

3D morphology of pharyngeal dentition in barbin fishes (Pisces: Teleostei: Cyprinidae): Implications for taxonomy, phylogeny and palaeobiogeography

Dissertation

der Mathematisch-Naturwissenschaftlichen Fakultät
der Eberhard Karls Universität Tübingen
zur Erlangung des Grades eines
Doktors der Naturwissenschaften
(Dr. rer. nat.)

vorgelegt von
MSc. Anna Ayvazyan
aus Martuni, Armenien

Tübingen
2019

Gedruckt mit Genehmigung der Mathematisch-Naturwissenschaftlichen Fakultät der Eberhard Karls Universität Tübingen.

Tag der mündlichen Qualifikation:	22.10.2019
Dekan:	Prof. Dr. Wolfgang Rosenstiel
1. Berichterstatter:	Prof. Dr. Madelaine Böhme
2. Berichterstatter:	Prof. Dr. Hervé Bocherens
3. <i>Berichterstatter:</i>	Prof. Dr. Jürgen Kriwet

Acknowledgments

First, I want to thank Prof. Dr. Madelaine Böhme for the opportunity to work under her supervision, for inspiring and encouraging me with this topic, as well as for her patience and endless hours for valuable discussions, which increase not only the quality of my work but also my professional competence. I am grateful to Prof. Dr. Hervé Bocherens for support and constrictive discussions during my work, as well as his valuable comments and corrections of my dissertation. I greatly acknowledge the support of my colleague Dr. Davit Vasilyan for accompanying me the long way from the beginning of my work, to sharing his professional experience and knowledge, which influenced my scientific understanding.

This work was partly funded by the German Academic Exchange Service (DAAD) and I am indebted to DAAD and its team for this opportunity to carry my research at the University of Tübingen. I am grateful to my contact person in DAAD Alexandra Sandic-Mangione for her great support during the first years of my study.

I furthermore highly appreciate the support and effort of my colleague Adrian Tröscher, who introduced me to the 3D software and taught me his knowledge until I was able to self-sufficiently work with the program. Further, I want to thank my friends and colleagues, especially all colleagues from “Terrestrial palaeoclimatology” for their encouragement and support. Many thanks to Hartmut Schulz, for his time and support to work with the SEM to photograph the fossil material. I also thank YXLON GmbH, especially Dirk Steiner, Andre Beerlink and Jean-Francios Metyer, as well as Christian Schulbert from Earlangen University for the opportunity to scan some of the studied material.

I gratefully thank Prof. Dr. Ignacio Doadrio and his working group to hosting me twice in National History Museum of Madrid (MNCN) and for the permission to work at the osteological collection, as well as for the possibility to scan the pharyngeal bones at the analytic laboratory of MNCN, with the great support of Christina Paradella and Laura Tormo.

I thank to Dr. Henriette Obermaier from the Bavarian State Collection for Anthropology and Palaeoanatomy for an access to the osteological collection,

Munich (SNSB), Prof. Dr. Samvel Pipoyan from Pedagogic State University of Armenia, Fabian Herder and Nisreen Alwan at Senckenberg Naturmuseum Frankfurt (SMF) for providing some of studied samples.

I am most grateful to my parents and my brother who kindly supported me under all possible circumstances during my study.

Table of Contents

Zusammenfassung	8
Summary	9
Abstract	10
List of publications	Fehler! Textmarke nicht definiert.
1. Introduction	12
1.1. The genus <i>Capoeta</i> and its biogeographical distribution	13
1.2. Cyprinid pharyngeal dentition	15
1.3. The fossil record of <i>Capoeta</i>	16
1.4. What is "species flock"?	18
1.5. Ecology and trophic preferences of <i>Capoeta</i>	18
1.6. 3D morphology and its importance.....	18
Objectives and expected outcome of doctoral research	20
2.1. Results	21
2.1.1. General aspects of the pharyngeal apparatus morphology of the genus <i>Capoeta</i> 21	
2.1.2. 3D morphology of the pharyngeal tooth: recorded characters and characterization.....	24
2.1.3. Recorded shape classes and distribution within studied species.....	27
2.1.4. Geological overview	28
2.1.5. Application of the established methodology to the fossil record of cyprinids	34
2.2. Discussion	44
2.2.1. Pharyngeal tooth morphology as a key for species level identification.....	44
2.2.2. Phylogenetic significance of pharyngeal tooth morphology	44
2.2.3. Taxonomy of the isolated fossil pharyngeal teeth from Çevirme.....	45
2.2.4. Possible influence of plasticity and allometry on high diversity of recorded shape classes 46	
2.2.5. Species flock scenario of evolution of the genus <i>Capoeta</i> : palaeogeographical interpretation of the fossil site Çevirme (palaeolake Tekman).....	47
2.2.6. Taxonomy of the isolated fossil pharyngeal teeth from Jradzor, Kısatibi, Kargı 1, Kargı 2, Harami1, Hancılı and Keseköy.....	48
3. Conclusion	50
4. Outlook	52
5. References	53
6. Appendix I: Published and Accepted Manuscripts	57
3D morphology of pharyngeal dentition of the genus <i>Capoeta</i> (Cyprinidae): Implications for taxonomy and phylogeny	57

Possible species-flock scenario for the evolution of the cyprinid genus *Capoeta*
(Cypriniformes: Cyprinidae) within late Neogene lake systems of the Armenian Highland . 69

7. Appendix II: Submitted Manuscript..... 100

Fish, amphibian and reptilian faunas from the latest Oligocene o middle Miocene localities
from Central Turkey 100

8. Appendix III: Supplementary material 184

Thesis

Zusammenfassung

Cyprinidae ist die zweitgrößte Fischfamilie der Welt und eine der am weitesten verbreiteten Fischgruppen im Süßwasser. Diese Fische zeigen einen hohen Endemismus für die Entwässerungssysteme in denen sie leben. Ihre geographische Verbreitung hängt von Süßwasseranschlüssen ab und spiegelt damit die Paläogeographie sowie die Geschichte der Wasserbecken dieses Gebietes wieder. Daher sind Süßwasserfische ein gut geeignetes Modell für paläo(bio)geographische und evolutionäre Studien. Dies ist jedoch nur möglich, wenn fossile Cypriniden auf Artniveau bestimmt werden können. Allerdings sind das rezente Vergleichsmaterial und die verfügbaren Methoden zur Taxonomie isolierter Knochen und Zähne von Cypriniden beschränkt. Innerhalb dieser Studie habe ich erfolgreich eine Methodik zur Identifizierung von isolierten Schlundzähnen barbiner Cypriniden auf Artenebene unter Verwendung der 3D Morphologie etabliert. Die Anwendung dieser Methode auf isolierte Schlundzähne von Kratzbarben der Gattung *Capoeta* ergab folgenden Ergebnisse:

- Die Morphologie von Schlundzähnen beinhaltet ein phylogenetisches Signal und erlaubt Schlussfolgerungen zur Evolution der Gattung zu ziehen;
- Die Evolution von *Capoeta* erfolgte wahrscheinlich in einem Artenschwamm während des Pliozän in See-Ökosystemen des Armenischen Hochlandes;
- Diese entwickelte Methode hat großes Potenzial die Evolutionsgeschichte anderer Barbini zu entschlüsseln.

Summary

Cyprinidae is the largest fish family in the world and one of the most widespread in freshwater and shows high endemism to the drainage systems, which they inhabit. Their distribution in water basins depends on freshwater connections and, therewith, reflects the palaeogeographic development as well as the history of the drainage systems of this area. Thus, the freshwater fishes are considered as a proper model for palaeo(bio)geographic and evolutionary studies. These studies can be possible only if the fossil remains are identified at species level. However, the recent comparative material as well as the methods for species level taxonomy of isolated bones and teeth of cyprinid fishes are limited. Here, I successfully provide a tool/methodology for species level identification of isolated pharyngeal teeth of barbini fishes by applying the analysis of the 3D morphology.

By applying this methodology to isolated pharyngeal teeth of extant ten *Capoeta* species as well as to the fossil record of *Capoeta*, I recorded:

- phylogenetic significance of pharyngeal tooth morphology and its insight into evolutionary scenario of the genus;
- the evolution of *Capoeta* was possibly represented by a species-flock model in a huge unrecognized palaeolake system in the present-day Armenian Highland at 4Ma;
- This method has great potential to disentangle the evolutionary history for other Barbini groups.

Abstract

Capoeta is a monophyletic clade of Barbini, endemic to Western Asian and Ponto-Caspian drainage basins. It serves as a valuable model for studying the history of the hydrographic system of this region, as well as provide the evolutionary model of this genus. This can be provided only in case of species level identification of the fossil remains of *Capoeta*, which are mainly represented by well-preserved isolated pharyngeal teeth. Until now, the specie level identification of teeth of any cyprinid is not recorded.

For the first time within this study, the methodology based on the 3D approaches is established to study the detailed morphology of isolated pharyngeal teeth of ten extant *Capoeta* species, to understand its taxonomic and phylogenetic significance. For this purpose, two 3D stage characters (lateral outline and transverse cross section) are imported to describe and categorize the isolated pharyngeal teeth into 18 shape classes. Results show that the detailed morphology can provide species level identification and has phylogenetic significance. This methodology is applied to the fossil record of cyprinids from the early Pliocene locality Çevirme (Turkey), Miocene sites Jradzor (Armenia) and Kısatibi (Georgia), and latest Oligocene to middle Miocene Kargı 1, Kargı 2, Harami1, Hancılı, Keseköy (all from Turkey) localities.

The isolated fossil pharyngeal teeth from Çevirme are identified at species level and four *Capoeta* species (*C. cf. umbla*, *C. cf. baliki*, *C. cf. sieboldi* and *C. cf. capoeta/C. cf. sevangi*) are recorded. This high local diversity of closely related four species I suggest to represent a species-flock model of the genus *Capoeta* in the Tekman palaeo-lake at 4 Ma. I hypothesized that the genus *Capoeta* evolved in the huge late Miocene to Pliocene palaeo-lake system in the present-day Armenian Highland (in the Tekman palaeo-lake). Later in the Pliocene, this extensive palaeo-lake system was disrupted by tectonic activities and resulted the present biogeographic distribution of *Capoeta* in West Asian and Ponto-Caspian drainage systems.

To get the complete view of the evolution of this genus as well as the history of the drainage systems of the Western Asian and Ponto-Caspian regions further studies of fossil sites from these regions are necessary. Within this thesis, two more fossil late Miocene sites (Jradzor and Kısatibi) and latest Oligocene to middle Miocene localities (Kargı 1, Kargı 2, Harami1, Hancılı, Keseköy) are included. The preliminary analyses of the fossil remains from these localities show the presence of the genus diagnostic

shape class "C" and, therewith, indicate that the studied material belongs to the genus *Capoeta*.

The isolated fossil pharyngeal teeth from the Kargı 1, Kargı 2, Harami1, Hancılı, Keseköy localities (Turkey) are identified at generic level and belong to the genera *Barbus* and *Luciobarbus*. However, the species level identification was not possible due to the lack of the detailed morphological studies of this element in the extant barbin species.

The 3D methodology applied within this study (on the example of the genus *Capoeta*) aimed to show that the detailed morphology of pharyngeal teeth provides significant taxonomic and phylogenetic information. Based on this example the similar methodology can be established for the other groups of cyprinid/barbin fishes as *Barbus* and *Luciobarbus*.

1. Introduction

This section consists of two parts. First part includes a brief overview of present day geographic distribution of the cyprinid genus *Capoeta*, its fossil record and its importance to palaeobiogeographic analysis of the Western Asian and Ponto-Caspian regions. The second part is devoted to the 3D morphology of the pharyngeal teeth as a useful tool for taxonomic and phylogenetic studies, as well as its application to the fossil record.

Freshwater fishes, as well as their fossil remains, are very suitable for zoogeographic and palaeobiogeographic studies since their migration(s) from one to another water basin depends largely on connections of the drainage basins. Thus, only the species level identification of these fishes provides the possibility to study the history of the hydrographic system and palaeogeography of the studied area (1).

The family Cyprinidae is the most diverse freshwater fish family represented with around 3000 species (2). The family includes several large clades (subfamilies), i.e. Cyprininae, Leuciscinae (3). Among cyprinins the genus *Capoeta* is not widely distributed. It inhabits only the water basins of Western Asia. This genus shows an endemism to this region, which makes it a valuable and interesting model to study palaeobiogeography as well as the history of the drainage system evolution of this area.

Currently, more than 30 *Capoeta* species are described (4–6). The earlier taxonomical studies of the genus *Capoeta* are mainly based on morphometric and meristic characters (7, 8), whereas the recent studies mostly on genetic analyses (4, 9). The cyprinid genus *Capoeta*, as other cyprinids, is also characterised by the presence of pharyngeal jaw. The pharyngeal jaws carry pharyngeal teeth, which are arranged in three rows. The number of the pharyngeal tooth rows and tooth number in the each row are mentioned as one of the significant taxonomic characters for the genus *Capoeta* (7, 8, 10, 11). Several studies have shown that the pharyngeal dentition, is an essential character complex at least at genus level, to study the evolution of cyprinids (12–16). Despite of this, the detailed morphological study of pharyngeal teeth of any cyprinid at species level is missing.

For the first time Heckel (1843) described the pharyngeal teeth of cyprinid fishes based on single morphological character (shape of grinding surface) and distinguished four

main groups and 13 subgroups. According to him, the pharyngeal teeth of the genus *Capoeta* belong to the subgroup "shovel-shaped teeth" and are characterized by 4.3.2 (outer, middle and last tooth rows) formula (17). Later studies recorded the presence of four or five teeth in the main, two to four in the second and two in the third rows (7, 8, 11).

Recent studies of the pharyngeal teeth are mainly concentrated on the number of the tooth rows, the tooth number in these rows, some measurements of teeth and pharyngeal bone as well as tooth shapes (11, 12, 14, 16, 18). However, the detailed morphological study of pharyngeal teeth and its significance for the taxonomy and phylogeny of any cyprinid, as well as the genus *Capoeta*, is missing. Besides this, the fossil remains of cyprinids are mainly represented by isolated pharyngeal teeth (19) therefore, the fossil record of many cyprinids, including the genus *Capoeta*, is still largely unknown. This is mainly caused by the problems with lower level (generic/specific levels) taxonomy of isolated pharyngeal teeth.

This dissertation aims to: 1) establish a new methodology to identify isolated pharyngeal teeth at species level; 2) apply it to the suitable group of cyprinids; 3) give an evolutionary model of the genus *Capoeta*; and 4) study the history of drainage basins and palaeobiogeography of the Western Asian and Ponto-Caspian regions.

1.1. The genus *Capoeta* and its biogeographical distribution

The genus *Capoeta* Valenciennes in Cuvier & Valenciennes, 1842, distributed across western Asia from Anatolia to the Levant, Transcaucasia, the Tigris and Euphrates basins, most of Iran, Turkmenistan, Northern Afghanistan and the upper reaches of the Amu-Darya and Syr-Darya drainages (20) (Figs. 1, 2).



Figure 1. *Capoeta damascina* from the Homs (Qattinah) Lake, Orontes River drainage, Syria (SYR08/25, SMF). The scale bar equals to 1cm.

The molecular genetic data shows that the genus *Capoeta* is a monophyletic group, which is nested within the *Luciobarbus* lineage and a sister group of *Luciobarbus subquincunciatus* (Fig. 3) (4, 21, 22). According to the phylogenetic analyses three main groups/clades within the genus *Capoeta* are distinguished: Mesopotamian, Anatolian-

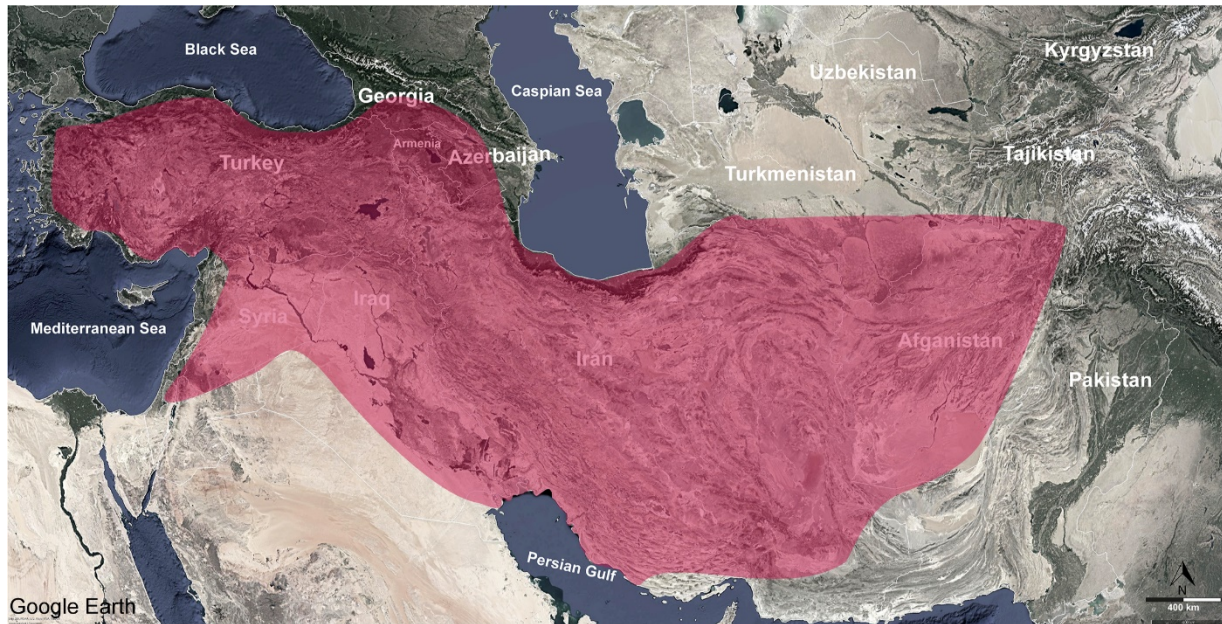
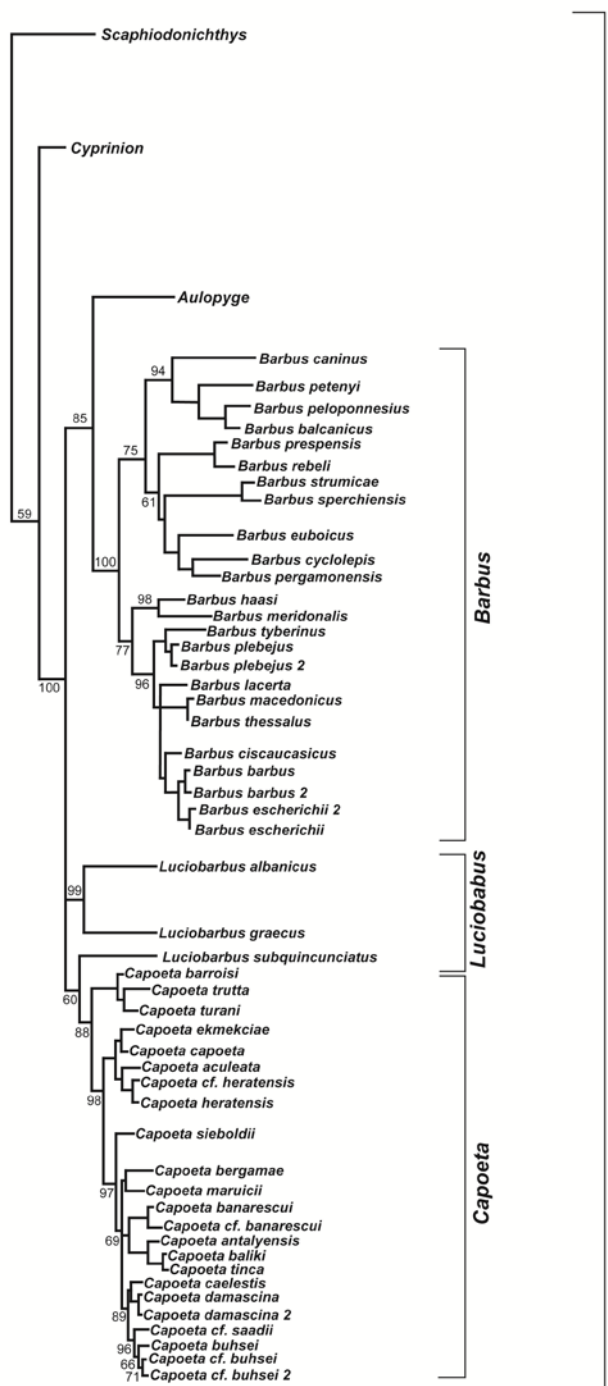


Figure 2. Map showing the present day distribution of the genus *Capoeta* (highlighted in red). © Google Earth Pro.

Iranian and Aralo-Caspian clades. The Mesopotamian group contains species distributed in the Tigris-Euphrates drainage system and adjacent water basins: *Capoeta trutta* (Heckel, 1843), *Capoeta turani* Özulu & Freyhof, 2008 and *Capoeta barroisi* Lortet, 1894. The Anatolian-Iranian group includes species inhabiting the Black Sea Basin: *Capoeta sieboldi* Steindachner, 1864, *Capoeta baliki* Turan, Kottelat, Ekmekçi & Imamoglu, 2006, *Capoeta banarescui* Turan, Kottelat, Ekmekçi & Imamoglu, 2006. The Mediterranean drainage basins (Anatolian-Iranian clade) of southeastern Turkey, the Tigris–Euphrates river system, and small rivers, which drain into the gulfs of Persia and Oman, as well as inland water bodies in Iran contain the following species: *Capoeta buhsei* Kessler, 1877, *Capoeta saadii* (Heckel, 1847), *Capoeta caelestis* Schöter, Özulu & Freyhof, 2009, *Capoeta damascina*, *Capoeta angorae* (Hankó, 1925) and *Capoeta kosswigi* Karaman, 1969. Finally, the Aralo-Caspian group includes the species distributed in the Kura and Araxes rivers, as well as Aral and Caspian Sea drainages: *Capoeta capoeta* Gldenstdt, 1773, *Capoeta sevangi* De Filippi, 1865, *Capoeta aculeata* (Valenciennes, 1844) (4, 6, 21)



Barbini Bleeker, 1859

Figure 3. Cladogram showing the location of the genus *Capoeta* on the phylogenetic tree based on the molecular genetic analysis. The phylogenetic tree is taken from Yang et al. 2015. Clades of *Luciobarbus*, *Cyprinion* and *Scaphiodonichthys* are simplified.

The detailed distribution of the studied extant *Capoeta* species see Table 1 Ayvazyan et al., 2018 (21).

1.2. Cyprinid pharyngeal dentition

Cyprinids are characterized by the toothless jaws (e.g. dentary, maxilla, premaxilla) and by presence of the pharyngeal bones. The pharyngeal jaws form as a result of ossification of the fifth left and right ceratobranchials. They are specialized for the food processing and are located in the posterior part of fish cranium (Fig. 4 A, B). The pharyngeal jaw carries pharyngeal teeth, which are arranged in up to three rows and can be represented by following formula: 4.3.2. - 2.3.4. – numbers indicate number of the teeth on the left and right jaws from the first to the third and the third to the first raw correspondingly (23, 24). As it is already mentioned, the numbers of

the rows and the number of the teeth in these rows have a taxonomic significance for cyprinid fishes and they are considered as one of the

criteria mentioned in identification keys.

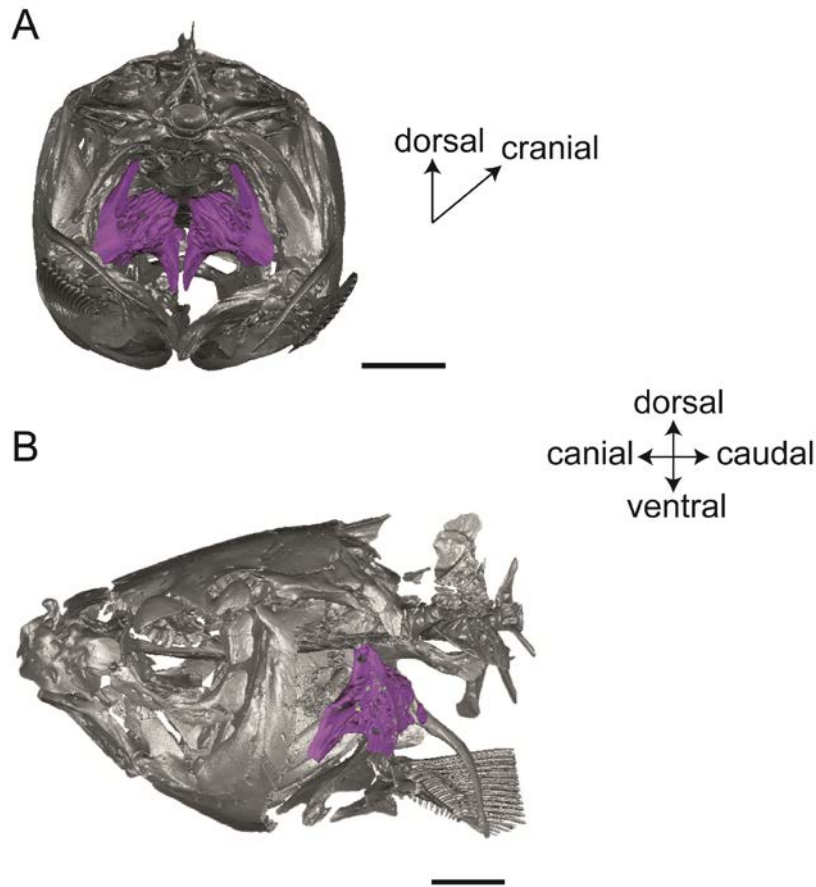


Figure 4. Anatomical location of the pharyngeal bones in *Capoeta sevangi*, Sevan Lake, (A) posterior and (B) lateral views. The scale bars equal to 1cm. Modified from Ayzazyan et al., 2018.

1.3. The fossil record of *Capoeta*

According to the molecular data, the genus *Capoeta* originated around the Langhian–Serravallian boundary (13.9 Ma) and diversification within the genus occurred along the middle Miocene – late Pliocene (Levin et al., 2012).

The fossil record of *Capoeta* is scarce. So far, until my dissertation they are known only from four localities. Two of them from the late Miocene and

other two from the Pleistocene localities. Miocene *Capoeta* fossils are known from Armenia and Georgia; both in the present-day Kura-Araxes drainage basin (Fig. 5).

The first fossil remains of *Capoeta* (*'Varhikorinius' nuntius*) have been described by Bogachev (1927) from the late Miocene (early Pliocene at that time) locality in the Kusatibi, Samtskhe-Javakheti region, Georgia (Fig. 5). The material was represented by three more or less complete and a few strongly destroyed skeletons as well as more than 70 bone fragments. Vasilyan & Carnevale (2013) have mentioned skeletons of *Capoeta* sp. from the Jradzor locality (latest Miocene) in Armenia (25).

The record of the genus *Capoeta* from the late Pliocene sediments of Ericek (Cameli Basin, SW Anatolia; Van den Hoek et al., 2015) is doubtful. The tooth morphologies (Fig. 4 a-d in Van den Hoek et al., 2015) are not found within pharyngeal teeth of the *Capoeta* species. Vasilyan et al. (2014) described two isolated pharyngeal teeth and two fragments of serrated dorsal fin rays referred to *Capoeta* sp. from the early

Pleistocene locality Paşınler (Erzurum Province, north-eastern Turkey). Fossil remains of *Capoeta damascina* Valenciennes, 1842 have been recorded during the study of the fish community of the palaeolake Hula (26). The site is situated in the northern part of the Dead Sea Rift, Israel and has been dated to the middle Pleistocene (0.78 Ma).

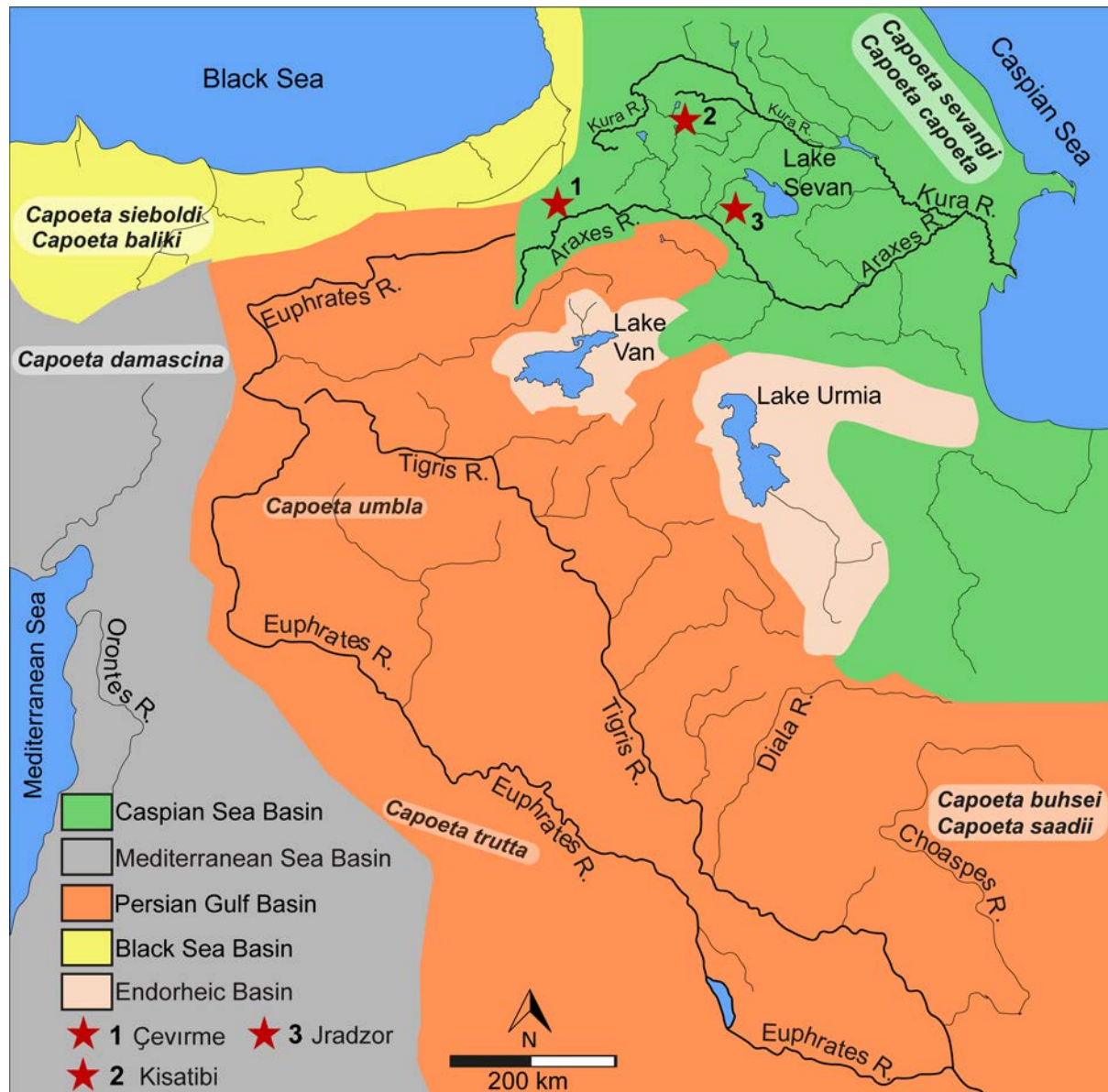


Figure 5. Geographical overview of the drainage systems of Western Asia and Ponto-Caspian regions (Euphrates-Tigris, Araxes-Kura). Red stars indicate the positions of the fossil localities of recorded fossil remains of the genus *Capoeta*.

1.4. What is "species flock"?

A species flock is a monophyletic group of closely related sympatric species inhabiting the same or geographically restricted area. Among both vertebrate and invertebrate animals examples of species flocks are recorded. This phenomena is connected to the rapid adaptive radiation, morphological divergence and speciation (27–30). The species flock concept is known within both living and fossil fishes (31–36) (details see Ayvazyan et al., 2019).

1.5. Ecology and trophic preferences of *Capoeta*

The monophyletic genus *Capoeta* includes herbivorous scrapers, feeding mainly on algae and periphyton, which they scrap from the substrate by the horny sheath on their lower lip. These species generally inhabiting the lakes and streams with fast and slow-flowing waters (7, 20, 37).

1.6. 3D morphology and its importance

3D morphology considered as a morphological study based on the 3D models of studied material. 3D models are created through (micro)computed tomography. Microcomputed tomography is an X-ray transmission technique. X-rays are emitted from generator and travel/penetrate through a sample. They are recorded by a detector on the other side to produce projection image of the sample. The final data of scanning consist of two-dimensional (2D) trans-axial projections, or slices of a scanned specimen, which should be reconstructed in 3D software to get the 3D models (38). These models are used for further examinations and measurements.

3D morphology is one of the modern methods widely applied to the different groups of organisms. The high demand of three-dimensional computed tomography has many reasons: 1) high-resolution images of the study objects are provided; 2) measurements of different morphological structures can be obtained; 3) the 3D image can be rotated easily by changing the rotational axis; 4) the inner structures can be observed by removing the outer surfaces; and 5) different effects or virtual experiments can be

applied (e.g. wearing process of teeth).

The role of the 3D morphology is priceless for the fossil record. Especially if the fossil remain is partly or completely in the sediment. By applying this technique, it is possible to get the complete view of the fossil, without losing any information/material, which could be in the sediment and invisible for us.

The disadvantage of this technique is that the possibility to scan the study material is limited and the costs are high. Besides this, the reconstruction and preparation of the material could be very time consuming.

Objectives and expected outcome of doctoral research

This research addresses to the questions regarding to the taxonomic and phylogenetic significance of the morphology of the isolated pharyngeal teeth of cyprinid fishes. I expected to establish a morphological methodology based on 3D methodology, which is applicable to identify the isolated pharyngeal teeth at species/generic level. For this purpose, the pharyngeal teeth of the monophyletic genus *Capoeta* are studied. This genus shows an endemism to the water basins of the Western Asia and Ponto-Caspian regions, therefore the low level taxonomic identification of the fossil remains (mainly represented by isolated pharyngeal teeth) can serve as a basis to track the evolution of this genus and to perform a palaeobiogeographical analysis of the water drainages of these regions.

Thus, the goals of the present study are:

- to establish methodology by applying 3D approaches to species level identification of isolated pharyngeal teeth of 10 extant *Capoeta* species;
- to check the interspecific and topologic variations of pharyngeal tooth morphology;
- to test the possible phylogenetic signal embedded in the tooth morphology;
- to apply the resulting methodology to the fossil record of *Capoeta*;
- to determine species composition within the fossil sample;
- to evaluate the history and coverage of lake system in Western Asia and Ponto-Caspian regions;
- to discuss evolutionary models for the genus *Capoeta* in respect to its biogeography;
- to test the applicability of this methodology to other barbin fishes.

2. Results and Discussion

2.1. Results

The results of this study are divided into three parts. The first part is devoted to the 3D morphology of the pharyngeal teeth of ten extant *Capoeta* species and its significance to the taxonomy and phylogeny.

The second part concerns to the fossil record of the genus *Capoeta* and the studied main fossil sites where fossil remains of *Capoeta* are recorded.

The third part includes the results of the applicability of the established methodology (within the first part of this study) to the fossil record of cyprinids.

Supplementary material (figures, graphs and tables) is included in Appendix III.

2.1.1. General aspects of the pharyngeal apparatus morphology of the genus *Capoeta*

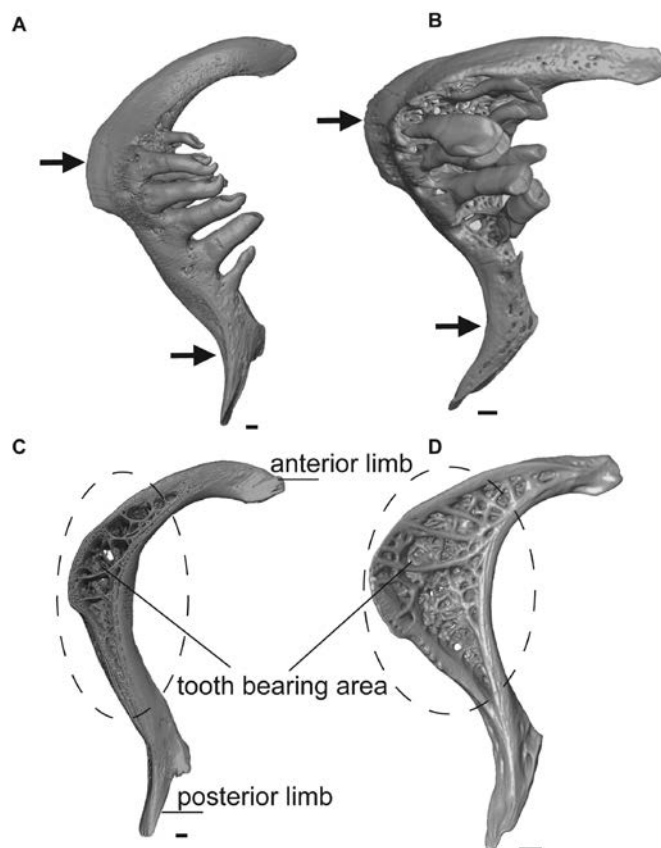


Figure 6. Morphological differences of pharyngeal bones in dorsal (A, B) and ventral (C, D) views: (A, C) *Barbus barbuis*; (B, D), *Capoeta umbla*. Black arrows point the main morphological characters and the circles marked the tooth bearing areas. Scale bars equal to 1mm.

The pharyngeal bones of the genus *Capoeta* are relatively robust and wide compare to the pharyngeal bones of the genus *Barbus* (Fig. 6 A, B). They are characterized by relatively large tooth bearing area and well-expressed anterior and curved posterior limbs. A well-developed pharyngeal bone is an evidence of the strong muscles attached to the bone (Fig. 6 C, D).

Each pharyngeal jaw possesses nine to ten pharyngeal teeth, which are arranged at the pharyngeal bone in three rows (I, II, III). Each of them has different tooth number.

The first or main row possesses four or five teeth (a1, a2, a3, a4, a5), the second row three (b1, b2, b3) and the third row two (c1, c2) teeth (Fig. 7, A). Each tooth consists of a tooth foot, a crown, a foot-crown border, a grinding surface and an edge of the grinding surface (Fig. 7 B).

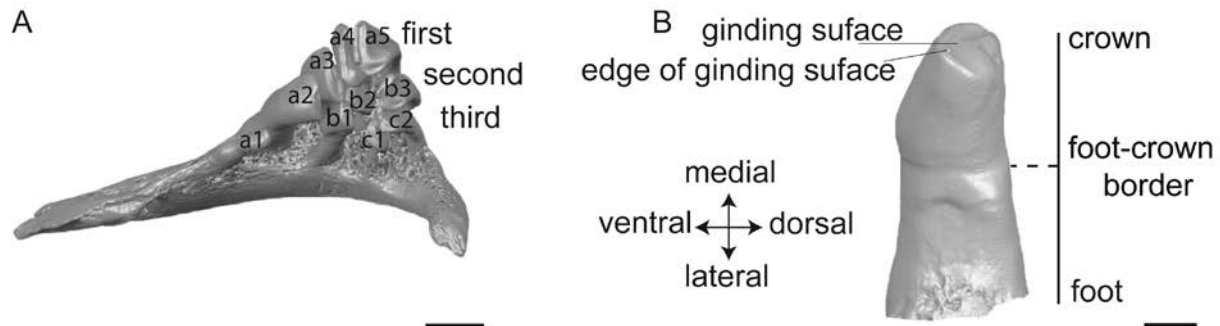


Figure 7. Pharyngeal bone of *C. damascina*: (A) the distribution of pharyngeal teeth into first (a1, a2, a3, a4 and a5), second (b1, b2 and b3) and third teeth (c1 and c2) rows; (B) *C. baliki*, tooth morphology. Scale bars equal to 1mm. Modified from Ayvazyan et al., 2018.

Within the studied ten extant *Capoeta* species from different water basins, two main formulas of the pharyngeal teeth distribution into tooth rows, are recorded: 1) 4.3.2-2.3.4 in *C. capoeta*, *C. sevangi*, *C. sieboldi*, *C. trutta* and *Capoeta sp.*; or 2) 5.3.2-2.3.5 in *C. damascina*, *C. umbla*, *C. buhsei*, *C. saadii* and *C. baliki*. The species with the second formula have a1 tooth or the tooth base, which indicates the possible presence of the a1. *Capoeta* shows a heterodont dentition based on recorded high morphological diversity among the studied ten species.

The teeth of the main/first row are relatively larger (except a1) than those of the second and third rows. The first tooth of the main row (a1) is a small accessorial tooth and can be easily broken. It is absent (*C. capoeta*, *C. sevangi*, *C. sieboldi*, *C. trutta* and *Capoeta sp.*), strongly reduced (*C. umbla*) or less reduced (*C. damascina*). In case of *C. saadii*, *C. buhsei* and *C. baliki* it is broken and only the tooth basis is visible (Fig. 8). As a rule, the second tooth of the main row (a2) is usually easily distinguished from other teeth. It is robust, relatively large with a wide tooth base and grinding surface. The other teeth of the main row (a3, a4, a5), as well as the teeth of two other rows (b2, b3, c1, c2) are slender compared to the a2. They widen distally and bent laterally. These characters are more pronounced ventrodorsally along the main row and well expressed in the most dorsal tooth (a5). The first tooth of the second row (b2) is the second largest tooth after the a2. The other teeth of the second row are slender and bent laterally. Two teeth of

the third row (c1, c2) are usually the smallest. The grinding surfaces in all three rows narrow ventradorsally. Among two control groups *C. sevangi* (n=9) and *C. capoeta*

(n=13) intraspecific variation, as well as left-right asymmetry are not recorded.

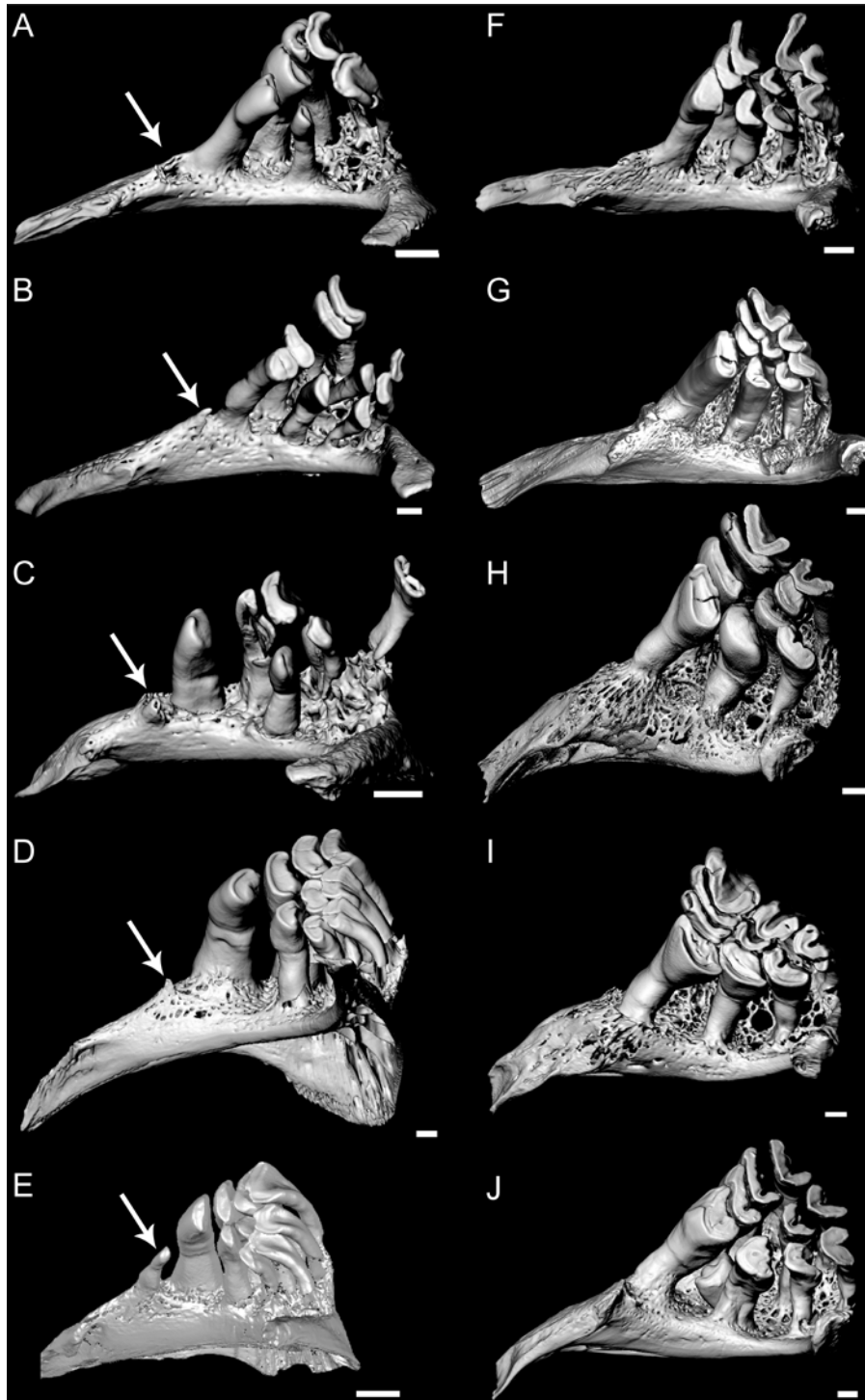


Figure 8. Images of 3D models of pharyngeal bones with teeth of the studied ten extant *Capoeta* species (A–J). (A) *Capoeta buhsei*; (B) *Capoeta umbla* (mirrored); (C) *Capoeta saadii*; (D) *Capoeta baliki*; (E) *Capoeta damascina* (mirrored); (F) *Capoeta capoeta*; (G) *Capoeta sevangi*; (H) *Capoeta sp.*; (I) *Capoeta trutta*; and (J) *Capoeta sieboldi*. The white arrows show a1 or presence of its bases. Scale bars equal to 1mm. From Ayvazyan et al., 2018.

2.1.2. 3D morphology of the pharyngeal tooth: recorded characters and characterization

The morphology of pharyngeal teeth is examined based on 3D models of isolated pharyngeal teeth (n=84) of studied ten extant species. Each pharyngeal tooth is virtually separated from the pharyngeal bone as an apart 3D model and the teeth set for each studied species is established to characterise and categorize these teeth into shape classes (morphotypes) (Fig. 9). Other set of teeth, including extant comparative material of the genus *Capoeta*, are included in Appendix, Figure S1.

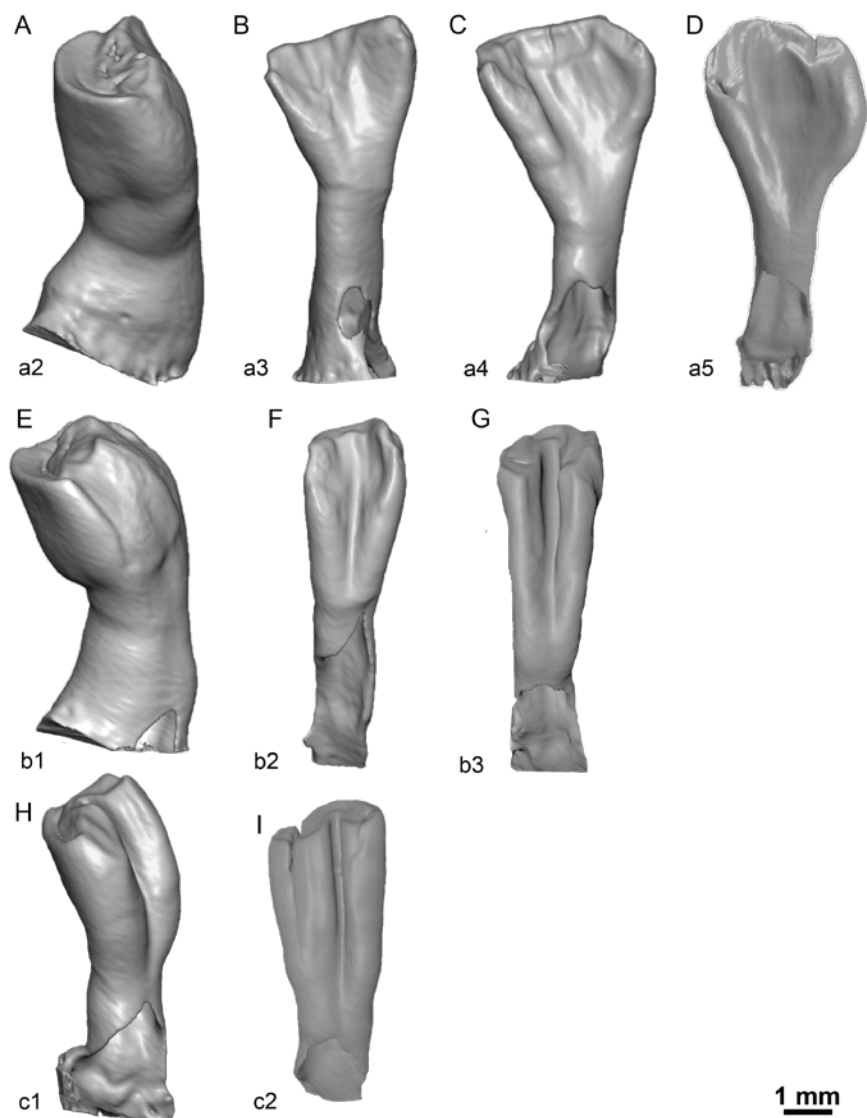


Figure 9. Set of the isolated pharyngeal teeth of *Capoeta trutta*. (A-D)Teeth of the first (a2, a3, a4 and a5), (E-G) second (b1, b2 and b3) and third (H, I) (c1 and c2) rows. Ayvazyan et al., 2018 (supplementary material).

The detailed examination of 3D models of isolated pharyngeal teeth is performed in the 3D software Avizo (8.0, 9.0), as well as under the light microscopes Leica DVM5000 digital- and M50 stereomicroscope (pharyngeal bones/teeth). To formulize better tooth morphology we introduced shape classes defined by character stages: lateral outline (α , the contour of the tooth body) and transverse cross-section (β , measured at the distal tooth crown) (Fig. 9 A, B). Within the studied pharyngeal teeth ($n=84$), we define 14 character stages of lateral outline (α_1 - α_{14}) (Fig. 10A). The most frequently lateral outline has a spatulate form. It occurs mainly in the a3-a5, b2-b3 and c1-c2 tooth positions. According to the transverse cross-section, we record in total eleven characters stages (β_1 - β_{11}) (Fig. 10B).

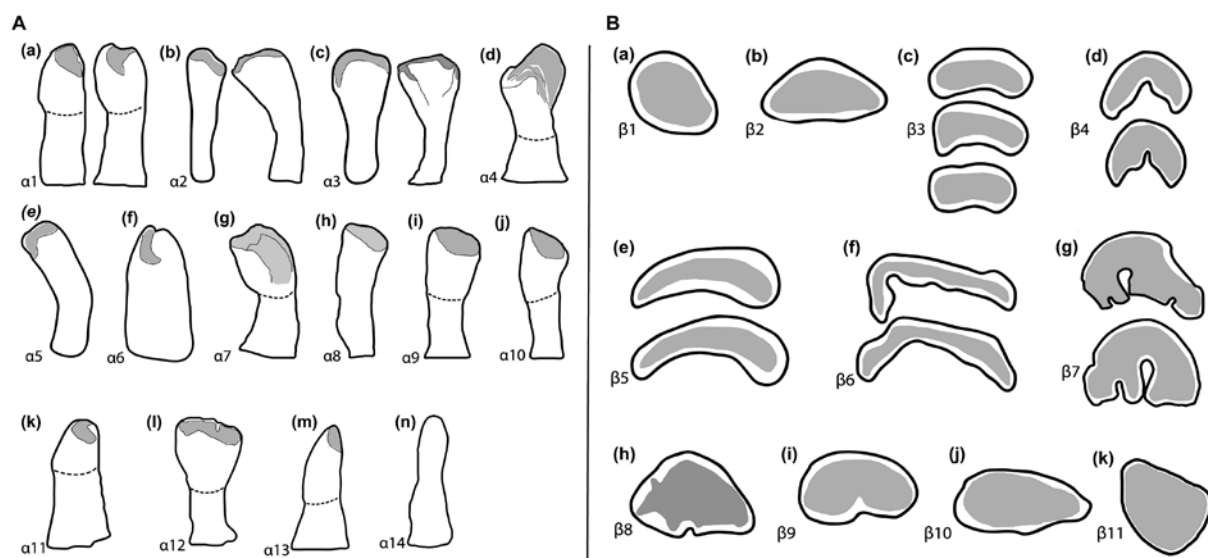


Figure 10. Illustration of character stages: (A) lateral outlines (α_1 - α_{14}) and (B) transverse cross sections (β_1 - β_{11}) of isolated pharyngeal tooth within the studied extant *Capoeta* species. Modified from Ayvazyan et al., 2018.

To check the robustness of the transverse cross-section the artificial (virtual) wear experiment is applied (for details see "Material and methods", Ayvazyan et al. 2018). In this experiment the different layers/slices from the top of the grinding surface were cutten to follow the variability, i.e. development of these characters during the wearing process. Thus, three different height sections from the top of the grinding surface (0.57mm, 0.87mm and 1.42mm) were processed. The results did not show any significant changes of transverse cross-section (β) and it stays stable during applied wearing process.

This virtual experiment allows to test also the stability of other characters e.g. foldity

and serrated posterior edge of the grinding surface, which were recorded but not applied to teeth description as these characters depend on degree of tooth wearing (S2 Fig. A1-A3).

Thus, two main groups of characters of the pharyngeal teeth can be identified: 1) applicable for the tooth description as the lateral outline (α) and transverse cross section (β); and 2) variable during the ontogeny as folded, serrated and sloped edge of the grinding surface. The first group of characters (α , β) can be applied to categorize the pharyngeal teeth of the studied ten *Capoeta* species into 18 shape classes. The detailed description of all the shape characters and classes can be found in the Appendix III (Fig. 11, Tables S1, S2).

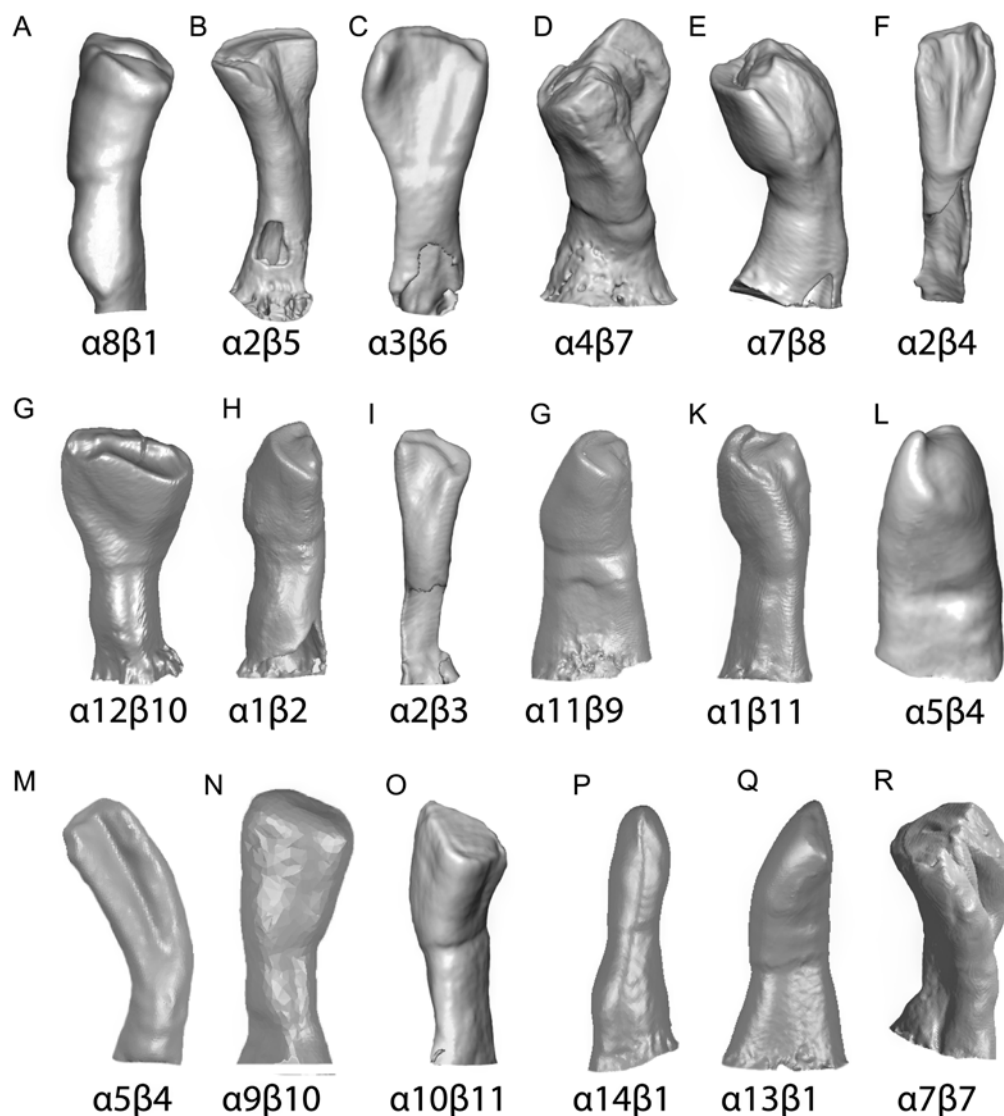


Figure 11. 3D images of the recorded shape classes of the pharyngeal tooth of the genus *Capoeta*. (A-R shape) classes proposed in the present work. The scales are not given in order to avoid scaling up of the figures (Ayvazyan et al., 2018).

2.1.3. Recorded shape classes and distribution within studied species

To test the potential taxonomic and phylogenetic signal of the pharyngeal tooth morphology a dendrogram is performed based on the distribution of recorded shape classes within studied ten extant *Capoeta* species. According to the dendrogram, the studied species are divided into four phenotypic clades: Clade I (*C. saadii*, *C. buhsei*, *C. damascina*, *C. umbla* and *C. baliki*), Clade II (*C. sieboldii*), Clade III (*C. capoeta* and *C. sevangi*) and Clade IV (*C. trutta* and *Capoeta* sp.) (Fig.12, Table S3).

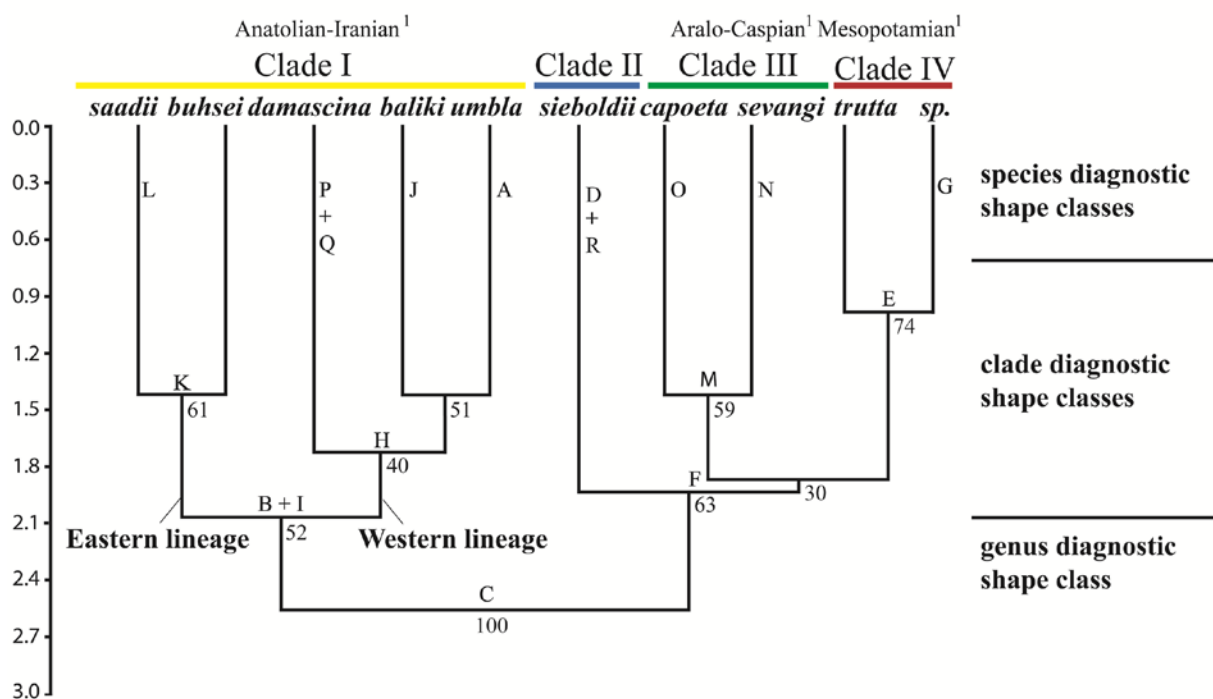


Figure 12. Phenotypic dendrogram generated based on the pharyngeal tooth shape classes of the *Capoeta* species. The letters (A-N) indicate the characteristic shape classes for nodes or branches. Numbers indicate the bootstrap support (branch support). ¹Distinguished clades of the genus *Capoeta* follows Levin et al. (2012). ²Eastern (E lineage) and Western (W lineage) lineages within the *C. damascina* complex established by Alwan et al., 2016. Modified from Ayyazyan et al., 2018.

Based on the distribution of the recorded 18 shape classes within studied species (shown on the dendrogram) three main groups of the shape classes are distinguished: diagnostic for the **genus**, **clade** and **species**. The **genus diagnostic shape class** is the shape class "C", since it occurs in all studied species and is characteristic for the genus *Capoeta*. Thus, this shape class is the most frequent within all recorded shape classes (S3 Fig.). The **clade diagnostic shape classes** are characteristic for a group of species, which belong to the same clade, e.g. shape classes "B, E, F, H, I, K and M".

The other shape classes are **species diagnostic**: "D, G, J, L, N, O, P, Q and R" are characteristic for certain species and can be used at **species level identification** of isolated pharyngeal teeth. They occur mainly at the tooth position a2 (S4 Fig). Based on the presence of the different level of shape classes (genus/species/clade diagnostic) and their distribution within ten extant species an identification key is established (S5 Fig.). I found a correlation between tooth positions and shape classes, e.g. shape class "C" occurs in tooth positions a3-a5 in all studied species, whereas species diagnostic shape classes mainly characterise the teeth at the tooth position a2 (except b1 tooth of *C. sieboldi*) (S6 Fig.).

2.1.4. Geological overview

2.1.4.1. Euphrates-Tigris and Kura-Araxes: A brief overview

Four main rivers of the northeast part of Western Asia are the Euphrates, Tigris, Kura and Araxes, which all originate in the Armenian Highland (Fig. 4). The Euphrates and Tigris with their tributaries are life arteries of the entire Mesopotamian area. Both rivers originate from numerous streams in the Armenian Highland (Turkish High Plateau according to Illies & Rzóska, 1980) near the Erzurum Province at an altitude of over 2000 m above sea level (39).

The Euphrates is about 2600 km long. It flows through Syria and Iraq to join the Tigris, form Shatt al-Arab and ends in the Persian Gulf. The Tigris is nearly 2000 km long. The river has five tributaries which drain the mountains (Khabur, Greater and Lesser Zab, Adheym and the Diyala) and carry their erosion products into the plain, where they join the Tigris. The water of the rivers is mainly supplied from the snowmelt and rain (39, 40).

The Kura-Araxes (Araxes also known as Aras and Araks) River Basin is located in the Southern Caucasus. The Kura River is the longest river in the Caucasus (around 1,364 km). It encompasses Turkey, Iran, Armenia (does not pass Armenia but its tributaries), Georgia and Azerbaijan. It starts in the Armenian Highland at the Kizil-Giadik Mountain, and flows southeast through Georgia into Azerbaijan. The main tributary of the Kura is the Araxes River (USAID, 2002) (41, 42). The Araxes River originates in the Bingöl Dağ region, Erzurum Province, where it is separated from headwaters of Euphrates River

through low divide. The total length of the Araxes is 1072 km. It flows through Turkey, Armenia, Azerbaijan and Iran (Kura-Aras River Basin Transboundary Diagnostic Analysis; Campana et al, 2012) (43).

2.1.4.2. Late Neogene lacustrine sedimentation in the Armenian Highland

Present-day Armenian Highland (Eastern Anatolia, Armenia, Iranian Azerbaijan, Samtskhe-Javakheti region of Georgia) is composed of the high mountainous landscapes of the Eastern Taurides and Lesser Caucasus with elevations between 1.700 to over 5.000 meters above sea level. Because of the dominant arid climate during the later Holocene, lakes are rare in this region. Two endorheic saline lakes, Lake Van and Lake Urmia, as well as Lake Sevan are notable exceptions (Fig. 13).



Figure 13. Map of the Armenian Highland. Three main lakes of the region: two endorheic saline lakes Van and Urmia, freshwater Lake Sevan. Figure is redrawn from Vasilyan et al., 2014, background data from © OpenStreetMap contributors, CC BY-SA. Modified from Ayvazyan et al., 2019.

However, geologic mapping revealed, that during the pre-Quaternary lacustrine, sedimentation was widespread and long lasting in this region. According to Altınlı

(1966) during the Late Miocene and Pliocene (11.6-2.6 Ma) lacustrine sedimentation dominates Eastern Anatolia with regional thicknesses of over 1.000 m. These sediments contain a rich freshwater fauna (e.g. diatoms, gastropods, mussels, ostracods, fishes) and have been variously attributed to the Horasan Formation, Gelinkaya Formation, Işıklar Formation (all in the Erzurum Province), Zırnak Formation (Bitlis Province), Çaybağı Formation (Elazığ Province), or to the Parçikan Formation (Malatya Province) (44–49). Despite extensive syn-sedimentary volcanism, none of these formations is fully radiometrically dated. However, few available K-Ar data (50) and rare rodent fossils (51, 52) suggest that the main lacustrine phase in Eastern Anatolia centred between 6 and 3 Ma, probably coeval with the supposed uplift of this region.

Late Miocene to Pliocene lacustrine sediments in Armenia are described from the 500 m thick Voghjaberd Suite (53). Index ostracods of the Caspian Productive Series (dated to between ~5.3 and 2.7 Ma, (54) and small mammals (55) point to Pliocene age of this formation, and recently discovered rodents from the *Capoeta* bearing site Jradzor have a latest Miocene age (25).

An older lacustrine period is documented in Iranian Azerbaijan, where fish bearing (Atherinidae, Cyprinodontidae, Leuciscinae, but no Barbinae) lake sediments from the Tabriz Basin ('lignite beds', 'fish beds') have been dated to between 12 and 7.5 Ma (56). These late Neogene lacustrine sediments have a tectonically fragmented exposure over a huge area in the Eastern Taurides stretching several hundreds of kilometres, notably including the upper reaches of present-day Euphrates, Tigris, Kura and Araxes rivers (Fig. 13).

2.1.4.3. Fossil locality Çevirme

The fossil site Çevirme (Erzurum Province, Tekman district) (Tekman palaeo-lake) is located 12 km west of the Hacıömer village on the road from Hacıömer to Tekman, 500 m after the bridge over the Araxes River (coordinates: N 39° 37' 37"; E 41° 38'; Figs. 5, 13 and 14).



Figure 14. High resolution map (from Google Earth Pro) showing the fossil locality Çevirme marked by red contoured circle. The whitish sediment north of the Araxes River represent the lacustrine Işıklar Formation. Modified from Ayvazyan et al., 2019.

The locality belongs to the Tekman Basin (East-Anatolian Taurides; Irrlitz, 1972), approximately 40 km south from the Pasinler Basin and 120 km north-northwest of Lake Van. Late Neogene sediments in the Tekman Basin laying discordantly over early Miocene marine limestones (57). The sedimentary facies of the basin infill change from fluvial-alluvial to lacustrine. The late Miocene sedimentary formation (Hacıömer Formation) is composed of an approximately 300 m thick reddish-brown sequence of conglomerates, sandstone and silts with minor intercalation of marls. In the south of the basin, the alteration with vulcanites appear. These terrestrial-fluvial fossils free layers intercalate in their upper parts with nearly 200 m thick lacustrine sediments of the Işıklar Formation, which mainly consist of light gray, as well as slightly reddish freshwater carbonates (see fig. 4 in Ayvazyan et al., 2019). Layers of marl, organic rich clay and tufa are also present. The section is covered by Pleistocene basalts from the Bingöl Dag area (57).

The fossil site Çevirme, discovered and first described by Sickenberg et al. (1975: 95), belongs to the lacustrine upper part of the Işıklar Formation (58). The 65 m thick stratigraphic section is subdivided based on lithological and sedimentological characters. The fossil remains of fishes, molluscs and mammals are found at 18 m of the section (see fig. 4 in Ayvazyan et al., 2018).

Earlier palynological studies at Çevirme section indicate an early Pliocene pollen

spectrum in accordance to the small mammal fauna (57, 58). A recent preliminary taxonomic update of the rodent association revealed among others the genera *Mimomys* and *Occitanomys*. This suggests correlation to MN15a mammal zone, roughly of about 4 Ma in the middle part of the Pliocene (51).

2.1.4.4. Fossil locality Jradzor, Armenia

The fossil locality Jradzor is located in the Yeranos mountainous range at the present-day elevation of the 1920 m asl (Central Armenia) (Figs. 5, 15). The fossil site is represented mainly by pure and porous diatomite rock with extremely low clay and sand content. It has thickness of about 8 m and lateral extension in the outcrop of ca. 150 m.



Figure 15. Fossil locality Jradzor, Central Armenia. The red arrow shows the diatomite sediment section from where the fossil remains of *Capoeta* were recorded.

The presence of two black sandstones in the lower part of the section, indicating erosion of the lake surrounding volcanic rocks and their fluvial transport. The upper 7 m thick diatomite bed shows red to yellow colouring and fine lamination. Several 2-10 cm thick layers rich of clay occur, indicating phases with terrestrial input during the lake development. Grey-brown clayey diatomite and overlying grey-bluish sandstone are composed in the uppermost 60 cm of the section. The diatomite is covered by conglomerate, showing sharp erosive contact with underlying beds. Laterally the upper bed is eroded and conglomerates lie directly on upper part of the 7 m thick diatomite pocket. The following stratigraphic markers are recorded: pennatic diatoms *Cymbella elongata* and *Pinnularia meisteri* f. *armenica*.

The diatomite deposit of the fossil site Jradzor provides well preserved fossil diatom algae, remains of fishes (*Leuciscus cf. souffia*, *Leuciscus* sp., *Garra* sp., *Capoeta* sp.), an amphibian (*Pelophylax cf. ridibundus*), a reptile (Geoemydae indet.) and mammals (? *Hypolagus* sp.). Both complete and incomplete skeletons of fishes are found. The taphonomy of the fish remains allow to conclude about their resident lacustrine populations in the lake, at least in earlier staged of the lake sedimentation. The overlying river and palaeosol deposits contain small mammal species characteristic for latest Miocene assemblages (25).

2.1.4.5. Fossil locality Kساتibi, Georgia

The fossil locality Kساتibi is a part of a large Goderdzskaya Formation (900-1100 m). Kساتibi is located in the Samtskhe-Javakheti region (southern Georgia), in the middle of the extended gorges of the Kura and Potskhovi rivers (Fig. 5) (59). Skhirtladze (1958) provides the sedimentary succession of the Goderdzskaya Formation at the fossil site Kساتibi (nearly 150 m) (59).

Palaeoflora of Kساتibi is represented by 22 species (59). The fossil remains of vertebrates are almost absent in Goderdzskaya Formation. Only the diatomite layers have relatively rich fossil fauna, which is mainly represented by fossil remains of freshwater fishes. The records of fossil mammals are rare.

Bogachev (1938) described all fish remains from Kساتibi as one genus *Varicorhinus* and as a new species *Varicorhinus nuntius*. Based on palaeontological and palaeobotanical data, he dated the fossil site Kساتibi to Pliocene (Late Miocene now days) (Gabelaja, 1976).

Later, Gabelaja (1976) studied the fossil remains of fishes from Kساتibi and record the presence of two genera *Barbus* and *Capoeta*. Wherein, the main part of the recorded fossil fish material belong to *Caepota nuntius* and relatively few specimens to *Barbus orientalis*.

2.1.4.6. Latest Oligocene to the middle Miocene localities from Tukey

Fossil locality Kargı is located in a coal quarry near the village of Dodurga. The sediments are represented by white limestones and dark green clays. The biostratigraphic correlations suggest that Kargı 2 lies at the Oligocene–Miocene transition (local zone A, MP 30–MN 1), and Kargı 3 is of Early Miocene age (local zone B, MN1). The fossil remains from Kargı are recovered from bioturbated, blackish, solid clay. Kargı 2 sediments, darkly coloured and bioturbated, indicate a typical lacustrine bottom. Kargı 3 sediments are grey clays, rich in diatomite (60, 61).

The Harami section constitutes the sedimentary overburden of the main coal level of the Harami mine near the town of Ilgin. It contains *Eumyarion* and *Spano/Democrisetodon* dominated assemblages attributed to zone MN 1 or 2. Greenbrown laminated or homogeneous clays comprise the main part of the section. At several levels small coal layers (1- 10 cm) are present (62).

Hancılı locality is a former lake. Its sediments are finely laminated, coalbearing and mildly bioturbated. It is considered as a MN 4 locality (61).

Keseköy locality is a coal quarry near the town of Kizilcahamam. The section predominantly consists of green-brown, partly laminated clays, intercalated with several coal layers. It contains an assemblage of small mammals that is attributed to the local zone D, being correlated to MN 3 (60, 61).

2.1.5. Application of the established methodology to the fossil record of cyprinids

The established methodology is applied to the fossil material represented by isolated fossil pharyngeal teeth as well as to the teeth founded within the skull or complete fish skeleton samples.

2.1.5.1. Isolated fossil pharyngeal teeth from Çevirme

Isolated fossil pharyngeal teeth (n=247) (Depository numbers and other details see Table 1, Ayvazyan et al., 2019) collected from the Pliocene age locality Çevirme (Erzurum Province, Tekman district) (BGR Çevirme 1-247) are studied based on already established methodology within the first part of this research. Distinguished two characters stages lateral outline and transverse cross section ($\alpha\beta$), recorded shape

classes and identification key are applied correspondingly to describe, categorise and identify these fossil isolated pharyngeal teeth. Each fossil tooth is characterised by lateral outline (α) and transverse cross section (β) (details see 2.1.2) (Fig. 16).

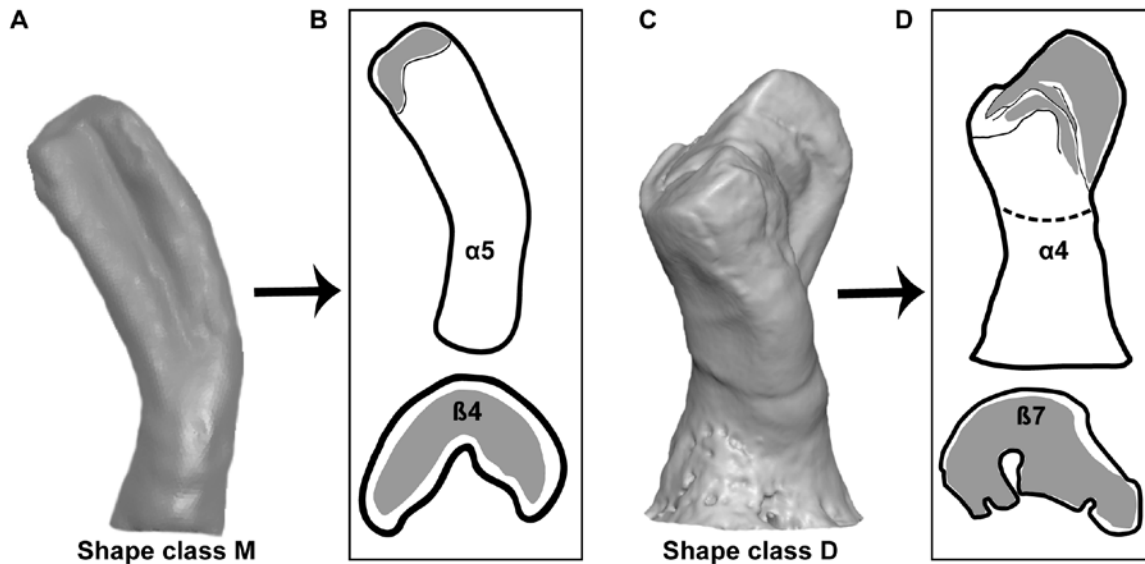


Figure 16. Methodology to describe the isolated pharyngeal teeth based on the character stages and shape classes. (A) shape class "M", b2 tooth of extant *C. capoeta*. (B) shape character $\alpha 5$ (lateral outline). (C) shape character $\beta 4$ (transverse cross-section). Shape class "M" is characterised by shape characters $\alpha 5$ and $\beta 4$. (D) shape class "D", a2 tooth of extant *C. sieboldi*. $\alpha 4$, shape character (lateral outline). $\beta 7$, shape character (transverse cross-section). Shape class "D" is characterised by shape characters $\alpha 4$ and $\beta 7$. The scales are not given to avoid scaling up of the figures. Avyazyan et al., 2019.

Within studied fossil material eight shape classes are recorded (Fig. 17). They represent **genus**, **species** and **clade** diagnostic shape classes, therefore, the studied fossil material is identified as pharyngeal teeth of the genus *Capoeta*. These three level of shape classes are illustrated on Figure 12. The most frequent shape class among fossil material is the genus diagnostic shape class "C" and relatively rare ones are the species diagnostic shape classes. Expectedly, the same pattern can be found through the study of the extant pharyngeal teeth (S3, S7 Figs.). In some cases due to the presence of three species diagnostic shape classes ("A", "J" and "R"), species level identification of isolated pharyngeal teeth was possible. Thus, three fossil *Capoeta* species are identified: *C. umbla*, *C. baliki* and *C. sieboldi*. The presence of the clade diagnostic shape class "M" indicates the presence of *C. capoeta*/*C. sevangi*, which compose the Ararlo-Caspian clade.

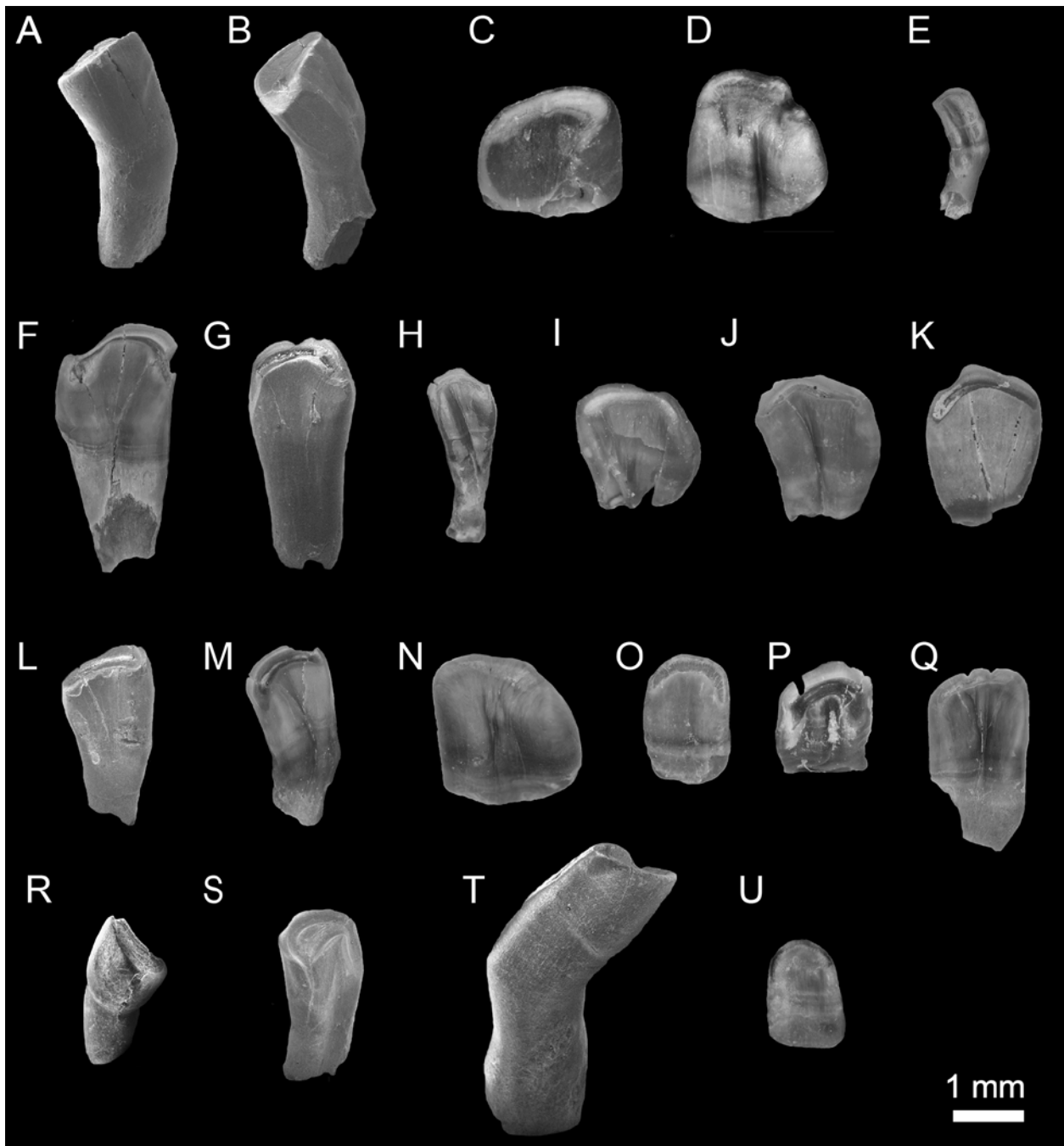


Figure 17. Isolated fossil pharyngeal teeth from the early Pliocene locality Çevirme (Erzurum Province, Tekman district). (A-E) species/clade diagnostic shape classes: (A) shape class "A" characteristic of *C. umbra* (BGR Çevirme 1). (B) shape class "R", characteristic of *C. sieboldi* (BGR Çevirme 3). (C-D) shape class "J", characteristic of *C. baliki* (BGR Çevirme 4, 5). (E), clade diagnostic shape class "M", characteristic of Aralo-Caspian clade of genus *Capoeta* (*C. sevanji* and *C. capoeta*) BGR Çevirme 23). (F-K) genus diagnostic shape class "C" (BGR Çevirme 24, 25, 26, 27, 28, 29). (L-S) common shape classes shared by different species. (L-N) shape class "B" (BGR Çevirme 155, 156, 157). (O-Q) shape class "F" (BGR Çevirme 195, 196, 197). (R-S) shape class "H" (BGR Çevirme 226, 227). (T) not identified, possibly tooth pathology (BGR Çevirme 237). (U) not identified (BGR Çevirme 238). Ayvazyan et al., 2019.

The clades recorded within the fossil material, based on the species/clade diagnostic shape classes are plotted on the phylogenetic tree based on the molecular genetic

analyses, which shows that the recorded shape classes belong to one monophyletic clade (Fig. 18).

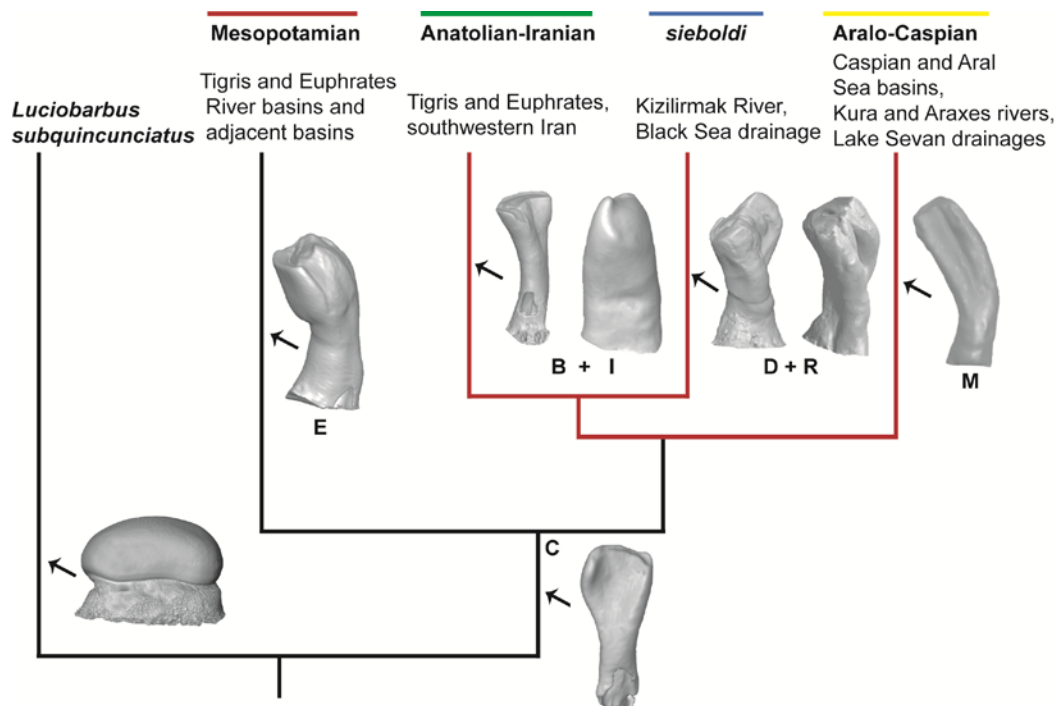


Figure 18. Phylogeny of the genus *Capoeta*: distinguished clades within the genus *Capoeta* (*Luciobarbus subquincunciatus* is the sister clade) (Levin et al., 2012). The clade diagnostic shape classes (capital letters) and respectively the 3D images of teeth of *Capoeta* as well as a2 tooth of *L. subquincunciatus* are mapped on the tree. The monophyletic Anatolia-Iranian/Aralo-Caspian/*sieboldi* clade, for which we propose a species flock model of evolution marked with red colour. Ayvazyan et al., 2019.

2.1.5.2. Fossil remains of *Capoeta* sp. from Jradzor (Armenia)

The fossil material from Jradzor is stored at the Institute of Geological Sciences, NASRA (IGS). Four fossil samples (excavations are continuing) are scanned and reconstructed at the University of Fribourg and YXLON International GmbH, Heilbronn. The main steps of the application of the X-ray computed tomography (μ CT) to the fossil material in the sediment is shown on the Figure 19. The material included in this work is represented by a complete fish skeleton and three skulls. The settings applied to scan the fossil material given in Table S4. The preliminary study of the 3D models of the isolated fossil pharyngeal teeth shows the presence of the shape class "C" (Fig. 19D), which is a species diagnostic for the genus *Capoeta* and indicates that the fossil specimens belong to the genus *Capoeta*. This material is not yet complete reconstructed, further studies are necessary for low-level taxonomic identification. Besides teeth, the skeletons of the fins and vertebra can give additional information

about these specimens and their taxonomy.

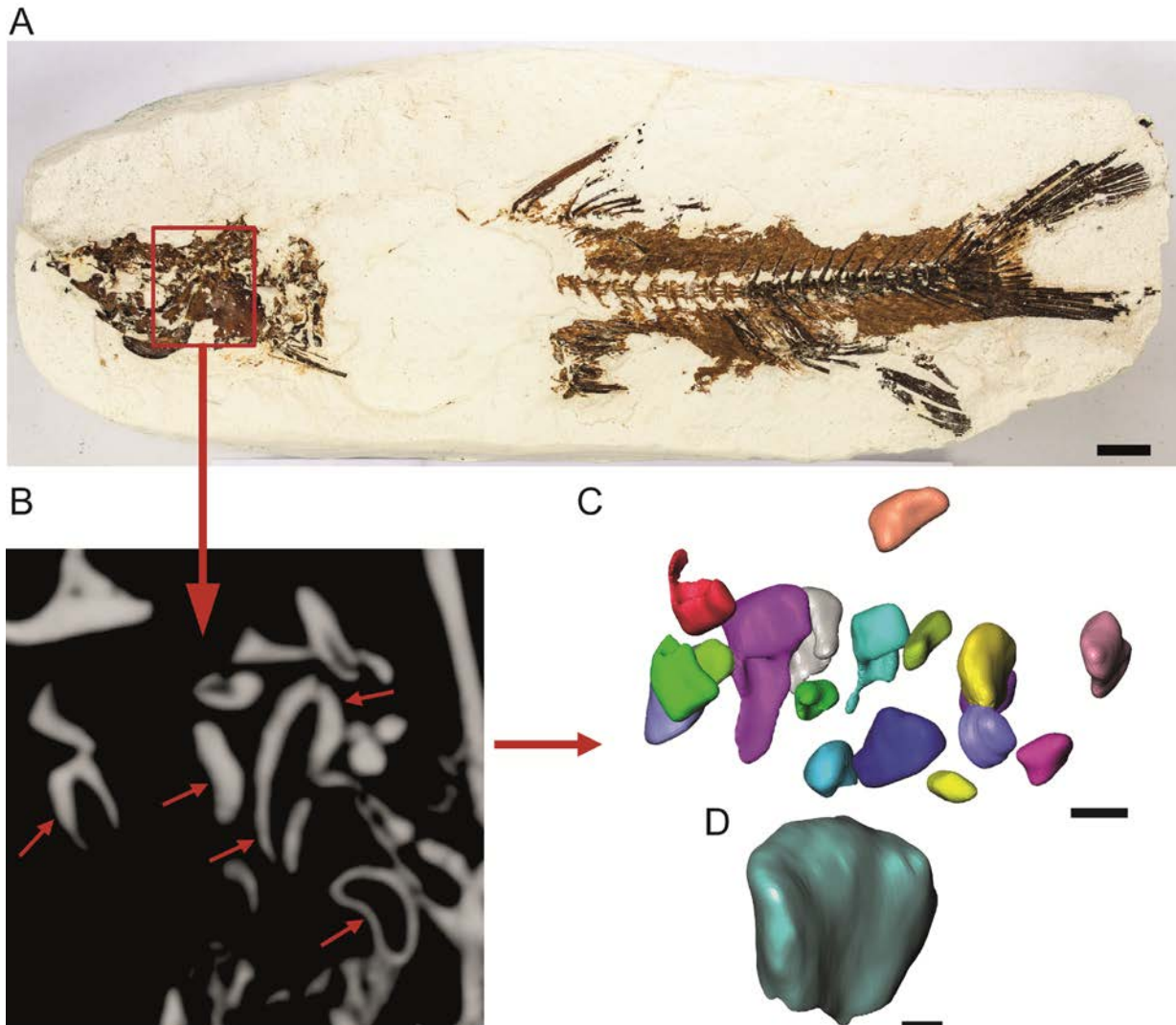


Figure 19. (A) *Capoeta* sp. (JRD-17/07); (B) a slice showing the teeth before reconstruction (teeth are marked by red arrows); (C) part of reconstructed isolated pharyngeal teeth; (D) recorded shape class "C".. The red quadrat shows the approximate locality of shown reconstruction in the sediment. Scale bar (A) = 1 cm, scale bar (C, D) = 1 mm.

2.1.5.3. Fossil remains of *Capoeta* from Ksatibi (Georgia)

The fossil material from the late Miocene locality Ksatibi is stored at the Georgian National Museum (GNM). This material was described by Bogachev, 1927 as a species *Capoeta nuntius*. There are more than 30 specimens in the collection of GNM. Four specimens (for now) are borrowed to restudy these samples by applying X-ray computed tomography and the methodology established by Ayzvazyan et al., 2018 (Table 1).



Figure 20. *Capoeta nuntius* (GNM 13-4) from the late Miocene locality Kisatbi, Georgia.

Four specimens are scanned and some of them are reconstructed (Fig.20). The preliminary results show the presence of a complete pharyngeal bone with the teeth (Fig. 21, GNM 10-1) as well as nearly 30 isolated teeth are reconstructed so far. The examination of the 3D models of the reconstructed fossil pharyngeal teeth the **shape class "C"** is recorded (Fig. 21C). Thus, the fossil material belongs to the genus *Capoeta*. Fortunately, one of the so far studied samples (GNM 8-2) contains a complete pharyngeal bone with the pharyngeal teeth on it (Fig. 21D). Interestingly, this **sample possess an a1 tooth** (Fig. 22), within studied extant *Capoeta* species only the species belong to Anatolia-Iranian or *damascina* clade have a1 tooth. The further research will allow to understand if the presence of a1 tooth is plesiomorphic character (reduction of a1) or homoplasy for the genus *Capoeta*. The settings applied to scan the fossil material given in Table S4.

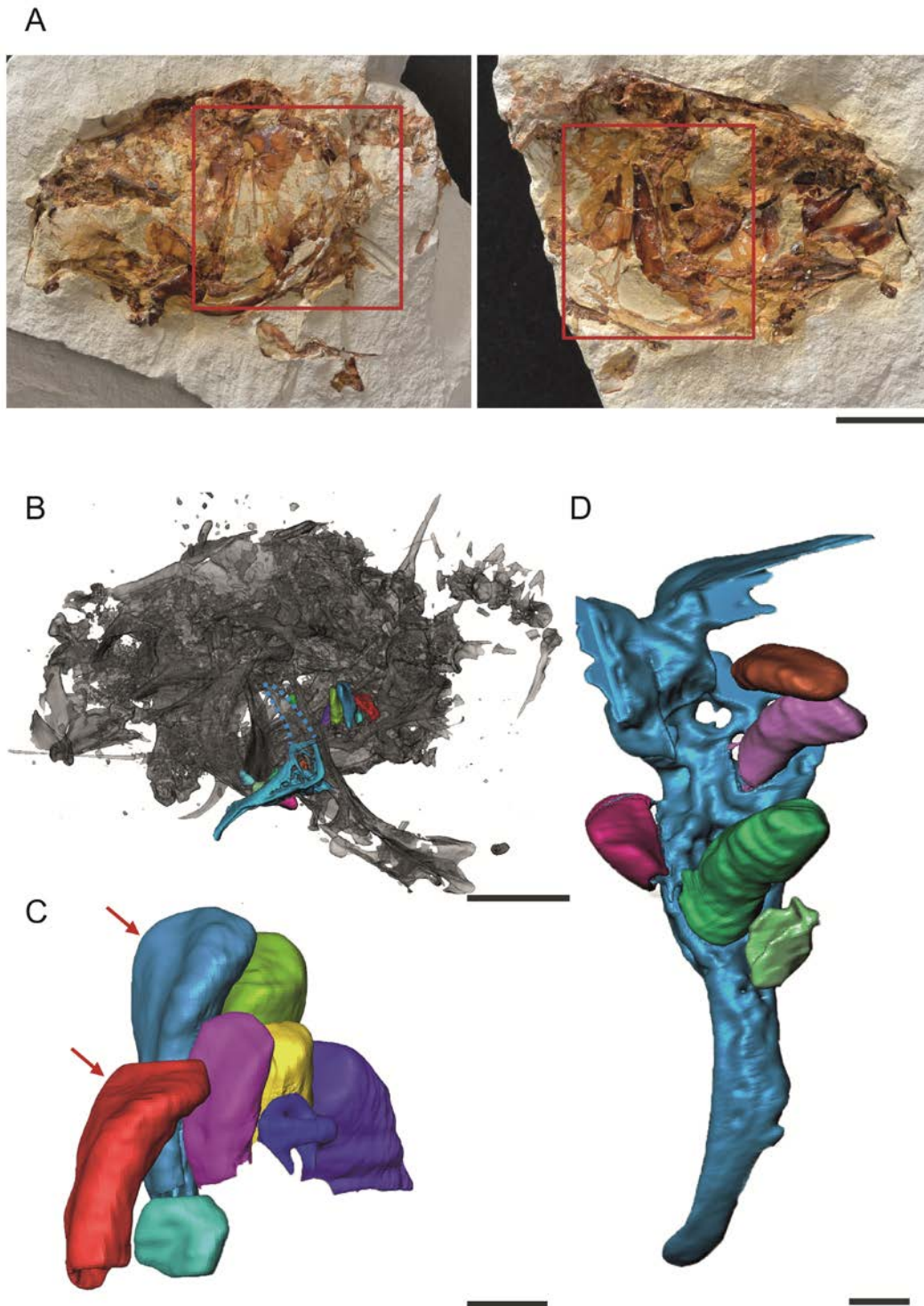


Figure 21. *Capoeta nuntius* (GNM 10-1): (A, B) reconstruction of the skull, (C) part of the reconstructed isolated pharyngeal teeth, (D) reconstructed pharyngeal bone with teeth. The red rectangles show the position of shown reconstruction in the sediment. The arrows show the teeth of shape class "C". Scale bar (A, B) = 1 cm, scale bars (C, D) = 1 mm.

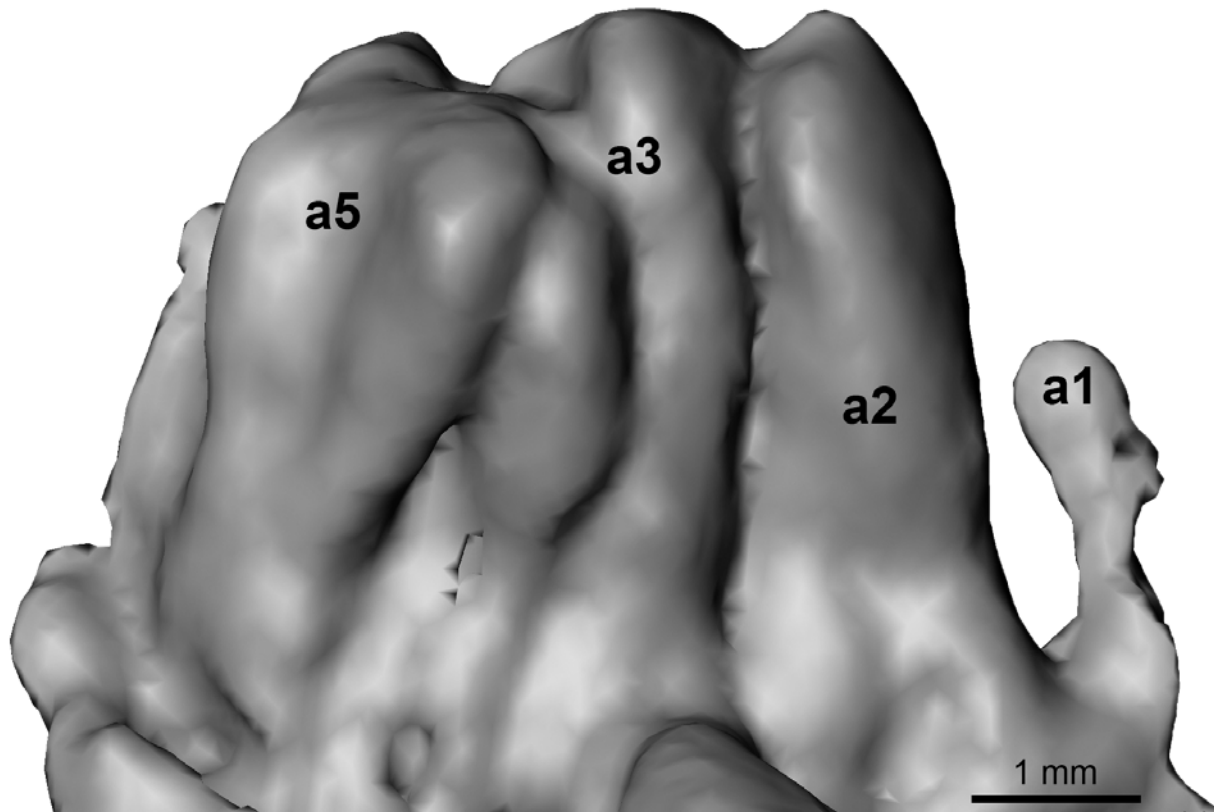


Figure 22. Surface view of the part of the pharyngeal bone with the teeth of *Capoeta nuntius* (GNM 8-1). a1, a2, a3 and a5 show respectively the teeth positions in the first tooth row.

2.1.5.4. Isolated pharyngeal teeth from Turkey

The fossil pharyngeal teeth (isolated or attached to the bone) (n=279) from latest Oligocene to middle Miocene localities Kargı 1, Kargı 2, Harami1, Hancılı, Keseköy (Turkey) are studied. The material is stored in the palaeontological collection of the University Utrecht (UU). The fossil material is compared to the extant material stored at the osteological collection of National Museum of Natural Sciences of Madrid (MNCN) and at the Bavarian State Collection for Anthropology and Palaeoanatomy, Munich (SNSB) (Depository numbers and other details see Table 2, Ayvazyan et al., 2019). The pharyngeal bones of the extant comparison material (*Barbus* and *Luciobarbus* species) are scanned using the microtomography systems NIKON XT H 160 at the Scanning electron microscopy at the analytic laboratory of MNCN (Fig. 23).

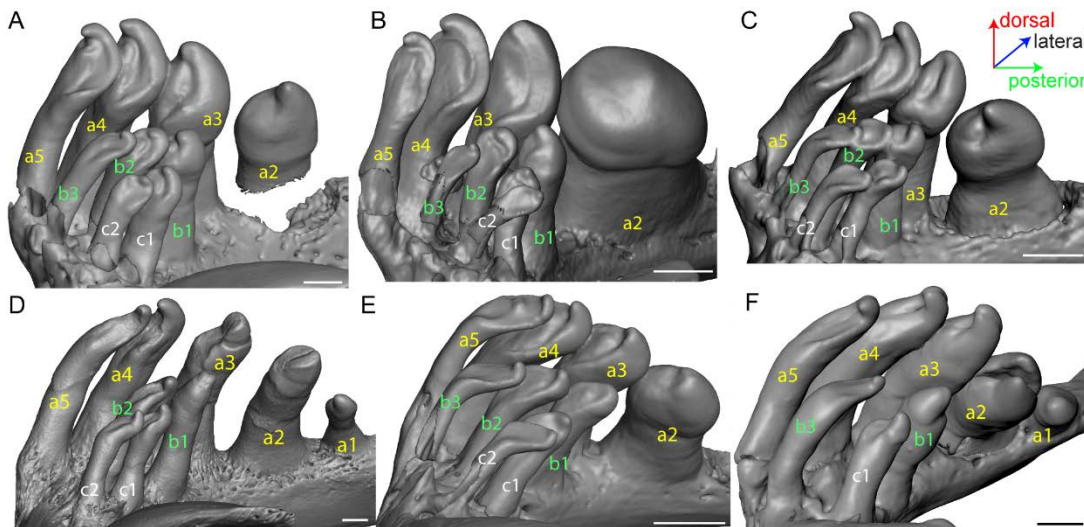


Figure 23. Images of the 3D models of the pharyngeal bones with teeth of the *Luciobarbus* and *Barbus* species. (A) *Luciobarbus comizo* (MNCN 69304), (B) *Luciobarbus longiceps* (MNCN E 54), (C) *Luciobarbus sclateri* (MNCN 69331), (D) *Barbus barbus* (SNSB SPAM-PI-00608), (E) *Barbus sacratus* (MNCN GUI 17), (F) *Barbus meridionalis* (MNCN 19933). The letters a, b, c correspond to the first (main), second and third row, the numbers (1-5) the tooth positions in those rows. The scale bars equal 1 mm. Vasilyan et al., unpublished.

The settings of the scanned pharyngeal bones are introduced in Table S6. The tomographic reconstruction was performed using Avizo 9.0 software at the Tübingen University.

Within the fossil material eight morphotypes of the pharyngeal teeth are distinguished (d1-d8). Morphological comparison with the 3D models of the extant *Barbus* and *Luciobarbus* species shows that seven from distinguished eight morphotypes (d1-d7) belongs to these two genera. This is additionally supported by the presence of the fossil remains of serrated rays of the dorsal fin (Fig. 24). The last d8 morphotype (Fig. 24 V, W) reminds the morphology of the pharyngeal teeth of the genus *Capoeta*, but this morphology is so far not recorded within the morphotypes of the extant *Capoeta* species distinguished by Ayvazyan et al., 2018.



Figure 24. Cyprinid remains from the studied localities. *Luciobarbus* sp., Morphotype d7 – from Hancılı, UU HAN 5315 (A); UU HAN 5316 (B); Morphotype d5 – UU HAN 5333 (C), UU HAR1 5300, loc. Hancılı (D); Morphotype d3 – UU HAN 5334, loc. Hancılı (E); UU HAN 5305, loc. Hancılı (F). *Barbus* sp., Morphotype d6 from the loc. Harami 1, UU HAR1 5301 (G), loc. Hancılı, UU HAN 5321 (H), UU HAN 5311 (I– J), UU HAN 5335 (K), Morphotype d4 - UU HAN 5308 (L), UU HAN 5309 (M). *Lucioarbus* vel *Barbus* sp., Morphotype d1 from loc. Hancılı, UU HAN 5300 (N – O), Morphotype d2, UU HAN 5303 (P), UU HAN 5306 (Q); Morphotype s1, UU HAN 5324 (R); Morphotype s2, UU HAN 5325 (S), UU HAN 5326 (T); Morphotype s3, UU HAN 5329 (U). aff. *Capoeta* sp. from the loc. Hancılı, UU HAN 5317 (V, W). Barbini indet. (Y – DD), UU KAR1 1304, loc. Kargı 1 (X), UU KAR1 1301, loc. Kargı 1 (Y), UU KAR2 1301, loc. Kargı 2 (AA), UU KAR2 1306, loc. Kargı 2 (DD), UU KAR2 1303, loc. Kargı 2 (EE), UU KE 5307, loc. Keseköy (BB), UU KE 5305, loc. Keseköy (CC). *Leuciscus* sp. from loc. Hancılı, UU HAN 5318 (FF). Vasilyan et al., in review.

The species level identification of the fossil material is not possible due to the absence of the detailed morphological report of the extant comparative material. The establishment of the identification key for these genera, which can be applied

for the identification of the isolated fossil pharyngeal teeth at low taxonomic level (species), is planned in my further research project.

2.2. Discussion

2.2.1. Pharyngeal tooth morphology as a key for species level identification

The detailed morphological study, based on the 3D approaches of the isolated pharyngeal teeth of ten extant *Capoeta* species, shows that the tooth morphology can serve as a key character for the species level identification. However, the species level identification is possible only based on the tooth morphology in the tooth position a2. Besides, the pharyngeal tooth morphology provides also an identification at the generic level based on the presence of the genus diagnostic shape class "C" (as the preliminary studies of the fossil material from Jradzor and Kısatibi show). More details see Ayvazyan et al., 2018.

2.2.2. Phylogenetic significance of pharyngeal tooth morphology

To test the possible phylogenetic signal embedded in the pharyngeal tooth morphology, the performed phenotypic dendrogram (based on the tooth morphology, respectively on the distribution of the recorded shape classes within studied species) is compared with three different phylogenetic trees based on the molecular genetic analyses of the genus *Capoeta*. This comparison shows a significant similarity of the results based on morphological and genetic data. The genetic data supports our results regarding to the recorded three main clades: Anatolian-Iranian or *Capoeta damascina* complex group, Aralo-Caspian or *Capoeta capoeta* complex group and Mesopotamian *Capoeta* or *Capoeta trutta* group (for details see Ayvazyan et al., 2018) (Fig. 25).

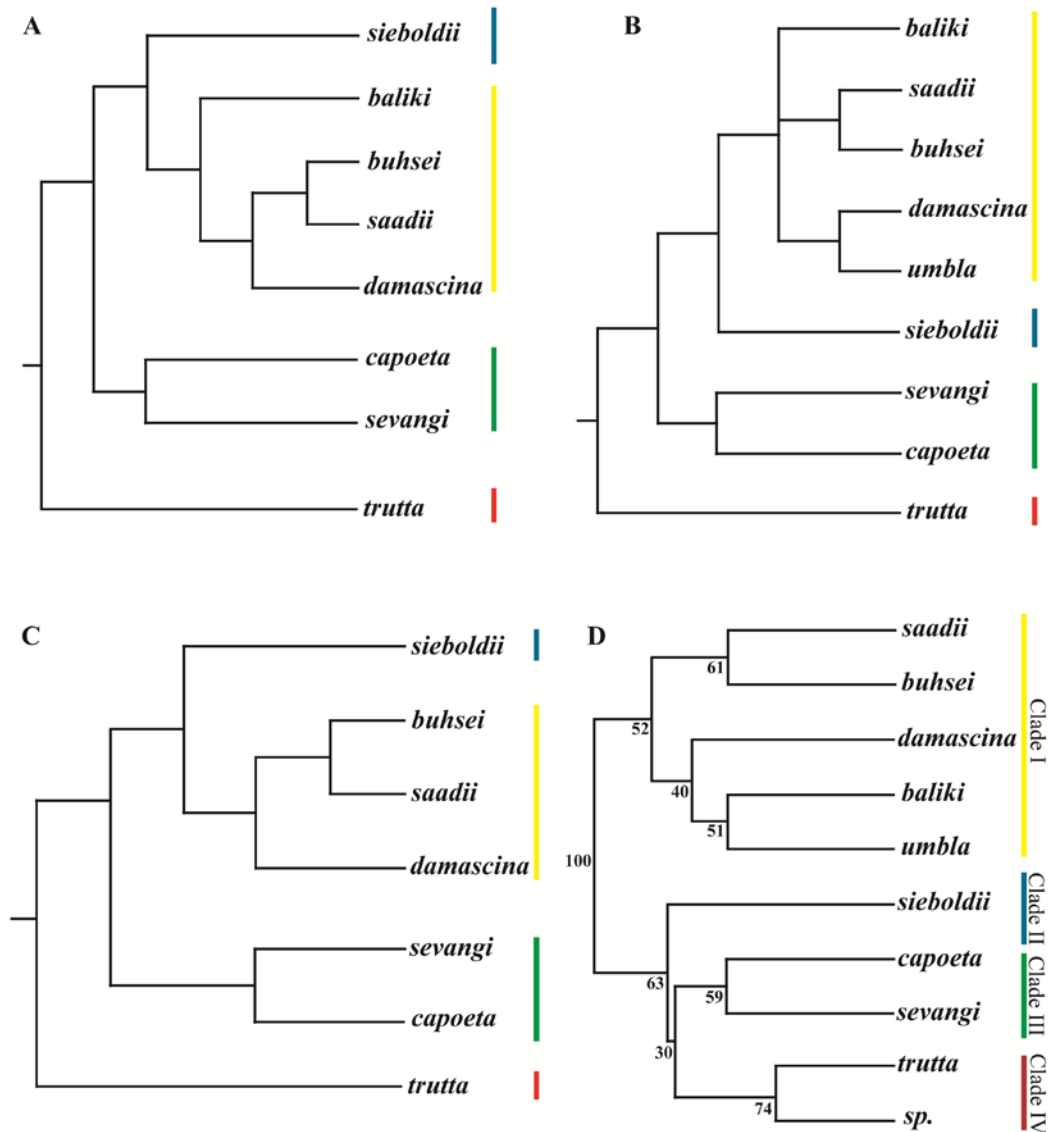


Figure 25. Simplified phylogenetic trees show the distribution of the studied *Capoeta* species within phylogenetic trees, based on genetic analyses of (A) Levin et al. 2012, (B) Bektas et al. 2017, (C) Zareian et al. 2016, (D) this study. Ayvazyan et al., 2018.

2.2.3. Taxonomy of the isolated fossil pharyngeal teeth from Çevirme

Within the isolated fossil pharyngeal teeth from Çevirme (Erzurum Province, Tekman District) eight shape classes are recorded where the shape class “C” is dominant in the assemblage (53%) (S6 Fig.) This indicates that the fossil material belongs to the genus *Capoeta*. Besides this, the presence of three species (A, J, R) and a clade diagnostic (M) shape classes suggests the presence of four palaeo-species (*C. cf. umbla*, *C. cf. baliki*, *C. cf. sieboldi* and *C. cf. capoeta/C. cf. sevangi*). In our days, the extant relatives of these species are distributed in three different water basins (Black

and Caspian Seas and Persian Gulf basins) (Fig. 5). According to the genetic and morphological (our data) data, they belong to different clades (Fig. 25). Whereas, the recorded palaeo-species (*C. cf. umbla*, *C. cf. baliki*, *C. cf. sieboldi* and *C. cf. capoeta/C. cf. sevangi*) belong to one monophyletic clade as it is shown on the Figure 18. Thus, the main questions are: 1) does the fossil assemblage represent one species characterised by high heterodonty, which was the ancestor of the genus *Capoeta* or it represents closely related four species; 2) is this high morphological diversity conditioned by plasticity or allometry; and 3) how does the present-day distribution of these species within the different water basins formed.

The recent *Capoeta* species are characterized by different degree of heterodonty, which varies between three and six shape classes per species. As it has been already mentioned, within fossil assemblage, eight shape classes are documented and it is unprecedented among extant species. It is also highly unlikely that a fossil species shows this degree of heterodonty, given the ten tooth positions at pharyngeal bones. Therefore, we consider the 'single species' interpretation as unlikely.

Based on the recoded four species/clade diagnostic shape classes the Çevirme assemblage is constituted by four species, which belong to three different clades (Anatolian-Iranian, Aralo-Caspian, and *sieboldi* clades) of the genus *Capoeta*. According to all molecular studies (5, 21, 63), these three clades are monophyletic and sister to the Mesopotamian clade (see Fig.) (more details see Ayvazyan et al., 2019).

2.2.4. Possible influence of plasticity and allometry on high diversity of recorded shape classes

The literature provides examples of the potential effects of plasticity on the dentary bone and tooth morphology mainly in cichlid fish cultures by applying contrasting diets (soft and hard) (64–66). These studies recorded some degree of phenotypic plasticity of dentary bone morphology and in some cases tooth size. The influence of these two diets on the development of the cyprinid pharyngeal dentition is also tested in the benthophagous cyprinid black carp. Dietary did not change the tooth morphology, but, instead, it has been found that broad diet may influence the frequency of tooth

replacement and size patterns (67). These studies are mainly based on aquarium experiments in benthophagous species where two extreme diets (commercial fish as a soft and snails as hard food) are tested. Under natural conditions, fishes are not forced to feed on only one type of food. Thus, it is data can be applied to, in the present paper studied algae-scraping species *Capoeta*, which are recorded from single geological layer and are sympatric individuals in a uniform environment. Considering this, the effect of feeding on different food should not be considered biasing on the carp pharyngeal tooth morphology, and, thus, we exclude the effect of plasticity on the studied fossil material.

Allometric shifts in pharyngeal tooth morphology cannot explain the high diversity of recorded shape classes in the studied fossil samples. Morphological shape remodeling in cyprinids happens in very early stages of their ontogeny. Juveniles (standard size of a few mm) have different tooth morphology than the adult samples, but the significant morphological changes are finalized in this early stage. Thus, the adult dentition in cyprinid fishes is completed by at the later larvae or juvenile stages (68). Our fossil material is represented by adult individuals, as the studied fossil pharyngeal teeth sizes vary between 0.8 – 3 mm (it is a sampling artifact introduced by mesh size limitation washing collection technique). Therefore, our fossil samples is composed of isolated pharyngeal teeth of adult individuals.

2.2.5. Species flock scenario of evolution of the genus *Capoeta*: palaeogeographical interpretation of the fossil site Çevirme (palaeolake Tekman)

We interpret this high local diversity of closely related species from the fossil site

Çevirme, **as a species-flock** model. Five main criteria are recorded to distinguish the group of animals as a species flock: 1) monophyly, 2) high species diversity (speciosity), 3) high level of endemism, 4) morphological and ecological diversity and 5) habitat dominance in terms of biomass (30, 69). A later study (70) suggests to concentrate on the three robust, easier to determine criteria such as monophyly, endemism and speciosity. The studied fossil *Capoeta* samples correspond to all five criteria sensu Eastman and McCune (2000) and can be regarded as a species flock (69) (details see Ayvazyan et. al., 2018). Thus, the species flock of the genus *Capoeta*, represented by four near related species, inhabited Tekman Basin 4 Ma years ago. This study hypothesizes, that the Tekman palaeo-lake (part of Armenian Highland) was the "center" of the speciation of *Capoeta* species related to the three recent clades of the genus (Anatolian-Iranian, Aralo-Caspian and *sieboldi*). It is already known, that the lake system of Armenian Highland was formed during the late Miocene and represents the source of all major rivers in Western Asia to which *Capoeta* is endemic (58). Thus, it could represent the center of origin of *Capoeta*.

According to the recent geologic work the tectonic reorganization in the region, starting about the Miocene-Pliocene transition (ca. 5.5 Myr) along the East and North Anatolian faults (71, 72), resulted in substantial surface uplift and probably caused the gradual reshaping of the hydrological network in the area. This could contribute to dispersal and speciation of the members of the species flock into their nowadays distribution areas. The other possible explanation of my results could be the concept of secondary contact. This scenario (speciation of hybrids) is very similar to the above suggested species flock model, however, without any genetic information, we cannot be confident about this hypothesis. More studies and more fossil sites inside and outside of the distribution area of *Capoeta* are needed to test these hypotheses. However, according to the current available data, the fossil species flock interpretation is the most plausible.

2.2.6. Taxonomy of the isolated fossil pharyngeal teeth from Jradzor, Kısatibi, Kargı 1, Kargı 2, Harami1, Hancılı and Keseköy

The studies on the fossil material from Jradzor and Kısatibi are still ongoing. The preliminary results show, however, that the both fossil material possibly belong to the

genus *Capoeta*, as the genus diagnostic shape class "C" is present. Species level identification is not completed, as the reconstruction of the scanned material is not yet finalized. The fossil remains of these both sites will be studied in more details in my further research project, including also the fossil remains of fin rays skeletons and vertebra. The fossil material from early Miocene (to middle Miocene) localities Kargı 1, Kargı 2, Harami1, Hancılı and Keseköy (Turkey) belongs to the family Cyprinidae. Above-mentioned localities provide fossil remains of barbin fishes, the remains of leuciscin are found only from Hancılı locality (Table S7). The studied oldest localities (Kargı 1, Kargı 2, Keseköy, latest Oligocene to early Miocene) can be assigned to a small-sized barbin.

The recorded tooth morphology from these localities cannot be referred to any fossil form known from Eurasia. Probably, they represent an ancient extinct barbin group. The fossil material from Harami 1 and Hancılı, based on the isolated fossil pharyngeal teeth, is identified as two widely distributed barbin genera *Luciobarbus* and *Barbus*. Besides the isolated pharyngeal teeth, the fossil remains of the three different morphotypes of serrated rays of the dorsal fin from Hancılı could indicate the presence of three barbin taxa in this locality. However, this cannot be stated with confidence due to the lack of comparative osteological studies of this element in the extant barbin species.

The record of the Harami 1 locality can be considered as the oldest known remains of *Barbus* and *Luciobarbus* genera (details see Vasilyan et al., in review). So far the oldest record of the genus *Luciobarbus* was known from the earliest late Miocene of Austria (loc. Mataschen, 73). Böhme & Ilg (74) mentioned oldest *Luciobarbus* from contemporaneous to Mataschen sites in Turkey, however, this material stays unfigured. We suggest that *Barbus* sp. Harami 1 and Hancılı should be considered as the oldest representatives of this genus, since earlier publications describing *Barbus* sp. do not represent the genus *Barbus* sensu Yang et al. (2015) (3). The results of this study would provide important information also for the calibration of the molecular trees, which estimates the divergence time and origination of different barbin clade.

3. Conclusion

For the first time, the methodology is applied to identify isolated pharyngeal teeth at species level (on the example of the cyprinid genus *Capoeta* and is applicable to the fossil record.

The results of my study show that the detailed 3D morphology is very promising tool applicable to the low level taxonomic identification of the isolated pharyngeal teeth. This pattern is very important not only for the taxonomy, but also for the fossil record of cyprinids, as the fossil remains of these fishes are mainly represented by isolated fossil pharyngeal teeth. Despite this, until now, the species level identification of isolated teeth is not recorded due to the lack of the comprehensive studies and comparative material of the pharyngeal dentition of the recent cyprinids. Within the palaeontological studies, the isolated teeth are generally identified only at the generic level. This study aimed to fill this gap by applying modern methodology to get maximum information about the morphological structures of the pharyngeal teeth, which can be the base for species level identification.

The species level identification of the fish fauna will allow to trace back the evolution of cyprinids, to investigate the history of the drainage basins evolution and provide details for the palaeobiogeographical analyses of the studied regions.

Besides its significance for taxonomy and the fossil record, the results of this study show that the 3D detailed morphology of the pharyngeal dentitions provides also phylogenetic signal, which is in accordance with the molecular genetic data. This additionally supports the study of the cyprinids evolution.

However, the applied methodology is quite time consuming, but as I already show, on an example of the genus *Capoeta*, it is feasible and very informative. This methodology can serve as a basis to establish the identifications keys (based on the detailed morphology of the pharyngeal teeth) of the isolated pharyngeal teeth of the other groups of cyprinids.

Summing up the results of this study, I conclude that:

- the detailed morphology using the 3D microtomography of pharyngeal teeth is a useful tool for the species and generic level identification of the isolated pharyngeal teeth, as well as in certain cases the tooth position in tooth rows etc.;

- the morphology of the pharyngeal teeth provides an obvious phylogenetic signal and highly supported by results derived from molecular genetic analyses;
- both these patterns are important for the taxonomy and can be also applied to the fossil record;
- the established methodology is applicable to the fossil record of the genus *Capoeta* and provides species level identification of the isolated fossil pharyngeal teeth;
- within fossil material from the Pliocene age locality Çevirme, eight shape classes are distinguished, four of them are species or clade diagnostic and indicate the presence of the four sympatric *Capoeta* species (*C. cf. sieboldi*, *C. cf. umbla*, *C. cf. baliki* and *C. cf. capoeta/sevangi*);
- this high local diversity of closely related four species is interpreted in terms of the species-flock model of *Capoeta* in the Tekman palaeo-lake at 4 Ma;
- I hypothesized that the genus *Capoeta* occurred in the huge late Miocene to Pliocene palaeo-lake system in the present-day Armenian Highland, more specifically in the Tekman palaeo-lake, which was a part of that huge palaeo-lake system;
- present-day distribution of the genus *Capoeta* in different water basins has been caused by Pliocene tectonic activities which disrupted this lake system and resulted in the very characteristic biogeographic distribution of *Capoeta* in Western Asian and Ponto-Caspian drainage systems;
- further studies of the fossil remains of the genus *Capoeta* from Jradzor (Armenia) and Kisatibi (Georgia) can give a complete view of the evolution of this genus as well as trace back the history of the drainage systems of this region;
- so far the preliminary results show that the recorded fossil remains belong to the genus *Capoeta*, as the genus diagnostic shape class "C" is recorded within both samples (ongoing project);
- the isolated fossil pharyngeal teeth from latest Oligocene to early Miocene localities Kargı 1, Kargı 2, Harami1, Hancılı and Keseköy are identified at generic level and belong to barbin genera *Luciobarbus* and *Barbus*;
- the species level identification of isolated fossil pharyngeal teeth from above mentioned localities is not possible, due to the lack of the comparative osteological studies of this element in the extant barbin species. The established

- methodology for the genus *Capoeta* can serve as a base for the similar study on the other barbin generas as *Barbus* and *Luciobarbus*.

4. Outlook

3D detailed morphology is useful tool to study the pharyngeal teeth morphology. This methodology is time consuming regarding to the material collection, microcomputed tomography, reconstruction of 3D models and further analyses. However, it worths, and there is a necessarily to apply this methodology and establish identification key of other groups of cyprinid fishes.

Besides the isolated teeth, it will be also very interesting to apply this methodology to study the morphology of the pharyngeal bones. I am inclined to think, that the morphology of the pharyngeal bones also embed important information. These patterns are included in my further research projects and would be studied.

5. References

1. Coad BW. Zoogeography of the freshwater fishes of Iran: In F. Krupp, W. Schneider, & R. Kinzelbach (Eds.), Proceedings of the Symposium on the Fauna and Zoogeography of the Middle East, Mainz, 1985. Beihefte zum Tübinger; 1987.
2. Nelson JS, Grande T, Wilson MVH. Fishes of the world. Fifth edition. Hoboken New Jersey: John Wiley & Sons; 2016.
3. Yang L, Sado T, Vincent Hirt M, Pasco-Viel E, Arunachalam M, Li J et al. Phylogeny and polyploidy: resolving the classification of cyprinine fishes (Teleostei: Cypriniformes). Mol Phylogenet Evol 2015; 85:97–116.
4. Alwan N, Esmaeili H-R, Krupp F. Molecular Phylogeny and Zoogeography of the *Capoeta damascina* Species Complex (Pisces: Teleostei: Cyprinidae). PLoS ONE 2016; 11(6):e0156434.
5. Zareian H, Esmaeili HR, Heidari A, Khoshkholgh MR, Mousavi-Sabet H. Contribution to the molecular systematics of the genus *Capoeta* from the south Caspian Sea basin using mitochondrial cytochrome b sequences (Teleostei: Cyprinidae). Mol Biol Res Commun 2016; 5(2):65–75.
6. Zareian H, Esmaeili HR, Gholamhosseini A, Japoshvili B, Özuluğ M, Mayden RL. Diversity, mitochondrial phylogeny, and ichthyogeography of the *Capoeta capoeta* complex (Teleostei: Cyprinidae). Hydrobiologia 2018; 806(1):363–409.
7. Karaman MS. Süßwasserfische der Türkei: Teil. Revision der kleinasiatischen und vorderasiatischen Arten des Genus *Capoeta* (*Varicorhinus*, partim). Mitteilungen aus dem Hamburgischen Zoologischen Museum und Institut, 66, 17-54.; 1969.
8. Krupp F. & Schneider W. The fishes of the Jordan River drainage basin and Azraq Oasis.: Fauna of Saudi Arabia, 10, 347-416.; 2008.
9. Turan C. Molecular systematics of *Capoeta* (Cyprinidae) species complex inferred from mitochondrial 16S rDNA sequence data. 2008; Acta Zoologica Cracoviensia, 51A(1-2), 1-14.
10. Howes G. J. Cyprinid Fishes.: Systematics and biogeography: an overview. Edited by Ian J. Winfield and Joseph S. Nelson; 1991.
11. Bănărescu P. The freshwater fishes of Europe; 1999.
12. Ahnelt H., Herdina A. N., Metscher B. D. Unusual pharyngeal dentition in the African Chedrin fishes (Teleostei: Cyprinidae): Significance for phylogeny and character evolution 2015.
13. Böhme M. Freshwater fishes from the Pannonian of the Vienna Basin with special reference to the locality Sandberg near Götzendorf, Lower Austria. 2002.
14. Pasco-Viel E, Charles C, Chevret P, Semon M, Tafforeau P, Viriot L et al. Evolutionary Trends of the Pharyngeal Dentition in Cypriniformes (Actinopterygii: Ostariophysi). PLoS ONE 2010; 5(6).
15. Zardoya R, Doadrio I. Molecular Evidence on the Evolutionary and Biogeographical Patterns of European Cyprinids. J Mol Evol 1999; 49(2):227–37.
16. Zeng Y, Liu H. The evolution of pharyngeal bones and teeth in Gobioninae fishes (Teleostei: Cyprinidae) analyzed with phylogenetic comparative methods. Hydrobiologia 2011; 664(1):183–97.
17. Heckel JJ. Fische Syriens: einer neuen Classification und Charakteristik sämtlicher Gattungen der Cyprinen; 1843.
18. Wautier K., Van der heyden C., Huysseune A. A quantitative analysis of pharyngeal tooth shape in the zebrafish (*Danio rerio*, Teleostei, Cyprinidae) 2000.
19. Böhme M IA. fosFARbase 2003; (Retrieved from: <http://www.wahre-staerke.com/>).
20. Bănărescu P. The freshwater fishes of Europe. Wiebelsheim: Aula-Verlag; 1999. (The freshwater fishes of Europe5, no. 1).

21. Levin BA, Freyhof J, Lajbner Z, Perea S, Abdoli A, Gaffaroğlu M et al. Phylogenetic relationships of the algae scraping cyprinid genus *Capoeta* (Teleostei: Cyprinidae). *Mol Phylogenet Evol* 2012; 62(1):542–9.
22. Ghanavi HR, Gonzalez EG, Doadrio I. Phylogenetic relationships of freshwater fishes of the genus *Capoeta* (Actinopterygii, Cyprinidae) in Iran. *Ecology and Evolution* 2016; 6(22):8205–22.
23. Nelson JS. *Fishes of the World*. 4th ed. Hoboken, New Jersey: John Wiley & Sons. Inc; 2006.
24. Howes GJ. *Cyprinid Fishes: Systematics, biology and exploitation*. 1st ed. New Dehli: Chapman and Hall; 1991.
25. Vasilyan D, Sahakyan L, Hovakimyan H, Lazarev L, Maul L, Rugenstein C J. New data on the upper Miocene continental record of Armenia. 2018.
26. Zohar I, Goren M, Goren-Inbar N. Fish and ancient lakes in the Dead Sea Rift: The use of fish remains to reconstruct the ichthyofauna of paleo-Lake Hula. *Palaeogeography, Palaeoclimatology, Palaeoecology* 2014; 405:28–41.
27. Shkil FN, Lazebnyi OE, Kapitanova DV, Abdissa B, Borisov VB, Smirnov SV. Ontogenetic mechanisms of explosive morphological divergence in the Lake Tana (Ethiopia) species flock of large African barbs (*Labeobarbus*; Cyprinidae; Teleostei). *Russ J Dev Biol* 2015; 46(5):294–306.
28. Sullivan JP, Lavoué S, Hopkins CD. Discovery and phylogenetic analysis of a riverine species flock of African electric fishes (Mormyridae: Teleostei). *Evol* 2002; 56(3):597.
29. Kosswig C. Ways of Speciation in Fishes. *Copeia* 1963; 1963(2):238.
30. Ribbink AJ. Is the species flock concept tenable? In *Evolution of Fish Species Flocks* (Echelle, A. A. & Kornfield, I., eds); 1984.
31. Schluter D. Ecological Character Displacement in Adaptive Radiation. *The American Naturalist* 2000; 156(S4):S4-S16.
32. Streelman J, Danley PD. The stages of vertebrate evolutionary radiation. *Trends in Ecology & Evolution* 2003; 18(3):126–31.
33. Verheyen E, Salzburger W, Snoeks J, Meyer A. Origin of the superflock of cichlid fishes from Lake Victoria, East Africa. *Science* 2003; 300(5617):325–9.
34. Altner M, Reichenbacher B. †Kenyaichthyidae fam. nov. and †*Kenyaichthys* gen. nov. - First Record of a Fossil Aplocheiloid Killifish (Teleostei, Cyprinodontiformes). *PLoS ONE* 2015; 10(4):e0123056.
35. Myers GS. The endemic fish fauna of Lake Lanao, and the evolution of higher taxonomic categories. *Evol* 1960; 14(3):323–33.
36. Echelle AAE, Kornfield IE. *Evolution of fish species flocks*; 1984.
37. Türkmen M, Erdoğan O, Yıldırım A, Akyurt İ. Reproduction tactics, age and growth of *Capoeta capoeta umbra* Heckel 1843 from the Aşkale Region of the Karasu River, Turkey. *Fisheries Research* 2002; 54(3):317–28.
38. Boerckel JD, Mason DE, McDermott AM, Alsberg E. Microcomputed tomography: approaches and applications in bioengineering. *Stem Cell Research & Therapy* 2014; 5(6):144. Available from: URL: <https://stemcellres.biomedcentral.com/track/pdf/10.1186/scrt534>.
39. Illies J. and Rzoska J. *Euphrates and Tigris, Mesopotamian Ecology and Destiny*. *Monographiae biologicae* 1980; 38.
40. Coad BW. *Fishes of the Tigris-Euphrates Basin: A Critical Checklist*; 1991.
41. Ewing A. *Water Quality and Public Health Monitoring of Surface Waters in the Kura-Araks River Basin of Armenia, Azerbaijan, and Georgia*. *Water Resources Professional Project Reports* 2010.
42. Coene F. *The Caucasus - An Introduction*; 2010.
43. Campana EM, Vener BB, Lee SB. Hydrostrategy, Hydropolitics, and Security in the Kura-Araks Basin of the South Caucasus. *Journal of Contemporary Water Research & Education* 2012; (149):22–32.
44. Altınlı E. *Geology of Eastern and Southeastern Anatolia* 1966; 66.
45. Yılmaz A, Terlemez I, Uysal Ş. Some stratigraphic and tectonic characteristics of the area around Hinis (Southeast of Erzurum) 1988; *Mineral Res. Expl. Bull.*,(108):1–21.

46. Nazik A, Türkmen I, Koc TC, Aksoy E, Avsar N, Yayik H. Fresh and Brackish Water Ostracods of Upper Miocene Deposits, Arguvan/Malatya (Eastern Anatolia); 2008.
47. Koç TC NA. Faunal content of lower Pliocene Çaybağı Formation and its relationship with depositional environments, Eastern Elazığ/Turkey 2012; (33 (2)).
48. Şafak Ü KM. Ostracod fauna and environmental characteristics of Köprükoy/Erzurum (East Anatolia) region. Bulletin of The Mineral Research and Exploration 2016; 153(25181):24–40.
49. Koçyigit A, Canoglu MC. Neotectonics and seismicity of Erzurum pull-apart basin, East Turkey. Russian Geology and Geophysics 2017; 58(1):99–122.
50. Keskin M, Pearce JA, Mitchell JG. Volcano-stratigraphy and geochemistry of collision-related volcanism on the Erzurum–Kars Plateau, northeastern Turkey. Journal of Volcanology and Geothermal Research 1998; 85(1-4):355–404.
51. Alpaslan Suata F., editor. Arkeometri sonuçları toplantısı. Ankara; 2011.
52. Ünay E, de Bruijn H, Suata-Alpaslan F. Rodents from the Upper Miocene Hominoid Locality Corakverler (Anatolia) 2006.
53. Nalivkin D. V. & Sokolov V. S. Stratigraphy of the USSR.: Neogene system: "Nedra"; 1986. Available from: URL: <https://books.google.de/books?id=e0sfOQAACAAJ>.
54. van Baak CGC, Krijgsman W, Stoica M. Mediterranean-Paratethys connectivity during the late Miocene to Recent: Unraveling geodynamic and paleoclimatic causes of sea-level change in semi-isolated basins. [Utrecht]: Utrecht University, Faculty of Geosciences, Department of Earth Sciences; 2016. (Utrecht studies in earth sciences; vol 87).
55. Melik-Adamyán HH. Stratigraphy and Palaeogeography of Pliocene and Late Pleistocene Lower Vertebrate Fauna of Central and North–Western Armenia. 2003.
56. Reichenbacher B, Alimohammadian H, Sabouri J, Haghfarshi E, Faridi M, Abbasi S et al. Late Miocene stratigraphy, palaeoecology and palaeogeography of the Tabriz Basin (NW Iran, Eastern Paratethys). 2011; (311).
57. Irrlitz W. Lithostratigraphie und tektonische Entwicklung des Neogens in Nordostanatolien. Beihefte zum Geologischen Jahrbuch 1972; Heft 120:61–85.
58. Sickenberg O. Geologisches Jahrbuch 1975; (Heft 15):95.
59. Gabelaya C. Fishes from Pliocene deposits of Georgia. Tbilisi; 1976.
60. Čerňanský A, Vasilyan D, Georgalis GL, Joniak P, Mayda S, Klembara J. First record of fossil anguines (Squamata; Anguinae) from the Oligocene and Miocene of Turkey. Swiss J Geosci 2017; 110(3):741–51.
61. Claessens L. Miocene reptilian and amphibian faunas of Anatolia; 1995.
62. Krijgsman W, Duermeijer CE, Langereis CG, Bruijn H de, Saraç G, Andriessen PAM. Magnetic polarity stratigraphy of late Oligocene to middle Miocene mammal-bearing continental deposits in Central Anatolia (Turkey). nos 1996; 34(1):13–29.
63. Bektas Y, Turan D, Aksu I, Ciftci Y, Eroglu O, Kalayci G et al. Molecular phylogeny of the genus *Capoeta* (Teleostei: Cyprinidae) in Anatolia, Turkey. Biochemical Systematics and Ecology 2017; 70:80–94.
64. Huysseune A. Phenotypic plasticity in the lower pharyngeal jaw dentition of *Astatoreochromis alluaudi* (teleostei: cichlidae). Archives of Oral Biology 1995; 40(11):1005–14.
65. Greenwood PH. Environmental effects on the pharyngeal mill of a cichlid fish, *Astatoreochromis alluaudi*, and their taxonomic implications. Proceedings of the Linnean Society of London 1965; 176(1):1–10.
66. Gunter HM, Fan S, Xiong F, Franchini P, Fruciano C, Meyer A. Shaping development through mechanical strain: the transcriptional basis of diet-induced phenotypic plasticity in a cichlid fish. Mol Ecol 2013; 22(17):4516–31.
67. Hung NM, Ryan TM, Stauffer JR, Madsen H. Does hardness of food affect the development of pharyngeal teeth of the black carp, *Mylopharyngodon piceus* (Pisces: Cyprinidae)? Biological Control 2015; 80:156–9.
68. Nakajima T. Larval vs. adult pharyngeal dentition in some Japanese cyprinid fishes. J Dent Res 1984; 63(9):1140–6.
69. Eastman JT, McCune AR. Fishes on the Antarctic continental shelf: evolution of amarine species flock?*. Journal of Fish Biology 2000; 57(sa):84–102.

70. Lecointre G, Améziane N, Boisselier M-C, Bonillo C, Busson F, Causse R et al. Is the species flock concept operational? The Antarctic shelf case. *PLoS ONE* 2013; 8(8):e68787.
71. Lechmann A, Burg J-P, Ulmer P, Guillong M, Faridi M. Metasomatized mantle as the source of Mid-Miocene-Quaternary volcanism in NW-Iranian Azerbaijan: Geochronological and geochemical evidence. *Lithos* 2018; 304-307:311–28.
72. Allen M, Jackson J, Walker R. Late Cenozoic reorganization of the Arabia-Eurasia collision and the comparison of short-term and long-term deformation rates. *Tectonics* 2004; 23(2):n/a-n/a.
73. Schultz O. Die Fischreste aus dem Unter-Pannonium (Ober-Miozän) von Mataschen, Steiermark (Österreich). *Joannea - Geologie und Paläontologie* 2004; 5:231–56.
74. Böhme M, Ilg A. fosFARbase. Available at www.wahre-staerke.com; 2003 [cited 2015 Dec 1].

6. Appendix I: Published and Accepted Manuscripts

3D morphology of pharyngeal dentition of the genus *Capoeta* (Cyprinidae): Implications for taxonomy and phylogeny

Accepted: 26 January 2018

DOI: 10.1111/jzs.12217

ORIGINAL ARTICLE

WILEY

JOURNAL OF
BIOLOGICAL SYSTEMATICS
= EVOLUTIONARY RESEARCH

3D morphology of pharyngeal dentition of the genus *Capoeta* (Cyprinidae): Implications for taxonomy and phylogeny

Anna Ayvazyan¹  | Davit Vasilyan^{2,3} | Madelaine Böhme^{1,4}

¹Department of Geosciences, Eberhard-Karls-University Tübingen, Tübingen, Germany

²JURASSICA Museum, Porrentruy, Switzerland

³Université de Fribourg, Fribourg, Switzerland

⁴Senckenberg Center for Human Evolution and Palaeoenvironment (HEP), Tübingen, Germany

Correspondence

Anna Ayvazyan
Email: anayvazyan@gmail.com

Funding information

This work was funded by the German Academic Exchange Service (DAAD) and the SYNTHESYS Grant (ES-TAF-5970) to the National Museum of Natural Sciences of Madrid (MNCN).

Contributing authors: Davit Vasilyan (davitvasilyan@gmail.com), davit.vasilyan@jurassica.ch; Madelaine Böhme (m.boehme@ifg.uni-tuebingen.de)

Abstract

Capoeta is a herbivorous cyprinid fish genus, widely distributed in water bodies of Western Asia. Recent species show a distinct biogeographic pattern with endemic distribution in large fluvial drainage basins. As other cyprinids, the species of this genus are characterized by the presence of the pharyngeal bone with pharyngeal teeth. Despite this, the detailed morphology of the pharyngeal teeth, its interspecific and topologic variations, and the importance for taxonomy and phylogeny of the genus *Capoeta* are still not established. For the first time, a detailed comprehensive study of the pharyngeal dentition of 10 *Capoeta* species has been provided. The morphologic study of the pharyngeal dentition bases on the 3D microtomography and follows the purpose to evaluate the potential taxonomic and phylogenetic signals of these elements, as well as to study interspecific and topologic variations of the pharyngeal teeth. In this study, we propose a new methodology to categorize the studied pharyngeal teeth in 18 shape classes. The results of this study show that the detailed 3D morphology of the pharyngeal teeth is a useful tool for the identification of isolated teeth at the generic and/or specific level and that in certain cases, the tooth position in the teeth rows can be identified. Additionally, the preliminary analysis shows that the morphology of the pharyngeal teeth provides a potential phylogenetic signal. Both these patterns are very important for the taxonomy of cyprinid fishes and especially can be applied to fossil records.

KEYWORDS

3D microtomography, *Capoeta*, Cyprinidae, pharyngeal teeth

1 | INTRODUCTION

Extant cyprinid fishes are known with more than 2,000 species and represent the most diverse family of bony fishes in Eurasia and Africa (Nelson, 2006). In fresh water bodies, they build the main part of the biodiversity of the fish community. The family includes several large clades (subfamilies), that is, Cyprininae and Leuciscinae. In Western Asia among cyprinids, one of the widely distributed genera is the cyprinine *Capoeta*, which is considered as endemic to the region. The monophyletic genus *Capoeta* includes herbivorous species, feeding mainly on algae and periphyton, which they scrap from the substrate by the horny sheath on their

lower lip (Banarescu, 1999; Karaman, 1969; Türkmen, Erdoğan, Yıldırım, & Akyurt, 2002).

Currently, more than 20 *Capoeta* species are described based on genetic studies and morphologic and meristic characters (Levin, Rubenyan, & Salnikov, 2005; Levin et al., 2012; Turan, Kottelat, & Ekmeççi, 2008). The earlier taxonomical studies of the genus *Capoeta* are based mainly on morphometrics and meristic characters (Karaman, 1969; Krupp & Schneider, 1989), whereas the recent studies mostly rely on genetic analyses (Alwan, Esmacili, & Krupp, 2016; Levin et al., 2012; Turan, 2008).

Levin et al. (2012) studied the phylogenetic relationships of the genus *Capoeta* based on the complete mitochondrial gene for

cytochrome *b* sequences obtained from 20 species. According to the study (Levin et al., 2012), three main groups are recognized: the Mesopotamian, the Anatolian-Iranian, and the Aralo-Caspian. Later, Zareian, Esmaeili, Heuidari, Khoshkholgh, and Mousavi-Sabet (2016) based on mitochondrial cytochrome *b* gene sequences distinguished three main groups: the *Capoeta trutta* group (the Mesopotamian *Capoeta* group), the *Capoeta damascina* complex group (the Anatolian-Iranian group), and the *Capoeta capoeta* complex group (the Aralo-Caspian group) (Zareian et al., 2016).

A diagnostic character of all cyprinid fishes is the presence of the pharyngeal bone with pharyngeal teeth located in up to three rows (Howes, 1991). It builds as a result of ossification of the right and left fifth ceratobranchials and forms tooth-bearing pharyngeal jaw, which is specialized for food processing. The morphology of the pharyngeal jaw and pharyngeal tooth shape and configuration also have taxonomic significance for cyprinids (Howes, 1991) and can be represented by a formula, for example, 4.3.2-2.3.4; these numbers indicate the amount of the teeth on the left and right jaws from the first to the third and the third to the first row correspondingly. The number of tooth rows and the amount of teeth in the each row are mentioned as one of the significant taxonomic characters for the genus *Capoeta* (Banareescu, 1999; Karaman, 1969; Krupp & Schneider, 1989). Besides this, several studies have shown that the pharyngeal dentition can also be considered as an essential character complex for the study of cyprinid evolution (Ahnelt, Herdina, & Metscher, 2015; Böhme, 2002; Pasco-Viel et al., 2010; Zardoya & Ignacio, 1999; Zeng & Liu, 2011). However, little is known about the morphology of pharyngeal bones and teeth of the genus *Capoeta*, as well as its significance for taxonomy and phylogeny.

Heckel (1843) described the pharyngeal teeth of cyprinid fishes for the first time. He classified them according to the grinding surfaces in four main groups and 13 subgroups. One of the subgroups described by him with "shovel-shaped teeth" includes the genus *Capoeta*. According to Heckel (1843), the teeth formula of the genus *Capoeta* is 2.3.4-4.3.2 (respectively from the third to the first and from the first to the third row). By examining different species of the genus, later studies (Banareescu, 1999; Karaman, 1969; Krupp & Schneider, 1989) found four or five teeth to be present in the main row, two to four in the second row, and two in the third row. Banareescu (1999) gave a rough morphologic description of the pharyngeal teeth and mentioned that the teeth in the main row are compressed and have irregular shape and those in the second and third rows are more or less cylindrical in shape (Banareescu, 1999). However, the detailed morphology, interspecific and topologic variations, and the importance of the tooth morphology for taxonomy and phylogeny of this genus are still not established.

Taking this into account, the main goals of this publication were (i) to provide a detailed morphologic description of pharyngeal teeth in 10 *Capoeta* species by applying 3D approaches; (ii) to check the interspecific and topologic variations of pharyngeal teeth; and (iii) to test the possible phylogenetic signal embedded in the tooth morphology.

2 | MATERIALS AND METHODS

2.1 | Sampling

Pharyngeal dentitions of 10 *Capoeta* species from different water basins of Anatolia, Iraq, Iran, Armenia, Georgia, and Syria are studied (Table 1). The comparative material of pharyngeal bones is stored at the Bavarian State Collection for Anthropology and Palaeoanatomy, Munich (SNSB); the National Museum of Natural Sciences of Madrid (MNCN); the Palaeontological Collection of Tübingen University (GPIT); and Senckenberg Naturmuseum Frankfurt (SMF). The sampled information about studied specimens and locations is listed in Table 1 and Figures 1 and 2. The osteologic and morphologic description of the pharyngeal bones and teeth follows the nomenclature introduced in Figure 3.

The left pharyngeal bones of adult individuals are used in the study (except for *Capoeta umbla* and *C. damascina*). Each pharyngeal bone possesses 9 to 10 teeth (pharyngeal teeth a3, a5, c1, and c2 in *Capoeta saadii* and b2, c1, and c2 in *Capoeta buhsei* are missing). So, in total, the morphologic characters of 84 teeth are examined and analyzed. The other samples of the same species were examined according to an established morphologic set of characters.

2.2 | Species identification

The studied species were collected and identified by different scholars. *C. saadii* and *C. buhsei* are collected by Ignacio Doadio in 2015, *C. umbla* by Angela Van den Driesch, *C. trutta* and *Capoeta* sp. by Eva Maria Cornelssen in 1978, *Capoeta baliki* and *Capoeta sieboldii* by Madelaine Böhme in 2010, *C. capoeta* by Samvel Pipoyan in 2012, *Capoeta sevangi* by Anna Ayvazyan in 2014, and *C. damascina* by Nisreen Alwan in 2008. All species are identified by the collectors based on external morphology and meristic characters.

Capoeta sp. from the Dokan Reservoir, Iraq, was collected by Cornelssen and stored as dried skeleton in SNSB as *Barbus belayewi*. According to our results, this specimen is closely related but not identical to the species *C. trutta*, which is also supported by the detailed study and comparison of the morphology of the last unbranched ray of the dorsal fin (unpublished results).

2.3 | X-ray microtomography

The pharyngeal bones were prepared in small polystyrene boxes for scanning.

The pharyngeal bones of the extant *Capoeta* species were scanned using X-ray computed tomography (μ CT). MicroCT images were taken using the microtomography system Phoenix v|tome|x s at the Tübingen University and Erlangen University, as well as NIKON XT H 160 at the Scanning electron microscopy and analytic laboratories of MNCN. The pharyngeal bones were scanned with the following settings: 0.025 mm resolution, 100 to 150 mA, and 83 to 150 kV depending on the size of the bones and teeth (the bigger the bone, the higher the voltage due to the increased thickness of

TABLE 1 *Capoeta* species included in the present study

Scientific name	Locality	Number of samples (n)	Depository
<i>Capoeta sieboldii</i>	Kizilirmak River, town of Avanos, Turkey	1	GPIT-OS-00858
<i>Capoeta baliki</i>	Kizilirmak River, Avanos, Turkey	1	GPIT-OS-00859
<i>Capoeta trutta</i>	Assad Sea, Syria	2	SAPM-PI-02908, SNSB SAPM-PI-02910, SNSB
<i>Capoeta capoeta</i>	Saghamo Lake, Georgia	13	GPIT-OS-00860 ^a
<i>Capoeta umbra</i>	Khata River, Adiyaman, eastern Turkey	1	SAPM-PI-00718, SNSB
<i>Capoeta sevangi</i>	Sevan Lake, Armenia	9	GPIT-OS-00861 ^a
<i>Capoeta</i> sp.	Dokan Reservoir, Iraq	2	SAPM-PI-00719, SNSB SAPM-PI-00721, SNSB
<i>Capoeta buhsei</i>	Soleghan River, Namak Lake, Tehran, Iran	1	AT241586, MNCN
<i>Capoeta saadii</i>	Shahpur River, Dalaki River, Bishapur, Iran	1	IR3, MNCN
<i>Capoeta damascina</i>	Homs or Qattinah Lake, Orontes River drainage, Syria	1	SYR08/25, SMF

SNSB, Bavarian State Collection for Anthropology and Palaeoanatomy, Munich; MNCN, National Museum of Natural Sciences of Madrid; GPIT, Palaeontological Collection of Tübingen University; SMF, Senckenberg Naturmuseum Frankfurt.

^aCollection numbers of scanned samples.

the element the X-rays must traverse). The tomographic reconstruction was performed using the following software: Phoenix datosx CT in Tübingen, VGStudio 3.0 in Erlangen, and Amira 8.0 in Madrid.

2.4 | Morphological analyses

The virtual sections and 3D volume renderings from the reconstructed volume images were evaluated in the Avizo package (version 8.0). The digitalization of the bones allows observing models from different sides and recording the microstructures of bones and teeth which are difficult to observe under a light microscope. The teeth were further edited in the Geomagic professional engineering (version 15.3.0) and Freeform Plus (2014.3.0. 172) software packages. Besides these, the pharyngeal bones were examined under the Leica DVM5000 digital microscope and Leica M50 stereomicroscope available at the University of Tübingen.

To study the morphology of each pharyngeal tooth, we reconstructed 3D models of pharyngeal bones and virtually separated each tooth as an isolated model (in Avizo and Geomagic). The isolated 3D tooth models allow for an examination of the tooth from different sides by rotating the models, as in the tooth rows the teeth are covered sidewise by others and it is difficult to observe all morphologic features of the teeth. Based on these 3D models, the set of teeth for each species is generated, which makes it easy to categorize teeth and record the intraspecific variation (Figure S1).

We established a set of shape characters: lateral outline (α) and transverse cross section (β). Based on them, the teeth were described and categorized into shape classes. To record the lateral outline of each tooth, we used the images of isolated 3D tooth models and marked the outlines using Adobe Illustrator. The lateral outlines were taken for each tooth in dorsal view, from the top of the tooth until its foot basis. The transverse cross section is performed using the tool "Slice" from the Avizo package. To record the cross sections, the tooth surfaces of every sample were virtually cut at the

same anatomical position where the surfaces of all teeth appear on the slice plate. To describe the shape characters, the coding used in phytolith (silicified plant particles) nomenclature is applied (Wautier, van der Heyden, & Huisseune, 2001). The same "Slice" tool is used to apply a virtual experiment to understand the robustness of the transverse cross section (β). For this experiment, the teeth surfaces of *C. sieboldii* were cut together in one slice and a4 of *C. buhsei* was cut separately from the other teeth to get the section at the uppermost part of the surface.

To describe and categorize the pharyngeal teeth of *Capoeta* species based on 3D models of 84 pharyngeal teeth, we used basic terminology (Wautier et al., 2001). In addition, to better formalize tooth morphology, we introduced shape classes defined by character stages α and β . To check the intraspecific variation of tooth morphology and left–right asymmetry among studied species, two control groups, *C. sevangi* ($n = 13$) and *C. capoeta* ($n = 9$), as well as all other species represented with two or more samples were examined.

To test the phylogenetic information of shape classes, the dendrogram has been performed using the morphologic characters by applying the Euclidean similarity index in the PAST (Paleontological Statistics, version 3) software.

3 | RESULTS

3.1 | General aspects of the pharyngeal tooth morphology of the genus *Capoeta*

Figure 3a and b shows the localization of the pharyngeal dentition in the fish body. The pharyngeal bones of the genus *Capoeta* can be distinguished by the well-developed dorsal and curved ventral limbs as well as the relatively large tooth-bearing area (Figure 3c and d). Each tooth consists of a tooth foot, a crown, a foot–crown border, a grinding surface, and an edge of the grinding surface (Figure 3e and f). The pharyngeal teeth of studied species are arranged at the

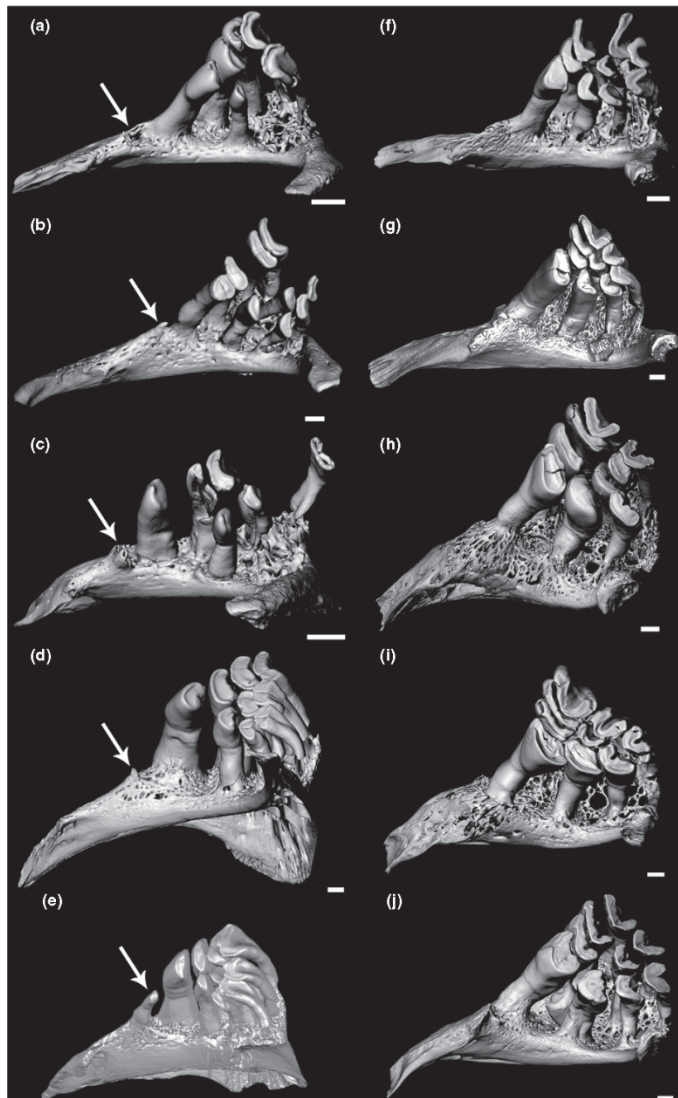


FIGURE 1 (a–j) Pharyngeal bones with teeth of the studied nine extant species of the genus *Capoeta*. (a) *Capoeta buhsei*; (b) *Capoeta umbla* (mirrored); (c) *Capoeta saadii*; (d) *Capoeta baliki*; (e) *Capoeta damascina* (mirrored); (f) *Capoeta capoeta*; (g) *Capoeta sevangi*; (h) *Capoeta* sp.; (i) *Capoeta trutta*; and (j) *Capoeta sieboldii*. The white arrows show a1 or presence of its bases. The scales are equal to 1 mm

pharyngeal bone in three rows. Each of them has different tooth count. The main row possesses five or four (a1, a2, a3, a4, a5), the second row three (b1, b2, b3), and the third row two (c1, c2) teeth (Figure 3c). The pharyngeal tooth formula is (i) 4.3.2–2.3.4 in *C. capoeta*, *C. sevangi*, *C. sieboldii*, *C. trutta*, and *Capoeta* sp.; or (ii) 5.3.2–2.3.5 in *C. damascina*, *C. umbla*, *C. buhsei*, *C. saadii*, and *C. baliki*, which have a1 (*C. damascina*) or the tooth base at the a1 position.

The pharyngeal bone of *Capoeta* shows heterodont dentition. The teeth of the main row are larger than those of the second and third

rows. The first tooth of the main row can be absent (*C. capoeta*, *C. sevangi*, *C. sieboldii*, *C. trutta*, and *Capoeta* sp.), strongly reduced (*C. umbla*), or less reduced as in *C. damascina*. A1 is a small accessorial tooth and can be easily broken. In the case of *C. saadii*, *C. buhsei*, and *C. baliki*, it is broken and only the tooth basis is visible.

As a rule, the second tooth of the main row (a2) within all studied species is robust and relatively large with a wide tooth base and grinding surface. The other teeth of the main row (a3, a4, a5) as well as the teeth of two other rows (b2, b3, c1, c2) compared to

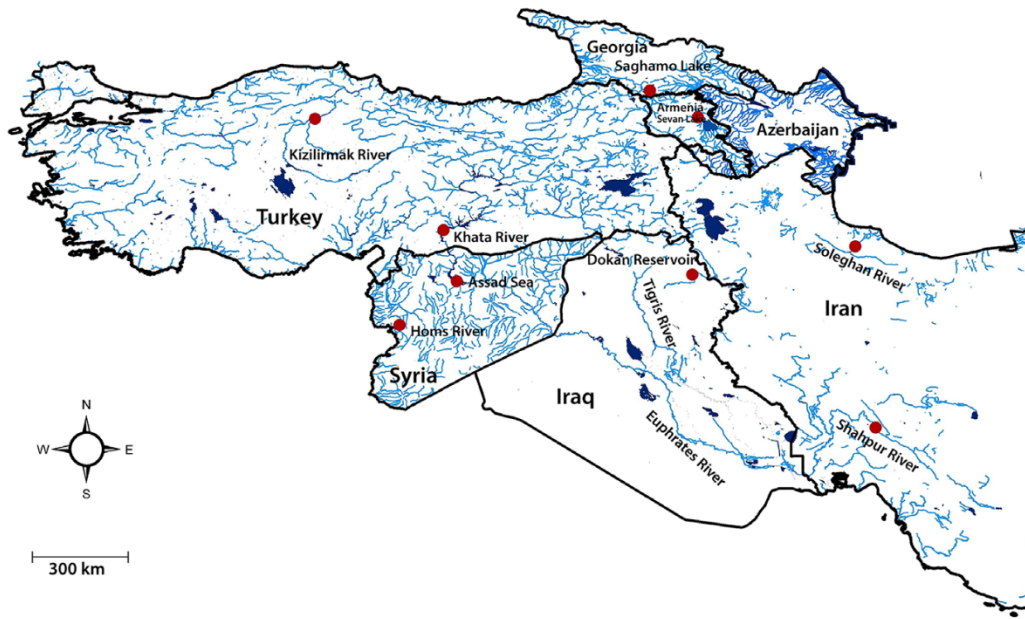


FIGURE 2 Drainage system of Western Asia (Turkey, Iraq, Iran, Armenia, Georgia, and Syria). The sampled (circles) localities of the studied *Capoeta* species

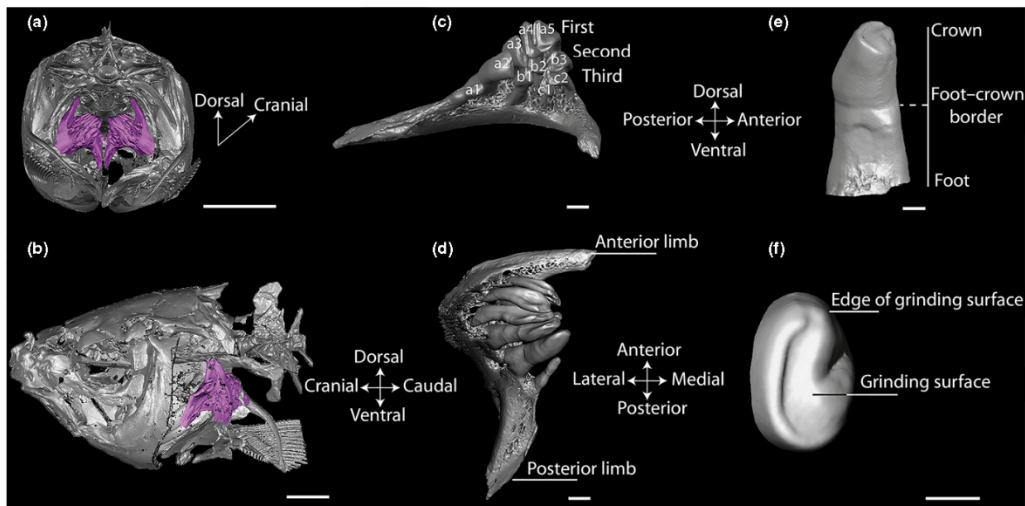


FIGURE 3 The terminology of the pharyngeal bones and teeth used in the present work: Skull of *Capoeta sevangi* in (a) posterior and (b) lateral views, showing the position of pharyngeal bones. Pharyngeal bone with teeth in (c) anterior and (d) medial views. The pharyngeal tooth (e) and grinding surface (f). The scale bars are equal to 1 cm (a, b) and 1 mm (c–f)

a2 are slender. They widen distally and are bent laterally. These characters are more pronounced ventrodorsally along the main row and well expressed in the most dorsal tooth (a5). The first tooth of

the second row (b1) is usually similar to the a2 with its morphology, but it is more slender. The other teeth of the second row are slender and bent laterally. Two teeth of the third row (c1, c2) are

usually the smallest. The grinding surfaces in all three rows narrow ventrodorsally.

The intraspecific variation and left–right asymmetry among both studied control groups (*C. sevangi* and *C. capoeta*) were not recorded.

3.2 | Pharyngeal tooth characterization and classification

On the basis of the 3D models and images of pharyngeal teeth, we describe *Capoeta* tooth morphology using two sets of the shape characters: lateral outline (α) and transverse cross section (β , measured at the distal tooth crown). According to the lateral outline, we define 14 character stages ($\alpha 1$ – $\alpha 14$; Figure 4; Table S1). Among the studied species, the most frequently occurring lateral outline has spatulate form. It occurs mainly in the $\alpha 3$ – $\alpha 5$, $\alpha 2$ – $\alpha 3$, and $\alpha 1$ – $\alpha 2$ tooth positions. As a rule, nearly all $\alpha 2$ teeth are molariform with a few differences.

The outline of the transverse cross section is variable among the studied teeth, and overall, eleven character stages ($\beta 1$ – $\beta 11$; Figure 5, Table S1) can be defined for them. The variability of the outline of the transverse cross section of the grinding surfaces is a result of the morphological diversity of the masticatory surface in the studied 10 species.

We applied the (virtual) artificial wear experiment (for details, see Materials and methods) to understand the robustness of the

transverse cross section (β). Different layers/slices from the top of the grinding surface were cut to follow the variability, that is, development of these characters during the wearing process. In this experiment, the pharyngeal teeth of *C. sieboldii* were examined as the folded edge of grinding surface is characteristic of them and the applied experiment allows to test the development of the crenated grinding surface during the wearing process. Therefore, three different height sections from the top of the grinding surface (0.57 mm, 0.87 mm, and 1.42 mm) were processed. The heights of the cut slices are the points after which the form of the examined characters (crenated edge of the grinding surface) was changed. As shown in Figure S2, there are no any significant changes of transverse cross section (β) and it stays stable during applied wearing process, while folds of the grinding surface can change during the wearing process: They deepen, enlarge, or disappear (Figure S2 A1–A3). Therefore, the number or deepening of these folds cannot be used to describe the tooth as they are not applicable for the comparison if the samples have different degree of tooth wearing. The other example is the serrated posterior edge of the grinding surface, which is well expressed in the $\alpha 4$ tooth of *C. buhsei* (Figure S2 B). Its presence can be considered as a character of an unworn or less worn tooth. The application of virtual wearing by applying four different height sections of grinding surface (0.42 mm, 0.78 mm, 1.31 mm, and 1.87 mm) allows to observe the development of the serration during the wearing process. As shown in Figure S2, the serration of the surface is disappearing after a few layers were cut which can be identified during the wearing process (Figure S2 C1–C4).

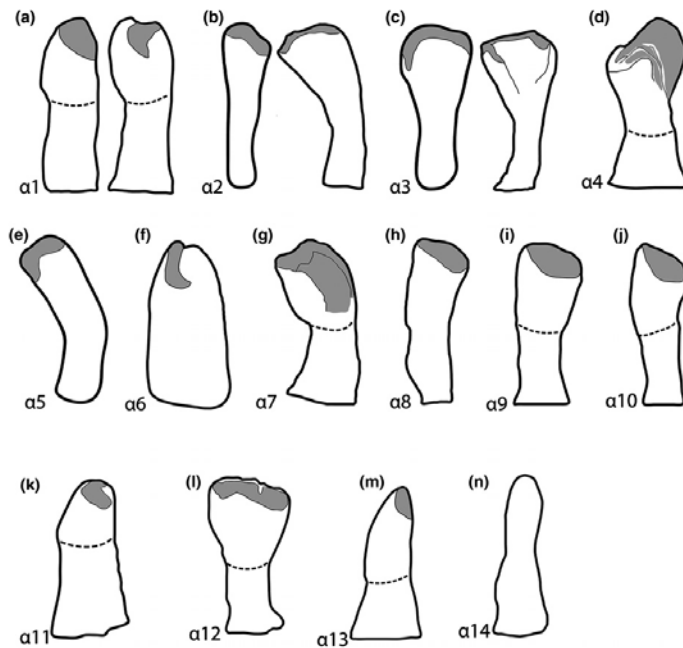


FIGURE 4 Lateral outlines of pharyngeal teeth in the studied *Capoeta* species. Illustrations (a–n) of the 14 character stages ($\alpha 1$ – $\alpha 14$) for the tooth lateral outline. The presence of the groove on the grinding surface is indicated in gray color

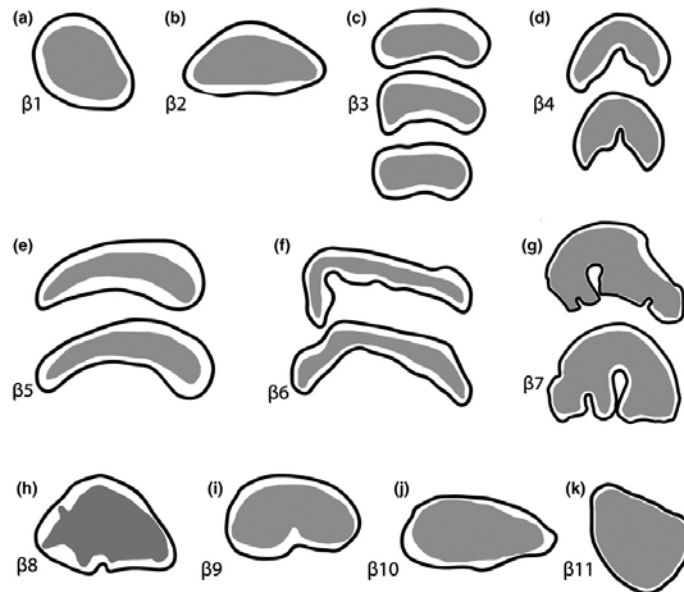


FIGURE 5 Eleven character stages ($\beta 1$ – $\beta 11$) (a–f) of the transverse cross sections of pharyngeal teeth of the studied *Capoeta* species. The gray color indicates the presence of the groove on the grinding surface, and the white color corresponds to the tooth “enamel”

The grinding surface of some studied dorsal teeth has sloped edges. This character appears in teeth of different rows and possibly points out the tooth's movement direction during the grinding or which part of the grinding surface is actively participating in the grinding process (Figure S2 D, E).

So two main groups of characters of the pharyngeal teeth were distinguished: (i) applicable for the teeth description as the lateral outline (α) and transverse cross section (β); and (ii) variable during the ontogeny as folded, serrated, and sloped edge of the grinding surface.

The lateral outline (α) and the outline of the transverse cross section (β) were used to categorize the pharyngeal teeth of the studied 10 *Capoeta* species into 18 shape classes (Figure 6a–r; Table S2). Within the described shape classes, the most frequent one is shape class “C,” which is common to all studied species (Figures S3 and S4).

The detailed description of all the shape classes can be found in the Supporting Information (Tables S1 and S2).

3.3 | Dendrogram based on the tooth shape classes

To test the potential taxonomic and phylogenetic signal of the pharyngeal tooth morphology, we performed a simple dendrogram based on the distribution (presence/absence) of the described shape classes within the studied species (Figure 7; Table S3). The dendrogram divided the studied species into four phenotypic clades: Clade I (*C. saadii*, *C. buhsei*, *C. damascina*, *C. umbla*, and *C. baliki*), Clade II (*C. sieboldii*), Clade III (*C. capoeta* and *C. sevangi*), and Clade IV (*C. trutta* and *Capoeta* sp.).

3.4 | Distribution of shape classes across species

The distribution of the studied species on the dendrogram is based on the morphological characters of these elements. The clustering of a few species inside one clade not only indicates that these species have similar (but not identical) tooth morphology, but also points out their close phylogenetic relationship.

According to the dendrogram, each clade is described with shape classes, and certain species on the dendrogram have own characteristic shape classes (Figure 7). Therefore, the described 18 shape classes are divided into three groups: diagnostic for the genus, clade, and species. The shape class “C” appears in all 10 studied *Capoeta* species, and it is the characteristic shape class of the genus *Capoeta*. The clade diagnostic shape classes are characteristic of a group of species which belong to the same clade, for example, shape classes “B, E, F, H, I, K, and M.” The other shape classes, “D, G, J, L, N, O, P, Q, and R,” are characteristic of certain species (Figure 7). Besides this, the described tooth shape classes are characteristic of certain tooth positions as well; for example, the shape class “C” is characteristic of teeth belonging to the main row (besides a1 and a2). To test the frequency of the occurrences of shape classes in different teeth positions, the graph was drawn (Figure S5). It shows that the teeth in a2 and b1 positions are the most heteromorph and the ones in position a5 are homomorph or less heteromorph. So the second tooth of the main row (a2) of each studied species (except *C. buhsei*) has a distinct shape class found only in one species; thus, a2 can be used for the identification at species level. The identification key of the pharyngeal teeth within the studied species was established based on the shape classes (Figure S6).

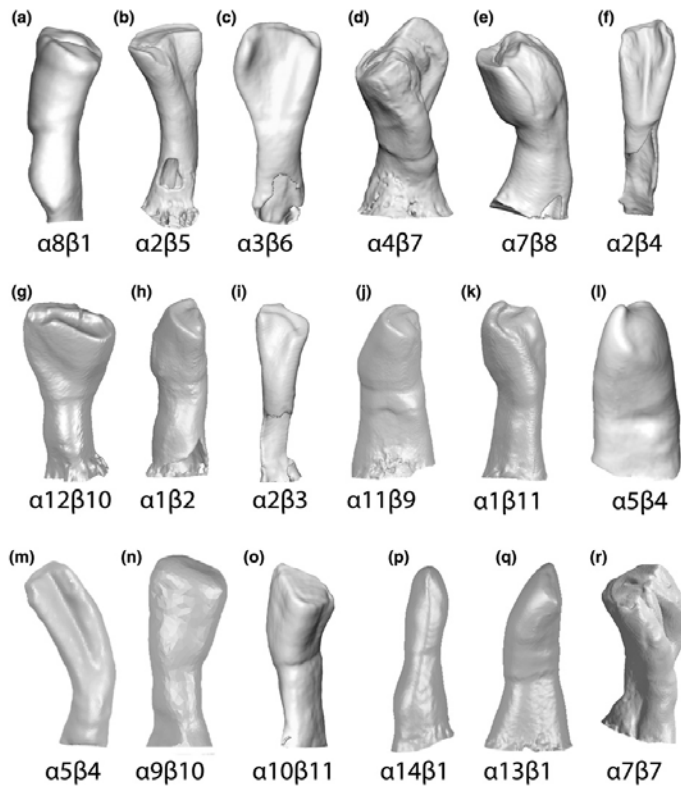


FIGURE 6 3D images of the recorded shape classes of the pharyngeal tooth of the genus *Capoeta*. (a–r) Shape classes proposed in the present work; for the descriptions, Tables S1 and S2. The scales are not given to avoid scaling up of the figures

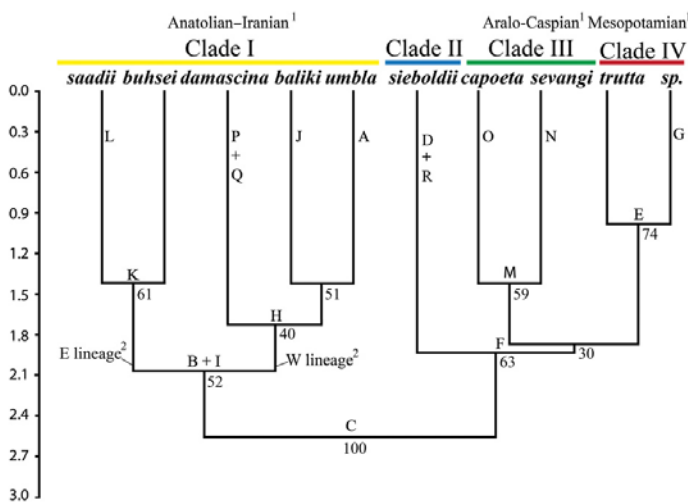


FIGURE 7 Phenotypic dendrogram generated based on the pharyngeal tooth shape classes of the *Capoeta* species. The letters (a–n) indicate the characteristic shape classes of nodes or branches. Numbers indicate the bootstrap support (branch support). ¹Distinguished clades of the genus *Capoeta* following Levin et al. (2012). ²Eastern (E lineage) and Western (W lineage) lineages within the *Capoeta damascina* complex established by Alwan, Esmacili, & Krupp, 2016; Alwan, Zareian, & Esmacili, 2016

4 | DISCUSSION

4.1 | Presence of a1 as a diagnostic character for Clade I

The presence of the a1 within 10 studied *Capoeta* species is characteristic of five of them, which are all clustered in Clade I: *C. saadi*, *C. buhsei*, *C. umbla*, *C. damascina*, and *C. baliki*. The tooth is well developed in *C. damascina*, and in the other above-mentioned species, it is reduced, missing, or broken, but the tooth base is well visible (Figures 1 and 8).

4.2 | Potential phylogenetic signal of the pharyngeal tooth morphology

The performed dendrogram shows not only the morphologic similarity of the species, which belong to the same clade, but also the potential phylogenetic relationship of these species.

C. damascina is considered as a complex of nearly related species with two distinguished lineages: the eastern represented by *C. buhsei*, *Capoeta coadi*, and *C. saadii* and the western represented by *Capoeta caelestis*, *C. damascina*, and *C. umbla*. In this study, the members of both lineages are included: *C. buhsei*, *C. saadii*, *C. damascina*, and *C. umbla*. As the dendrogram shows, these species are clustered (based on their pharyngeal tooth morphology as well as the presence of the a1) in one group and form the *damascina* complex clade (Clade I, Anatolian–Iranian group), respectively with the

western and eastern lineages as it has been shown based on genetic analyses (Alwan, Zareian, & Esmacili, 2016; Alwan, Esmacili, & Krupp, 2016).

To check the correspondence between morphological and genetic results, we simplify already existing phylogenetic trees based on genetic analyses to show how the studied species cluster within phylogenetic trees based on genetic and morphologic analyses (Figure 9). Therefore, phylogenetic trees from three recent studies were used (Bektas et al., 2017; Levin et al., 2012; Zareian et al., 2016). The comparison of dendrograms (Figure 9) shows that the species of Anatolian–Iranian or *C. damascina* complex group (*saadi*, *buhsei*, *damascina*, *umbla*, and *baliki*) cluster within one clade (indicated by yellow color). The Aralo-Caspian or *C. capoeta* complex group (*C. sevangi* and *C. capoeta*) cluster together in the same clade and are indicated in green. *C. trutta* in all three dendrograms as well as in our results clusters as the distinct clade Mesopotamian *Capoeta* or *C. trutta* group and is indicated in red.

According to the dendrogram (Figure 7), *C. sp.* from Dokan Reservoir clusters within the *trutta* clade, and we suppose it is one of the closely related species of the *trutta* complex.

The studies of Levin et al. (2012) and Zareian et al. (2016) have shown that *C. sieboldii* clusters as a sister lineage to the *damascina* complex. According to Bektas et al. (2017), *C. sieboldii* is easily distinguishable from all *Capoeta* species distributed in Anatolian rivers by its pleated lips and single-paired barbels (the other *Capoeta* species distributed in Anatolian rivers are characterized by double-paired barbels) and represented as a separate clade. This

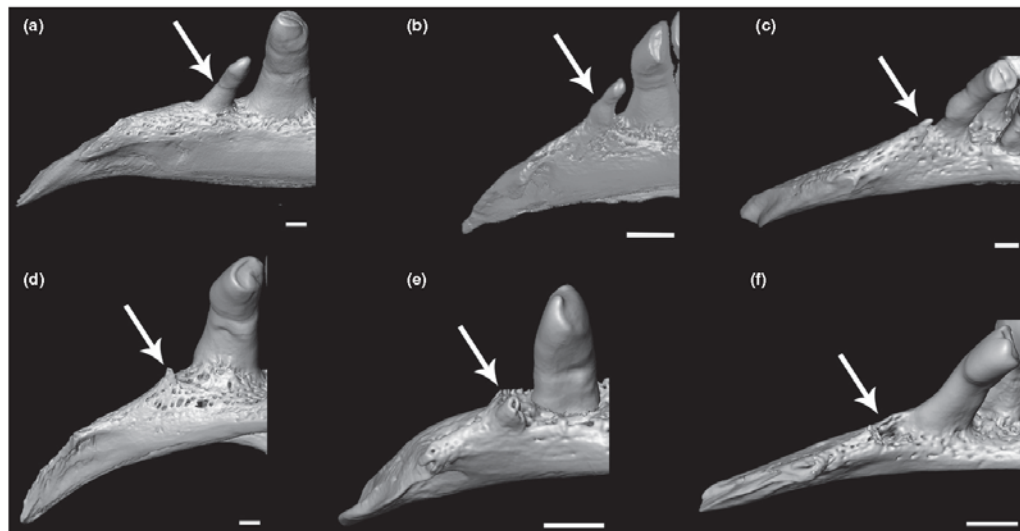


FIGURE 8 Reduction of the a1 tooth in the genus *Capoeta* in comparison with *Barbus barbatus*. (a) *B. barbatus*, (b) *Capoeta damascina*, (c) *Capoeta umbla* (strongly reduced), (d) *Capoeta baliki* (tooth broken), (e) *Capoeta saadii* (tooth broken), and (f) *Capoeta buhsei* (resorption pit visible). The white arrows show the a1 tooth or the position of its tooth basis. The scale bars are equal to 1 mm

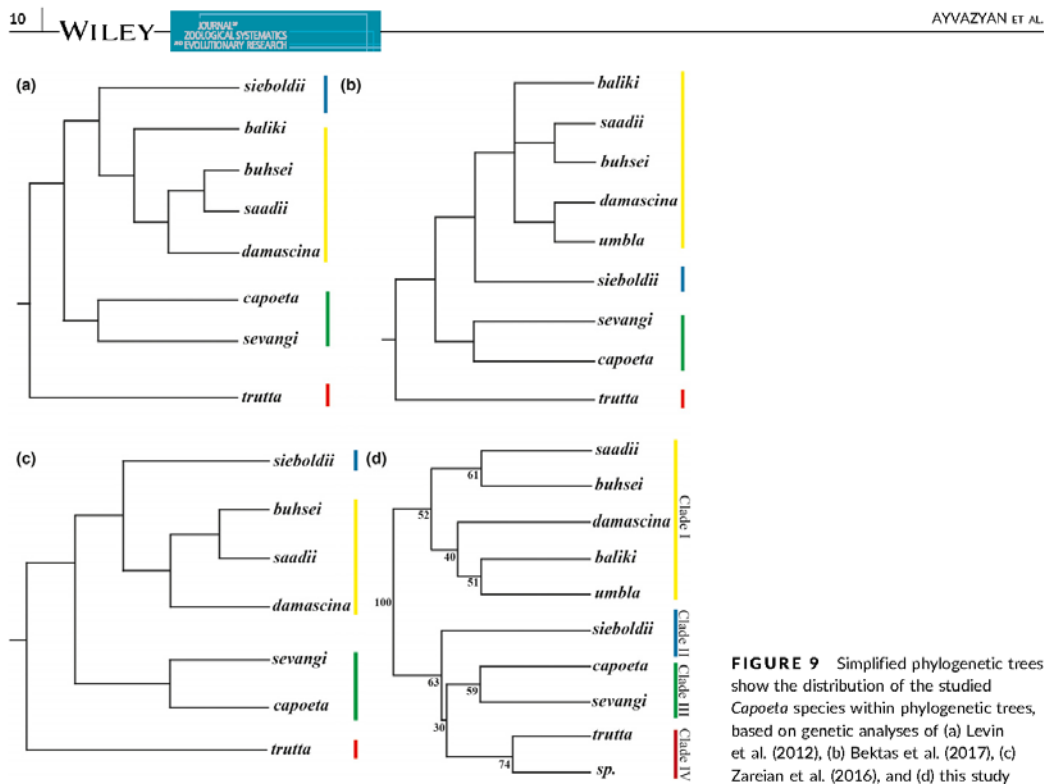


FIGURE 9 Simplified phylogenetic trees show the distribution of the studied *Capoeta* species within phylogenetic trees, based on genetic analyses of (a) Levin et al. (2012), (b) Bektas et al. (2017), (c) Zareian et al. (2016), and (d) this study

pattern is also supported by our results. According to our data, *C. sieboldii* is represented as a distinct clade (Figure 7, in blue color, Clade II). However, our analysis shows only one difference from genetic results (Bektas et al., 2017): *C. sieboldii* is placed as a sister clade to Aralo-Caspian (Clade III) and Mesopotamian (Clade IV) clades (Figure 7), whereas the genetic data cluster it as a sister clade to *C. damascina* (Clade I, small scale; Bektas et al., 2017).

4.3 | Is the reduction of a1 plesiomorphic or apomorphic for the genus *Capoeta*?

The phylogenetic tree based on molecular analyses of the genus *Capoeta* published by Levin et al. (2012) was simplified to show the presence of the a1 in different clades within this genus and its sister groups (Figure 10). The pharyngeal bones most of species of *Barbus* and *Luciobarbus* clades were available to us and the presence/absence of a1 was recorded first-hand, and the information about missing species was taken from the existing literature. This dendrogram shows that a1 tooth or its basis is present in representatives of clade *Barbus* and clade B (*Capoeta* clade), but absent in the other two sister groups (*Luciobarbus* and *L. subquincunciatus*). We assume that the absence of a1 is plesiomorphic for the genus *Capoeta*, which means it was lost among the species of clades A and C and reappeared or was regained in the species of

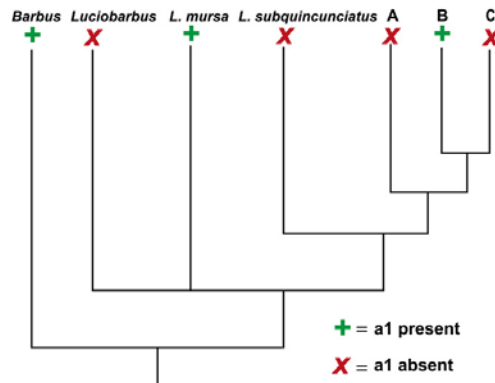


FIGURE 10 Presence/absence of a1 tooth shown on the phylogenetic tree based on mitochondrial gene for cytochrome b sequences (Levin et al., 2012). The clades are respectively corresponding to the clades mentioned in the work. A, B, and C the Mesopotamian group (A), the Anatolian-Iranian group (B), and the Aralo-Caspian group (C), are included in the clade *Capoeta*

clade B. The other possibility is that the presence of a1 tooth or its basis is a derived character that distinguishes the *damascina* clade.

4.4 | Potential ecological signal of the pharyngeal tooth

The preliminary interpretation of the possible ecological signal or the connection between feeding habits and pharyngeal tooth morphology of the studied species is provided based on literature data (Coad, 2010; Karaman, 1969; Krupp & Schneider, 1989).

The studies regarding the feeding habits of the genus *Capoeta* are unanimous and suggest that these species are herbivorous and feeding mainly on algae and periphyton, which they scrape from the substrate using the horny sheath on their lower lip (Banareescu, 1999; Karaman, 1969; Krupp & Schneider, 1989; Türkmen et al., 2002). The similar feeding habits should indicate that the tooth morphology is identical, in other words that the studied species should have homodont dentitions if the main driven factor is ecology, which has not been supported by our study. According to our results, the studied *Capoeta* species have heterodont dentitions and there is an interspecific variation of tooth morphology and tooth numbers within the studied species. Besides this, the dense packaging of the tooth arrangement in the tooth rows on the tooth-bearing area differs as well.

On the other hand, in case the a1 tooth is an apomorphic character of the *C. damascina* clade, a more omnivorous diet of the species of this complex could be suggested, as in *L. subquincunciatus* having a specialized dentition for feeding on algae or benthos. Thus, the a1 tooth could not be considered to provide selective advantage. This indicates the possible trophic segregation within these species.

The mouth and the lower lip covered by horny sheath are used mainly to scrap the algae; therefore, their morphology could also be an important trait to understand the trophic variation of the species and its reflection in tooth morphology.

Within the genus *Capoeta*, two types of mouth forms have been described: horseshoe-shaped and transverse (Karaman, 1969). The horseshoe-shaped is the basal form and can develop into the highly specialized transverse form. In the study by Karaman (1969), it has also been mentioned that all studied populations, during their development, first have the horseshoe mouth form without horny sheath. So we can assume that the horseshoe form of the mouth is a plesiomorphic and the transverse form is an apomorphic character. The mouth form has been described in different studies (Banareescu, 1999; Coad, 2010; Krupp & Schneider, 1989), but we could not find any significant difference between the given morphological descriptions.

So additional morphologic and ecologic studies are necessary to understand whether there is indeed trophic segregation between the *Capoeta* clades and whether there is a possible relation of the tooth morphology and feeding habits.

5 | CONCLUSION

5.1 | Pharyngeal tooth characterization and classification

For the first time, the detailed comprehensive study of pharyngeal dentition of 10 species of the genus *Capoeta* has been provided. The

morphology of the pharyngeal dentition has been studied using the 3D microtomography to test its potential relevance for answering to taxonomic and phylogenetic questions. Special tools in the 3D software Avizo 8.0 allow to perform different effects (wearing process) and to test the stability of the morphological characters. These can be applied for the characterization and identification of pharyngeal teeth.

In this study, the set of morphological characters ($\alpha\beta$) were established to categorize the studied pharyngeal teeth into 18 shape classes. The results of different analyses based on the described shape classes show that based on the detailed morphology of these elements, the isolated pharyngeal teeth can be identified at the generic or specific level. Besides this, it is also possible to determine the relative or even the exact position of the isolated tooth in the tooth rows.

The identification key of the pharyngeal teeth of the studied species could be used for the identification of the isolated pharyngeal teeth, which is important not only for the taxonomy of recent species but also for the fossil record, as mainly the isolated pharyngeal teeth are found in the fossil record.

5.2 | Correspondence between morphological and molecular results

The comparison of the results of morphology and genetic analyses shows significant similarities of the generated trees. This supports our assumption that the pharyngeal tooth morphology of this genus has not only taxonomic but also phylogenetic relevance. The morphological results strongly support the presence of four clades: (i) *C. damascina* clade; (ii) *C. sieboldii* clade; (iii) *C. capoeta* clade; and (iv) *C. trutta* clade.

Summing up our results, we conclude that:

1. the detailed morphology using the 3D microtomography of pharyngeal teeth is a useful tool for the identification of the isolated pharyngeal teeth at the generic and specific levels, as well as in certain cases the tooth position in tooth rows;
2. the morphology of the pharyngeal teeth provides an obvious phylogenetic signal, supporting results derived from molecular genetic analyses;
3. both these patterns are important for the taxonomy of the genus and can be applied for the fossil records as well;
4. the a1 tooth is an apomorphic character for the *C. damascina* complex;
5. there is possible trophic segregation (the species of the *C. damascina* complex are more omnivorous/less dietary specialized); further studies are necessary to confirm this.

ACKNOWLEDGEMENTS

The first author thanks Prof. I. Doadrio for his support and access to the osteological collection; his working group, namely Silvia Perea, Miriam Casal-Lopez, and Hamid Reza Ghanavi, for the hosting in Madrid, as well as Christina Paradella and Laura Tomo for the support with scanning the studied material in the National

Museum of Natural Sciences of Madrid (MNCN); Dr. Marton Rabi and Silvia Perea for the discussions regarding phylogeny; Adrian Tröscher for technical support; Prof. Bettina Reichenbacher for the support; Dr. Jorg Feyhof for fruitful discussions about some taxonomic issues; Prof. Samvel Pipoyan for providing one of the studied species; and Stefan Riede for critically reading the manuscript.

The authors are grateful to Dr. Henriette Obermaier from the Bavarian State Collection for Anthropology and Palaeoanatomy, Munich (SNSB), for access to the osteological collection; Fabian Herder and Nisreen Alwan at Senckenberg Naturmuseum Frankfurt (SMF) for providing one of the studied samples; and Christian Schulbert for making it possible to scan some material at Micro-Computed Tomography Laboratory in Erlangen University.

ORCID

Anna Ayvazyan  <http://orcid.org/0000-0003-3484-9398>

REFERENCES

- Ahnelt, H., Herdina, A. N., & Metscher, B. D. (2015). Unusual pharyngeal dentition in the African Chedrin fishes (Teleostei: Cyprinidae): Significance for phylogeny and character evolution. *Zoologischer Anzeiger - A Journal of Comparative Zoology*, 255, 85–102. <https://doi.org/10.1016/j.jcz.2015.02.007>
- Alwan, N., Esmaili, H. R., & Krupp, F. (2016). Molecular phylogeny and zoogeography of the *Capoeta damascina* species complex (Pisces: Teleostei: Cyprinidae). *PLoS One*, 11(6), e0156434. <https://doi.org/10.1371/journal.pone.0156434>
- Alwan, N. H., Zareian, H., & Esmaili, H. R. (2016). *Capoeta coadi*, a new species of cyprinid fish from the Karun River drainage, Iran based on morphological and molecular evidences (Teleostei, Cyprinidae). *ZooKeys*, 572, 155–180. <https://doi.org/10.3897/zookeys.572.7377>
- Banarescu, P. M. (1999). *The freshwater fishes of Europe*. Wiesbaden, Germany: AULA-Verlag.
- Bektas, Y., Turan, D., Aksu, I., Ciftci, Y., Eroglu, O., Kalayci, G., & Belduz, A. O. (2017). Molecular phylogeny of the genus *Capoeta* (Teleostei: Cyprinidae) in Anatolia, Turkey. *Biochemical Systematics and Ecology*, 70, 80–94. <https://doi.org/10.1016/j.bse.2016.11.005>
- Böhme, M. (2002). Freshwater fishes from the Pannonian of the Vienna Basin with special reference to the locality Sandberg near Götzen-dorf, Lower Austria. *CFS Courier Forschungsinstitut Senckenberg*, 237, 151–173.
- Coad, B. W. (2010). *Freshwater fishes of Iraq*. Sofia, Bulgaria; Moscow, Russia: PENSOFT.
- Heckel, J. J. (1843). *Abbildungen und Beschreibungen der Fische Syriens*. Howes, G. J. (1991). *Cyprinid fishes: Systematics, biology and exploitation*, 1st edn. New Delhi: Chapman and Hall.
- Karaman, M. S. (1969). *Süßwasserfische der Türkei*. Hamburg, Germany: Mitteilungen des Hamburg Zoologisches Museum und Institut.
- Krupp, F., & Schneider, W. (1989). The fishes of the Jordan River drainage basin and Azraq Oasis. *Fauna of Saudi Arabia*, 10, 347–416.
- Levin, B. A., Freyhof, J., Lajbner, Z., Perea, S., Abdoli, A., Gaffaroglu, M., ... Doadrio, I. (2012). Phylogenetic relationships of the algae scraping cyprinid genus *Capoeta* (Teleostei: Cyprinidae). *Molecular Phylogenetics and Evolution*, 62(1), 542–549. <https://doi.org/10.1016/j.ympev.2011.09.004>
- Levin, B. A., Rubenyan, A. R., & Sainikov, V. B. (2005). Phenetic diversity of khramulya *Capoeta capoeta* (Ostariophysi, Cyprinidae). *Journal of Ichthyology*, 45(9), 754–767.
- Nelson, J. S. (2006). *Fishes of the world*, 4th edn. Hoboken, NJ: John Wiley & Sons, Inc..
- Pasco-Viel, E., Charles, C., Chevret, P., Semon, M., Tafforeau, P., Viriot, L., & Laudet, V. (2010). Evolutionary trends of the pharyngeal dentition in Cypriniformes (Actinopterygii: Ostariophysi). *PLoS One*, 5(6), e11293. <https://doi.org/10.1371/journal.pone.0011293>
- Turan, C. (2008). Molecular systematics of the *Capoeta* (Cypriniformes: Cyprinidae) species complex inferred from mitochondrial 16S rDNA sequence data. *Acta Zoologica Cracoviensia - Series A: Vertebrata*, 51A(1), 1–14. https://doi.org/10.3409/azc.51a_1-2.1-14
- Turan, D., Kottelat, M., & Ekmekçi, F. G. (2008). *Capoeta erhani*, a new species of cyprinid fish from Ceyhan River, Turkey (Teleostei: Cyprinidae). *Ichthyological Exploration of Freshwaters*, 19, 263–270.
- Türkmen, M., Erdoğan, O., Yıldırım, A., & Akyurt, İ. (2002). Reproduction tactics, age and growth of *Capoeta capoeta umbra* Heckel 1843 from the Askale Region of the Karasu River, Turkey. *Fisheries Research*, 54(3), 317–328. [https://doi.org/10.1016/S0165-7836\(01\)00266-1](https://doi.org/10.1016/S0165-7836(01)00266-1)
- Wautier, K., van der Heyden, C., & Huysseune, A. (2001). A quantitative analysis of pharyngeal tooth shape in the zebrafish (*Danio rerio*, Teleostei, Cyprinidae). *Archives of Oral Biology*, 46(1), 67–75. [https://doi.org/10.1016/S0003-9969\(00\)00091-1](https://doi.org/10.1016/S0003-9969(00)00091-1)
- Zardoya, R., & Ignacio, D. (1999). Molecular evidence on the evolutionary and biogeographical patterns of European cyprinids. *Journal of Molecular Evolution*, 49(2), 227–237. <https://doi.org/10.1007/p100006545>
- Zareian, H., Esmaili, H. R., Heudari, A., Khoshkholigh, R. M., & Mousavi-Sabet, H. (2016). Contribution to the molecular systematics of the genus *Capoeta* from the south Caspian Sea basin using mitochondrial cytochrome b sequences (Teleostei: Cyprinidae). *Molecular Biology Research Communications*, 5(2), 65.
- Zeng, Y., & Liu, H. (2011). The evolution of pharyngeal bones and teeth in Gobioninae fishes (Teleostei: Cyprinidae) analyzed with phylogenetic comparative methods. *Hydrobiologia*, 664(1), 183–197. <https://doi.org/10.1007/s10750-010-0598-8>

SUPPORTING INFORMATION

Additional Supporting Information may be found online in the supporting information tab for this article.

How to cite this article: Ayvazyan A, Vasilyan D, Böhme M. 3D morphology of pharyngeal dentition of the genus *Capoeta* (Cyprinidae): Implications for taxonomy and phylogeny. *J Zool Syst Evol Res*. 2018;00:1–12. <https://doi.org/10.1111/jzs.12217>

Possible species-flock scenario for the evolution of the cyprinid genus *Capoeta* (Cypriniformes: Cyprinidae) within late Neogene lake systems of the Armenian Highland

PLOS ONE

Possible species-flock scenario for the evolution of the cyprinid genus *Capoeta* (Cypriniformes: Cyprinidae) within late Neogene lake systems of the Armenian Highland

--Manuscript Draft--

Manuscript Number:	PONE-D-18-32717R2
Article Type:	Research Article
Full Title:	Possible species-flock scenario for the evolution of the cyprinid genus <i>Capoeta</i> (Cypriniformes: Cyprinidae) within late Neogene lake systems of the Armenian Highland
Short Title:	Possible species-flock scenario for the evolution of the cyprinid genus <i>Capoeta</i>
Corresponding Author:	Anna Ayvazyan Eberhard Karls Universitat Tübingen Tübingen, GERMANY
Keywords:	Erzurum, fishes, fossils, palaeobiogeography, pharyngeal teeth, Tekman, Çevirme
Abstract:	We studied 4 Ma old isolated pharyngeal teeth from lake sediments of Çevirme (Tekman Palaeolake, Erzurum Province) based on 3D morphology. As a result, we found that the Pliocene lake constitutes sympatric occurrence of four <i>Capoeta</i> species (<i>C. cf. umbla</i> , <i>C. cf. baliki</i> , <i>C. cf. sieboldi</i> and <i>C. sp. sevangi/capoeta</i>), whose modern relatives belong to a monophyletic clade inhabiting three different drainage systems of this region (Euphrates River, Kura River and Black Sea). We interpreted this high local diversity of closely related species in terms of the species-flock model. The Tekman palaeolake was a part of an unrecognized extended late Miocene to Pliocene palaeolake system in the present-day Armenian Highland, which has been disrupted by Pliocene tectonic activities. Surface uplift of the Armenian Highland contributed to the very characteristic biogeographic distribution and endemism of <i>Capoeta</i> in West Asian drainage systems. Thus, we proposed a species-flock scenario for the evolution and dispersal of the cyprinid genus <i>Capoeta</i> in a huge unrecognized palaeolake system in the present-day Armenian Highland.
Order of Authors:	Anna Ayvazyan Davit Vasilyan Madelaine Böhme
Opposed Reviewers:	
Response to Reviewers:	Rebuttal PONE-D-18-32717R1 Possible species-flock scenario for the evolution of the cyprinid genus <i>Capoeta</i> (Cypriniformes: Cyprinidae) within late Neogene lake systems of the Armenian Highland Comment #1: Using '3D shape characters' for inferring results as indicated in the abstract still is ambiguous, because you do not provide any corresponding analysis (as indicated by the reviewer). Just changing "3D morphology" into "3D shape characters" is not sufficient since 'lateral outline' and 'transverse cross sections' are 2D rather than 3D aspects! Therefore, using 3D referring to such characters is incorrect. To analyse 3D shape characters you have to use sophisticated analytical procedures such as geometric morphometrics, which, you, however argue to not be possible. I wonder if this really is true, because from my experience you are always able to find at least a few homologous points (even if there are only three to five). This, nevertheless, is still sufficient in most cases to produce results. Of course, you also have to use teeth from the same position for this, which has to be clarified before. Concluding: You have to change this if you are using 2D characters, or you have to make a detailed justification why these characters are 3-dimensionally in the method's section. Respond. We changed this part in abstract "Based on shape characters defined for 3D

Powered by Editorial Manager® and ProduXion Manager® from Aries Systems Corporation

	<p>models of modern species..." as these characters are distinguished within our previous study (Ayvazyan et al. 2018) based on the 3D models of studied samples.</p> <p>Comment #2: Please include Table 2 based on a modification of Table 1 of your previous publication and add the necessary size information. Respond: Table 2 is added.</p> <p>Comment #3: Change the captions of figures 1 and 2 into "... redrawn and modified from..." Respond: Done.</p> <p>Comment #4: Please make sure that the newly included section (lines 380 ff) will be proof read by a native speaker. There are some typos, grammar and wording errors (e.g., line 389, third word: it should read 'provides'; line 393: it should read "... also tested in benthophagous"; line 396: delete punctuation before "These..."; line 402: it should read "... should not be considered..."; line 407: "teeth" should read "tooth" Respond: Thank you, we took all the corrections in consideration and newly proof this section.</p> <p>Comment #5: You answered in detail the questions concerning the patterns of tooth wear in your letter to the editor but you did not include any of this in the manuscript. Please include a summary of your answer in the method's section and also a short paragraph in the discussion's section that tooth wear patterns are not considered by you as taxonomic characters based on Ayvazyan et al. (2018). Respond. We added a summary regarding to the patterns of tooth wear in Material and methods We think this information does not fit into any section of Discussion.</p> <p>Comment #6: - Please finally check if you are using any copyrighted figures. Respond. There is no any other copyrighted figures except the mentioned ones.</p> <p>Comment #7: - You need to include a final statement: No permits were required for the described study, which complied with all relevant regulations. Respond: Added in the end of manuscript.</p>
<p>Additional Information:</p>	
<p>Question</p>	<p>Response</p>
<p>Financial Disclosure</p> <p>Enter a financial disclosure statement that describes the sources of funding for the work included in this submission. Review the submission guidelines for detailed requirements. View published research articles from PLOS ONE for specific examples.</p> <p>This statement is required for submission and will appear in the published article if the submission is accepted. Please make sure it is accurate.</p>	<p>This study was funded in part by the German Academic Exchange Service (DAAD), ID: 57076385. This scholarship (Research fellowships for doctoral candidates and young scientists) was awarded to AA. The funder had no role in study design, data collection and analyses, decision to publish, or preparation of manuscript. No additional external funding was received for this study.</p> <p>German Academic Exchange Service (DAAD) website: https://www.daad.de/de/.</p>

<p>Unfunded studies Enter: <i>The author(s) received no specific funding for this work.</i></p> <p>Funded studies Enter a statement with the following details:</p> <ul style="list-style-type: none"> • Initials of the authors who received each award • Grant numbers awarded to each author • The full name of each funder • URL of each funder website • Did the sponsors or funders play any role in the study design, data collection and analysis, decision to publish, or preparation of the manuscript? • NO - Include this sentence at the end of your statement: <i>The funders had no role in study design, data collection and analysis, decision to publish, or preparation of the manuscript.</i> • YES - Specify the role(s) played. <p>* typeset</p>	
<p>Competing Interests</p> <p>Use the instructions below to enter a competing interest statement for this submission. On behalf of all authors, disclose any competing interests that could be perceived to bias this work—acknowledging all financial support and any other relevant financial or non-financial competing interests.</p> <p>This statement will appear in the published article if the submission is accepted. Please make sure it is accurate. View published research articles from PLOS ONE for specific examples.</p>	<p>The authors have declared that no competing interests exist.</p>

<p>Unfunded studies Enter: <i>The author(s) received no specific funding for this work.</i></p> <p>Funded studies Enter a statement with the following details:</p> <ul style="list-style-type: none"> • Initials of the authors who received each award • Grant numbers awarded to each author • The full name of each funder • URL of each funder website • Did the sponsors or funders play any role in the study design, data collection and analysis, decision to publish, or preparation of the manuscript? • NO - Include this sentence at the end of your statement: <i>The funders had no role in study design, data collection and analysis, decision to publish, or preparation of the manuscript.</i> • YES - Specify the role(s) played. <p>* typeset</p>	
<p>Competing Interests</p> <p>Use the instructions below to enter a competing interest statement for this submission. On behalf of all authors, disclose any competing interests that could be perceived to bias this work—acknowledging all financial support and any other relevant financial or non-financial competing interests.</p> <p>This statement will appear in the published article if the submission is accepted. Please make sure it is accurate. View published research articles from PLOS ONE for specific examples.</p>	<p>The authors have declared that no competing interests exist.</p>

<p>NO authors have competing interests</p> <p>Enter: <i>The authors have declared that no competing interests exist.</i></p> <p>Authors with competing interests</p> <p>Enter competing interest details beginning with this statement:</p> <p><i>I have read the journal's policy and the authors of this manuscript have the following competing interests: [insert competing interests here]</i></p>	
<p>* typeset</p> <p>Ethics Statement</p> <p>Enter an ethics statement for this submission. This statement is required if the study involved:</p> <ul style="list-style-type: none"> • Human participants • Human specimens or tissue • Vertebrate animals or cephalopods • Vertebrate embryos or tissues • Field research <p>Write "N/A" if the submission does not require an ethics statement.</p> <p>General guidance is provided below. Consult the submission guidelines for detailed instructions. Make sure that all information entered here is included in the Methods section of the manuscript.</p>	<p>The studied fossil material already housed in the Bundesanstalt für Geowissenschaften und Rohstoffe, Hannover (BGR collection numbers) and no additional excavation of fossils was undertaken.</p> <p>Recent comparative material (pharyngeal bones) is represented by adult individuals and comes from following collections: Bavarian State Collection for Anthropology and Palaeoanatomy Munich (SNSB), Palaeontological Collection of Tübingen University (GPIT) and National Museum of Natural Sciences of Madrid (MNCN) (including these of Fig 7, S2 Table). Both fossil and extant specimens publicly deposited in the above-mentioned collections and accessible by others in a permanent repository.</p>

Powered by Editorial Manager® and ProduXion Manager® from Aries Systems Corporation

<p>NO authors have competing interests</p> <p>Enter: <i>The authors have declared that no competing interests exist.</i></p> <p>Authors with competing interests</p> <p>Enter competing interest details beginning with this statement:</p> <p><i>I have read the journal's policy and the authors of this manuscript have the following competing interests: [insert competing interests here]</i></p>	
<p>* typeset</p> <p>Ethics Statement</p> <p>Enter an ethics statement for this submission. This statement is required if the study involved:</p> <ul style="list-style-type: none"> • Human participants • Human specimens or tissue • Vertebrate animals or cephalopods • Vertebrate embryos or tissues • Field research <p>Write "N/A" if the submission does not require an ethics statement.</p> <p>General guidance is provided below. Consult the submission guidelines for detailed instructions. Make sure that all information entered here is included in the Methods section of the manuscript.</p>	<p>The studied fossil material already housed in the Bundesanstalt für Geowissenschaften und Rohstoffe, Hannover (BGR collection numbers) and no additional excavation of fossils was undertaken.</p> <p>Recent comparative material (pharyngeal bones) is represented by adult individuals and comes from following collections: Bavarian State Collection for Anthropology and Palaeoanatomy Munich (SNSB), Palaeontological Collection of Tübingen University (GPIT) and National Museum of Natural Sciences of Madrid (MNCN) (including these of Fig 7, S2 Table). Both fossil and extant specimens publicly deposited in the above-mentioned collections and accessible by others in a permanent repository.</p>

Powered by Editorial Manager® and ProduXion Manager® from Aries Systems Corporation

<p>Format for specific study types</p> <p>Human Subject Research (involving human participants and/or tissue)</p> <ul style="list-style-type: none"> • Give the name of the institutional review board or ethics committee that approved the study • Include the approval number and/or a statement indicating approval of this research • Indicate the form of consent obtained (written/oral) or the reason that consent was not obtained (e.g. the data were analyzed anonymously) <p>Animal Research (involving vertebrate animals, embryos or tissues)</p> <ul style="list-style-type: none"> • Provide the name of the Institutional Animal Care and Use Committee (IACUC) or other relevant ethics board that reviewed the study protocol, and indicate whether they approved this research or granted a formal waiver of ethical approval • Include an approval number if one was obtained • If the study involved <i>non-human primates</i>, add <i>additional details</i> about animal welfare and steps taken to ameliorate suffering • If anesthesia, euthanasia, or any kind of animal sacrifice is part of the study, include briefly which substances and/or methods were applied <p>Field Research</p> <p>Include the following details if this study involves the collection of plant, animal, or other materials from a natural setting:</p> <ul style="list-style-type: none"> • Field permit number • Name of the institution or relevant body that granted permission 	
<p>Data Availability</p> <p>Authors are required to make all data underlying the findings described fully available, without restriction, and from the time of publication. PLOS allows rare exceptions to address legal and ethical concerns. See the PLOS Data Policy and FAQ for detailed information.</p>	<p>Yes - all data are fully available without restriction</p>

Powered by Editorial Manager® and ProduXion Manager® from Aries Systems Corporation

<p>Format for specific study types</p> <p>Human Subject Research (involving human participants and/or tissue)</p> <ul style="list-style-type: none"> • Give the name of the institutional review board or ethics committee that approved the study • Include the approval number and/or a statement indicating approval of this research • Indicate the form of consent obtained (written/oral) or the reason that consent was not obtained (e.g. the data were analyzed anonymously) <p>Animal Research (involving vertebrate animals, embryos or tissues)</p> <ul style="list-style-type: none"> • Provide the name of the Institutional Animal Care and Use Committee (IACUC) or other relevant ethics board that reviewed the study protocol, and indicate whether they approved this research or granted a formal waiver of ethical approval • Include an approval number if one was obtained • If the study involved <i>non-human primates</i>, add <i>additional details</i> about animal welfare and steps taken to ameliorate suffering • If anesthesia, euthanasia, or any kind of animal sacrifice is part of the study, include briefly which substances and/or methods were applied <p>Field Research</p> <p>Include the following details if this study involves the collection of plant, animal, or other materials from a natural setting:</p> <ul style="list-style-type: none"> • Field permit number • Name of the institution or relevant body that granted permission 	
<p>Data Availability</p> <p>Authors are required to make all data underlying the findings described fully available, without restriction, and from the time of publication. PLOS allows rare exceptions to address legal and ethical concerns. See the PLOS Data Policy and FAQ for detailed information.</p>	<p>Yes - all data are fully available without restriction</p>

48 system include rather short and small but numerous drainage systems of the
49 Mediterranean Sea Basin (this territory includes southern Anatolia, Syria, Lebanon, Israel,
50 the Arabian Peninsula), Black Sea Basin (northern Anatolia and Western Georgia), the
51 Tigris-Euphrates (Persian Sea Basin) and Kura-Araxes basins, most of Iranian territory
52 (Caspian Sea Basin) [1].

53 The four main rivers of Western Asia and the Ponto-Caspian region (Euphrates, Tigris,
54 Kura and Araxes) all originate in the Armenian Highland (Fig 1a). The history and
55 formation of these water basins remain largely unknown. To track the evolution of
56 drainage basins, fossil records of aquatic faunas can be used. Recently, Vasilyan &
57 Carnevale (2013) shown, using the fossil record of the genus *Garra* from Armenia, that
58 area including the upper reaches of the present-day Araxes River drainage system
59 belonged to the Protoeuphrates-Tigris drainage system in the latest Miocene [7, 8] [earlier
60 [7] the age of the locality has been dated to Pliocene, the new results [8] suggest slightly
61 older age latest Miocene].

62 In the present study, we trace back the fossil record of the genus *Capoeta* to 4 Ma, using
63 fossil material found at the Pliocene age locality Çevirme (Erzurum Province, Tekman
64 district) in Eastern Turkey (Fig. 1a and 1b). The study sets the following goals: (1) to apply
65 the established methodology [9] for species-level identification of isolated pharyngeal
66 teeth of *Capoeta*; (2) to determine species composition within the fossil sample; (3) to
67 evaluate the history and coverage of lacustrine sediments in Western Asia and the Ponto-
68 Caspian region; and (4) to discuss evolutionary models for the genus *Capoeta* with
69 respect to its biogeography.

48 system include rather short and small but numerous drainage systems of the
49 Mediterranean Sea Basin (this territory includes southern Anatolia, Syria, Lebanon, Israel,
50 the Arabian Peninsula), Black Sea Basin (northern Anatolia and Western Georgia), the
51 Tigris-Euphrates (Persian Sea Basin) and Kura-Araxes basins, most of Iranian territory
52 (Caspian Sea Basin) [1].

53 The four main rivers of Western Asia and the Ponto-Caspian region (Euphrates, Tigris,
54 Kura and Araxes) all originate in the Armenian Highland (Fig 1a). The history and
55 formation of these water basins remain largely unknown. To track the evolution of
56 drainage basins, fossil records of aquatic faunas can be used. Recently, Vasilyan &
57 Carnevale (2013) shown, using the fossil record of the genus *Garra* from Armenia, that
58 area including the upper reaches of the present-day Araxes River drainage system
59 belonged to the Protoeuphrates-Tigris drainage system in the latest Miocene [7, 8] [earlier
60 [7] the age of the locality has been dated to Pliocene, the new results [8] suggest slightly
61 older age latest Miocene].

62 In the present study, we trace back the fossil record of the genus *Capoeta* to 4 Ma, using
63 fossil material found at the Pliocene age locality Çevirme (Erzurum Province, Tekman
64 district) in Eastern Turkey (Fig. 1a and 1b). The study sets the following goals: (1) to apply
65 the established methodology [9] for species-level identification of isolated pharyngeal
66 teeth of *Capoeta*; (2) to determine species composition within the fossil sample; (3) to
67 evaluate the history and coverage of lacustrine sediments in Western Asia and the Ponto-
68 Caspian region; and (4) to discuss evolutionary models for the genus *Capoeta* with
69 respect to its biogeography.

70 **Fig 1. The Armenian Highland.** (a), Fossil locality marked by red contoured circle in a relation to
71 the Euphrates-Tigris and Araxes-Kura water basins. (b), map showing the fossil locality marked
72 by red contoured circle. Map data: Figure 1 (a, b) is redrawn and modified from U. S. Geological
73 Survey, CC BY 4.0.

74 **Species flock concept in ichthyology**

75 A species flock is a monophyletic group of closely related sympatric species inhabiting the
76 same area or geographically restricted area. The species flock is common for both
77 vertebrate and invertebrate animals, which show rapid adaptive radiation, morphological
78 divergence and speciation [10–13]. The examples of species flock are recorded in
79 different groups of animals: insects, fishes, lizards and birds, [14–19]. Especially
80 monophyletic groups of fishes represent a particular interest, as one of the criteria of the
81 species to be considered as a species flock is the monophyly of the described
82 groups/species [20, 21].

83 Two main well-known species flocks of cyprinids fishes are found in the Philippine Lake
84 Lanao and the Ethiopian Lake Tana [18, 22–24]. Besides the extant species flocks, some
85 potential fossil species flocks are also reported, e.g., from the Eocene site in Tanzania,
86 the upper Miocene Lukeino Formation in the Tugen Hills of the Central Rift Valley of Kenya
87 [17].

88

89 **Cyprinid pharyngeal dentition**

90 The oral jaws (e.g. dentary, maxilla, premaxilla) of cyprinids are toothless. Instead they
91 have pharyngeal teeth located on the pharyngeal bones [25]. Both left and right fifth
92 ceratobranchials are modified into pharyngeal jaws, which have the function of food

93 processing [25, 26]. The pharyngeal bones and teeth provide important taxonomic
94 characters for systematics of the cyprinid fishes. The number and arrangement of the
95 pharyngeal teeth in tooth rows are recognized and widely used diagnostic characters for
96 cyprinid classification [27].

97 The fossil remains of cyprinids are mainly represented by isolated pharyngeal teeth [28]
98 and it is hard to identify specimens based on sole isolated teeth. Therefore, the fossil
99 record of many cyprinids, included the genus *Capoeta*, is still largely unknown.

100

101 **The fossil record of the genus *Capoeta***

102 According to the molecular data, the genus *Capoeta* originates around the Langhian–
103 Serravallian boundary (13.9 Ma) and diversification within the genus occurs along the
104 Middle Miocene – Late Pliocene period [29].

105 The scarce fossil record of *Capoeta* comes from four localities, two from the late Miocene
106 and two from the Pleistocene. Miocene *Capoeta* fossils are known from Armenia and
107 Georgia, both in the present-day Kura-Araxes drainage basin (Fig 2). The first fossil
108 remains of *Capoeta nuntius* are described by Bogachev (1927) at the late Miocene locality
109 in the Kistibi, Samtskhe-Javakheti region, Georgia [30, 31]. The material is represented
110 by three more or less complete and a few strongly damaged skeletons as well as more
111 than 70 isolated bone fragments. Vasilyan & Carnevale (2013) describe skeletons of
112 *Capoeta* sp. from the Jradzor locality (latest Miocene) in Armenia [32]. The record of
113 *Capoeta* from late Pliocene sediments at Ericek (Cameli Basin, SW Anatolia) is doubtful
114 [33], since the tooth morphologies (Fig 4 a-d in [33]) are not found within pharyngeal teeth

5

115 of the *Capoeta* species. Instead of this, they resemble the morphology of the genus
116 *Luciobarbus*; as the reported cobitid and gobiid remains are snake jawbones. Vasilyan et
117 al. (2014) describe two isolated pharyngeal teeth and two fragments of serrated dorsal fin
118 rays referred to *Capoeta* sp. from the early Pleistocene locality Pasinler (Erzurum
119 Province, north-eastern Turkey). Fossil remains of *Capoeta damascina* Valenciennes,
120 1842 are also recorded from the Hula Palaeolake [34]. The site is situated in the northern
121 part of the Dead Sea Rift, Israel and dated to the Middle Pleistocene (0.78 Ma).

122 **Fig 2. Geographical overview of the drainage systems of Western Asia and the Ponto-**
123 **Caspian regions (Euphrates-Tigris, Araxes-Kura).** Red star (1) indicates the position of the
124 Çevirme locality. The red circle shows the possible extension of palaeolake system of the
125 Armenian Highland. The arrows show the late distribution of the recorded fossil *Capoeta* species
126 into the different water basins due to the tectonic disruption of the Lake system during the Pliocene
127 uplift period. The two already known late Miocene fossil sites Kısatibi (red star 2) and Jradzor (red
128 star 3) are included as well. Map data: Figure 2 is redrawn and modified from U. S. Geological
129 Survey CC BY 4.0.

130

131 **Biogeographical distribution of extant *Capoeta* species**

132 According to the molecular data, the monophyletic genus *Capoeta* is represented by three
133 main clades: Mesopotamian, Anatolian-Iranian and Aralo-Caspian clades and nested
134 within the genus *Luciobarbus* as a sister group of the species *Luciobarbus*
135 *subquincunciatus* [29, 35, 36] (Fig 3a and 3b). The Mesopotamian group contains species
136 distributed in the Tigris-Euphrates drainage system and adjacent water basins: *Capoeta*
137 *trutta* (Heckel, 1843), *Capoeta turani* Özulu & Freyhof, 2008 and *Capoeta barroisi* Lortet,
138 1894. The Anatolian-Iranian group includes species inhabiting the Black Sea Basin:

6

139 *Capoeta sieboldi* Steindachner, 1864, *Capoeta baliki* Turan, Kottelat, Ekmekçi &
140 Imamoglu, 2006, *Capoeta banarescui* Turan, Kottelat, Ekmekçi & Imamoglu, 2006. The
141 Mediterranean drainage basins (Anatolian-Iranian clade) of southeastern Turkey, the
142 Tigris–Euphrates river system, and small rivers, which drain into the gulfs of Persia and
143 Oman, as well as inland water bodies in Iran contain the following species: *Capoeta*
144 *buhsei* Kessler, 1877, *Capoeta saadii* (Heckel, 1847), *Capoeta caelestis* Schöter, Özulu
145 & Freyhof, 2009, *Capoeta damascina*, *Capoeta angorae* (Hankó, 1925) and *Capoeta*
146 *kosswigi* Karaman, 1969. Finally, the Aralo-Caspian group includes the species
147 distributed in the Kura and Araxes rivers, as well as Aral and Caspian Sea drainages:
148 *Capoeta capoeta* Gldenstdt, 1773, *Capoeta sevangi* De Filippi, 1865, *Capoeta aculeata*
149 (Valenciennes, 1844) (S1 Table) [29].

150 A recent phylogenetic analysis [9], using the morphologies of pharyngeal teeth of ten
151 *Capoeta* species, groups them in four main clades. Three of these clades show the same
152 tree topography that the molecular data provides, the remaining clade groups differently
153 [9].

154 **Fig 3. Phylogeny of the genus *Capoeta*.** (a), distinguished clades within the genus
155 *Capoeta* (*Luciobarbus suquincunciatus* is the sister clade) (Levin et al., 2012). The clade
156 diagnostic shape classes of recorded clades within the fossil material (see Fig.7,
157 Ayvazyan et al. 2018) are given in capital letters included 3D images of teeth of *Capoeta*
158 as well as the a2 tooth of *L. subquincunciatus*. The monophyletic Anatolia-Iranian/Aralo-
159 Caspian/*sieboldi* clade, for which we propose a species flock model of evolution, is
160 marked by red colour. (b), the location of *Capoeta* clade within phylogenetic tree based
161 on the molecular genetic analysis (Levin et al., 2012).

162

163 **Late Neogene lacustrine sedimentation in the Armenian Highland**

164 Present-day Armenian Highland (Eastern Anatolia, Armenia, Iranian Azerbaijan,
165 Samtskhe-Javakheti region of Georgia) is composed of the high mountainous landscapes
166 of the Eastern Taurides with elevations between 1.700 to over 5.000 meters above sea
167 level. Because of the dominant arid climate during the late Holocene, lakes are rare in this
168 region. Two endorheic saline lakes, Lake Van and Lake Urmia, as well as the freshwater
169 Lake Sevan are notable exceptions (Figs 1a and 2). However, geologic mapping revealed,
170 that during the pre-Quaternary lacustrine, sedimentation was widespread and long lasting
171 in this region. According to Altınlı (1966) during the Late Miocene and Pliocene (11.6-2.6
172 Ma) lacustrine sedimentation dominated Eastern Anatolia with regional thicknesses of
173 deposits over 1.000 m. These sediments contain a rich freshwater fauna (e.g. diatoms,
174 gastropods, bivalvs, ostracods, fishes); [37–42] and have been variously attributed to the
175 Horasan Formation, Gelinkaya Formation, Işıklar Formation (all in the Erzurum Province),
176 Zırnak Formation (Bitlis Province), Çaybağı Formation (Elazığ Province), or to the
177 Parçikan Formation (Malatya Province). Despite extensive syn-sedimentary volcanism,
178 none of these formations are radiometrically dated, but available K-Ar data [43] and rare
179 rodent fossils [44, 45] suggest that the main lacustrine phase in Eastern Anatolia centred
180 between 6 and 3 Ma, probably coeval with the supposed uplift of this region [46].

181 An older lacustrine period is documented in Iranian Azerbaijan, where fish bearing
182 (Atherinidae, Cyprinodontidae, Leuciscinae, but no Barbinae) lake sediments from the
183 Tabriz Basin ('lignite beds', 'fish beds') have been dated to between 12 and 7.5 Ma [47].

184 These late Neogene lacustrine sediments have tectonically fragmented exposure over a
185 huge area in the Eastern Taurides stretching several hundreds of kilometres, notably

186 including the upper reaches of present-day Euphrates, Tigris, Kura and Araxes rivers (Fig
187 2).

188

189 **Fossil locality Çevirme**

190 The fossil site Çevirme (Erzurum Province, Tekman district) is located 12 km west of the
191 Hacıömer village on the road from Hacıömer to Tekman, 500 m after the bridge over the
192 Araxes River (coordinates: N 39° 37' 37"; E 41° 38'; Figs 1a, 1b and 2). The locality
193 belongs to the Tekman Basin (East-Anatolian Taurides), approximately 40 km south from
194 the Pasinler Basin and 120 km north-northwest of Lake Van. Late Neogene sediments in
195 the Tekman Basin laying discordant over early Miocene marine limestones [48]. The
196 sedimentary facies of the basin infill change from fluvial-alluvial to lacustrine. The late
197 Miocene sedimentary formation (Hacıömer Formation) is composed of an approximately
198 300 m thick reddish-brown sequence of conglomerates, sandstone and silts with minor
199 intercalation of marls. In the south of the basin, the alteration with vulcanites appear. These
200 terrestrial-fluvial fossil free layers intercalate in their upper parts with nearly 200 m thick
201 lacustrine sediments of the Işıklar Formation, which mainly consist of light grey, as well as
202 slightly reddish freshwater carbonates (Fig 1b). Layers of marl, organic rich clay and tufa
203 are also present. The section is covered by Pleistocene basalts from the Bingöl Dag area
204 [48].

205 The fossil site Çevirme, discovered and first described by Sickenberg (1975), belongs to
206 the lacustrine upper part of the Işıklar Formation. The 65 m thick stratigraphic section is
207 subdivided based on lithological and sedimentological characters. The fossil remains of
208 fishes, molluscs and mammals are found at 18 m depth of the section (Fig 4). Earlier

9

368 shape classes "A", "J" and "R" (a2 tooth position) comprise 10% of studied isolated fossil
369 pharyngeal teeth (S1 and S2 Figs).

370 Morphological observations of isolated fossil pharyngeal teeth revealed, besides the main
371 distinguished characters (lateral outline (α) and transverse cross-section (β)), further
372 characters commonly occurring within both recent and fossil *Capoeta*. They are "ruptures"
373 of the grinding surface and the crenated edge of the grinding surface, which are variable
374 and depending on the degree of tooth wearing (Fig 7) (details see Ayvazyan et al., 2018).
375 These structures are not considered as a species characteristic.

376 **Fig 7. Additional morphological characters (besides the shape characters ($\alpha\beta$) in**
377 **fossil and extant pharyngeal teeth (not to scale).** (a), *Capoeta* sp., b3 tooth (extant)
378 (SAPM-PI-00719, SNSB). (b), *C. trutta*, a5 tooth (extant) (SAPM-PI-02908, SNSB). (c-d),
379 isolated fossil pharyngeal teeth (identified as shape class "C" and "F" respectively) (BGR
380 6, 16). (e), isolated fossil pharyngeal tooth (BGR 5). (f), *C. capoeta*, b2 tooth (extant)
381 (GPIT-OS-00860^a), both are identified as shape class "M". The ruptures of grinding
382 surface are marked by red arrows (a, b, c, d) and an example of very similar tooth
383 morphology in fossil (e) and extant (f) isolated pharyngeal teeth.

384

385 Discussion

386 In our fossil samples, we record eight shape classes where the genus diagnostic shape
387 class "C" dominates the assemblage (53%). Identified shape classes as species or clade
388 diagnostic (A, J, R, M) compose 10% of the assemblage (S1 Fig).

389 **Possible influence of plasticity and allometry on high diversity of recorded shape**
390 **classes**

391 The literature provides examples of the potential effects of plasticity on the dentary bone
392 and tooth morphology mainly in cichlid fish cultures by applying contrasting diets (soft and
393 hard) [50–53]. These studies recorded some degree of phenotypic plasticity of dentary
394 bone morphology and in some cases tooth size. The influence of these two diets on the
395 development of the cyprinid pharyngeal dentition is also tested in the benthophagous
396 cyprinid black carp. Dietary did not change the tooth morphology, but, instead, it has been
397 found that broad diet may influence the frequency of tooth replacement and size patterns
398 [54]. These studies are mainly based on aquarium experiments in benthophagous species
399 where two extreme diets (commercial fish as a soft and snails as hard food) are tested.
400 Under natural conditions, fishes are not forced to feed on only one type of food. Thus, it
401 is data can be applied to, in the present paper studied algae-scraping species *Capoeta*,
402 which are recorded from single geological layer and are sympatric individuals in a uniform
403 environment. Considering this, the effect of feeding on different food should not be
404 considered biasing on the carp pharyngeal tooth morphology, and, thus, we exclude the
405 effect of plasticity on the studied fossil material.

406 Allometric shifts in pharyngeal tooth morphology cannot explain the high diversity of
407 recorded shape classes in the studied fossil samples. Morphological shape remodeling in
408 cyprinids happens in very early stages of their ontogeny. Juveniles (standard size of a few
409 mm) have different tooth morphology than the adult samples, but the significant
410 morphological changes are finalized in this early stage. Thus, the adult dentition in cyprinid
411 fishes is completed by at the later larvae or juvenile stages [55]. Our fossil material is

412 represented by adult individuals, as the studied fossil pharyngeal teeth sizes vary between
413 0.8 – 3 mm (it is a sampling artifact introduced by mesh size limitation washing collection
414 technique). Therefore, our fossil samples is composed of isolated pharyngeal teeth of
415 adult individuals.

416

417 **Taxonomic assignment**

418 For species-level taxonomy we discuss two possible interpretations. The assemblage can
419 be interpreted to document either a single, very heterodont species or several *Capoeta*
420 species.

421 **1. The fossil assemblage documents one species.** The recent *Capoeta* species are
422 characterized by different degree of heterodonty, which varies between three and six
423 shape classes per species. For instance, *C. damascina*, the most heterodont extant
424 species, is characterized by six different shape classes [9]. The second most heterodont
425 species *C. umbla* (Heckel, 1843) is characterized by five different shape classes, four of
426 them are shared with *C. damascina*. Eight shape classes, as found in our fossil samples,
427 is unprecedented among extant species. It is also highly unlikely that a fossil species
428 shows this degree of heterodonty, given the ten tooth positions at pharyngeal bones are
429 present. Therefore, we consider the 'single species' interpretation as rather unlikely.

430 **2. The fossil assemblage represents more than one species.** The specific
431 identification of extant *Capoeta* species is possible only on the morphology of the teeth at
432 the tooth position a2 [9]. The Çevirme association contains four shape classes, which are
433 species-specific among recent taxa at the a2 position: the shape class "A" characterizes

20

434 *C. umbla*, the shape class “J” is typical for *C. baliki* (both species belong to the Anatolian-
435 Iranian clade) and the shape class “R” is found only in *C. sieboldi* (*sieboldi* clade). The
436 shape class “M” is shared at the a2 position by two closely related Aralo-Caspian species
437 *C. capoeta* and *C. sevangi*. Therefore, we assume that the Çevirme assemblage is
438 constituted of four species.

439 The four discussed extant species are also characterized by other shape classes, which
440 are not found within the studied fossil material. The shape class “I” is common in *C. umbla*
441 and *C. baliki*, it occurs at the topological positions b2, b3 and c2. These teeth are small
442 and may not be found due to taphonomic or sampling bias (tooth diameter is smaller than
443 0.8 mm). Two additional shape classes “N” and “O”, which are missing in our sample,
444 characterize the two Aralo-Caspian *Capoeta* species *Capoeta sevangi* and *Capoeta*
445 *capoeta*, at the tooth position a2. We interpret the lack of these species characteristic
446 shape classes by younger divergence of these species (see below).

447 Our results indicate the presence of possible four species in the fossil assemblage, which
448 belong to three different clades (Anatolian-Iranian, Aralo-Caspian, and *sieboldi* clades) of
449 the genus *Capoeta*. According to all molecular studies [29, 56, 57], these three clades are
450 monophyletic and sister groups to the Mesopotamian clade (Fig 3a).

451 **The evolution of the genus *Capoeta* as a species flock scenario**

452 Greenwood (1984) suggests that, in order to identify a group of organisms as species
453 flock, the representatives should be monophyletic and endemic to an area they inhabiting
454 [21]. Later on, five main criteria are distinguished to detect the flock species [13, 58]: 1)
455 monophyly, 2) high species diversity (speciosity), 3) high level of endemism, 4)
456 morphological and ecological diversity; and 5) habitat dominance in terms of biomass. A

21

457 later study [59], suggests to concentrate on three robust, easier to determine criteria such
458 as monophyly, endemism and speciosity. This study suggests ranking the ecological
459 criterion as secondary. Our fossil *Capoeta* samples correspond to all five criteria sensu
460 Eastman and McCune (2000) and can thus be regarded as a species flock. The extant
461 *Capoeta* is a monophyletic phytophagous barbin genus, widely distributed in West Asian
462 and the Ponto-Caspian water basins and comprise 30 extant species [5, 29, 35, 56]. Our
463 four fossil species (*Capoeta cf. umbla*, *C. cf. baliki*, *C. cf. sieboldi*, *C. sp. capoeta/sevangi*)
464 belong to a monophyletic clade composed of *Capoeta sieboldi*, Anatolian-Iranian and
465 Aralo-Caspian species (Fig 3a) endemic to the drainage systems of the Black and Caspian
466 seas and Persian Gulf (Fig 2), thus, fulfilling the three main criteria for species flock
467 recognition [59]. Certainly, we cannot be fully definite that our fossil taxa are also
468 monophyletic. However, considering that the phylogenetic analysis using the morphology
469 of extant pharyngeal teeth [9] placed the species in the same topology as the molecular
470 phylogenetic analysis, we are confident that the fossil species attribution correspond to
471 extant taxa. Nevertheless, as in every biological study species identification retain certain
472 degree of uncertainty, which would potentially affect the probable monophyly of the fossil
473 taxa.

474 The endemic occurrence of the genus *Capoeta* in Western Asia and the Ponto-Caspian
475 region is supported by its exclusive extant and fossil record in the region [7, 30, 60–62].
476 The taxonomic studies of this genus show the morphological and meristic diversity of the
477 extant *Capoeta* species [9, 39, 63–65], but detailed ecologic studies are lacking so far.
478 The fifth criteria (habitat dominance in terms of biomass) is more difficult to access for the
479 fossil palaeocommunity. However, within the studied samples from the locality Çevirme
480 *Capoeta* dominates not only by the species richness over *Leuciscus* (one undetermined

481 medium-size species), but also in terms of numbers of specimens (247 *Capoeta* teeth
482 versus 41 *Leuciscus* teeth), suggesting habitat dominance of *Capoeta* in the Tekman
483 Palaeolake of the Işıklar Formation 4 Ma ago.

484 Our results are largely in agreement with estimated divergence times within *Capoeta* [57],
485 showing that at 4 Ma *C. sieboldi* is already diverged and the Aralo-Caspian clade species
486 *C. capoeta* and *C. sevangi* are not yet separated, which explains the lack of their species-
487 specific tooth shape classes "N" and "O". The fossil Aralo-Caspian clade taxon may,
488 therefore, represent a new undescribed species ancestral to the extant members of this
489 clade. However, published divergence times seem to be overestimated since the fossil
490 calibration points used for the molecular clock are too old, maybe by a factor of two *Barbus*
491 sp. set at 18 Ma citing Böhme & Ilg 2003 refer in fact to *Barbus* s. l., which is probably
492 closer related to *Cyprinion*; the oldest *Barbus* s. s. fossils are known from sediments of
493 age at least 8 Ma, Böhme unpublished data) [66]. Nevertheless, the oldest unequivocal
494 *Luciobarbus* with affinities to *L. subquincunciatus* (the sister clade of *Capoeta*, Fig. 3a and
495 3b) is *L. vindobonensis* from 9.8 Ma old deposits in Austria [67], suggesting that the
496 evolution of *Capoeta* is largely a late Miocene event.

497 The presence of a four-million-year old *Capoeta* species flock in the Tekman Basin with
498 members of three recent clades is very remarkable. We hypothesize, that the Tekman
499 Palaeolake, which was part of a large Armenian Highland lake system, was a place of the
500 speciation of *Capoeta* species related to the three recent clades of the genus (Anatolian-
501 Iranian, Aralo-Caspian and *sieboldi*). Moreover, the huge Armenian Highland lake system,
502 which formed during the late Miocene and represents the source of all major rivers in

503 Western Asia and the Ponto-Caspian region where *Capoeta* is widely distributed, could
504 represent the centre of origin of *Capoeta* including its Mesopotamian clade.

505 A recent study shows that tectonic reorganization in the region, starting about the
506 Miocene-Pliocene transition (ca. 5.5 Ma) along the East and North Anatolian faults [46,
507 68]. It resulted in substantial surface uplift and probably caused the gradual reshaping of
508 the hydrological network in the area. This could largely contribute to dispersal and further
509 speciation of the members of the species flock into their distribution areas nowadays.

510 The possible species flock scenario of the genus *Capoeta* as well as the reorganization
511 of the palaeolake system in Armenian Highland are hypothetically illustrated in Figure 8,
512 where three main stages of lake evolution.

513 **Fig 8. Hypothetical evolutionary stages of the palaeolake system of Armenian**
514 **Highland since latest Miocene.** Three main stages are suggested (marked by blueish
515 colours): formation, maximum of lake expansion, decay and fully development of present-
516 day drainage system. The monophyletic clade of recorded species within the fossil
517 material shows the presence of the species flock of *Capoeta* at 4 Ma ago in palaeolake
518 system of Armenian Highland.

519 The other possible explanation of our results could be the concept of secondary contact.
520 This scenario (speciation of hybrids) is very similar to the above suggested species flock
521 model, however, without any genetic information we cannot be precise about this
522 hypothesis. More studies and more fossil sites inside and outside distribution area of
523 *Capoeta* are needed to test our hypothesis, but according to the current available data,
524 the fossil species flock interpretation is the most plausible.

525 **Conclusions**

526 For the first time, a detailed study of the isolated fossil pharyngeal teeth of the genus
527 *Capoeta* (n=247) is provided. The description and identification of the fossil material
528 from Çevirme (Erzurum Province, Tekman district) is based on the methodology
529 introduced by Ayzazyan et al. 2018. We show that our methodology is applicable to
530 the fossil record of the genus *Capoeta* and allows identification of the isolated fossil
531 pharyngeal teeth at species level. Within the studied fossil material eight shape classes
532 are distinguished, four of them are species or clade diagnostic and indicate the
533 presence of the four sympatric *Capoeta* species (*C. cf. sieboldi*, *C. cf. umbla*, *C. cf.*
534 *baliki* and *C. sp. capoeta/sevangi*) in the Tekman Palaeolake at 4 Ma. These four
535 species belong to a monophyletic clade of the genus and today they are distributed in
536 different water basins (Euphrates/Kura/Black Sea) of Western and Ponto-Caspian
537 region. We interpret this high local diversity of closely related species in terms of the
538 species-flock model.

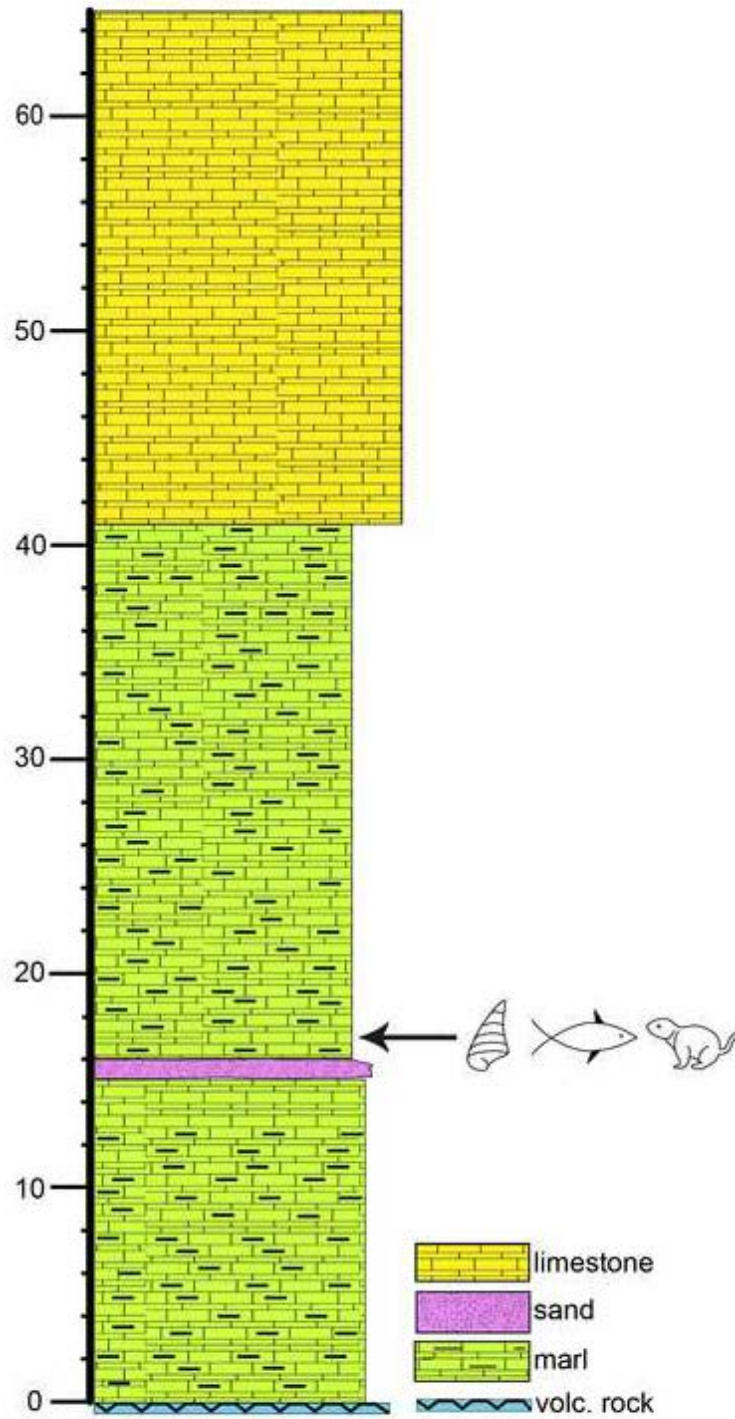
539 Literature review suggests that the Tekman Palaeolake was part of an unrecognized
540 huge late Miocene to Pliocene palaeolake system in the present-day Armenian
541 Highland and we hypothesized that the evolution of *Capoeta* occurred there during the
542 late Miocene. Pliocene tectonic activities disrupted this lake system and resulted in the
543 very characteristic biogeographic distribution of *Capoeta* in West Asian and Ponto-
544 Caspian drainage systems today.

545

546 **Acknowledgments**

Figure

[Click here to access/download;Figure;Fig4_new.tif](#)



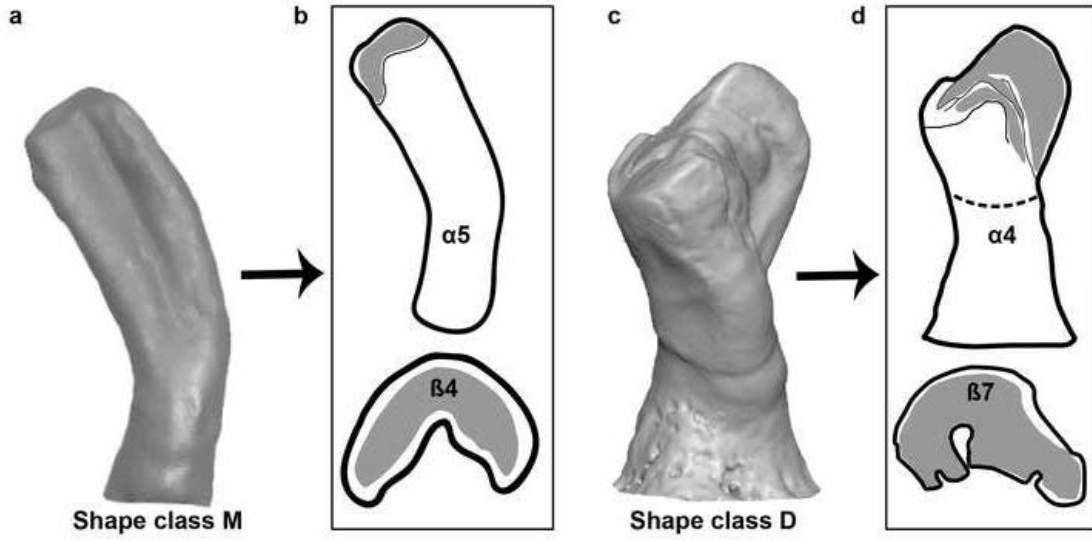
Figure

[Click here to access/download:Figure;Fig5.tif](#)



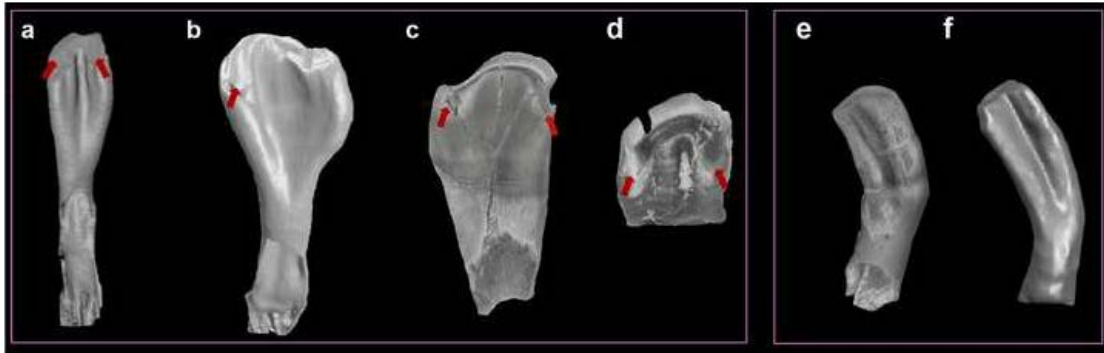
Figure

[Click here to access/download;Figure;Fig6.tif](#)



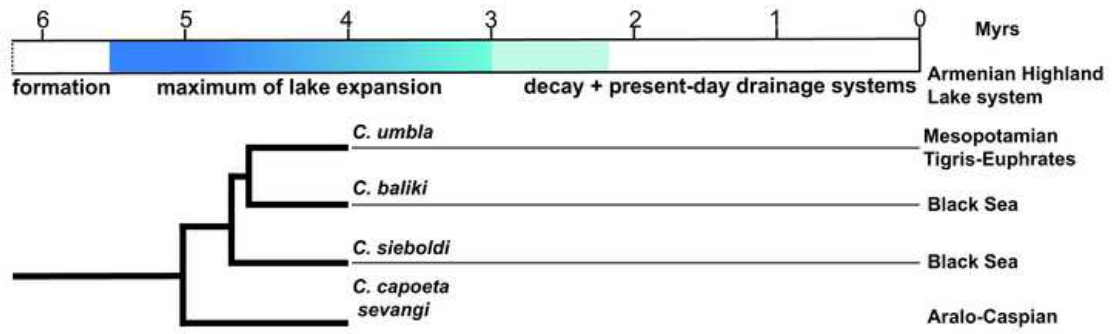
Figure

[Click here to access/download;Figure;Fig7.tif](#)



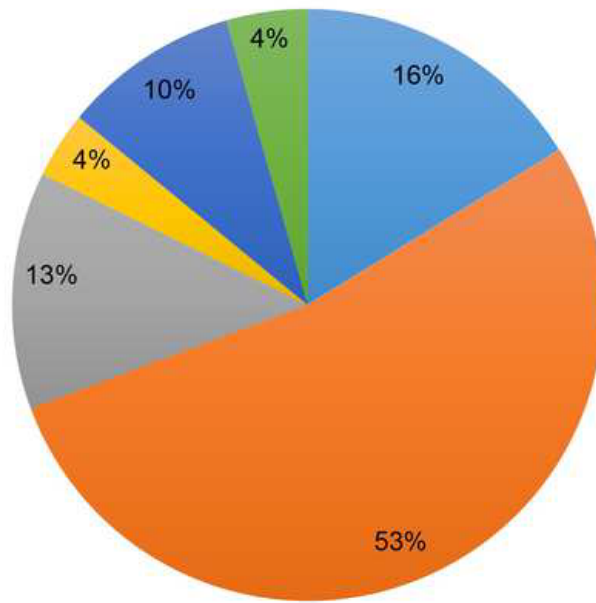
Figure

[Click here to access/download;Figure;Fig8.tif](#)



S1_Fig

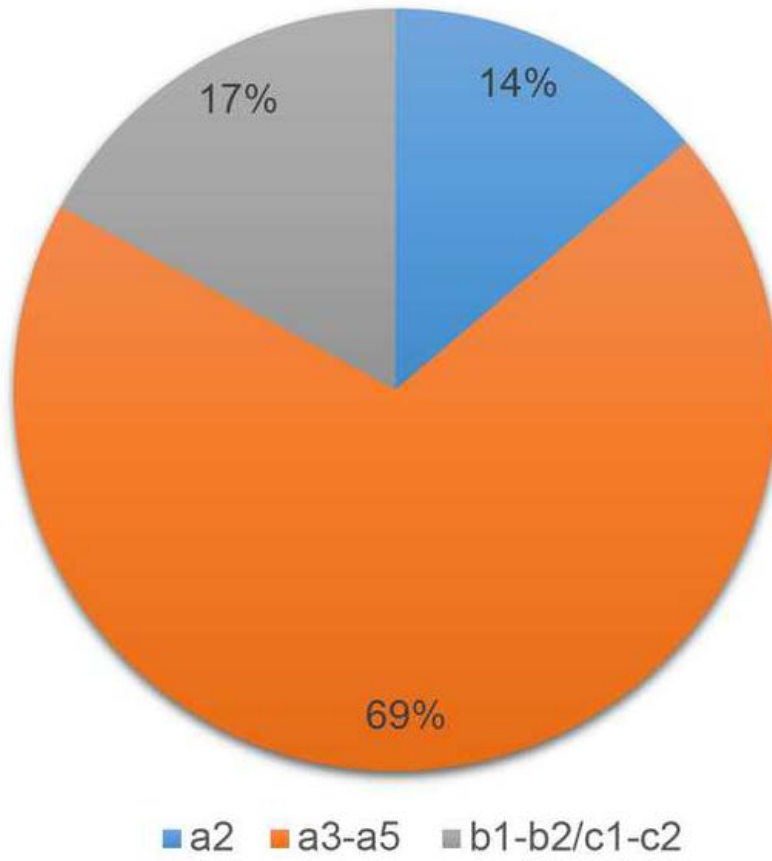
[Click here to access/download:Figure:S1_Fig.tif](#)



- | | | | |
|-----------------|------------------|----------------------------|--------------------|
| ■ shape class B | | ■ shape class H | |
| ■ shape class C | genus diagnostic | ■ shape classes A, J, R, M | species diagnostic |
| ■ shape class F | | ■ other shape classes | |

S2_Fig

[Click here to access/download;Figure;S2_Fig.tif](#)



7. Appendix II: Submitted Manuscript

Fish, amphibian and reptilian faunas from the latest Oligocene o middle Miocene localities from Central Turkey

Palaeobiodiversity and Palaeoenvironments

Fish, amphibian and reptilian faunas from the latest Oligocene to middle Miocene localities from Central Turkey
--Manuscript Draft--

Manuscript Number:	
Full Title:	Fish, amphibian and reptilian faunas from the latest Oligocene to middle Miocene localities from Central Turkey
Article Type:	Original Paper
Corresponding Author:	Davit Vasilyan JURASSICA Museum Porrentruy, SWITZERLAND
Corresponding Author Secondary Information:	
Corresponding Author's Institution:	JURASSICA Museum
Corresponding Author's Secondary Institution:	
First Author:	Davit Vasilyan
First Author Secondary Information:	
Order of Authors:	Davit Vasilyan Zbyněk Roček Anna Ayvazyan Leon Claessens Roček Zbyněk Leon Claessens
Order of Authors Secondary Information:	
Funding Information:	Institute of Geology of the CAS (RVO67985831) Prof. Dr. Zbyněk Roček
Abstract:	In this paper, we describe ectothermic vertebrate assemblages from the Kargı 1, Kargı 2, Kargı 3, Haramı1, Haramı 3, Hancıllı, Keseköy, Çandır, Bağıcı localities in Turkey. The ages of these localities range from the latest Oligocene to the middle Miocene. The preserved non-mammalian fauna of the studied localities includes fishes (<i>Luciobarbus</i> sp., <i>Barbus</i> sp., <i>Luciobarbus</i> vel <i>Barbus</i> sp., aff. <i>Capoeta</i> sp., <i>Barbini</i> indet., <i>Leuciscus</i> sp.), anurans (<i>Bufo</i> indet., <i>Pelobatidae</i> indet., <i>Latonia</i> sp., <i>Palaeobatrachidae</i> indet.), lizards (<i>Pseudopus</i> sp., <i>Lacertidae</i> indet. 1, <i>Lacertidae</i> indet. 2, <i>Lacertidae</i> indet. 3, <i>Lacertidae</i> indet. 4, <i>Blaniidae</i> indet. (? <i>Blanus</i> sp.)), snakes (<i>Albaneryx</i> sp., <i>Erycinae</i> indet.) and crocodiles (<i>Crocodylia</i> indet.). Here we describe, for the first time, the fossil occurrence of the genera <i>Salamandra</i> , <i>Albaneryx</i> and <i>Pseudopus</i> from Anatolia, as well as the first fossil representative of the clade of the Western Asian lizards (<i>Lacertidae</i> indet. 3). Our study provides the earliest known fossil occurrence for the genera <i>Luciobarbus</i> , <i>Barbus</i> , <i>Pseudopus</i> and <i>Albaneryx</i> . Palaeobiogeographic relationships of each studied group are discussed and compared with the European and Asiatic record. A tentative palaeoenvironmental reconstruction is provided for each locality.
Suggested Reviewers:	Martin Ivanov mivanov@sci.muni.cz he is a specialist of fossil amphibians and reptiles Krister Smith Krister.Smith@senckenberg.de he is a specialist of fossil reptiles

	Villa Andrea andrewjayhouse@gmail.com he is a specialist of fossil amphibians and reptiles
	Olga Otero olga.otero@univ-poitiers.fr she is a specialist of fossil fishes
	Tomáš Přikryl prikryl@gli.cas.cz he is a specialist in fossil fishes and amphibians
Opposed Reviewers:	

Manuscript

[Click here to access/download;Manuscript;Vasliyan Manuscript.docx](#)[Click here to view linked References](#)

- 1 1 Fish, amphibian and reptilian faunas from the latest Oligocene to middle Miocene localities
2
3 2 from Central Turkey
4
5 3
6
7
8 4 Davit Vasilyan^{1,2,*}, Roček Zbyněk³, Anna Ayvazyan⁴, Leon Claessens⁵
9
10
11 5
12
13
14 6 ¹JURASSICA Museum, Route de Fontenais 21, 2900 Porrentruy, Switzerland
15
16
17 7 ²Department of Geosciences, University of Fribourg, Chemin du musée 6, 1700 Fribourg,
18
19 8 Switzerland
20
21
22 9 ³Department of Palaeobiology, Geological Institute, Czech Academy of Sciences, Rozvojová
23
24 10 136, CZ-165 00 Prague 6, Czech Republic
25
26
27 11 ⁴Department of Geosciences, Eberhard-Karls-University Tübingen, Hölderlinstr. 12,
28
29 12 72076, Tübingen, Germany
30
31
32 13 ⁵Department of Biology, College of the Holy Cross, 1 College Street, Worcester, MA 01610,
33
34 14 USA.
35
36
37 15
38
39 16 Davit Vasilyan <https://orcid.org/0000-0001-8712-0678>
40
41
42 17
43
44 18 * davit.vasilyan@jurassica.ch, tel.: 0041324209211
45
46
47
48 19
49
50
51 20 Keywords
52
53
54 21 Fishes, amphibians, reptiles, Turkey, latest Oligocene – middle Miocene,
55
56 22 palaeobiogeography.
57
58
59
60 23
61
62
63
64
65

24 **Abstract**

1
2
3 25 In this paper, we describe ectothermic vertebrate assemblages from the Kargı 1, Kargı 2,
4
5 26 Kargı 3, Harami1, Harami 3, Hancılı, Keseköy, Çandır, Bağçi localities in Turkey. The ages of
6
7 27 these localities range from the latest Oligocene to the middle Miocene. The preserved non-
8
9 28 mammalian fauna of the studied localities includes fishes (*Luciobarbus* sp., *Barbus* sp.,
10
11 29 *Luciobarbus* vel *Barbus* sp., aff. *Capoeta* sp., Barbini indet., *Leuciscus* sp.), anurans
12
13 30 (*Bufo*idae indet., *Pelobatidae* indet., *Latomia* sp., *Palaeobatrachidae* indet.), lizards
14
15 31 (*Pseudopus* sp., *Lacertidae* indet. 1, *Lacertidae* indet. 2, *Lacertidae* indet. 3, *Lacertidae* indet.
16
17 32 4, *Blanidae* indet. (?*Blanus* sp.)), snakes (*Albaneryx* sp., *Erycinae* indet.) and crocodiles
18
19 33 (*Crocodylia* indet.). Here we describe, for the first time, the fossil occurrence of the genera
20
21 34 *Salamandra*, *Albaneryx* and *Pseudopus* from Anatolia, as well as the first fossil representative
22
23 35 of the clade of the Western Asian lizards (*Lacertidae* indet. 3). Our study provides the earliest
24
25 36 known fossil occurrence for of the genera *Luciobarbus*, *Barbus*, *Pseudopus* and *Albaneryx*.
26
27 37 Palaeobiogeographic relationships of each studied group are discussed and compared with the
28
29 38 European and Asiatic record. A tentative palaeoenvironmental reconstruction is provided for
30
31 39 each locality.
32
33
34
35
36
37
38
39
40
41
42
43
44
45
46
47
48
49
50
51
52
53
54
55
56
57
58
59
60
61
62
63
64
65

42 Introduction

1
2
3 43 Multiple publications dealing with assemblages of small and large mammals have
4
5 44 summarized the rich fossil record of this group in Anatolia (Marković et al. 2018; Wang et al.
6
7 45 2013). In contrast, fossil fishes, amphibians and reptiles from Anatolia have not been
8
9
10 46 thoroughly investigated. In order to understand migrations of vertebrates between Asia and
11
12 47 Europe in the late Paleogene and early Neogene (Bruijn et al. 2013; Rössner and Heissig
13
14 48 1999), it is essential to have an understanding the fossil record of Anatolia, which likely lay
15
16
17 49 on the migration route between Europe and Asia for many species.
18
19
20 50 A brief overview (Böhme et al. 2003), based on disarticulated fossil material, stood at the
21
22
23 51 basis for a review of the possible relationships between the Anatolian Neogene freshwater fish
24
25 52 fauna and those of Europe and Asia. Similarities of the Anatolian fauna were recognized: 1)
26
27 53 with that from the central Europe for the most part of the early Miocene; 2) with those from
28
29
30 54 Central Asia for the late early Miocene and early middle Miocene. Few early Miocene
31
32 55 localities, e.g., Ağaöz (Paicheler et al. 1978) and Alpagut-Dodurga (Rückert-Ülkümen 1998),
33
34
35 56 provided articulated skeletons of cyprinid fishes. However, this material does not allow
36
37
38 57 observation of the morphology of the pharyngeal teeth, or association to postcranial and other
39
40 58 cranial elements.
41
42
43 59 Hitherto published amphibians of Anatolia include Salamandridae indet., *Pelobates*,
44
45 60 *Pelophylax*, *Rana* (Paicheler et al. 1978), Palaeobatrachidae indet. and *Bufo* (Claessens
46
47 61 1997). Claessens (1997) also suggested a migration route for the genus *Bufo* from Asia to
48
49
50 62 Europe via Anatolia.
51
52
53 63 Recently, Vasilyan et al. (2017) analysed the European and Western Asian amphibian and
54
55 64 reptilian Neogene record, suggested that Anatolia played an important role in the dispersal of
56
57
58 65 some amphibians and reptilian lineages, especially during the early Miocene. Around a dozen
59
60
61 66 publications have studied the non-mammalian vertebrate faunas from Anatolia (Table 1).

1
2
3
4
5
6
7
8
9
10
11
12
13
14
15
16
17
18
19
20
21
22
23
24
25
26
27
28
29
30
31
32
33
34
35
36
37
38
39
40
41
42
43
44
45
46
47
48
49
50
51
52
53
54
55
56
57
58
59
60
61
62
63
64
65

67 Among them, the recent study by Čerňanský et al. (2017) suggested relations of the
68 *Ophisaurus* sp. from the Kargi 2 locality (Oligo-Miocene boundary) with *Ophisaurus* from
69 the Middle Miocene of Kazakhstan (Vasilyan et al. 2016).

70 Further ectothermic vertebrates, such as lizards *Pseudopus* and *Varanus*, have their earliest
71 appearances in Europe during the early Miocene, around 18-17 Ma, during the so-called
72 Proboscidean Datum Event. As it has been documented for mammals, they arrived to Europe
73 from Anatolia (Rössner and Heissig 1999). Similar migrations, however, have never been
74 documented for other vertebrate groups. Only the discovery of the genus *Bavariboa* in the
75 eastern Anatolia (Szyndlar and Hoşgör 2013) provided a strong evidence of biogeographic
76 connection of the European and southwestern Asian ophidian faunas at the
77 Oligocene/Miocene boundary.

78 Summarizing the known fossil record of Anatolia in the context of those from Europe and
79 Asia, holds significant potential for Cenozoic fish, amphibians and reptiles from Anatolia for
80 resolution of numerous palaeogeographic questions about the origin of European groups as
81 well as for shedding light on timing of migration events for fish, amphibians and reptiles
82 between Europe, Asia and Africa.

83 In the present study, we present: (1) our results focused on ectothermic vertebrates recovered
84 from localities previously studied for small mammals; (2) their interpretations in
85 palaeobiogeographic context; and (3) tentative palaeoenvironmental interpretations of the
86 localities.

87 **Materials and methods**

- 1
2
3 88 The fossil material described in this study originates from nine latest Oligocene to middle
4
5 89 Miocene localities (Kargı 1, Kargı 2, Kargı 3, Harami1, Harami 3, Keseköy, Çandır, Hancılı,
6
7 90 Bağrı). Part of the material has been studied and discussed by one of the authors in his
8
9
10 91 unpublished Master's thesis (Claessens 1996). The depositional environments, small mammal
11
12 92 faunas, biochronologic correlations and absolute ages of the localities has been discussed and
13
14 93 summarized in Bruijn et al. (2013); Čerňanský et al. (2017); Claessens (1996); Kaymekci
15
16 94 (2000); Krijgsman et al. (1996); Krijgsman (2003) (Figure 1).
17
18
19
20 95 The studied fossil material has been collected from the fossiliferous horizons by screen
21
22 96 washing of the sediment samples and later picked from the sediment residue. The described
23
24 97 material is stored in the palaeontological collection of the University Utrecht (UU). The
25
26 98 material has been photographed by the digital microscope, Leica DVM5000 (Tübingen,
27
28 99 Germany), the electronic microscope FEI XL 30 Sirion, and a Canon EOS 50D camera.
29
30
31
32
33 100 The extant comparison material of fishes is stored at the osteological collection of National
34
35 101 Museum of Natural Sciences of Madrid (MNCN) and at the Bavarian State Collection for
36
37 102 Anthropology and Palaeoanatomy, Munich (SNSB). The pharyngeal bones of the extant
38
39 103 *Barbus and Luciobarbus* species are scanned using X-ray computed tomography (μ CT).
40
41
42 104 MicroCT images were taken using the microtomography systems NIKON XT H 160 at the
43
44 105 Scanning electron microscopy, analytic laboratories of MNCN. The scan settings of the
45
46 106 pharyngeal bones are introduced in Supplementary Material 1. The tomographic
47
48 107 reconstruction was performed using Avizo 9.0 software in the Tübingen University.
49
50
51
52
53 108
54
55 109 **Systematic palaeontology**
56
57
58 110 Class Actinopterygii Cope, 1887
59
60
61
62
63
64
65

- 111 Clade Teleostomorpha Arratia, 2000
1
2
- 112 Order Cypriniformes Bleeker, 1859
3
4
5
- 113 Family Cyprinidae Rafinesque, 1815
6
7
8
- 114 Subfamily Cyprininae (Rafinesque, 1815) (sensu Yang et al., 2015)
9
10
11
- 115 Tribe Barbini Bleeker, 1859 (sensu Yang et al., 2015)
12
13
14
- 116 Genus *Luciobarbus* Heckel, 1843
15
16
17
- 117 Fig. 2a-c
18
19
20
21
- 118
22
23
- 119 Below we provide short notes on the pharyngeal dentition of the genus *Luciobarbus* and
24
25
- 120 illustrate the teeth, using the following species *Luciobarbus longiceps* (MNCN E 54),
26
27
- 121 *Luciobarbus comizo* (MNCN 69304) and *Luciobarbus sclateri* (MNCN 69331). The
28
29
30
- 122 pharyngeal teeth of the studied *Luciobarbus* species are arranged on the pharyngeal bone in
31
32
- 123 three rows. The first (a) row contains four teeth, the second (b) three and the third row (c) two
33
34
35
- 124 teeth.
36
37
38
- 125 The pharyngeal tooth of the first row (a2-a5) are larger than the others in other two rows [since
39
40
41
- 126 the a1 tooth in the studied species is reduced (absent), the first tooth in the first (main) row is
42
43
- 127 the a2 tooth]. The tooth at the a2 position is molariform with a small “hook” (*L. longiceps* and
44
45
- 128 *L. sclateri*) or has flat surface (*L. comizo*). The a3 tooth is the second large tooth of the main
46
47
48
- 129 row after the a2. The tooth foot is longer than the crown, the foot-crown border is well-
49
50
- 130 distinguished. The crown is posteriorly convexed. The grinding surface has a C-shape with the
51
52
- 131 hook on the top of it (not well developed at a3 of *L. longiceps* (Fig. 2b) and *L. sclateri* (Fig.
53
54
- 132 2c)). The teeth at the tooth positions a4 and a5 are spoon-shaped and compressed
55
56
57
- 133 anteroposteriorly. A hook is present at the laterodorsal corner of tooth, which projects anteriorly
58
59
60
- 134 over the grinding surface.
61
62
63
64
65

135 The pharyngeal teeth at the second (b1-b3) and third (c1-c2) rows are smaller in comparison to
 136 those of the first row. Within the studied three extant *Luciobarbus* species, the teeth of the
 137 second and third rows can be grouped in two tooth morphogroups: 1) b1, c1 and 2) b2-b3 and
 138 c2. The teeth of the first morphogroup (b1 and c1 tooth positions) have posteriorly bent rounded
 139 tooth body. The foot-crown border is well distinguished. In anterior view, the grinding surface
 140 ruptures slightly and possesses one or two enhancements. The grinding surface has a well-
 141 developed, antrodorsally oriented hook on its tip. The second tooth morphogroups (b2, b3 and c2
 142 tooth positions) are slender among all teeth. The tooth body widens distally and is compressed
 143 anteroposteriorly. The grinding surface ruptures anteriorly and have one or two enhancements.
 144 These teeth are also characterized by the presence of the hook on the top of the grinding surface.
 145 In comparison to the teeth of the first tooth morphogroup, the grinding surface of these teeth
 146 (b2, b3, c2) are more expanded.

147

148 *Luciobarbus* sp.

149 Fig. 3a-g

150

151 **Material:** loc. Hancılı: tooth morphotype d3 – eight pharyngeal teeth (UU HAN 5304, 5305,
 152 5334); tooth morphotype d5 – four pharyngeal teeth (UU HAN 5332–5333) and one
 153 pharyngeal tooth (HAR1 5300); tooth morphotype d7 – 21 pharyngeal teeth (UU HAN 5313–
 154 5316).

155 **Description and remarks:**

156 *Tooth morphotype d3.* The teeth are elongate to robust, with either straight or medially
 157 bending tooth crown (Fig. 3f-g). The tooth crown possesses a hook, located either at the tooth
 158 axis or lateral from it. The hook is anteriorly pointed. The grinding surface is located at the

159 anterior surface of the bone. It bears moderately high longitudinal eminence (“crest”), which
1
2
3 160 length varies depending on tooth crown height. The lateral margins of the grinding surfaces
4
5 161 are elevated, dorsally the margins reduce in height at the basis of the hook, building
6
7 162 constrictions. A similar morphology can be observed at the b1 and c1 tooth positions of some
8
9 163 extant *Luciobarbus* spp (Fig. 2a-c).
10
11
12 164 *Tooth morphotype d5*. The tooth is elongate and slightly curved along its longitudinal axis and
13
14 165 bends medially (Fig. 3d-e). The anterior surface of the tooth crown is concave. The grinding
15
16 166 surface is narrow. It extends lateromedially on the tooth dorsal surface and extends ventrally,
17
18 167 parallel to the medial margin of the tooth. The posterior margin of the tooth is significantly
19
20 168 higher than the anterior margin. It possesses an anteriorly directed reduced, pointy and
21
22 169 medially oriented hook, which is located slightly lateral from the tooth center. This tooth
23
24 170 morphotype can be found at the b2, b3 and c2 tooth positions of the recent genus *Luciobarbus*
25
26 171 (Fig. 2a-c).
27
28
29 172 *Tooth morphotype d7*. The tooth crown is spoon-shaped, anteroposteriorly compressed. Its
30
31 173 anterior surface is concave (Fig. 3a-c). The grinding surface has a C-shape and is located on
32
33 174 the dorsal tip of the bone. The lateral corner of the tooth possesses an anteriorly oriented
34
35 175 hook, which shows different degree of development in different individuals. The medial
36
37 176 corner of the grinding surface, in teeth with more pronounced hook, extends slightly ventrally
38
39 177 to the tooth foot. The anterior margin of the tooth (anterior wall of the grinding surface) is
40
41 178 lower than the posterior one. It has either convex or concave surfaces, corresponding to less or
42
43 179 more degree of tooth wearing. This tooth morphotype is characteristic for the genus
44
45 180 *Luciobarbus* and can be found at the a4 to a5 tooth positions (Fig. 2b).
46
47
48
49
50
51
52
53
54
55 181
56
57
58
59 182 Genus *Barbus* Cuvier and Cloquet, 1816 (sensu Yang et al., 2015)
60
61
62
63
64
65

183 Fig. 2d-f
 1
 2
 3 184
 4
 5
 6 185 The morphology of the pharyngeal dentition of the genus *Barbus* follows using *Barbus*
 7
 8 186 *barbus* (SNSB SPAM-PI-00608), *Barbus meridionalis* (MNCN 19933) and *Barbus sacratus*
 9
 10 187 (MNCN GUI 17).
 11
 12
 13
 14 188 The pharyngeal teeth of the genus *Barbus* within studied three extant species are located in
 15
 16 189 three rows. Five teeth are present at the first (a) row, three in the second (b) and two in the
 17
 18
 19 190 third (c) row. The teeth in the first row are larger than those in other two rows, excepting the
 20
 21 191 a1 tooth. The a1 tooth is small. It has wide tooth base which narrows distally. The tooth body
 22
 23
 24 192 is compressed at the foot-crown border. The tooth crown is slightly narrower than the tooth
 25
 26 193 base. The grinding surface bears a hook on the top of it. The second tooth of the first row (a2)
 27
 28
 29 194 has molariform morphology, somewhat comparable to the a1 tooth. However, the a2 tooth is
 30
 31 195 several times larger than the a1. The teeth from the a3 to a5 tooth positions shows gradual
 32
 33
 34 196 transition from the tooth morphology with robust teeth with thick crowns; rather small
 35
 36 197 grinding surface (a3) to tooth morphology with slender teeth, narrow crown with expanded
 37
 38
 39 198 grinding surface. In all these tooth positions the teeth are bent, possesses hooks and smooth
 40
 41 199 grinding surface, which is delimited by a high (a3, a4) or low (a4, a5) ridge.
 42
 43
 44 200 The tooth body of the b1 tooth narrows distally. The crown is robust. The tooth body bends
 45
 46
 47 201 slightly posteriorly at the foot-crown border. The grinding surface ruptures anteriorly and
 48
 49
 50 202 possesse hook on the top. In anterior view, few grooves are observable on the grinding
 51
 52
 53 203 surface. The b2 tooth has a straight tooth body, whereas the tooth crown is bent posteriorly.
 54
 55
 56 204 The grinding surface is spilled with the hook on the top. Anteriorly the grinding surface is
 57
 58
 59 205 ruptured. The morphology of the b3 and c2 teeth are similar and nearly same as the one of b2,
 60
 61 206 but these teeth are slender and they bend extremely posteriorly. Besides this, the grinding
 62
 63
 64 207 surfaces of those teeth are narrower than that grinding surface of the b1. The c1 tooth has a
 65

- 208 straight body as the b1, but it is shorter and smaller than the b1. The grinding surface is with
1
2
3
4
5
6
7
8
9
10
11
12 210
13
14
15 211 *Barbus* sp.
16
17
18 212 Fig. 3h-n
19
20
21
22
23 213
24
25
26 214 **Material:** Loc. Hancılı: tooth morphotype d4 – 23 pharyngeal teeth (UU HAN 5307, 5307-1,
27
28
29 215 5308, 5309); tooth morphotype d6 – 28 pharyngeal teeth (UU HAN 5310-5312, 5321, 5335).
30
31
32 216 Loc. Harami 1: tooth morphotype d6 – one pharyngeal tooth (UU HAR1 5301).
33
34
35
36 217 **Description and remarks:**
37
38
39 218 *Tooth morphotype d6.* The teeth are elongate, rather slender and bent medially. They are
40
41
42 219 twisted along their longitudinal axis (Fig. 3h-l). The grinding surface is well expressed,
43
44 220 oriented and exposed anteriorly. It has rough surface composed of longitudinally running
45
46 221 crests. The grinding surface is encircled by a moderately high, thin margin. The lateral margin
47
48 222 of the grinding surface can be slightly serrated. The ventral wall of this margin in some teeth
49
50 223 can reduced so that the grinding surface flows in the tooth foot. The tooth crown possesses a
51
52 224 pointy hook directed anteriorly and projects over the grinding surface. This morphotype of the
53
54 225 pharyngeal tooth can be observed at the tooth positions a3-a5, b1-b3 of the extant genus
55
56 226 *Barbus* (Fig. 2d-e).
57
58
59 227 *Tooth morphotype d4.* The teeth are elongate, slightly bent, rather thick and robust. The tooth
60
61 228 crown is shorter than the tooth foot (Fig. 3m-n). The grinding surface is less developed than in
62
63 229 the Morphotype d6. It is limited mostly to the most dorsal portion of the tooth crown. The
64
65 230 grinding surface is rather smooth but still can possess few uneven structures. The grinding

- 231 surface is encircled mostly by high and sharp lateral walls possessing irregular margins. The
 1
 2
 3 232 ventral wall can be reduced or well-developed. Dorsally, a pointy hook is projecting over the
 4
 5 233 grinding surface. The hook can be reduced or moderately developed, but never reaches the
 6
 7 234 size of that in the Morphotype d6. Its orientation varies in the available teeth from dorsally
 8
 9 235 directed to anteriorly directed ones. A comparable morphology can be found at the b2 tooth
 10
 11
 12 236 position of the genus *Barbus* (Fig. 2d, f).
 13
 14
 15 237
 16
 17
 18 238 *Luciobarbus* vel *Barbus* sp.
 19
 20
 21 239 Fig. 3o-v
 22
 23
 24 240
 25
 26
 27 241 **Material:** Loc. Hancılı: tooth morphotype d1 – 15 pharyngeal teeth (UU HAN 5300, 5301,
 28
 29 242 5321), tooth morphotype d2 – 27 pharyngeal teeth (UU HAN 5302, 5303, 5306). Dorsal fin
 30
 31
 32 243 spine morphotype s1 – seven unbranched last spine of the dorsal fin (UU HAN 5322 – 5324);
 33
 34 244 dorsal fin spine morphotype s2 – five unbranched last spine of the dorsal fin (UU HAN 5325
 35
 36 245 – 5328); dorsal fin spine morphotype s3 – two unbranched last spine of the dorsal fin (UU
 37
 38 246 HAN 5329 – 5330).
 39
 40
 41
 42
 43 247 **Description and remarks:**
 44
 45
 46 248 *Tooth morphotype d1.* The teeth are large and robust. In cross section, the teeth are either
 47
 48 249 rounded or lateromedially compressed (Fig. 3o-p). The tooth foot is always longer than the
 49
 50
 51 250 tooth crown. The grinding surface is reduced and it has irregular surface. The margins of the
 52
 53 251 grinding surface are distinct and possess uneven (serration-like) structures. The hook is
 54
 55
 56 252 moderately pointy and shows anterodorsal orientation. This tooth morphology is
 57
 58 253 characteristic for the b1 tooth position of *Barbus* genera (Fig. 2d-e).
 59
 60
 61
 62
 63
 64
 65

1
2
3
4
5
6
7
8
9
10
11
12
13
14
15
16
17
18
19
20
21
22
23
24
25
26
27
28
29
30
31
32
33
34
35
36
37
38
39
40
41
42
43
44
45
46
47
48
49
50
51
52
53
54
55
56
57
58
59
60
61
62
63
64
65

254 *Tooth morphotype d2*. The teeth are rounded, robust, small in size, lateromedially compressed
255 (Fig. 3q-r). Both tooth foot and crown are short, in some of teeth a constriction marks the foot
256 crown boarder. The tooth crown has a molariform shape. The grinding surface is either fully
257 absent or extremely reduced. In those teeth with grinding surface, its surface is exposed
258 dorsally or anteriorly. The griding surface is rough and laterally bordered by low walls. The
259 hook is small and dorsally oriented. The described tooth morphology is characteristic of the
260 first tooth of the main row (a2) of *Barbus* and *Luciobarbus* genera (Fig. 3a, f).

261 *Morphotype s1*. The preserved spine fragments shows no serration at their posterior margins
262 (Fig. 3s). Slightly above the base of the spine, small posteroventrally pointed serrae appears,
263 dorsally they become longer. The dorsal serrae are sharp and possess poorly-pronounced
264 edges. In lateral and medial views, the spine body is narrow, although in larger individuals, it
265 can widen slightly.

266 *Morphotype s2*. The spine body is slender. It possesses directly at its base short posteriorly
267 directed serrae (Fig. 3t-u). Dorsally, the serrae become longer and cylindrical in shape,
268 sometimes they can have curved shape and point with their tip dorsally. The serrae surfaces
269 do not possess any structures.

270 *Morphotype s3*. In lateral and medial views, the bodies of the spines are broad (Fig. 3v). The
271 ventral margin of the preserved portions of the bones nearly lacks serration. Only on the
272 preserved upper part (most probably, corresponding to the middle portion of the spine)
273 possesses very small serrae.

274 The described forms of the unbranched last spine of the dorsal fin clearly can be distinguished
275 from each other, including that of the Barbini indet, from the locality Kargı 2 by: 1) the shape,
276 orientation and surface structure of the serrae; 2) the position, where the serration appears on
277 the spine; 3) the dimensions of the spine body.

278 In the neoichthyological studies the unbranched last spine of the dorsal fin and its serration is
1
2 279 broadly used for taxonomic proposes within different genera or among species of the same
3
4
5 280 genus (Kottelat and Freyhof 2007). Doadrio (1990) made an attempt to use the morphology
6
7 281 and peculiarities of this spine for intergeneric taxonomy, but, unfortunately, did not include
8
9 282 all barbin genera.
10
11
12 283 Taking into account, the presence of three different morphotypes of the unbranched last spine
13
14
15 284 of the dorsal fin and eight tooth morphotypes in the locality Hancılı, we can state about the
16
17 285 presence of at least three different barbin taxa, which could belong to the genera *Barbus*
18
19 286 and/or *Luiobarbus*. More comprehensive studies on recent barbin genera are necessary, to be
20
21
22 287 able to identify certain tooth morphologies or dorsal spine morphotypes to certain species.
23
24
25
26 288
27
28 289 Genus *Capoeta* Valenciennes, 1842 in Cuvier and Valenciennes, 1842
29
30
31 290
32
33
34
35 291 aff. *Capoeta* sp.
36
37
38 292 Fig. 3w-x
39
40
41 293
42
43
44 294 **Material:** Loc. Hancılı: tooth morphotype d8 – one tooth (UU HAN 5317).
45
46
47 295 **Description and remarks:** a single tooth is rather anterodorsally compressed and spoon-
48
49 296 shaped. The grinding surface is reduced and it is represented in a form of a narrow strip. The
50
51 297 anterior margin of the tooth (anterior wall of the grinding surface) is lower than the posterior
52
53 298 one. This morphology remind the morphology of the pharyngeal teeth of the genus *Capoeta*
54
55 299 (*Ayvazyan et al. 2018*) corresponding to the character stage $\alpha 2$ of the lateral outline and $\beta 5$ of
56
57 300 the transverse cross section, however, so far a comparable morphology have not been reported
58
59
60
61
62
63
64
65

1 301 for *Capoeta* (Ayvazyan et al. 2018). This tooth can be characterized by character stage $\beta 5$ of
 2 302 the transverse cross section, but no corresponding character stage α of the lateral outline is
 3
 4 303 found within the given character stages by Ayvazyan et al. (2018). However, so far a
 5
 6 304 comparable morphology have not been reported for *Capoeta* (Ayvazyan et al. 2018). Taking
 7
 8 305 into account these observations, as well as that the tooth is only one so far found, we prefer to
 9
 10 306 assign tentatively the tooth to the genus *Capoeta*.
 11
 12
 13
 14
 15 307
 16
 17 308 Barbini indet.
 18
 19
 20
 21 309 Fig. 3y-ee
 22
 23
 24 310
 25
 26
 27 311 **Material:** Loc. Kargı 1: 15 pharyngeal teeth isolated or attached to pharyngeal bone (UU
 28
 29 312 KAR1 1300 – 1305). Loc. Kargı 2: 19 pharyngeal teeth isolated or attached to pharyngeal
 30
 31 313 bone (UU KAR2 1301 – 1302, 1304-1306), one unbranched dorsal fin ray (UU KAR2 1303).
 32
 33 314 Loc. Keskoy: 116 pharyngeal teeth isolated or attached to pharyngeal bone (UU KE 5305 –
 34
 35 315 5310).
 36
 37
 38
 39
 40 316 **Description:** the pharyngeal teeth are mediolaterally compressed, small-sized and slender.
 41
 42 317 The grinding surface is located at the anterior side of the tooth crown (Fig. 3z, dd, aa, bb). It is
 43
 44 318 narrow and dorsoventrally elongated. In short teeth, the grinding surface is shifted dorsally,
 45
 46 319 whereas in long teeth it corresponds to the half of the entire tooth length. The grinding surface
 47
 48 320 is surrounded by a moderately high crest, which displays uneven structures (serration-shaped)
 49
 50 321 at its lateral wall. A well-developed hook projected over the grinding surface. The hook is
 51
 52 322 variously oriented – dorsoanteriorly (Fig. 3y) to anteriorly (Fig. 3z). At the posterior tooth
 53
 54 323 positions (a1 or a2; Fig. 3y, 3aa) the teeth are more robust, the grinding surface is reduced.
 55
 56
 57
 58
 59
 60
 61
 62
 63
 64
 65

- 1
2
3
4
5
6
7
8
9
10
11
12
13
14
15
16
17
18
19
20
21
22
23
24
25
26
27
28
29
30
31
32
33
34
35
36
37
38
39
40
41
42
43
44
45
46
47
48
49
50
51
52
53
54
55
56
57
58
59
60
61
62
63
64
65
- 324 The preserved fragment of the last unbranched spine of the dorsal fin possesses three rather
325 robust, short, pointy, ventroposteriorly directed serrae. Their surface is smooth (Fig. 3ee).
- 326 **Remarks:** The morphology of the pharyngeal teeth is so far (to the authors knowledge)
327 unknown both in the fossil record and among recent species. The shape of the teeth and the
328 grinding surface has similarities with e.g. *Barbus* sp. from Gračanica, Bosnia and
329 Herzegovina, middle Miocene (Vasilyan in review). Besides the tooth material, the presence
330 of a fragment of the serrated last unbranched spine of the dorsal fin suggests also the presence
331 of barbin (Kottelat and Freyhof 2007) fishes in the locality Kargı 1. Due to lack of the
332 comprehensive studied and comparative material of the pharyngeal dentition of the recent
333 barbins, we prefer to assign these remains to the tribe Barbini.
- 334
- 335 Subfamily Leuciscinae Bonaparte, 1835
- 336 Genus *Leuciscus* Cuvier, 1816-1817
- 337 *Leuciscus* sp.
- 338 Fig. 3ff
- 339
- 340 **Material:** Loc. Hancılı: three isolated pharyngeal teeth (UU HAN 5318–5320).
- 341 **Description and remarks:** The teeth are lateromedially compressed (Fig. 3ff-1, 3ff-3). The
342 grinding surface is elongate, narrow and located at the anterior side of the tooth. Its surface is
343 nearly smooth with some rugosities. Its lateral margin possesses up to five denticles with
344 rounded tips. Ventrally they become smaller. The dorsal tip of the tooth terminates with an
345 anteriorly oriented hook. This morphology resembles that of the genus *Leuciscus* (Rutte
346 1962).

- 347
1
2
3 348 Cyprinidae indet.
4
5
6 349
7
8
9 350 **Material:** Loc. Keseköy: 17 fragments of the pharyngeal bones (UU KE 5302 – 5304).
10
11
12 351 **Remarks:** fragments of the pharyngeal bone, showing the places (if different sizes) of the
13
14 352 attachment of the pharyngeal teeth are present. One or two rows are observable on pharyngeal
15
16 353 bones, where the teeth have been arranged. Pharyngeal bones with dentition are widely known
17
18 354 in cypriniform fishes, specially in the family Cyprinidae (Winfield and Nelson 1991). Taking
19
20 355 into account the fact that in this locality only cyprinid remains are known, we tentatively
21
22 356 assign this material to the family Cyprinidae.
23
24
25
26
27 357
28
29
30
31 358 Teleostei indet.
32
33
34 359
35
36
37 360 **Material:** Loc. Kargı 1: 14 vertebrae (UU KAR1 1303). Loc. Kargı 2: ten vertebrae (UU
38
39 361 KAR2 1300). Loc. Keseköy: 17 atlases (UU KE 5301) and 128 trunk/caudal vertebrae (UU
40
41 362 KE 5300). Loc. Hancılı: one vertebra (UU HAN 5331).
42
43
44
45 363 **Description and remarks:** numerous vertebrae, including those from trunk and caudal
46
47 364 positions, as well as the atlases, have been found. They show amphicoelous morphology, the
48
49 365 atlases are anteroposteriorly strongly flattened. Any further identification of the material is
50
51 366 impossible.
52
53
54
55 367
56
57
58
59 368 Class Amphibia Linnaeus, 1758
60
61
62
63
64
65

- 369 Order Caudata Scopoli, 1777
1
2
- 370 Family Salamandridae Goldfuss, 1820
3
4
5
- 371 Genus *Salamandra* Garsault et al., 1764
6
7
8
- 372
9
10
11
- 373 *Salamandra* sp.
12
13
14
- 374 Fig. 4a-l
15
16
17
- 375
18
19
20
- 376 **Material:** Loc. Harami 1: one caudal vertebra (UU HAR1 5055). Loc. Bağıçi: one trunk
21
22
23
- 377 vertebrae (UU BAG 1002) and two humeri (UU BAG 1003, UU BAG 1004).
24
25
26
- 378 **Description:** A relatively well preserved trunk vertebra (UU BAG 1002) is present from the
27
28
29
- 379 locality Bağıçi (Fig. 4a-e). It is remarkable with its large size; the centrum length measures 6
30
31
- 380 mm. In lateral view, the neural arch and centrum are dorsoventrally flattened, due to this they
32
33
- 381 are low and broad. The opisthocelous centrum is flexuous. The praezygapophysis is
34
35
36
- 382 connected with the parapophysis by a posteroventrally directed accessory allar process,
37
38
- 383 whereas the postzygapophysis is connected with the diapophysis by a horizontally directed
39
40
41
- 384 dorsal lamina. In anterior and posterior views, the neural canal is round and narrow. Several
42
43
- 385 foramina of different sizes are piecing the bases of the prezygapophysis. The neural spine is
44
45
- 386 missing, but the neural arch possesses traces of its base, suggesting that it reached nearly the
46
47
48
- 387 anterior tip of the neural arch.
49
50
51
- 388 The anterior portion of a caudal vertebra (UU HAR1 5055) is preserved (Fig. 4f-i). In ventral
52
53
54
- 389 view, the lateral edges of the vertebral centrum possess the bases of the haemapophysis. The
55
56
- 390 centrum possesses an anterior condyle, suggesting a probable opisthocelous morphology of
57
58
- 391 the vertebra. In anterior view, the neural arch is rounded, only its base is flat. Distinct
59
60
61
62
63
64
65

- 1
2 392 subprezygapophyseal foramina are observable at the base of the praezygapophysis. In lateral
3
4
5 393 view, the neural spine is visible which arises behind the short zygosphenes.
6
7 394 Distal portions of two humeri are present in the locality Bağıçi. The bones are lateromedially
8
9 395 flattened. The lateral surface of the distal tip of the humeri possesses a longitudinal and rather
10
11 396 shallow olecranon fossa. The shallow cubital ventral fossa of the humeri is observable on the
12
13 397 medial surface of the bones. It has semilunar outline. The capitulum (radial condyle) is located
14
15 398 at its base (UU BAG 1004, fig. 4j) or is missing (UU BAG 1003, fig. 4k-l). The humeri, at
16
17 399 their mid-diaphyseal position possesses a small remnant of the humeral dorsal crista. The
18
19 400 longest preserved humerus fragments (representing the distal half of the bone) measures 6
20
21 401 mm, suggesting the humerus had the length of around 11-12 mm.
22
23
24
25 402 **Remarks:** The large size of the bones and the observed morphology, i.e. dorsoventrally
26
27 403 flattened, broad and robust trunk vertebrae; caudal vertebra with round neural canal and
28
29 404 neural spine; and the general morphology of the humeral fragments, agrees with the genus
30
31 405 *Salamandra* (Estes and Hoffstetter 1976; Rage 1984). Also the large bone sizes agrees with
32
33 406 that of the *Salamandra sansaniensis* (Estes and Hoffstetter 1976; Rage and Hossini 2000).
34
35 407 Nevertheless, the lack of the studies on vertebral morphology of all recent *Salamandra*
36
37 408 species, including that of the largest representative of the genus, i.e., *Salamandra*
38
39 409 *infraimmaculata*, makes the reliable identification of the fossil remains impossible.
40
41
42
43
44
45
46 410
47
48
49 411 Order Anura Fischer, 1813
50
51
52 412 Family Pelobatidae Bonaparte, 1850
53
54
55 413
56
57
58 414 Pelobatidae indet.
59
60
61
62
63
64
65

415 Figure 4m-v
 1
 2
 3 416
 4
 5
 6 417 **Material:** Loc. Harami 1: one fragmentary maxilla (UU HAR1 5051). Loc. Keseköy: one
 7
 8 418 fragmentary maxilla (UU KE 5006). Loc. Hançılı: three frontoparietals (UU HAN 5051–
 9
 10 419 5053). Loc. Bağiçi: one fragmentary maxilla (UU BAG 1001).
 11
 12
 13 420 **Description:** All maxillae are fragmentary. The labial surface bears the pit-and-ridge
 14
 15 421 ornamentation. The specimen UU HAR1 5051 (Harami 1; Fig. 4m, n) represents the smallest
 16
 17 422 individual; it is rather weathered, due to which its surface structures are poorly pronounced. In
 18
 19 423 UU KE 5006 (Keseköy; Fig. 4q, r), the bone is provided with the dorsal, posterodorsally
 20
 21 424 inclined and rather pointed zygomaticomaxillar process, and with the posterior process. Its
 22
 23 425 end is most probably undamaged (judging by the intact zygomaticomaxillar process),
 24
 25 426 suggesting a broad contact with a short but robust quadratojugal. Between both processes, the
 26
 27 427 margin of the bone is concave. In lingual view, UU KE 5006 (loc. Keseköy) and UU BAG
 28
 29 428 1001 (loc. Bağiçi) possess a moderately developed pit behind the pterygoid process (Fig. 4p,
 30
 31 429 r). The pterygoid process is the well prominent posterior termination of the horizontal lamina
 32
 33 430 roofing the tooth row dorsally. The lamina horizontalis is represented by a rather sharp and
 34
 35 431 not high flange in UU HAR1 5051 (loc. Harami 1), or by a distinct, robust flange with a
 36
 37 432 rounded surface in UU KE 5006 (loc. Keseköy) and UU BAG 1001 (loc. Bağiçi). The latter
 38
 39 433 maxilla, however, differs from that from Keseköy in absence of the pterygoid process and in
 40
 41 434 subdivided zygomaticomaxillar process. Unless these two features are artifacts caused by
 42
 43 435 fossilization, they could represent significant taxonomic differences.
 44
 45
 46
 47
 48
 49
 50
 51
 52
 53 436 Two frontoparietals from Hançılı roughly correspond to one another in their general shape
 54
 55 437 and size (Figs. 4s–v). They are paired, which means that they were in contact with their
 56
 57 438 counterparts from the opposite side in a slightly serrated median suture. Their orbital margin
 58
 59 439 is nearly straight or only slightly concave, and it is deflected ventrally. Consequently, the
 60
 61
 62
 63
 64
 65

1 440 tectum supraorbitale is poorly developed and does not extend into the orbit. The margo
2
3 441 orbitalis ends posteriorly in a lateral process, which is discernible only because the margin of
4
5 442 the frontoparietal breaks here and runs posteromedially. There, it terminates in a process
6
7 443 which represents the most posterior part of the frontoparietal. The margin then turns sharply
8
9 444 and runs anteromedially towards the posterior end of the median suture. This suggests that
10
11 445 posteromedial margins of both frontoparietals enclosed nearly rectangular, wedge-like space.
12
13 446 The frontoparietal incassation on the ventral surface of the bone is typically pelobatid-like,
14
15 447 which means that it is undivided, broad posteriorly and narrower anteriorly. In a living
16
17 448 animal, it fitted in a large fenestra in the roof of the endocranial braincase. The dorsal surface
18
19 449 of the frontoparietal is covered by sculpture; that in UU HAN 5051 (Figs. 4s, t) is represented
20
21 450 by indistinct mounds, arranged radially from the center of the bone, that in UU HAN 5052
22
23 451 (Figs. 4u, v) is pustular in the middle, with indistinct radial mounds in the peripheral parts of
24
25 452 the bone.
26
27
28
29
30
31 453 **Remarks:** General morphology of the maxilla, together with morphology of the
32
33 454 frontoparietals that corresponds to a postmetamorphic but not-yet ultimate developmental
34
35 455 stage of the Pelobatidae, and the pit-and-ridge type of ornamentation, is a combination of
36
37 456 characters that indicate relations to the Pelobatidae (Roček 1981), but do not allow
38
39 457 identification at the generic level (see Discussion).
40
41
42
43
44 458
45
46
47 459 Family Bufonidae Gray, 1825
48
49
50
51 460
52
53
54 461 Bufonidae indet.
55
56
57 462 Figure 4w-y
58
59
60 463
61
62
63
64
65

- 1
2
3 **464 Material:** Loc. Keseköy: one ilium (UU KE 5001).
4
5 **465 Description:** The fragment of this ilium measures 4.2 mm at its highest portion,
6
7 **466** corresponding to the highest point of the dorsal tubercle and lowest preserved point of the
8 **467** pars descendens. The anterior portion of the acetabulum and posterior part of the iliac shaft
9
10 **468** are preserved. The dorsal tubercle is pointy and well-pronounced, it is relatively high and
11
12 **469** broad. It is composed of two or three lobes (Fig. 4w). The anterior border of the acetabular
13
14 **470** rim is high. The pars descendens is moderately high. It narrows ventrally. A small
15
16 **471** preacetabular fossa pierces the anterodorsal corner between acetabulum and pars descendens.
17
18 **472** The iliac shaft has rounded outline and flat surface. It does not possess any structures. (Fig.
19
20 **473** 4w).
21
22
23
24
25 **474 Remarks:** The preserved ilium can be assigned to the family Bufonidae based on
26
27 **475** combination of the following characters: pointy, bi-(tri-)lobed dorsal tubercle, flat medial
28
29 **476** surface, the iliac shaft is smooth and does not possess a dorsal crest (Blain et al. 2010). The
30
31 **477** family Bufonidae represents a group with numerous species distributed in both Old and New
32
33 **478** Worlds (Frost 2014). The morphology of the ilium is broadly uniform in many forms (Sánchez
34
35 **479** 1998; Tihen 1962) and other skeletal elements are necessary for closer identification. The
36
37 **480** comparison with both recent and fossil Western Asian bufonids reveals strong similarities
38
39 **481** with its morphology and size to the genus *Pseudepidalea* (Blain et al. 2010) and clearly can
40
41 **482** be separated from the genus *Bufo*. Due to the incomplete preservation of the ilium and the
42
43 **483** lack of further skeletal elements as well as poor knowledge of the osteology of the family, we
44
45 **484** prefer to name the fossil bone from the locality Keseköy as Bufonidae ident. (?
46
47
48
49
50 **485** *Pseudepidalea*).
51
52
53
54
55 **486**
56
57
58
59 **487** Family Alytidae Fitzinger, 1843
60
61
62
63
64
65

- 1
2
3 488 Genus *Latonia* Meyer, 1843
4
5
6 489
7
8
9 490 *Latonia* sp.
10
11
12 491 Figure 5
13
14
15 492
16
17 493 **Material:** Loc. Kargı 1: four cranial bones (UU KAR1 1001 - 1005), seven maxillae (UU
18 494 KAR1 1006 -1011), one atlas (UU KAR1 1012), one vertebra (UU KAR1 1013), one costa
19
20 495 (UU KAR1 1014), two sacral vertebrae (UU KAR1 1015–1016), one ilium (UU KAR1 1054),
21
22 496 two urostyles (UU KAR1 1017–1018), one coracoid (UU KAR1 1019), one humerus (UU
23
24 497 KAR1 1020), two radioulnae (UU KAR1 1021–1022). Loc. Kargı 2: eight maxillae (UU
25
26 498 KAR2 1006–1012), three angulars (UU KAR2 1013–1015), one atlas (UU KAR2 1013), one
27
28 499 vertebra (UU KAR2 1014), two transverse processes (UU KAR2 1015, 1016), two costae
29
30 500 (UU KAR2 1017, 1018), 11 ilia (UU KAR2 1022 –1032), three urostyles (UU KAR2 1019 –
31
32 501 1021), two coracoids (UU KAR2 1033, 1034), six humeri (UU KAR2 1035 –1040). Loc.
33
34 502 Kargı 3: three maxillae (UU KAR3 1001 –1003), one ilium (UU KAR3 1207). Loc. Harami
35
36 503 1: nine maxillae (UU HAR1 5062, 5062-1, 5062-2, 5062-3). Loc. Harami 3: one maxilla (UU
37
38 504 HAR3 5052), one angular (UU KAR3 5012), two scapulae (UU HAR3 5051), one sacral
39
40 505 vertebra (UU HAR3 5013), one costa (UU HAR3 5014), one ilium (UU HAR3 5015), one
41
42 506 ischium (UU HAR3 5016). Loc. Keseköy: three anglars (UU KE 5012–5014), 71 maxillae
43
44 507 (UU KE 5012–5019, 5055–5057), two atlases (UU KE 5020–5021), six scapulae (UU KE
45
46 508 5022–5025, 5051), four costae (UU KE 5026–5029), six transverse processes (UU KE 5030 –
47
48 509 5035), 49 urostyles (UU KE 5052–5053). Loc. Hancılı: two frontoparietals (UU HAN 5054,
49
50 510 5055), four maxillary fragments (UU HAN 5056), one parasphenoid (UU HAN 5058), three
51
52
53
54
55
56
57
58
59
60
61
62
63
64
65

1
2
3
4
5
6
7
8
9
10
11
12
13
14
15
16
17
18
19
20
21
22
23
24
25
26
27
28
29
30
31
32
33
34
35
36
37
38
39
40
41
42
43
44
45
46
47
48
49
50
51
52
53
54
55
56
57
58
59
60
61
62
63
64
65

511 vertebrae (UU HAN 5057). Loc. Çandır: six maxillae (UU CD 5001), three cranial bones (UU
512 CD 5004), one atlas (UU CD 5002), three vertebral centra (UU CD 5003).

513 **Description and remarks:** The frontoparietal (UU HAN 5055) (Fig. 5a, b) preserved only its
514 anterolateral portion, which is, however, important for determination of the genus (Roček
515 1994). Its dorsal surface is horizontal, extending into the orbit by a thin supraorbital tectum.
516 The dorsal surface in that part is covered by antero-posteriorly oriented rounded ridges,
517 typical for *Latonia gigantea* (Roček 1994; fig. 7F). The frontoparietal incassation in the
518 middle portion of the inner surface of the bone is depressed, but rimmed with a prominent
519 crista, which was part of the contacting surface with the braincase in living animal. The
520 scapula (UU HAR3 5051) (Fig. 5c, d) has incomplete anterior margin, so its shape cannot be
521 restored with certainty. It seems that it was rather short and squarish. The maxillae are
522 preserved as short fragments (Fig. 5g-l) but a typical morphology of its inner surface, with the
523 sulcus for the nasolacrimal duct, which is manifested also on the dorsal margin of the bone, is
524 a typical feature of *Latonia*. On the lateral surface of the ilium, at the level of the anterior
525 margin of the acetabulum, there is a typical triangular depression which in its most posterior
526 part is pierced by several foramina (filled with whitish sediment in Fig. 5m). This is also a
527 typical feature of the genus *Latonia*. Finally, opisthocoelous atlas, although with neural arches
528 broken off, seems to be another evidence of *Latonia*. However, it differs from the atlas of
529 *Latonia* from the middle Miocene of Sansan and La Grive St. Alban in that both cotyles are
530 interconnected (Fig. 5f). Morphology of the cranio-vertebral articulation is often considered
531 important in anuran taxonomy, but nothing is known about individual and developmental
532 variation of this anatomical character.

533 The material is too fragmentary for more precise taxonomic evaluations, but the mentioned
534 fragments of the frontoparietal (UU HAN 5055), maxilla (UU HAR1 5062-1) and ilium
535 represent doubtless evidence of *Latonia* in the sample (Roček 1994).

- 536
1
2
3 537 Family Palaeobatrachidae
4
5
6 538 Palaeobatrachidae indet.
7
8
9 539
10
11
12 540 Figures 6, 7
13
14
15 541 **Material:** Loc. Kargı 1: one angular (UU KAR1 1052), two neural arches (UU KAR1 1053).
16
17 542 Loc. Kargı 2: one angular (UU KAR2 1104), two scapulae (UU KAR2 1105), one humerus
18
19 543 (UU KAR2 1001). Loc. Harami 1: one maxilla (UU HAR1 5059), six sphenethmoids (UU
20
21 544 HAR1 5005 – 5007, 5060), eight angulars (UU HAR1 5001 – 5004, 5061), one scapula (UU
22
23 545 HAR1 5009), one coracoid (UU HAR1 5010), 25 humeri (UU HAR1 5011 – 5035), one
24
25 546 illium (UU HAR1 5008), two neural arches (UU HAR1 5054). Loc. Harami 3: one
26
27 547 sphenethmoid (UU HAR3 5003), eight humeri (UU HAR3 5004 – 5011), two angulars (UU
28
29 548 HAR3 5001 – 5001). Loc. Keseköy: five maxillae (UU KE 5054), one urostyle (UU KE
30
31 549 5011).
32
33
34
35
36
37 550 **Description:** The largest of the three sphenethmoids from Harami 1 is UU HAR1 5005 (Fig.
38
39 551 6a-c); its widest diameter is 5.65 mm, so it represents a medium-sized individual, probably
40
41 552 not exceeding SVL of 60 mm. Its lateral processes display spongy bone, but are symmetrical
42
43 553 and not too prominent beyond the lamina supraorbitalis; this suggests that they were
44
45 554 completed by cartilage in living animal and exposed spongy bone is not an artifact. Similarly,
46
47 555 the anterior median process (i.e., ossified part of the septum nasi) is not too much prominent
48
49 556 beyond the floor of the nasal capsules (i.e., ossified part of the solum nasi). The anterior
50
51 557 margin of the floor of the nasal capsules is almost straight, thick, and was undoubtedly
52
53 558 extended by cartilage, whereas the anterior margin of the roof of the nasal capsules (i.e.,
54
55 559 ossified part of the tectum nasi) is deeply concave (Fig. 6a), thin, and was not completed by
56
57
58
59
60
61
62
63
64
65

560 cartilage (Fig. 6c). The articular facet for the frontoparietal is slightly depressed due to
1
2 561 elevated margins, covered by a few irregular and indistinct grooves. The borderline between
3
4
5 562 the contact facets for the nasals and the frontoparietal indicates the shape of the anterior
6
7 563 margin of the frontoparietal, which extended in a median point. On the right side, the
8
9
10 564 posterior margin of the lateral braincase wall is covered by periost, which suggests its natural
11
12 565 antero-posterior extent. This, compared with the maximum width of the bone, suggests that
13
14 566 the sphenethmoid was not elongated, but approximately as long as broad. The bottom of the
15
16
17 567 braincase reached posteriorly at least the same level as the lateral walls or more, the roof is
18
19 568 only moderately incised anteriorly (*incisura semielliptica sensu* Hossini and Rage 2000). The
20
21
22 569 ventral surface of the bottom of the braincase is rimmed by a rounded ridge on either side; the
23
24 570 ridges are at the transition between the bottom and lateral walls of the braincase, and delimit
25
26
27 571 laterally the groove-like articular facet for the parasphenoid. The braincase is connected with
28
29 572 each nasal capsule by a canal for the olfactorius nerve (*canalis olfactorius*). The medial
30
31
32 573 section of the ossified part of the postnasal wall is pierced by a canal for the medial branch of
33
34 574 the ophthalmic nerve (*ramus medialis nervi ophthalmici*), which enters the nasal capsule
35
36 575 dorsolateral to the orifice of the *canalis olfactorius* (Fig. 6c). Although the orbitonasal canal is
37
38
39 576 ellipsoid in cross-section, the longest diameters of both canals are about the same.
40
41 577 In contrast to UU HAR1 5005 (Fig. 6a-c), UU HAR1 5006 (Fig. 6d-f) is small, with its widest
42
43
44 578 diameter about 3.6 mm; this should correspond to an individual with SVL of about 40 mm.
45
46 579 Although this sphenethmoid is rather worn out both anteriorly and posteriorly (hence shorter
47
48
49 580 than broad), the nasal facets and the groove for the parasphenoid are similar to UU HAR1
50
51 581 5005. Principal differences between both bones are the narrow contact facet for the
52
53
54 582 frontoparietal (Fig. 6d) and deeply V-incised *incisura semielliptica*, which reaches up to the
55
56 583 level of the partition between both olfactory canals. Also the canals entering the nasal
57
58
59 584 capsules are rather different (*canalis olfactorius* is much larger than that for the medial branch
60
61 585 of the ophthalmicus nerve). On the left side of the bone, both fuse with one another close to

1 586 their entrance into the nasal capsule, but this may be a matter of individual variation. The
2 587 most important is that both the floor and the roof of the nasal capsules were completed by
3
4 588 cartilage in life, which rather suggests that the differences between both sphenethmoids are
5
6 589 due to degree of development, rather than indication of two different species. Alternatively,
7
8
9 590 they might be a result of developmental heterochrony of two closely related species, which is
10
11
12 591 the case with recent *Bombina bombina* and *B. variegata*.
13
14 592 A relative complete maxilla is from Harami 1 (UU HAR1 5059; Fig. 6o, p). It is obvious that
15
16 593 the tooth row terminates below the posterior base of the frontal process, that the most
17
18 594 posterior tooth position is of the same size as the more anterior ones, and that the orbital
19
20 595 margin is a flat, horizontal plate extending labially in a distinct ledge (marked by arrow in
21
22 596 Fig. 6p). In addition, the frontal process is clearly inclined towards the anterior.
23
24
25 597 The angulars UU HAR1 5004 (Fig. 6g), UU HAR1 5002 (Fig. 6h), and UU HAR1 5001 (Fig.
26
27 598 6i, j) all have the dorsoventrally compressed coronoid process, which continues posteriorly by
28
29 599 a long, horizontal ridge extending to the dorsomedial margin of the bone where it meets with
30
31 600 the gradually lowering medial wall of Meckel's groove (marked by arrow in Fig. 6g) whereas
32
33 601 anteriorly, the coronoid process terminates rather abruptly. Besides, all these angulars have a
34
35 602 tubercle or protuberance on the dorsal edge of the medial wall of the Meckel's groove, and a
36
37 603 smooth, depressed area for the adductor mandibulae externus muscle. There is some variation
38
39 604 in shape of the coronoid process – it may be divided by a delicate ridge or crista into the
40
41 605 anterior and posterior flat or slightly depressed areas, or can be a single convexity. Right
42
43 606 angular UU HAR1 5003 (Fig. 6k, l), however, is different, especially in the position and
44
45 607 shape of the coronoid process. In medial view (Fig. 6l), the coronoid process has a markedly
46
47 608 oblique position, with its longitudinal axis slanting down posteriorly, so its posterior margin is
48
49 609 located almost at the level of the ventral surface of the bone. In the dorsal aspect, it is
50
51 610 markedly prominent medially. Besides, the medial wall of the Meckel's groove is not
52
53 611 extended dorsally. It rather recalls MNHN LAU 11 from the early Miocene of Laugnac
54
55
56
57
58
59
60
61
62
63
64
65

612 (Hossini and Rage 2000, fig. 1-2). Two angulars from Harami 3 are less well preserved (Fig.
1
2 613 6m, n), but they fit into variation range of the angulars from Harami 1 (and of
3
4
5 614 *Palaeobatrachus* in general).
6
7 615 One fragmentary scapula (UU HAR1 5009) from Harami 1 is available (Fig. 7a–c). Both its
8
9
10 616 anterior and posterior margins are concave and its distal (suprascapular) portion is narrower
11
12 617 than the proximal part. As in other *Palaeobatrachidae*, the glenoidal and acromial parts with
13
14 618 their articular cavities are separated by a deep depression (Fig. 7c), but not by a complete
15
16 619 incisure into the outlines of the bone. The urostyle (UU KE 5011) from Keseköy is rather
17
18
19 620 worn out, such that both condyloid fossae lost their lateral margins and the intercondyloid
20
21
22 621 process seems to be remarkably prominent anteriorly (Fig. 7f), but this can be due to
23
24 622 preservation. On the other hand, two longitudinal, parallel ridges close to the midline on the
25
26 623 dorsal surface of the bone, typical for *Palaeobatrachus*, are well seen both in dorsal and
27
28
29 624 anterior aspects. The ilium (UU HAR1 5008) from Harami 1 markedly differs from the ilia of
30
31 625 other *Palaeobatrachidae* by reduced pars ascendens (even if it can be partly damaged in this
32
33
34 626 part), extremely large acetabulum (well seen in medial aspect; Fig. 7e), indistinct tuber
35
36 627 superius which is neither prominent dorsally nor laterally, and by a spike-like spina iliaca
37
38
39 628 (marked by arrow in Fig. 7e).
40
41 629 The humeri (Fig. 7h-u) are the most numerous among all skeletal elements, even if none of
42
43
44 630 them is complete. They vary in their size, proportions of the medial and lateral epicondyles,
45
46 631 and by relative size and position of the caput humeri. In great majority of them there is no
47
48 632 cubital fossa, so the caput humeri is continuous with the ventral surface of the humeral shaft,
49
50
51 633 but it seems that in large individuals there is a narrow, semilunar depression parallel with the
52
53 634 proximal surface of the caput humeri (Fig. 7h). This would suggest that relatively large
54
55
56 635 individuals bent the fore limb in the elbow joint, such that the capitulum of the radioulna
57
58 636 inserted into this depression, whereas in smaller (= younger) individuals the fore limbs were
59
60
61 637 stretched forwards, as is the case with swimming *Xenopus*. Besides this speculative

638 interpretation, no taxonomic conclusions can be inferred from morphological variation of the
 1
 2 639 humeri.
 3
 4 640 **Remarks:** The sphenethmoid is the ossified portion of the anterior part of the braincase with
 5
 6 641 adjacent parts of the septum nasi and postnasal walls, so the degree of its ossification may be
 7
 8
 9 642 used in assessing relative ontogenetic stages. In fully developed adults, ossified parts of
 10
 11 643 postnasal walls, septum nasi, and braincase walls should be more extensive, compared with
 12
 13 644 their cartilaginous portions, than in juveniles of the same species. In *Palaeobatrachus*, this
 14
 15 645 may be combined with fusion of the sphenethmoid with some dermal bones, like the
 16
 17 646 frontoparietal and parasphenoid. The maxilla is remarkable by obviously reduced number of
 18
 19 647 tooth positions, which is characteristic for Pliocene and Pleistocene species of
 20
 21 648 *Palaeobatrachus*, such as *P. eurydices* and *P. langhae*, whereas Oligocene taxa have higher
 22
 23 649 number of small teeth. The scapula seems to be different from those in Oligocene species by
 24
 25 650 its markedly concave anterior margin and narrow suprascapular portion; for instance,
 26
 27 651 *Palaeobatrachus* from Enspel has the anterior margin straight, meeting with the suprascapular
 28
 29 652 margin in a right angle.
 30
 31 653
 32
 33 654 *Anura* indet.
 34
 35 655 Figures 4z-cc
 36
 37 656
 38
 39 657 **Material:** loc. Kargı 1: one maxilla fragment (UU KAR1 1051). Loc. Harami 1: three
 40
 41 658 radioulnae (UU HAR1 5052), one neural arch (UU HAR1 5053), three phalanges (UU HAR1
 42
 43 659 5056–5058). Loc. Bağıcı: one radioulna (UU BAG 1203).
 44
 45 660 **Description:** Two different morphotypes of phalanges are present in Harami 1. Those of the
 46
 47 661 morphotype A (one phalanx, UU HAR1 5056, Fig. 4bb) are robust and triangular, the bulb is
 48
 49
 50
 51
 52
 53
 54
 55
 56
 57
 58
 59
 60
 61
 62
 63
 64
 65

- 1
2 662 large and possesses well-developed rugosities on its surface. The phalanges of the
3
4 663 morphotype B (two phalanges, UU HAR1 5057, 5058, Figs. 4cc) are shorter but slender, the
5
6 664 bulb is rounded with less rugosities than in the morphotype A.
7
8 665 The fragment of a maxilla (UU KAR1 1051) with both teeth and tooth pedicles is preserved
9
10 666 from the locality Kargı 1 (Fig. 4z-aa). The teeth are bicuspid and inclined lingually at their
11
12 667 tips. The labial cusps are smaller than the lingual ones. Its labial surface is smooth with few
13
14 668 small nutrition foramina.
15
16
17
18 669 **Remarks:** The phalanges can be clearly assigned to the Anura based on their morphology
19
20 670 (Kamermans and Vences 2009), but any precise identification is impossible. The tooth
21
22 671 morphology of the maxilla from Kargı 1 resembles that of e.g. Ranidae, Alytidae,
23
24 672 Pelobatidae, Bombinatoridae, Hylidae (Greven and Laumeier 1987; Greven and Ritz
25
26 673 2008/2009). Other families, such as Palaeobatrachidae (with non-pedicellated and
27
28 674 monocuspid teeth, lack of knobs between teeth) (Wuttke et al. 2012), Bufonidae (no teeth on
29
30 675 maxilla) (Sanchíz 1998) can be excluded. Taking this into account, this maxilla can be
31
32 676 considered only as Anura indet.
33
34
35
36
37
38 677
39
40
41 678 Class Reptilia Laurenti, 1768
42
43
44 679 Order Squamata Oppel, 1811
45
46
47 680 Family Anguidae Gray, 1825
48
49
50
51 681 Genus *Pseudopus* Merrem, 1820
52
53
54 682 *Pseudopus* sp.
55
56
57 683 Figure 8a-b
58
59
60 684
61
62
63
64
65

- 1
2
3
4
5
6
7
8
9
10
11
12
13
14
15
16
17
18
19
20
21
22
23
24
25
26
27
28
29
30
31
32
33
34
35
36
37
38
39
40
41
42
43
44
45
46
47
48
49
50
51
52
53
54
55
56
57
58
59
60
61
62
63
64
65
- 685 **Material:** Loc. Kargı 1: one jaw fragment (UU KAR1 1205). Loc. Kargı 2: one tooth (UU
686 KAR2 1204).
- 687 **Description and remarks:** A jaw fragment with two teeth (UU KAR1 1205, Fig. 8a) and an
688 isolated tooth (UU KAR2 1204, Fig. 8b) are preserved. The teeth are robust, cylindrical to
689 conical, subpleurodont and stout. Lateromedially they are slightly compressed. There are
690 distinct striae observable on the crown. The lateral and medial surfaces of the crowns possess
691 striae directed vertically (to the tooth axis). The anterior and posterior edges possess
692 moderately (UU KAR1 1205) or weakly developed (UU KAR2 1204) cutting edges. The
693 observed morphology on the available tooth material allows its identification as *Pseudopus*
694 (Klembara et al. 2014). Also the rather molariform morphology of teeth suggest their origin
695 from the posterior part of the jaws (Klembara et al. 2014).
- 696
- 697 *Ophisaurus* sp.
- 698 **Material:** Loc. Kargı 2: five trunk vertebra (UU KAR2 1201).
- 699 **Description and remarks:** These remains represent additional bone remains to the earlier
700 published material of *Ophisaurus* sp. in Čerňanský et al.(2017). See description and
701 discussion therein.
- 702
- 703 Anguinae indet.
- 704 Figure 8c-e
- 705

- 1
2
3
4
5
6
7
8
9
10
11
12
13
14
15
16
17
18
19
20
21
22
23
24
25
26
27
28
29
30
31
32
33
34
35
36
37
38
39
40
41
42
43
44
45
46
47
48
49
50
51
52
53
54
55
56
57
58
59
60
61
62
63
64
65
- 706 **Material:** Loc. Kargı 2: one right dentary (UU KAR2 1203), two osteoderms (UU KAR2
1202). Loc. Kargı 3: two osteoderms (UU KAR3 1202). Loc. Çandır: 22 osteoderms (UU CD
5207, 5208), one vertebra (UU CD 5209). Loc. Bağiçi: three osteoderms (UU BAG 1200).
- 709 **Description and remarks:** An anterior portion of a dentary (UU KAR1 1203, Fig. 8c) is
710 available from the locality Kargı 2. The labial surface is smooth, possessing only three mental
711 foramina. In lingual view, five tooth positions are visible. The base of the preserved tooth
712 pedicles are pierced by small foramina. The subdental shelf (sensu Evans 2008; dental crest
713 sensu Klembara et al. 2014) is low and have rounded surface. The dental lamina is more than
714 twice as high as the subdental shelf. The Meckelian groove is narrow and exposed ventrally.
715 The symphysis projects linguoposteriorly. The preserved anterior portion of the dentary
716 without teeth, can be identified as *Anguinae* indet. based on the ventrally exposed Meckelian
717 groove and general shape of the bone (Klembara et al. 2014).
- 718 Besides the herein described jaw material, we list in the material a further vertebra and
719 osteoderms representing an additional material to the already published remains of anguins
720 from Turkish localities (Čerňanský et al. 2017).
- 721
- 722 Family Lacertidae
- 723 Lacertidae indet. 1
- 724 Figure 8f-h
- 725
- 726 **Material:** Loc. Kargı 1: one dentary (UU KAR1 1206).
- 727 **Description:** The dentary is partially preserved with 14 tooth positions. The bone is robust,
728 the subdental shelf is thick, massive, and widens anteriorly (Fig. 8h). The Meckelian groove

- 1 729 opens lingually. The teeth are pleurodont, bicuspid, short, robust. They are located close to
 2
 3 730 each other. Their apices are oriented posterolingually. The tooth crown possess a large main,
 4
 5 731 blunt casp and a small mesial (anterior) caps. The main caps shows at its lingual surface
 6
 7 732 vertical striae terimating apically at the caps tip. The dental lamina is relatively high, reaching
 8
 9 733 the bases of the tooth crown (Fig. 8f). The labial surface of the dentary, is pierced by five
 10
 11
 12 734 small-sized mental foramina, which are arranged in a row and located in the lower half of the
 13
 14 735 bone.
 15
 16
 17 736 **Remarks:** see Remarks of Lacertidae indet. 4
 18
 19
 20
 21 737
 22
 23
 24 738 Lacertidae indet. 2
 25
 26
 27 739 Figure 8i-o
 28
 29
 30 740
 31
 32
 33 741 **Material:** Loc. Keseköy: ten maxillae (UU KE 5200 – 5202), 15 dentaries (UU KE 5203 –
 34
 35 742 5206, 5213). Loc. Çandır: one dentary (UU CD 5200).
 36
 37
 38 743 **Description:** The dentary is slender. The subdental shelf is flat posteriorly to rounded
 39
 40
 41 744 anteriorly (Fig. 8j). It has nearly the same height along its length but at the 9-10th tooth
 42
 43 745 positions, it increases in height. The ventral margin of the bone and the subdental shelf run
 44
 45 746 close and subparallel to each other. The Meckelian groove is lingually exposed, but anteriorly
 46
 47 747 it changes its orientation rather ventrally (Fig. 8j, 8l). The symphyseal part of the bone is
 48
 49 748 reduced. The dentition is remarkably heterodont: four different tooth morphologies can be
 50
 51 749 observed.
 52
 53
 54
 55
 56 750 The first morphotype resembles that of the skinks. Located at the first tooth positions (1-5th
 57
 58
 59 751 positions in UU KE 5213, Fig. 8l, 8n; 1(?)-7th positions in UU KE 5206, Fig. 8j, 8k), the
 60
 61
 62
 63
 64
 65

- 1 752 teeth are slender, monocuspid and pointed. At the lingual surface, the tooth crown possesses
2
3 753 vertical striae, directed to the tooth tip. The crista lingualis and crista labialis are separated
4
5 754 (not connection with carina intercuspidalis) and run parallel to each other. The former one in
6
7 755 less pronounced than the former. The antrum intercristatum is broad. The crista labialis is
8
9 756 slightly projecting over the antrum intercristatum.
10
11
12 757 The second morphotypes is characterised by rather short, robust bicuspid teeth, with rounded
13
14 758 crowns. The lingual surface of the crown possess vertical striae fusing at the tip of the tooth.
15
16 759 The main casp is larger and higher than the lateral one. In the tooth row, the second
17
18 760 morphotype can be observed posteriorly from the teeth of the first morphotype (8th tooth
19
20 761 position, UU KE 5206, Fig. 8k) and on maxilla (UU KE 5200, Fig. 8i).
21
22
23 762 The third tooth morphotype resembles the typical lacertid morphology, widely found in
24
25 763 European Neogene and recent forms. The tooth is bicuspic, cylindrical, with sharp apex. The
26
27 764 tooth crown composes of a large main caps and small lateral (anterior) casp. The lingual
28
29 765 surface of the tooth crown is nearly flat or bears weakly-developed vertical striae. The third
30
31 766 morphotype can be observed in the middle or posterior half of the dentary (15th tooth
32
33 767 positions in UU KE 5200, Fig. 8j and UU KE 5213, Fig. 8l).
34
35
36 768 The fourth morphotype is represented by short and robust tricuspid teeth. The crown has
37
38 769 smooth surface. It is composed of the main (central) large cusp and two anterior and posterior
39
40 770 cusps. The anterior cusp is slightly larger than the posterior one (last tooth positions, UU KE
41
42 771 5219, fig. 8o).
43
44
45 772 The teeth are oriented in the first three tooth positions anteriorly. Posteriorly in the tooth row
46
47 773 the teeth change their orientation to posterior direction. In labial view, the dentary has smooth
48
49 774 surface and possess at least five mental foramina, which are arranged in a row. The first
50
51 775 foramen is located very close to the symphysis and opens anteriorly. Three first foramina are
52
53
54
55
56
57
58
59
60
61
62
63
64
65

- 1
2
3
4
5
6
7
8
9
10
11
12
13
14
15
16
17
18
19
20
21
22
23
24
25
26
27
28
29
30
31
32
33
34
35
36
37
38
39
40
41
42
43
44
45
46
47
48
49
50
51
52
53
54
55
56
57
58
59
60
61
62
63
64
65
- 776 located close to each other (at the 1st, 4th and 7th tooth positions correspondingly) whereas
- 777 the last two ones 11th and 16-15th tooth positions correspondingly (UU KE 5213, Fig. 8l-n)
- 778 **Remarks:** see Remarks of Lacertidae indet. 4
- 779
- 780 Lacertidae indet. 3
- 781 Figure 8p-r
- 782
- 783 **Material:** Loc. Keseköy: eight maxillae (UU KE 5207 – 5210), 16 dentaries (UU KE 5211 –
- 784 5212, 5214 – 5216, 5220). Loc. Hancılı: one maxilla (UU HAN 5200). Loc. Çandır: four jaw
- 785 bones (UU CD 5201, 5210).
- 786 **Description:** The dentaries are fragmentary preserved. The subdental shelf is flat. The
- 787 Meckelian groove exposes lingually. All teeth including the posterior ones are bicuspid,
- 788 cylindrical, with sharp apices. The main cusp is large and pointed, it possesses at its lingual
- 789 surface weakly-developed vertical striae. The small lateral (anterior) cusp is significantly
- 790 lower than the main one. All preserved teeth are oriented posteriorly. In labial view, the bone
- 791 possesses four rather large mental foramina (UU KE 5215, Fig. 8aa), which are located in the
- 792 preserved specimen at the first 12 tooth positions.
- 793 **Remarks:** see Remarks of Lacertidae indet. 4.
- 794
- 795 Lacertidae indet. 4
- 796 Figure 8s-u
- 797

- 1
2
3 798 **Material:** Loc. Çandır: one dentary (UU CD 5202).
- 4
5 799 **Description:** The preserved dentary is robust. The dental shelf is high with a flat surface. The
6
7 800 symphysis is reduced. The teeth are arranged close to each other. The dentition is heterodont.
8
9 801 At the sixth tooth position, the tooth crown is bicuspid, with large main cusps and small
10
11 802 anterior cusp (Fig. 8u). At the seventh tooth position, the tooth is thick; the tooth crown is
12
13 803 bicuspid with clearly separated pointy cusps, which are nearly similar in height. The 9-10th
14
15 804 tooth positions, the tooth crowns are monoscutid, with rounded, spoon-shaped cusp. All
16
17 805 teeth have smooth lingual surfaces. The Meckelian groove is narrow and opens
18
19 806 linguoventrally, anteriorly it turns more ventrally. The labial surface of the bone is pierced by
20
21 807 six, closely situated, rather large mental foramina. Among them, the first one is located
22
23 808 slightly ventrally from the main row (Fig. 8t).
24
25
26
27
28 809 **Remarks:** The described four forms of lacertid lizards can be clearly distinguished from each
29
30 810 other by several characters:
31
32
33 811 1) the mental foramina:
34
35
36 812 a. in Lacertidae indet. 1 they are small in size, arranged at the ventral half of the bone and not
37
38 813 very far from each other;
39
40
41
42 814 b. in Lacertidae indet. 2 the foramina are larger than in Lacertidae indet. 1, and the first three-
43
44 815 four foramina are closely located to each other, a further foramen is located significantly far
45
46 816 from the rest;
47
48
49
50 817 c. in Lacertidae indet. 3 the foramina are larger and they are arranged rather close to each
51
52 818 other in Lacertidae indet. 2;
53
54
55
56 819 d. the mental foramina are small and located very close to each other in Lacertidae indet. 4.
57
58
59 820 2) dentition:
60
61
62
63
64
65

- 1
2
3
4
5
6
7
8
9
10
11
12
13
14
15
16
17
18
19
20
21
22
23
24
25
26
27
28
29
30
31
32
33
34
35
36
37
38
39
40
41
42
43
44
45
46
47
48
49
50
51
52
53
54
55
56
57
58
59
60
61
62
63
64
65
- 821 a. Lacertidae indet. 2 and 4 have heterodont dentition with four and (at least) two
822 morphotypes correspondingly.
- 823 b. Lacertidae indet. 1 has the shortest and thickest teeth in comparison to other studied forms.
- 824 c. Lacertidae indet. 3 has a typical lacertid dentition, commonly found in all fossil and recent
825 species of the genus.
- 826 3) the subdental shelf:
- 827 a. it is robust, massive and (most) well-pronounced in Lacertidae indet. 1,
- 828 b. Lacertidae indet. 4 has slightly less robust subdental shelf than in Lacertidae indet. 1, but is
829 is still more pronounced than in Lacertidae indet. 2 and Lacertidae indet. 3;
- 830 c. Lacertidae indet. 2 and Lacertidae indet. 3 have slender subdental shelf, which is
831 significantly less developed than in Lacertidae indet. 1 and/or Lacertidae indet. 4.
- 832 **Taxonomic considerations:** Remarkable is the presence of two lizards Lacertidae indet. 2
833 and 4 with heterodont dentition. Heterodont dentition has been earlier reported in fossil
834 lizards, e.g. *Miolacerta* (Roček 1984), *Lacerta filholi* (Müller 1996), Scincidae gen. et sp.
835 indet. from Gratkorn (Böhme and Vasilyan 2014) (which should be considered to belong to
836 the family Lacertidae, pers. observations of DV). In many forms the heterodonty was
837 characterised by the presence of anterior monocuspid teeth, posteriorly they become bicuspid
838 or tricuspid, those forms with bicuspid teeth changes posteriorly to fully to tricuspid tooth
839 morphology. Until now in different works, these forms have been described by comparing
840 limited number of lacertid genera, without including e.g. Anatolian (*Anatololacerta*,
841 *Parvilacerta*) and Southern Caucasian (e.g. *Darevskia*, *Iranlacerta*) genera. Kosma (2004)
842 provides rather comprehensive study on dentition of this family, describing the dentition of
843 some species from non-European genera. According to him, among lacertids the heterodont
844 dentition, with up to three different tooth morphotypes (mono-, bi- and tricuspid), can be

1 845 observed in some species of the genera *Darevskia*, *Algyroides*, *Lacerta*, *Iberolacerta*. Among
2 846 these lizards, *Darevskia rudis* (Kosma, 2004: fig. 28) is characterised by three tooth
3
4 847 morphotypes (1-3), which we observe in Lacertidae indet. 2. Moreover, the tooth crown in *D.*
5
6 848 *rudis* is divided into a prominent cuspis labialis and a lower cuspis lingualis and bears
7
8 849 lingulally fine striation. This characters have been also found in the Lacertidae indet. 2, both
9
10 850 from Keseköy and Çandır localities. *Darevskia chlorogaster* (Kosma 2004), do not show the
11
12 851 tricuspid teeth (only mono- and bicuspid) but has a similar structure of the tooth crown.
13
14 852 Nonetheless, to refer the Lacertidae indet. 2 to *Darevskia*, *Algyroides* or other genera, a large
15
16 853 comparative osteological study is necessary, in order to document the osteological differences
17
18 854 among the genera and species. However, the affiliation of the Lacertidae indet. 2 to the
19
20 855 Western Asian lacertids seems most plausible.
21
22
23
24
25
26 856 It is important to note, that our observations question also the validity of the genus *Miolacerta*
27
28 857 (Roček 1984) considering also the fact that the genus has been erected using only limited
29
30 858 lacertid genera for comparison.
31
32
33
34 859 Further identification or comparison of Lacertidae 1, 3 and 4 is difficult due to the presence of
35
36 860 generous characteris (bicuspic teeth) or the lack of available both osteological collections and
37
38 861 comprehensive osteological studied of lizards.
39
40
41
42
43 862
44
45
46 863 Lacertidae indet.
47
48
49 864 Figure 8v-w
50
51
52
53 865
54
55
56 866 **Material:** Loc. Keseköy: five dentaries (UU KE 5217). Loc. Çandır: one dentary (UU CD
57
58 867 5203). Loc. Bağiçi: one maxilla (UU BAG 1201).
59
60
61
62
63
64
65

- 868 **Description and Remarks:** The available dentaries are poorly preserved. They possess few
1 bicuspids of different sizes, which are characteristic to the family Lacertidae (Kosma
2 869
3 2004). Due to the poor preservation, any further taxonomic identification is impossible.
4 870
5
6
7
8 871 The partially preserved maxilla possesses pleurodont, linguoposteriorly directed bicuspid
9
10 872 teeth (Fig. 8v-w). Parallel to the ventral margin of the maxilla a row of four rounded foramina
11
12 873 for mandibular division of the fifth cranial nerve are present. Above the foramina, the bone
13
14 874 possesses dermal ornamentation on the labial surface of the bone, composed of small pits
15
16 875 (Fig. 8v). The premaxillar process is mainly broken. In lingal view, a prominent arched ridge
17
18 876 is present, which builds the anteriodorsal wall for a rather deep cavity. Anteriorly from the
19
20 877 arched ridge the surface of the bone concave and builds rather deep depression. The
21
22 878 combination of characters as bicuspid pleurodont teeth, presence of the dermal ornamentation,
23
24 879 have been found in *Lacerta* cf. *viridis* (Venczel 2006), however, as recently have been
25
26 880 reported (Villa 2018) the dermal ornamentation can be found in different lacertid genera.
27
28 881 Thus, an open nomenclature at the familiar level is preferable for the maxilla from Çandır
29
30 882 (*Lacertidae* indet.)
31
32
33
34
35
36
37
38 883
39
40
41 884 *Amphisbaenia* Gray, 1844
42
43
44 885 Family *Blanidae* (Kearney, 2003)
45
46
47 886 *Blanidae* indet. (? *Blanus* sp.)
48
49
50 887 Figure 8x-y
51
52
53 888
54
55
56 889 **Material:** Loc. Çandır: one dentary (UU CD 5204).
57
58
59
60
61
62
63
64
65

890 **Description:** the posterior part of a dentary with the single most posterior tooth is preserved.
1
2 891 The tooth is short, conical and oriented anterodorsally. Its tip has a small, sharp, posteriorly
3
4
5 892 oriented tip. Basis of two further teeth are present anteriorly from the last teeth. Considering
6
7 893 the large diameter of the tooth traces, their larger sizes in comparison to the last tooth can be
8
9 894 concluded. Resorption pits are present and have circular outlines. In labial view, the bone
10
11
12 895 surface is smooth, it is pierced only by a rather small mental foramina (Fig. 8x). In lingual
13
14 896 view, the subdental shelf of dentary is high and has flat lingual surface. It has the same height
15
16 897 along its length, only at the last tooth position it narrows and projects dorsally terminating
17
18 898 behind the last tooth. The Meckelian canal is open, it widens posteriorly. The intermandibular
19
20 899 septum is preserved. It has a triangular shape and is located ventrally from the last tooth. The
21
22 900 posterior cavity is large. Posteriorly, the ventral margin of the dentary extends ventrally, and
23
24 901 builds a “cavity” corresponding, most probably, to the articulation surface with angular.
25
26 902 Ventrally from the intermandibular septum, a shallow distinct anteroposteriorly directed
27
28 903 deepening is visible, corresponding to the surface of attachment with the splenial. The
29
30 904 coronoid process is partially preserved. It shows thin coronoid facet, which is dorsally broken
31
32 905 off.
33
34
35
36
37
38
39 906 **Remarks:** The combination of the following features, characteristic for the family Blanidae
40
41 907 (Čerňanský et al. 2016), can be observed on the Çandır dentary: 1) Meckelian groove is open
42
43 908 and well developed; 2) pleurodont teeth; 3) presence of the splenial (can be assumed based on
44
45 909 the available attachment surface). Further characters observable in the Çandır dentary such as
46
47 910 4) intermandibular septum extending anteriorly and reaching/surpassing the level of the
48
49 911 posterior end of the tooth row; 5) a strong splenial facet in the posteroventral region of the
50
51 912 dentary have been mentioned to be characteristic for Blanidae and Bipedidae (Folie et al.
52
53 913 2013). Nevertheless, Čerňanský et al. (2016) did not mention either splenial bone or splenial
54
55 914 facet to be characteristic for the family Bipedidae. Due to incomplete preservation of the
56
57
58
59
60
61
62
63
64
65

- 915 dentary, the number and size of the teeth and mental foramina, which are diagnostic for
 1
 2 916 familiar or generic attribution of the remains (Cernanski et al., 2016/2017 Herrlingen 11+9),
 3
 4 917 can not be counted. The presence of slightly posteriorly recurved teeth in the Çandır specimen
 5
 6 918 suggests its attribution of the European *Blanus* (Cernanski et al., 2016/2017 Herrlingen 11+9).
 7
 8 919 The comparison of the described specimen with the only known worm lizard from Turkey
 9
 10 920 (*Blanus* ssp., loc. Gebeceler Georgalis et al. 2018) does not reveal any differences. Thus, an
 11
 12 921 assignment of the Çandır dentary to the genus *Blanus* appears to be possible, but an
 13
 14 922 identification of the material at the family level is preferable.
 15
 16
 17
 18
 19
 20 923
 21
 22
 23 924 *Lacertilia* indet.
 24
 25
 26 925 Figure 8z
 27
 28
 29
 30 926
 31
 32
 33 927 **Material:** Loc. Kargı 1: one ilium (UU KAR1 1208). Loc. Çandır: one autotomy septa (UU
 34
 35 928 CD 5209).
 36
 37
 38 929 **Description and Remarks:** The ilium from Kargı 1 is a robust bone, the bone body is thick.
 39
 40 930 The preacetabular process is thick, pointy and oriented posteriorly (Fig. 8z). The acetabular
 41
 42 931 fossa has lunar shape. The morphology of the ilium is typical to lizards (Russell and Bauer
 43
 44 932 2008). The autotomy septum (UU CD 5209) is small in size and corresponds to the anterior
 45
 46 933 portion. The septum has a trapezoid form and possesses two small and short transverse
 47
 48 934 processes. The morphology of the septum corresponds to the “pattern (b)” or “type 3 of
 49
 50 935 Etheridge” sensu Hoffstetter and Gasc (1969), which is characteristic to e.g. Teiidae,
 51
 52 936 Lacertidae, Anguidae and some Scincidae. In the locality Çandır both Lacertidae and
 53
 54 937 Anguidae have been recorded and most probably, this septum could belong to one of these
 55
 56 938 groups.
 57
 58
 59
 60
 61
 62
 63
 64
 65

- 939
1
2
3 940 Clade Serpentes Linnaeus, 1758
4
5
6 941 Family Boidae Gray, 1825
7
8
9 942 Subfamily Erycinae Bonaparte, 1831
10
11
12 943 Genus *Albaneryx* Hoffstetter and Rage, 1972
13
14
15 944 *Albaneryx* sp.
16
17
18 945 Figure 9a-e
19
20
21
22 946
23
24
25 947 **Material:** Loc. Kargı 3: one trunk vertebra (UU KAR3 1204).
26
27
28 948 **Description:** The vertebra UU KAR3 1204 is fragmentary preserved, the dia-, para-, pre- and
29
30 949 postzygapophyses and condyle are missing. The vertebra, judging by its preserved
31
32 950 dimensions, was longer than short (cl=2 mm (+ ~0.3 mm condyle), naw=2.33, cl/naw=0.86
33
34 951 (0.98 with condyle)). The lateral walls of the zygosphenes are rounded. The lateral lobes project
35
36 952 slightly dorsally, the cranial margin is provided by a short central lobe (Fig. 9d). The neural
37
38 953 arch is low and is located at the posterior half of the neural arch. It arises dorsoposteriorly
39
40 954 directly behind the zygosphenes and bends caudally after reaching its highest point. In dorsal
41
42 955 view, the neural spine is thickened and has a triangular shape. In anterior view, the
43
44 956 paracotylar foramina are absent (Fig. 9a). Deep depressions are present on both lateral sides
45
46 957 of the cotyle. The cotyle is round. In ventral view, the vertebra centrum possesses a distinct
47
48 958 and well-expressed haemal keel. Two small subcentral foramina are present at both sides of
49
50 959 the haemal keel. They are located in anteroposteriorly running subcentral grooves, which
51
52 960 extends cranially. The lateral foramina are small and located in the corner between weakly-
53
54 961 pronounced interzygapophyseal ridge and synapophysis (Fig. 9c).
55
56
57
58
59
60
61
62
63
64
65

- 1
2
3
4
5
6
7
8
9
10
11
12
13
14
15
16
17
18
19
20
21
22
23
24
25
26
27
28
29
30
31
32
33
34
35
36
37
38
39
40
41
42
43
44
45
46
47
48
49
50
51
52
53
54
55
56
57
58
59
60
61
62
63
64
65
- 962 **Remarks:** The small size of the vertebra (cl=2 mm), the absence of paracotylar foramina, the
963 presence of the pronounced haemal keel, low and expended neural spine allow to attritute the
964 vertabra to the family Erycinae (Ivanov et al. 2018; Rage 1984), excluding the genera
965 *Bransateryx* and *Gonglophis* which have larger sizes of vertebra (Szyndlar 1987; Szyndlar
966 and Schleich 1993). UU KAR3 1204 resemble the genus *Albaneryx* and distinguished from
967 the genera *Eryx* and *Gongylophis* by tickened neural spine, situated at the posterior half of the
968 neural arch directely behind the zygosphene (Ivanov et al. 2018; Szyndlar and Schleich 1993).
969 Additionally, the vertebra differs from *Eryx* by pronounced haemal keel of the vertebra
970 centrum (Blain 2016; Szyndlar 1991). Further vertebra comparison with species of the genus
971 *Albaneryx* is difficult due to the poor preservation of the bone.
- 972
- 973 Erycinae indet.
- 974 Figure 9f-n
- 975
- 976 **Material:** Loc. Harami 1: one trunk vertebra (UU HAR1 5200).
- 977 **Descriptions and Remarks:** the vertebra UU HAR1 5200 (Fig. 9f-i) is smaller than the UU
978 KAR3 1204 (*Albaneryx* sp.) (Fig. 9a-e), its centrum length (cl) equals 1.29 mm (+~0.2 mm
979 condyle). The vertebra is wide (naw=1,62 mm) than long, cl/naw=0.8 mm (0.92 with
980 condyle). In anterior view, the neural arch is high and has rounded outline. The cotyle is
981 incomplete. The paracotylar foramina are absent in the broad depressions on both sided of the
982 cotyle (Fig. 9f). In lateral view, the vertebrae centrum bents posteroventrally and possesses a
983 weakly-pronounced haemal keel. The preserved anterior portion of the neural spine is low and
984 rises slightly posteriorly (Fig. 9i). In dorsal view, the right lateral lobe of the zygosphene is
985 observable, as well as it is visible that the neural spine arises not directly behind the

- 1 986 zygosphenes, but slightly posteriorly (Fig. 9h). In ventral view, two subcentral foramina are
 2
 3 987 present laterally on both sides of the haemal keel at the anterior half of the vertebra centrum
 4
 5 988 (Fig. 9g). The small vertebrae sizes, $cl/naw > 1$, absence of the paracotylar foramina suggest
 6
 7 989 the assignment of the vertebra to the subfamily of Erycinae (Szyndlar 1991). UU HAR1 5200
 8
 9 990 can be distinguished from UU KAR3 1204 (*Albaneryx* sp.) by its smaller size, less developed
 10
 11
 12 991 haemal keel and shorter neural spine. Herewith this vertebra can be considered to belong to
 13
 14 992 different taxa than *Albaneryx* sp. However, the poor preservation of the vertebra does not
 15
 16
 17 993 allow any further identification.
 18
 19
 20 994 **Material:** Loc. Bağçı: one caudal vertebra (UU BAG 1202).
 21
 22
 23 995 **Descriptions and Remarks:** The preserved caudal vertebra is fragmentary preserved. Its
 24
 25
 26 996 surface is eroded. The vertebra is small, with longer preserved vertebra centrum ($cl=1.13$ mm)
 27
 28 997 and shorter *naw* value equalling 0.96, $cl/naw=1.19$. Prezyg-, postzyg- and haem- and
 29
 30 998 pleurapophyses are broken.
 31
 32
 33 999 In anterior view, the neural canal is small and rounded. The cotyle is anterodorsally flattened.
 34
 35
 36 1000 The paracotylar depressions are deep and possess paracotylar foramina (Fig. 9j). The neural
 37
 38 1001 arch rises posteriorly. The neural spine is broken but, based on its preserved portion, it can be
 39
 40
 41 1002 assumed that it was high (Fig. 9k). In dorsal view, it is visible that the neural spine is short
 42
 43 1003 and arises behind the zygosphenes (Fig. 9n). The small size of vertebra and its dimensions
 44
 45
 46 1004 suggests its assignment to subfamily Erycinae (Szyndlar 1991). Its further identification,
 47
 48 1005 however, is difficult, due to its poor preservation.
 49
 50
 51 1006
 52
 53
 54 1007 *Serpentes* indet.
 55
 56
 57 1008 Figure 9o-t
 58
 59
 60
 61 1009
 62
 63
 64
 65

- 1010 **Material:** Loc. Kargı 1: one tooth (UU KAR1 1207). Loc. Kargı 3: two vertebra (UU KAR3
1
2
3
4
5
6
7
8
9
10
11
12
13
14
15
16
17
18
19
20
21
22
23
24
25
26
27
28
29
30
31
32
33
34
35
36
37
38
39
40
41
42
43
44
45
46
47
48
49
50
51
52
53
54
55
56
57
58
59
60
61
62
63
64
65
- 1011 1203, 1205, 1206). Loc. Keseköy: one tooth (UU KE 5218). Loc. Bağıcı: one axis (UU BAG
1012 1204).
- 1013 **Descriptions and Remarks:** the preserved teeth are conical and posteriorly oriented. UU
1014 KAR1 1207 has sharp tip without any canal (Fig. 9t).
- 1015 The preserved axis (UU BAG 1204) lacks the posterior (third) intercentrum (hypapophysis),
1016 transverse process and neural spine. The odontoid process is flattened anteriorly, with clear
1017 two articulation surfaces (Fig. 9o). Ventrally from the odontoid process, the anteroventrally
1018 exposed articulation surface of the second intercentrum is visible. The vertebra centrum
1019 between the second and third intercentra in concave. The neural arch is long. In posterior
1020 view, the roof of the neural arch shows a shape of dorsally flattened triangle. The
1021 postzygapophysis is nearly horizontally oriented (Fig. 9q). The posteroventral corners of the
1022 neural arch, located above the postzygapophyses, possess weakly pronounced posteriorly
1023 oriented processes. The articulation surface of the zyngatrum is oriented at about 45°. The
1024 observed morphology of the preserved axis resembles mostly that of the natricin snakes (the
1025 weakly pronounced posterior processes of the neural arch, long axis) (Szyndlar 1991).
1026 However, due to lack of the comparative material of other groups we prefer to assign the axis
1027 to snakes.
- 1028 Three further vertebrae (UU KAR3 1203, 1205, 1206) are very fragmentary preserved, which
1029 makes any identification impossible.
- 1030
- 1031 *Crocodylia* Gmelin, 1789
- 1032 *Crocodylia* indet.
- 1033 Figure 9u-w

- 1034
1
2
3 1035 **Material:** Loc. Kargı 1: 78 teeth (UU KAR1 1200 – 1202), four osteoderms (UU KAR1
4
5 1036 1203, 1204). Loc. Kargı 2: 97 teeth (UU KAR2 1200). Loc. Kargı 3: five teeth (UU KAR3
6
7
8 1037 1201). Loc. Harami 1: six teeth (UU UU HAR1 5202). Loc. Hancılı: 49 teeth (UU KE 5201).
9
10 1038 Loc. Çandır: one tooth (UU CD 5205).
11
12
13 1039 **Description and remarks:** All studied teeth belong to small-sized individuals. They are
14
15
16 1040 lingolabially compressed and conical in shape. They are represented by different
17
18 1041 morphologies from slender, high and narrow to rather blunt, short, broad. At their bases, they
19
20
21 1042 show a crown-root construction. The both lingual and labial tooth surfaces possess weakly-
22
23 1043 pronounced striae (Fig. 9u-v). The anterior and posterior tooth margins possess sharp cutting
24
25
26 1044 edges. The fragments of osteoderms displays characteristic for crocodiles ornamentation
27
28 1045 composed of deep rounded well-pronounced pits (Fig. 9w).
29
30
31 1046
32
33 1047 **Discussion**
34
35
36 1048 Collectively, the fish, amphibian and reptilian faunal record of the Kargı 1, Kargı 2, Kargı 3,
37
38
39 1049 Harami1, Harami 3, Hancılı, Keseköy, Çandır, and Bağıcı localities is diverse (Table 2), and
40
41 1050 contains carps (*Luciobarbus* sp., *Barbus* sp., *Luciobarbus* vel *Barbus* sp., aff. *Capoeta* sp.,
42
43
44 1051 *Barbini* indet., *Leuciscus* sp.), a salamander (*Salamandra* sp.), anurans (Bufonidae indet.,
45
46 1052 Pelobatidae indet., *Latonia* sp., Palaeobatrachidae indet.), lizards (*Pseudopus* sp., Lacertidae
47
48 1053 indet. 1, Lacertidae indet. 2, Lacertidae indet. 3, Lacertidae indet. 4, Blanidae indet. (?*Blamus*
49
50
51 1054 sp.)), snakes (*Albaneryx* sp., Erycinae indet.) and crocodiles (Crocodylia indet.). However,
52
53 1055 each individual locality yielded only a very limited number of taxa and, moreover, all studied
54
55
56 1056 samples are represented by small, disarticulated bones and skeletal fragments. Fossil remains
57
58 1057 of some groups, such as turtles and tortoises, are not included in the samples. In this light, the
59
60
61 1058 assemblages reported here are unlikely to represent complete reconstructions of

1059 paleoherpetological assemblages, due to both sampling (washing and subsequent screening
1
21060 which resulted in sampling bones of just certain size range) and taphonomic biases.
3
4
51061 Consequently, our palaeobiogeographic and palaeoecological inferences are tentative.
6
7
81062
9
10
111063 Cyprinids
12
13
141064 The identifiable fish material from the studied localities belongs to the family Cyprinidae.
15
161065 Only the locality the Hancılı provided leuciscin remains, the other localities contain abundant
17
18
191066 remains of barbin fishes (Table 2). The oldest fish remains from the studied localities (Kargı
20
211067 1, Kargı 2, Keseköy, latest Oligocene to early Miocene) can be assigned to a small-sized
22
23
241068 barbin. The observed tooth morphology cannot be referred to any fossil form known from
25
261069 Eurasia. Most probably, they could represent an ancient extinct barbin group. Both Harami 1
27
28
291070 and Hancılı localities provide remains of two widely distributed barbin genera *Luciobarbus*
30
311071 and *Barbus*. Indeed, the barbin record from the Hancılı, which is identified by isolated
32
33
341072 pharyngeal teeth as *Barbus* sp. and *Luciobarbus* sp., could include three barbin taxa, if
35
361073 considering only the three different morphotypes of the serrated rays of the dorsal fin.
37
38
391074 However, this cannot be stated with confidence due to the lack of comparative osteological
40
411075 studies of this element in the extant barbin species.
42
43
441076 The record of the Harami 1 locality can be considered as the oldest known remains of *Barbus*
45
461077 and *Luciobarbus* genera. So far the oldest record of the genus *Luciobarbus* was known from
47
48
491078 the earliest late Miocene of Austria (loc. Mataschen, Schultz 2004). Böhme and Ilg (2003)
50
511079 mentioned oldest *Luciobarbus* from contemporaneous to Mataschen sites in Turkey, however,
52
53
541080 this material stays unfigured. We suggest that *Barbus* sp. Harami 1 and Hancılı should be
55
561081 considered as the oldest representatives of this genus, since earlier publications describing
57
58
591082 *Barbus* sp. do not represent the genus *Barbus* sensu Yang et al. (2015). Our finds would
60
61
62
63
64
65

1083 provide important information also for the calibration of the molecular trees, which estimates
1
2 1084 the divergence time and origination of different barbin clades.
3
4
5 1085 Amphibians
6
7
8 1086 The only caudate taxon from the studied Anatolian sites is *Salamandra* sp., recovered from
9
10
11 1087 the localities Harami 1 and Bağıcı. It is the first fossil record of the genus in this region. The
12
13 1088 genus is well known from the Neogene of Europe, but its out-of-Europe occurrence was
14
15 1089 hitherto unknown. Our records is the evidence of caudate amphibians in Anatolia as early as
16
17 1090 in the earliest Miocene and at least during middle Miocene. Because of absence of
18
19 1091 osteological data on the genus *Salamandra*, it is not possible to decide whether this fossil is
20
21 1092 related to the recent species *Salamandra infraimmaculata* distributed in Anatolia and Middle
22
23 1093 East. Until now, the fossil record of caudates in Anatolia was represented by imprints of
24
25 1094 Salamandridae indet. from the locality Ağaöz, early Miocene (Paicheler et al. 1978) which,
26
27 1095 however, can not be compared with our specimens.
28
29
30 1096 Hitherto, only few fossil anuran taxa have been reported from Anatolia, mainly from the early
31
32 1097 and middle Miocene (Table 1). They include brown frog (*Rana*), green frogs (*Pelophylax*,
33
34 1098 originally described as *Rana* sp. in Paicheler et al. (1978)), and spadefoot toad (*Pelobates* sp.).
35
36 1099 The evidence of *Pelobates* is based on premetamorphic tadpoles (Dubois et al. 2010;
37
38 1100 Paicheler et al. 1978) in which, however, it is difficult to decide whether they belong to
39
40 1101 *Pelobates* or *Eopelobates*. Similarly, Wassersug and Wake (1995) reported on two tadpoles
41
42 1102 from the middle Miocene of Gürcü (not included in Table 1) that they assigned to *Pelobates*
43
44 1103 sp.
45
46 1104 In the studied localities, the remains of the genus *Latonia*, found in nearly all of them (Table
47
48 1105 2), suggest presence of this genus in central Anatolia from the latest Oligocene to middle
49
50 1106 Miocene. The remains represent small to large individuals (e.g. Fig. 4). The oldest record of
51
52 1107 the genus is known from the earliest Oligocene of Europe (e.g., localities Grafenmühle 10,
53
54
55
56
57
58
59
60
61
62
63
64
65

1108 Möhren 12 and 13; Böhme and Ilg 2003). Their appearance in Europe coincides with the
1
21109 Grande Coupure event, during which the vertebrate fauna of Europe has been replaced by new
3
4
51110 arrivals including large and small mammals (Hooker 2010; Legendre 1989), as well as
6
71111 amphibians and reptiles (Rage 2012; Vasilyan 2018). Whether *Latonia* invaded Europe (e.g.,
8
9
101112 via Anatolia) or evolved here from some other discoglossoids by means of heterochrony
11
121113 (which may be suggested by the fact that *Latonia* is sometimes accompanied by discoglossoid
13
141114 anurans of smaller size which, although being adult, correspond to early developmental stages
15
16
171115 of *Latonia*) can be only hypothesized. In order to illustrate this background, one can mention
18
191116 *Discoglossus troscheli* from the Oligocene and *Opisthocoeellus weigelti* and *O. hessi* from
20
21
221117 the Eocene and Oligocene of central Europe, or *Eodiscoglossus*, *Iberobatrachus*,
23
241118 *Bakonybatrachus* or *Paralatonia* from the Cretaceous of Spain, Hungary and Romania (see
25
26
271119 literature summerized in Roček 2013).
28
291120 Because of uniformity of species within the genus *Palaeobatrachus* and because majority of
30
31
321121 them was based on articulated skeletons, disarticulated bones of the Palaeobatrachidae usually
33
341122 provide only a limited information for taxonomic assignments. However, our material is an
35
361123 exception. Taking into account that the earliest palaeobatrachids were recorded from the
37
38
391124 Cretaceous of Iberian Peninsula from where they only in the Eocene and post-Eocene times
40
411125 spread to the central and eastern part of Europe (Wuttke et al. 2012), and that they occurred
42
43
441126 only in Europe (with a few exceptions, one of them being Anatolia), it can be taken granted
45
461127 that the palaeobatrachids from Anatolia must have their origin in pre-Miocene Europe and
47
48
491128 that they are not immigrants from Asia (Fig. 9). Their occurrences in the late Miocene of
50
511129 northern Caucasus (Syromyatnikova 2018; Tesakov et al. 2017) and in the Pliocene and
52
53
541130 Pleistocene of the east-European Plateau (Wuttke et al. 2012) seem to be relatively late for
55
561131 immigration of palaeobatrachids to Anatolia. An interesting problem associated with
57
581132 Anatolian Miocene occurrences of palaeobatrachids is the record of *Palaeobatrachus* from the
59
60
611133 locality Gaverdovsky in northern Caucasus (Syromyatnikova 2018; Tesakov et al. 2017),
62
63
64
65

1134 whose contact with the main area of pre-Miocene distribution of palaeobatrachids in Europe
 1
 21135 was probably during a very short time (Fig. 10).
 3
 4
 51136 The remains of Pelobatidae indet. from the Harami 1, Keseköy, Bağiçi provide new data on
 6
 7
 81137 the early Miocene record of the family in Anatolia. Earlier, tadpoles assigned to *Pelobates* sp.
 9
 101138 were described from the early Miocene localities Ağaöz and Ahlath Dere (Dubois et al. 2010;
 11
 12
 131139 Paicheler et al. 1978) and from the the early Miocene of Gürcü Valley (Beşkonak and Akoz
 14
 151140 (Ağaöz sites) (Wassersug and Wake 1995). The former two localities are situated in the
 16
 171141 Beşkonak sequence of lacustrine origin of the Dereköy piroclasts, at the base of the GÜvem
 18
 19
 201142 Formation (Paicheler 1978). The locality Keseköy is also in the Beşkonak sequence (Yavuz-
 21
 221143 Işık 2008). The age of the sequence has been dated using the radiometric analysis between
 23
 24
 251144 19.7 Ma (underlying Çukurviran dacite) and 17.9 Ma (overlying Bakacak andesite) (Denk
 26
 271145 et al. 2017; Wilson et al. 1997; Yavuz-Işık 2008). Pelobatidae indet. from the locality Harami
 28
 29
 301146 1 represents the oldest record (early early Miocene, 22.2 – 22.3 Ma) of the family in Anatolia,
 31
 321147 whereas the Bağiçi specimen is the so far known youngest (late middle Miocene) form of the
 33
 34
 351148 family in Anatolia.
 36
 371149 At first sight, the frontoparietals from Hancılı, obviously belonging to adult individuals, differ
 38
 39
 401150 in their overall appearance from those in recent pelobatids, which are coalesced. However,
 41
 421151 when the development of the frontoparietal in *Eopelobates* and *Pelobates* (both recent and
 43
 441152 fossil) is followed (Maus and Wuttke 2004; e.g. Roček 1981; fig. 43; Roček et al. 2014; fig.
 45
 46
 471153 11-n; Roček and Wuttke 2010; fig. 8), then we see that the frontoparietal takes its origin from
 48
 491154 a pair of bones, which later come in contact along the midline. Besides, another, unpaired
 50
 51
 521155 median ossification arises posteriorly and inserts into the wedge-like space between the
 53
 541156 posterior parts of both frontoparietals. It is only during metamorphosis when all three parts
 55
 56
 571157 fuse into a single frontoparietal complex. It was discovered recently that the developmental
 58
 591158 scheme of the tripartite pelobatid frontoparietal may persist till adulthood in some taxa (e.g.,
 60
 61
 62
 63
 64
 65

1159 *Eopelobates deani*; Roček et al. 2014; fig. 4c). Arrested development of the frontoparietal in
 1
 21160 some extinct pelobatids may be thus taken as a case of heterochrony. Our frontoparietals
 3
 4
 51161 could have been parts of a larger complex, as seems to be supported by the fact that the
 6
 71162 frontoparietal incassation on the inner surface of the bones reached their medial margin (i.e.,
 8
 9
 101163 the incassation extended onto the opposite frontoparietal), and the same holds for the
 11
 121164 posteromedial margin of the bone, which can be taken as an evidence that the incassation
 13
 141165 extended onto the ventral surface of the posterior unpaired element. Pelobatidae were for the
 15
 16
 171166 whole period of their existence restricted to Europe, even if their earliest representatives
 18
 191167 probably invaded Europe from North America in the early Eocene (Roček et al. 2014; Wang
 20
 21
 221168 et al. 2017). One may speculate that heterochrony could have been a response to conditions in
 23
 241169 the marginal areas of distribution, such as today's Anatolia. Whereas isolated bones of adults
 25
 26
 271170 and of the mentioned fossil tadpoles may be considered unequivocal evidence of the
 28
 291171 Pelobatidae, their generic assignment (either to the genus *Eopelobates* or *Pelobates*) is more
 30
 31
 321172 difficult. It was already mentioned above (see Description) that the maxillae rather differ in
 33
 341173 shape of their zygomaticomaxillar process, which is almost pointed and inclined posteriorly in
 35
 361174 UU KE 5006 (Fig. 4q, r) and probably also in UU HAR1 5051 (Fig. 4m, n), whereas the
 37
 38
 391175 maxilla in UU BAG 1001 (Fig. 4o, p) is different – it has its zygomaticomaxillar process
 40
 411176 divided in two parts (which means that its contact with the squamosum was longer than in
 42
 43
 441177 *Pelobates*), the maxilla had its articulation with pterygoid by means of a deep but not
 45
 461178 prominent horizontal lamina instead of processus pterygoideus, sculpture on its labial surface
 47
 48
 491179 is of the pit-and-ridge type. All these characters point to *Eopelobates*. This is also supported
 50
 511180 by the tripartite frontoparietal, only moderately extended laterally (Figs. 4s-v). Thus, it is
 52
 53
 541181 possible that there occurred representatives of both genera in Anatolia, or at least some sort of
 55
 561182 transitional form between them, as it was, e.g., in Gritsev (Roček et al. 2014). However,
 57
 581183 occurrence of pelobatid tripartite frontoparietals from Anatolia (Figs. 4s-v) not necessarily
 59
 60
 611184 mean that they represent pelobatids closely related to *E. deani*. Rather, they could support the

1185 view that some characters, such as those associated with rate of development, could evolve
1
2 1186 independently in forms distant both geographically and chronologically.
3
4
5 1187 As regards the tadpoles, their generic assignment is also not easy. Tadpoles of
6
7 1188 *Eopelobates* have the posterior part of the parasphenoid covered with sculpture whereas it is
8
9 1189 smooth in *Pelobates*. Such details, however, are not discernible in our tadpoles, so their
10
11
12 1190 generic assignment remains open.
13
14 1191 The true toad record has very limited stratigraphic occurrence. It has been only found
15
16
17 1192 from the locality Keseköy (Table 2). In Claessens (1996, 1997) it has been referred to the
18
19 1193 genus *Bufo*, which we after critical revision refer to as *Bufo* indet. Whether *Bufo*
20
21 1194 has entered from Asia to Europe via Turkey (Claessens 1997; Vasilyan et al. 2017), we can
22
23
24 1195 not state here. Further finds from early Miocene localities, would allow to shed more light on
25
26 1196 this palaeobiogeographic question.
27
28
29 1197 Surprisingly, the samples from our studied localities do not contain any ranid remains
30
31 1198 which, however, can be a result of limited sampling or taphonomic bias.
32
33
34
35 1199
36
37 1200 Lizards
38
39
40 1201 *Pseudopus* sp. from the localities Kargı 1 and Kargı 2 represents the first and oldest known
41
42 1202 record of the genus from Anatolia and entire Eurasia. So far, *Pseudopus* was known
43
44
45 1203 exclusively from Europe since the earliest Miocene until the Late Pleistocene (Čerňanský et
46
47 1204 al. 2015; e.g. Klembara et al. 2010). The oldest European record of the genus (*Pseudopus* aff.
48
49
50 1205 *ahnikoviensis*) has been described from the locality Wiesbaden-Amöneburg, Germany of the
51
52 1206 late Aquitanian age (21-22 Ma) (Čerňanský et al. 2015). Thus, *Pseudopus* sp. from the two
53
54
55 1207 studied Turkish localities Kargı 1 and Kargı 2 of latest Oligocene and latest Oligocene-earliest
56
57 1208 Miocene (earliest Aquitanian) ages respectively, can be considered as the earliest documented
58
59
60 1209 remains of the genus from Eurasia. Taking into account the European and Anatolian records
61
62
63
64
65

1210 of the genus, we hypothesis that the genus, being present in Anatolia during the latest
 1
 21211 Oligocene and earliest Miocene, could migrate into Europe during the early Miocene from
 3
 4
 51212 Anatolia. Considering the present finds, the probable origin of the genus in Anatolia and its
 6
 71213 later dispersed by establishing landbridges can be suggested. However, when it could
 8
 91214 happened, stays unclear, since the European record is scarce and restricted to the Central
 10
 11
 121215 Europe. Further finds from Eastern and Southern Europe will be necessary to trace the
 13
 141216 migration routes of this genus.
 15
 16
 171217 The lacertid lizards are represented by at least four forms in the studied localities. Lacertidae
 18
 19
 201218 indet. 1 is the oldest (latest Oligocene, loc. Kargı 1) form. Lacertidae indet. 2 and Lacertidae
 21
 221219 indet. 3 occur in late early Miocene and/to middle Miocene localities (Keseköy, Hancılı,
 23
 24
 251220 Çandır), whereas Lacertidae indet. 4 is known only from the middle Miocene locality Çandır.
 26
 271221 Lacertidae indet. 1 and Lacertidae indet. 3 have tooth morphology well-known from
 28
 29
 301222 numerous Neogene localities of Europe, but forms with morphology (shape of bone and teeth)
 31
 321223 comparable to Lacertidae indet. 1 can not be found. We suggest that Lacertidae indet. 3 from
 33
 34
 351224 loc. Keseköy and Çandır represents a fossil form of recent Western Asian genera like
 36
 371225 *Darevskia*, *Algyroides*, indicating the presence of this group in the region already since the
 38
 39
 401226 early Miocene.
 41
 42
 431227 Until recently, worm lizards have been completely unknown from the Anatolian fossil record.
 44
 451228 A fossil form of the *Blanus trauchi* complex have been newly described from the middle
 46
 47
 481229 Miocene (13.6 Ma) Gebeceler locality in Western Turkey (Georgalis et al. 2018). Here we
 49
 501230 report another worm lizard (Blanidae indet. ? [*Blanus* sp.]) record from Turkey coming from
 51
 521231 the Çandır locality, which has comparable or slightly older age than Gebeceler fossil. Our find
 53
 54
 551232 suggest that this lizard group was distributed in the middle Miocene much northern and
 56
 571233 eastern from both their known fossil and recent distribution areas. This provides an excellent
 58
 59
 60
 61
 62
 63
 64
 65

- 1234 example that the reptilian fossil record of Anatolia is understudied and numerous important
 1
 21235 fossil finds are still waiting to be uncovered.
 3
 4
 51236
 6
 7
 81237 Snakes
 9
 10
 111238 Among the scarce snake finds the most interesting is the vertebra referable to the the genus
 12
 13
 141239 *Albaneryx* (*Albaneryx* sp.) from the locality Kargı 3 (earliest Miocene). Until now, the
 15
 161240 stratigraphic record of this genus covered very short time period (several few million years)
 17
 18
 191241 from the middle Miocene to the earliest late Miocene of Europe and Western Asia (Böhme
 20
 211242 and Ilg 2003; Ivanov et al. 2018). The oldest record of the genus is known from the middle
 22
 23
 241243 Miocene age (13.5-13.7 Ma) locality Sansan (Augé and Rage 2000), whereas the youngest
 25
 261244 record is documented from the e.g. Grytsiv, Ukraine (11.1 Ma) (Zerova 1989). Considering
 27
 28
 291245 the morphological similarities of *Albaneryx* with the North American genus *Lichanura*, it has
 30
 311246 been hypothesised (Augé and Rage 2000; e.g. Zerova 1989) that the genus arrived in Europe
 32
 33
 341247 from Northern America via Asia. However, no evidences for this hypothesis have been
 35
 361248 provided and the appearance of the genus in Europe stays still enigmatic.
 37
 38
 391249 Interestingly, the oldest record of *Albaneryx* coincides with the end of the Miocene Climatic
 40
 41
 421250 Optimum (MCO) (loc. Sansan), when a significant temperature drop has been observed
 43
 441251 (Böhme 2003; Zachos et al. 2001). The new early Miocene find of the genus from Central
 45
 461252 Anatolia favours to the hypothesis of their arrival from Asia into Europe, which was, most
 47
 48
 491253 probably, linked to peculiar climatic conditions necessary for their dispersal and live,
 50
 511254 prevailing in Europe after the MCO.
 52
 53
 541255 Further finds of small-sized erylins from the localities Harami 1 and Bağıçi, suggests the
 55
 56
 571256 (rather continuous) presence of this groups in the Neogene fossil record of the Central
 58
 59
 60
 61
 62
 63
 64
 65

- 1257 Anatolia. More fragmentary preserved snake material (Table 2, Serpentes indet.) is available
 1
 21258 from the studied localities, but too poorly preserved for any consideration.
 3
 4
 51259
 6
 7
 81260 Crocodiles
 9
 10
 111261 The crocodile remains are present in five studied localities suggesting their presence (with
 12
 13 some gaps) in Central Anatolia from the latest Oligocene (Kargı 1) to middle Miocene
 141262 (Çandır) (Fig. 1, table 2). So far, the fossil crocodiles (*Diplocynodon* sp.) from Turkey is
 15
 161263 known from the early early Miocene of eastern Turkey (loc. Tuz-6, Turabi Formation) (Sen et
 17
 18 al. 2011) and mid Oligocene – mid Miocene of western Turkey (Küçükdoğanca Kökü)
 191264 (Schleich 1994). However, since based on tooth material any identifications are not
 20
 211265 appropriate (Delfino 2002), this fossils should be considered as Crocodylia indet. As
 22
 231266 suggested by Böhme (2003), the presence of crocodiles indicate a warm climate with a mean
 24
 251267 annual temperature not lower than 15.7° C, minimal cold and warm month temperatures not
 26
 271268 lower than -1.7° C and 18.3° C respectively.
 28
 291269
 30
 311270
 32
 331271
 34
 35
 36
 371272 **Palaeoenvironmental interpretations**
 38
 39
 401273 We reconstructed tentatively palaeoenvironments of the localities taking into account both
 41
 421274 depositional environments of the fossiliferous horizons and assemblage of the ectothermic
 43
 441275 vertebrates. The fossil faunas of Kargı 1 is found from organic reach black clays; Kargı 2 –
 45
 461276 most probably from comparable sediments as in Kargı 1; Kargı 3 – from greyish clays rich in
 47
 481277 diatomite; Harami 1 – from darkish clay/coal; Harami 3 – from a layer of fine laminated coal
 49
 501278 (Claessens 1996); Keseköy – from green-brown, partly laminated clays and marly clays
 51
 521279 (Krijgsman et al. 1996; Yavuz-Işık 2008); Hancılı – from fine laminated clays and coal
 53
 541280 (Kaymekci 2000). The depositional palaeoenvironment of the sites Kargı 1, Kargı 2, Harami
 55
 56
 57
 58
 59
 60
 61
 62
 63
 64
 65

1281 1, Harami 3 and Hancılı can be interpreted as swamp or marsh, whereas for Kargı 3 and
1
21282 Keseköy a lacustrine environment are characteristic, for Hancılı mix of lake and swampy
3
4
51283 environment can be suggested. The fossil fauna of Çandır is yielded from the reddish silts
6
71284 (Krijgsman 2003), that likely represent pedogenically modified package of the coastal lagoons
8
9
101285 or lake margin. The sedimentology of the Bağıcı locality is unknown but lacustrine
11
121286 environment has been suggested (Claessens 1996).
13
14
151287 Palaeoenvironmental reconstructions for the studied localities, considering the assemblages of
16
171288 ectothermic vertebrates, reflect a mosaic of different environments. In Kargı 1 and 2 an
18
19
201289 environment with transition from water (Barbini indet., *Palaeobatrachus* sp., Crocodylia
21
221290 indet.) to (wet) nearshore (semi-terrestrial *Latonia* sp.) and terrestrial open habitats
23
24
251291 (*Pseudopus* sp., *Ophisaurus* sp., Lacertidae indet. 1) can be suggested. The few fossil remains
26
271292 from Kargı 3 suggest the presence of water body (Crocodylia indet.) with surrounding it
28
29
301293 sandy (*Albaneryx* sp.) wet nearshore (*Latonia* sp.) areas, whereas in Harami 3 water body
31
321294 (*Palaeobatrachus* sp.) and wet nearshore areas (*Latonia* sp.). The Harami 1 represents among
33
34
351295 the studied localities the most diverse palaeoenvironments from aquatic habitats (*Luciobarbus*
36
371296 sp., *Barbus* sp., *Palaeobatrachus* sp., Crocodylia indet.), to nearshore areas (*Latonia* sp.) with
38
39
401297 sandy soils (Pelobatidae indet., Erycinae indet.) and forested areas (*Salamandra* sp.). The
41
421298 Keseköy assemblage of the ectothermic vertebrates suggests the presence of an aquatic
43
441299 environment (Barbini indet., *Palaeobatrachus* sp.), surrounding it nearshore habitats (*Latonia*
45
46
471300 sp.) with sandy soils (Pelobatidae indet.) and large areas with open stony areas (Bufonidae
48
491301 indet., *Ophisaurus* sp., Laceridae indet. 1 and 2). The Hancılı locality is dominated by aquatic
50
51
521302 groups (at least three barbins, *Leuciscus* sp., Crocodylia indet.), but groups inhabiting
53
541303 nearshore areas (*Latonia* sp.) with sandy soils (Pelobatidae indet.) and open habitats
55
56
571304 (Lacertidae indet. 3) were also present. The Çandır association is dominated by terrestrial
58
591305 heliophile groups such as *Ophisaurus* sp., Lacertidae indet. 1, Lacertidae indet. 2 and
60
61
62
63
64
65

- 1306 Lacertidae indet. 3, but also aquatic (*Crocodylia* indet.), semiterrestrial (*Latonia* sp.) and
 1
 2
 3 1307 woodland (*Blanidae* indet.) forms were also present. The herpetofaunistic assemblage of the
 4
 5 1308 Bağıçi locality suggest a terrestrial environment with sandy cover (*Pelobatidae* indet.,
 6
 7 1309 *Erycinae* indet.), forested area (*Salamandra* sp., *Anguis* sp.) and open habitats (*Ophisaurus*
 8
 9 1310 sp., *Laceridae* indet.).
 10
 11
 12
 13 1311
 14
 15
 16 1312 **Conclusions**
 17
 18
 19 1313 The results of the present study significantly enlarge the knowledge of the fish, amphibian and
 20
 21 1314 reptilian fossil record of Anatolia and shed more light on the palaeobiogeographic importance
 22
 23
 24 1315 and significance of the Anatolia for the distribution of the these vertebrate groups.
 25
 26
 27 1316 The earlier studies of the Anatolian fish record documented several species of the genera
 28
 29 1317 *Leuciscus*, *Barbus*, *Tinca* from early Miocene (to middle Miocene) (Table 1). However, the
 30
 31
 32 1318 fossil material has been assigned to a given genus only using cranial and postcranial bone
 33
 34 1319 characteristics, and did not include the characters of the pharyngeal dentition. This makes
 35
 36
 37 1320 impossible to compare them with fossil material from our study and vice versa. Since we can
 38
 39 1321 not securely assign the pharyngeal tooth material of our study to a recent genera, we are aware
 40
 41
 42 1322 of comparing with the known fossil record. More studies and better material are necessary to
 43
 44 1323 provide data for linking the cyprinid taxa identified by the pharyngeal teeth and other skeletal
 45
 46 1324 elements.
 47
 48
 49 1325 Previously among early to middle Miocene amphibians four different taxa have been
 50
 51
 52 1326 documented in the Anatolia record (Table 1). Our present study found two comparable groups
 53
 54 1327 (*Salamandra* sp. and *Pelobatidae* indet.) and added three more taxa (*Latonia* sp.,
 55
 56
 57 1328 *Palaeobatrachus* sp. and *Bufo* indet.). Earlier known both green (*Pelophylax* sp.) and
 58
 59 1329 brown (*Rana* sp.) have not been documented in our study.
 60
 61
 62
 63
 64
 65

1330 Until recently, no fossil lizards have been recorded from Anatolia. Čerňanský et al. (2017)
 1
 21331 and Georgalis et al. (2018) have reported first anguid and amphisbaenids from Turkey. The
 3
 4
 51332 studied localities provided addition lizard material, such as the oldest *Pseudopus* record,
 6
 71333 diverse lacertids (Lacertidae sp. 1 – 4). Earlier known snake record from Turkey is limited to
 8
 91334 Colubroidea indet. and *Bavariboa* sp. (Table 1). As Szyndlar and Hoşgör (2013) has
 10
 11
 121335 suggested, the find of *Bavariboa* sp. evidence about the link between terrestrial faunas of Asia
 13
 141336 and Europe. Our find of *Albaneryx* sp. provide additional support for this hypothesis.
 15
 16
 171337 In summary, the latest Paleogene and middle Miocene fish, amphibian and reptilian fauna of
 18
 19
 201338 Central Turkey (Anatolia) is represented by the following groups: Barbini, Leuciscinae,
 21
 221339 Salamandridae, Pelobatidae, Bufonidae, Alytidae, Palaeobatrachidae, Ranidae, Anguinae,
 23
 24
 251340 Lacertidae, Amphisbaena, Erycinae, Boinae, Chelydridae, Crocodylia. All these groups are
 26
 271341 broadly known in the fossil record of the Europe and suggest strong link between European
 28
 29
 301342 and Anatolian ectothermic faunas. The present study is an outstanding example, showing the
 31
 321343 important role of Anatolia in the dispersal of the other vertebrate groups than mammals, as
 33
 34
 351344 well as how much informative can be poor samples. Further studies on the Anatolian fossil
 36
 371345 record of these groups will provide important clues of the understanding of the formation and
 38
 391346 shaping the European fossil record.
 40
 41
 42
 43
 44
 45
 46
 47
 48
 49
 50
 51
 52
 53
 54
 55
 56
 57
 58
 59
 60
 61
 62
 63
 64
 65

1347 **Acknowledgements**
1
2
31348
4
5
61349 We would like to thank Wilma Wessels (University Utrecht) for support and providing all
7
81350 necessary details about the studied material and locality. We would like to acknowledge
9
10
111351 Sevket Sen for the information about the Hancılı locality. Contribution by ZR was funded by
12
131352 the research plan of the Institute of Geology of the CAS (RVO67985831).
14
15
161353
17
18
191354 **Conflict of Interest:** The author declares that he has no conflict of interest.
20
21
22
231355
24
25
261356
27
28
29
30
31
32
33
34
35
36
37
38
39
40
41
42
43
44
45
46
47
48
49
50
51
52
53
54
55
56
57
58
59
60
61
62
63
64
65

- 1357 References
- 1 1358 Arratia G (2000) New teleostean fishes from the Jurassic of southern Germany and the systematic
2 problems concerning the 'pholidophoriforms'. *Paläontologische Zeitschrift* 74:113–143. doi:
3 10.1007/BF02987957
- 4 1360 Augé ML, Rage J-C (2000) Les Squamates (Reptilia) du Miocène moyen de Sansan. *Mémoires du*
5 Muséum national d'histoire naturelle 183:263–313
- 6 1362 Ayvazyan A, Vasilyan D, Böhme M (2018) 3D morphology of pharyngeal dentition of the genus
7 *Capoeta* (Cyprinidae): Implications for taxonomy and phylogeny. *Journal of Zoological*
8 Systematics and Evolutionary Research 255:85. doi: 10.1111/jzs.12217
- 9 1364 Blain H-A (2016) Amphibians and Squamate Reptiles from Azokh 1. In: Fernandes Jalvo Y, King T,
10 Yepiskoposyan L, Andrews P (eds) *Azokh Caves and the Transcaucasian Corridor*. Springer Verlag,
11 pp 1–20
- 12 1366 Blain H-A, Gibert L, Ferràndez-Cañadell C (2010) First report of a green toad (*Bufo viridis* sensu lato)
13 in the Early Pleistocene of Spain: Palaeobiogeographical and palaeoecological implications.
14 *Comptes Rendus Palevol* 9:487–497
- 15 1371 Bleeker P (1859) Enumeratio specierum piscium hucusque in Archipelago indico observatarum,
16 adjectis habitationibus citationibusque, ubi descriptiones earum recentiores reperiuntur, nec non
17 speciebus Musei Bleekeriani Bengalensibus, Japonicis, Capensibus, Tasmanicisque. *Neerlandense*
18 6:1–276
- 19 1375 Böhme M (2003) The Miocene Climatic Optimum: Evidence from ectothermic vertebrates of Central
20 Europe. *Palaeogeography, Palaeoclimatology, Palaeoecology* 195:389–401
- 21 1377 Böhme M, Ilg A (2003) fosFARbase. Available at www.wahre-staerke.com. Accessed 1 December
22 2015
- 23 1379 Böhme M, Vasilyan D (2014) Ectothermic vertebrates from the late Middle Miocene of Gratkorn
24 (Austria, Styria). *Palaeobiodiversity and Palaeoenvironments* 94:21–40
- 25 1381 Böhme M, Reichenbacher B, Schulz-Mirbach T (2003) Neogene freshwater fishes from Anatolia – a
26 key for understanding the (palaeo-)biogeography of European freshwater fishes. In: unknown
27 (ed) *International Symposium of Fisheries and Zoology*
- 28 Bonaparte CL (1831) *Saggio di una distribuzione metodica degli animali vertebrati*. Antonio Bouzaler,
29 Rome
- 30 1386 Bonaparte CL (1835) *Prodromus systematis ichthyologiae*. *Nuovi Annali delle Scienze naturali*
31 Bologna. *Nuovi Annali delle Scienze naturali Bologna* 1:181-196, 272-277
- 32 1388 Bonaparte CL (1850) *Conspectus systematum. Mastrozoologiae. Ornithologiae. Herpetologiae et*
33 *Amphibiologiae. Ichthyologiae*. E. J. Brill, Lugduni Batavorum
- 34 1390 Bruijn H de, Ünay E, Hordijk K (2013) A review of the Neogene Successions of the Muridae and
35 Dipodidae from Anatoli, with special reference to taxa known from Asia and/or Europe. In: Wang
36 X, J FL, Fortelius M (eds) *Fossil mammals of Asia: Neogene biostratigraphy and chronology*.
37 Columbia University Press, New York
- 38 1394 Čerňanský A, Rage J-C, Klembara J (2015) The Early Miocene squamates of Amöneburg (Germany):
39 the first stages of modern squamates in Europe. *Journal of Systematic Palaeontology* 13:97–128.
40 doi: 10.1080/14772019.2014.897266
- 41 1397 Čerňanský A, Klembara J, Müller J (2016) The new rare record of the late Oligocene lizards and
42 amphisbaenians from Germany and its impact on our knowledge of the European terminal
43 Palaeogene. *Palaeobiodiversity and Palaeoenvironments* 96:559–587. doi: 10.1007/s12549-015-
44 0226-8
- 45 1401 Čerňanský A, Vasilyan D, Georgalis GL, Joniak P, Mayda S, Klembara J (2017) First record of fossil
46 anguines (Squamata; Anguidae) from the Oligocene and Miocene of Turkey. *Swiss J Geosci*
47 110:741–751. doi: 10.1007/s00015-017-0272-5
- 48 1402

- 1405 Claessens L (1996) Miocene reptilia and amphibian faunas of Anatolia: with special emphasis on the
1406 anura. Diploma thesis, Utrecht Universitij
- 1407 Claessens L (1997) On the herpsteofauna of some Neogene Eastern Mediterranean localities and the
1408 occurrence of *Palaeobatrachus* and *Bufo* (Amphibia, Anura) in the Lower Miocene of Turkey.
1409 Journal of Vertebrate Paleontology 17:39
- 1410 Cope ED (1887) Zittel's manual of palaeontology. American Naturalist 21:427–448
- 1411 Cuvier G (1816-1817) Le Règne Animal distribué d'après son organisation pour servir de base à
1412 l'histoire naturelle des animaux et d'introduction à l'anatomie comparée. Avec Figures, dessinées
1413 d'après nature. Contenant Les reptiles, les poissons, les mollusques et les annélides. Deterville,
1414 Paris
- 1415 Cuvier G, Cloquet N (1816) N. genus *Barbus*. In: Levrault FG (ed) Dictionnaire des sciences naturelles,
1416 2nd. F. G. Levrault, Strasbourg
- 1417 Cuvier G, Valenciennes A (1842) Histoire naturelle des poissons, vol 16. P. Bertrand, Paris
- 1418 Delfino M (2002) Erpetofauna italiana del Neogene e del Quaternario, Università degli Studi di
1419 Modena e Reggio Emilia
- 1420 Denk T, Güner TH, Kvaček Z, Bouchal JM (2017) The early Miocene flora of Güvem (Central Anatolia,
1421 Turkey): a window into early Neogene vegetation and environments in the Eastern
1422 Mediterranean. Acta Palaeobotanica 57:250. doi: 10.1515/acpa-2017-0011
- 1423 Doadrio I (1990) Phylogenetic relationships and classification of western palaeartic species of the
1424 genus *Barbus* (Osterechthyes, Cyprinidae). Aquatic and Living Resources 3:265–282
- 1425 Dubois A, Grossjean S, Paicheler J-C (2010) Strange tadpoles from the lower Miocene of Turkey: Is
1426 paedogenesis possible in anurans? Acta Palaeontologica Polonica 55:43–55
- 1427 Estes R, Hoffstetter R (1976) Les Urodèles du Miocène de la Grive-Saint-Alban (Isère, France). Bulletin
1428 du Muséum National d'Histoire Naturelle, 3e Série, Science de la Terre 57:297–343
- 1429 Evans SE (2008) The skull of lizards and tuatara. In: Gans C (ed) The skull of Lepidosauria, Volume 20,
1430 Morphology H. Society for the Study of Amphibians and Reptiles, Ithaca, pp 1–347
- 1431 Fischer G (1813) Zoognosia. Tabulis Synopticis Illustrata, in Usurum Prælectionum Academiae Imperialis
1432 Medico-Chirurgicae Mosquensis Edita, 3rd edn., vol 1. Typis Nicolai Sergeidis Vsevolozsky,
1433 Moscow
- 1434 Fitzinger L (1843) Systema Reptilium. Fasciculus Primus. Braumüller et Seidel, Wien
- 1435 Folie A, Smith R, Smith T (2013) New amphisbaenian lizards from the Early Paleogene of Europe and
1436 their implications for the early evolution of modern amphisbaenians. Geologica Belgica 16:227–
1437 235
- 1438 Frost DR (2014) Amphibian Species of the World: an Online Reference. Version 6.0 (9 January, 2013).
1439 Accessed 24.02.20152014
- 1440 Garsault FAd, Defehrt AJ, Prévost BL, Duflos P, Martinet FN, Geoffroy É-F (1764) Les figures des
1441 plantes et animaux d'usage en medecine décrits dans La matiere medicale de Mr. Geoffroy
1442 medecin. Chez l'auteur rue St. Dominique porte St. Jacques, Paris
- 1443 Georgalis GL, Halaçlar K, Mayda S, Kaya T, Ayaz D (2018) First fossil find of the *Blanus strauchi*
1444 complex (Amphisbaenia, Blanidae) from the Miocene of Anatolia. Journal of Vertebrate
1445 Paleontology 2234:e1437044. doi: 10.1080/02724634.2018.1437044
- 1446 Gmelin JF (1789) Regnum animal. Caroli a Linne Systema Naturae per regna tri naturae, secundum
1447 classes, ordines, genera, species, cum characteribus, differentiis, synonymis, locis. Beer, Leipzig
- 1448 Goldfuss GA (1820) Handbuch der Zoologie, Bd. 2. J. L. Schrag, Nürnberg
- 1449 Gray JE (1825) A synopsis of the genera of reptiles and Amphibia, with a description of some new
1450 species. Annals of Philosophy, London 10:193–217
- 1451 Gray JE (1844) Catalogue of tortoises, crocodilians, and amphisbaenians in the collection of the
1452 British Museum. British Museum, Natural History, London

- 1453 Greven H, Laumeier I (1987) A comparative SEM-Study on the Teeth on 10 Anuran Species.
 11454 Anatomische Anzeige 164:103–116
- 1455 Greven H, Ritz A (2008/2009) Tricuspid teeth in Anura (Amphibia). Acta Biologica Benrodis 15:67–74
- 1456 Heckel JJ (1843) Abblidungen und Beschreibungen der Fische Syriens, nebst einer neuen
 1457 Classification und Charakteristik sämmtlicher Gattungen der Cyprinen. E. Schweizerbart'sche
 1458 Verlagsbuchhandlung, Stuttgart
- 1459 Hoffstetter R, Gasc J-P (1969) Vertebrae and ribs of modern reptiles. In: Gans C (ed) Morphology A,
 1460 Biology of the Reptilia. Academic Press, London, New York, pp 201–310
- 1461 Hoffstetter R, Rage J-C (1972) Les Erycinae fossiles de France (Serpentes, Boidae). Compréhension et
 1462 histoire de la sous-famille. Annales de Paléontologie 58:81–124
- 1463 Hooker JJ (2010) The “Grande Coupure” in the Hampshire Basin, UK: taxonomy and stratigraphy of
 1464 the mammals on either side of this major Palaeogene faunal turnover. In: Whittaker JE, Hart MB
 1465 (eds) Micropalaeontology, sedimentary environments and stratigraphy: A tribute to Dennis Curry
 1466 (1912-2001). Geological Society, London, pp 147–215
- 1467 Hossini S, Rage J-C (2000) Palaeobatrachid frogs from the earliest Miocene (Agenian) of France, with
 1468 description of a new species. Geobios 33:223–231. doi: 10.1016/s0016-6995(00)80019-4
- 1469 Ivanov M, Vasilyan D, Böhme M, Zazhigin VS (2018) Miocene snakes from northeastern Kazakhstan:
 1470 new data on the evolution of snake assemblages in Siberia. Historical Biology 183:1–20. doi:
 1471 10.1080/08912963.2018.1446086
- 1472 Kamermans M, Vences M (2009) Terminal phalanges in ranoid frogs, morphological diversity and
 1473 evolutionary correlation with climbing habits. Alytes 26:117–152
- 1474 Kaymekci N (2000) Tectono-stratigraphical evolution of the Çankırı Basin (Central Anatolia, Turkey).
 1475 Geologica Ultraiectina. Mededelingen van de Faculteit Aardwetenschappen Universteit Utrecht,
 1476 vol 190. Universiteit Utrecht, Utrecht
- 1477 Kearney M (2003) Systematics of the Amphisbaenia (Lepidosauria: Squamata) based on
 1478 morphological evidence from recent and fossil forms. Herpetological Monographs 17:1–74
- 1479 Klembara J, Böhme M, Rummel M (2010) Revision of the Anguine Lizard *Pseudopus laurillardi*
 1480 (Squamata, Anguinae) from the Miocene of Europe, with Comments on Paleocology. Journal of
 1481 Paleontology 84:159–196
- 1482 Klembara J, Hain M, Dobiašová K (2014) Comparative anatomy of the lower jaw and dentition of
 1483 *Pseudopus apodus* and the interrelationships of species of subfamily Anguinae (Anguimorpha,
 1484 Anguinae). The Anatomical Record 297:516–544. doi: 10.1002/ar.22854
- 1485 Kosma R (2004) The dentition of recent and fossil scincomorphan lizards (Lacertilia, Squamata) -
 1486 Systematics, Functional Morphology, Palaeoecology, Fachbereich Geowissenschaften und
 1487 Geographie, Universität Hannover
- 1488 Kottelat M, Freyhof J (2007) Handbook of European freshwater fishes, Bd. 13. Publications Kottelat,
 1489 Berlin
- 1490 Krijgsman W (2003) Magnetostratigraphic dating of the Çandır fossil locality (middle Miocene,
 1491 Turkey). Courier Forschungsinstitut Senckenberg 240:41–49
- 1492 Krijgsman W, Duermeijer CE, Langereis CG, Bruijn H de, Saraç G, Andriessenm Paul A. M. (1996)
 1493 Magnetic polarity stratigraphy of late Oligocene to middle Miocene mammal-bearing continental
 1494 deposits in Central Anatolia (Turkey). Newsletters on Stratigraphy 34:13–29
- 1495 Laurenti JN (1768) Specimen medicum, exhibens synopsis reptilium emendatum cum experimentis
 1496 circa venena et antidota Reptilium Austriacorum. Typ. Joan. Thom. nob. de Trattnern, Viennae
- 1497 Legendre S (1989) Les communautés de mammifères du Paléogène (Eocène supérieur et Oligocène)
 1498 d'Europe Occidentale: structures, milieux et évolution. Münchner Geowissenschaftliche
 1499 Abhandlungen (A) 116:1–110

- 1500 Linnaeus C (1758) *Systema naturae per regna tria naturae, secundum classes, ordines, genera,*
11501 *species, cum characteribus, differentiis, synonymis, locis, Editio decima, reformata.* Stockholm, L.
21502 Salvi
31503 Marković Z, Wessels W, van de Weerd, Andrew A., Bruijn H de (2018) On a new diatomyid (Rodentia,
41504 Mammalia) from the Paleogene of south-east Serbia, the first record of the family in Europe.
51505 *Palaeobiodiversity and Palaeoenvironments* 98:459–469. doi: 10.1007/s12549-017-0301-4
61506 Maus M, Wuttke M (2004) The ontogenetic development of *Pelobates* cf. *decheni* tadpoles from the
71507 Upper Oligocene of Enspel (Westerwald/Germany). *Neues Jahrbuch für Geologie und*
81508 *Paläontologie - Abhandlungen* 232:215-203
91509 Merrem B (1820) Versuch eines Systems der Amphibien. Johann Christian Krieger, Marburg
101510 Meyer H von (1843) Mittheilung an Professor Bronn gerichtet. *Neues Jahrbuch für Geologie und*
111511 *Paläontologie, Geognasie, Geologie und Petrefactenkunde*:579–590
121512 Müller J (1996) Eine neue Art der Echten Eidechsen (Reptilia: Lacertilia: Lacertidae) aus dem Unteren
131513 Miozän von Poncenat, Frankreich. *Mainzer geowissenschaftliche Mitteilungen* 25:79–88
141514 Oppel M (1811) Die Ordnungen, Familien und Gattungen der Reptilien als Prodrum einer
151515 *Naturgeschichte derselben.* Joseph Lindauer, München
161516 Paicheler J-C (1978) Volcanic paleoenvironment and examples of sedimentary incidences at Tertiary
171517 Beşkonak Lake (Northern Anatolia – Turkey). *Bulletin of the Geological Society of Turkey* 21:11–
181518 25
191519 Paicheler J-C, Broin F de, Gaudant J, Mourer-Chauviré C, Rage J-C, Vergnaud-Grazzini C (1978) Le
201520 bassin lacustrine Miocène de Bes-Konak (Anatolie-Turquie): Géologie et intruduction a la
211521 paléontologie des vertébrés. *Geobios* 11:43–65
221522 Rafinesque CS (1815) *Analyse de Nature, ou Tableau de l’Universe et des Corps Organisés.* Jean
231523 Barravecchia, Palermo
241524 Rage J-C (1984) *Serpentes.* Handbuch der Paläoherpetology – Encyclopedia of Paleoherpology, vol
251525 11. Gustav Fischer, Stuttgart, New York
261526 Rage J-C (2012) Amphibians and squamates in the Eocene of Europe: What do they tell us?
271527 *Palaeobiodiversity and Palaeoenvironments* 92:445–457. doi: 10.1007/s12549-012-0087-3
281528 Rage J-C, Hossini S (2000) Les Amphibiens du Miocène moyen de Sansan. *Mémoires du Muséum*
291529 *national d’histoire naturelle* 183:177–217
301530 Roček Z (1981) Cranial anatomy of frogs of the family Pelobatidae Stannius, 1856, with outlines of
311531 their phylogeny and systematics. *Acta Universitatis Carolinae - Biologica* 1980:1–164
321532 Roček Z (1984) Lizards (Reptili: Sauria) from the Lower Miocene locality Dolnice (Bohemia,
331533 Czechoslovakia). *Řada matematických a přírodních věd* 94:4–69
341534 Roček Z (1994) Taxonomy and distribution of Tertiary discoglossids (Anura) of the genus *Latonia* V.
351535 Meyer, 1843. *Geobios* 27:717–751
361536 Roček Z (2013) Mesozoic and Tertiary Anura of Laurasia. *Palaeobiodiversity and Palaeoenvironments*
371537 93:397–439. doi: 10.1007/s12549-013-0131-y
381538 Roček Z, Wuttke M (2010) Amphibia of Enspel (Late Oligocene, Germany). *Palaeobiodiversity and*
391539 *Palaeoenvironments* 90:321–340. doi: 10.1007/s12549-010-0042-0
401540 Roček Z, Wuttke M, Gardner J, Singh Bhullar B-A (2014) The Euro-American genus *Eopelobates*, and a
411541 re-definition of the family Pelobatidae (Amphibia, Anura). *Palaeobiodiversity and*
421542 *Palaeoenvironments* 94:529–567. doi: 10.1007/s12549-014-0169-5
431543 Rögl F (1999) Mediterranean and Paratethys. Facts and hypotheses of an Oligocene to Miocene
441544 paleogeography (short overview). *Geologica Carpathica* 50:339–349
451545 Rössner G, Heissig K (eds) (1999) *The Miocene Land Mammals of Europe.* Dr. Friedrich Pfeil,
461546 München
47
48
49
50
51
52
53
54
55
56
57
58
59
60
61
62
63
64
65

- 1547 Rückert-Ülkümen N (1998) Cyprinidae (Pisces) aus dem Jungtertiär von Alpagut-Dodurga bei Çorum
 11548 (Mittellanatolien, Türkei). Mitteilungen der Bayerischen Staatssammlung für Paläontologie und
 21549 historische Geologie 38:167–181
 31550 Rückert-Ülkümen N (2003) Fossil ranids from miocene deposits of Central Anatolia. Istanbul Üniv.
 41551 Müh. Fak. Yerbilimleri Dergisi 16:71–74
 61552 Russell AP, Bauer AM (2008) The Appendicular Locomotor Apparatus of *Sphenodon* and Normal-
 71553 limbed Squamates. In: Gans C, Gaunt AS, Adler Kraig (eds) The skull and Appendicular Locomotor
 81554 Apparatus of Lepidosauria, Volume 21, Morphology 1. Society for the Study of Amphibians and
 91555 Reptiles, Ithaca, pp 1–465
 111556 Rutte E (1962) Schlundzähne von Süßwasserfischen. Palaeontographica Abteilung A 120:165–212
 121557 Sanchiz B (1998) Salientia. Handbuch der Paläoherpetologie. Verlag Dr. Friedrich Pfeil, München
 131558 Schleich H-H (1994) Fossile Schildkröten- und Krokodilreste aus dem Tertär Thrakiens (W-Türkei).
 141559 Courier Forschungsinstitut Senckenberg 173:137–151
 151560 Schultz O (2004) Die Fischreste aus dem Unter-Pannonium (Ober-Miozän) on Mataschen, Steiermark
 161561 (Österreich). Joannea - Geologie und Paläontologie 5:231–256
 171562 Scopoli GA (1777) Introductio ad historiam naturalem, sistens genera lapidum, plantarum et
 181563 animalium hactenus detecta, characteribus essentialibus donata, in tribus divisa, subinde ad leges
 191564 naturae. Apud Wolfgangum Gerle, Prague
 201565 Sen S, Antoine P-O, Varol B, Ayyildiz T, Sözeri K (2011) Giant rhinoceros *Paraceratherium* and other
 211566 vertebrates from Oligocene and middle Miocene deposits of the Kağızman-Tuzluca Basin,
 221567 Eastern Turkey. Naturwissenschaften 98:407–423. doi: 10.1007/s00114-011-0786-z
 231568 Syromyatnikova E (2018) Palaeobatrachid frog from the late Miocene of Northern Caucasus, Russia.
 241569 Palaeontologia Electronica. doi: 10.26879/861
 251570 Szyndlar Z (1987) Snakes from the Lower Miocene Locality of Dolnice (Czechoslovakia). Journal of
 261571 Vertebrate Paleontology 7:55–71
 271572 Szyndlar Z (1991) A review of Neogene and Quaternary snakes of central and eastern Europe. Part 1:
 281573 Scolecophidia, Boidae, Colubrinae. Estudios Geologicos 47:103–126
 291574 Szyndlar Z, Hoşgör I (2013) *Bavarioboa* sp. (Serpentes, Boidae) from the Oligocene / Miocene of
 301575 eastern Turkey with comments on connections between European and Asiatic snake faunas.
 311576 Acta Palaeontologica Polonica 57:667–671
 321577 Szyndlar Z, Schleich H-H (1993) Description of Miocene Snakes from Petersbuch 2 with Comments on
 331578 the Lower and Middle Miocene Ophidian Faunas of Southern Germany. Stuttgarter Beiträge zur
 341579 Naturkunde. Serie B (Geologie und Paläontologie) 192:1–47
 351580 Tesakov AS, Titov VV, Simakova AN, Frolov PD, Syromyatnikova EV, Kurshkov SV, Volkova NV,
 361581 Trikhunkov YI, Sotnikova MV, Kruskop SV, Zelenkov NV, Tesakova EM, Palatov DM (2017) Late
 371582 Miocene (Early Turolian) vertebrate faunas and associated biotic record of the Northern
 381583 Caucasus: Geology, palaeoenvironment, biochronology. Fossil Imprint 73:383–444
 391584 Tihen JA (1962) A review of New World fossil bufonids. The American Midland Naturalist 68:1–50
 401585 Vasilyan D (in review) Fish, amphibian and reptile fauna from the middle Miocene locality Gračanica,
 411586 Bosnia and Herzegovina. Palaeobiodiversity and Palaeoenvironments
 421587 Vasilyan D (2018) Eocene Western European endemic genus *Thaumastosaurus*: New insights into the
 431588 question “Are the Ranidae known prior to the Oligocene?”. PeerJ
 441589 Vasilyan D, Böhme M, Klembara J (2016) First record of fossil *Ophisaurus* (Anguimorpha, Anguidae,
 451590 Anguinae) in Asia. Journal of Vertebrate Paleontology:1–6. doi:
 461591 10.1080/02724634.2016.1219739
 471592 Vasilyan D, Zazhigin VS, Böhme M (2017) Neogene amphibians and reptiles (Caudata, Anura,
 481593 Gekkota, Lacertilia, Testudines) from south of Western Siberia, Russia and Northeastern
 491594 Kazakhstan. PeerJ 5. doi: 10.7717/peerj.3025
 50
 51
 52
 53
 54
 55
 56
 57
 58
 59
 60
 61
 62
 63
 64
 65

- 1595 Venczel M (2006) Lizards from the Late Miocene of Polgárdi (W-Hungary). *Nymphaea, Folia naturae*
 1596 *Bihariae* 33:25–38
- 1597 Villa A (2018) Neogene and Quaternary Neogene and Quaternary palaeodiversity of the European
 1598 lizards (Reptilia, Squamata), Università degli Studi di Torino
- 1599 Wang X, J FL, Fortelius M (eds) (2013) Fossil mammals of Asia: Neogene biostratigraphy and
 1600 chronology. Columbia University Press, New York
- 1601 Wang Y, Roček Z, Dong L (2017) A new pelobatoid frog from the lower Eocene of southern China.
 1602 *Palaeobiodiversity and Palaeoenvironments*
- 1603 Wassersug RJ, Wake DB (1995) Fossil tadpoles from the Miocene of Turkey. *Alytes* 12:145–157
- 1604 Wilson M, Tankut A, Guleç N (1997) Tertiary volcanism of the Galatia province, north-west Central
 1605 Anatolia, Turkey. *Lithos* 42:105–121. doi: 10.1016/S0024-4937(97)00039-X
- 1606 Winfield IJ, Nelson JS (eds) (1991) Cyprinid Fishes, Systematics, biology and exploitation. Chapman &
 1607 Hall, London, New York, Tokyo, Melbourne, Madras
- 1608 Wuttke M, Přikryl T, Ratnikov VY, Dvořák Z, Roček Z (2012) Generic diversity and distributional
 1609 dynamics of the Palaeobatrachidae (Amphibia: Anura). *Palaeobiodiversity and*
 1610 *Palaeoenvironments* 92:367–395. doi: 10.1007/s12549-012-0071-y
- 1611 Yang L, Sado T, Vincent Hirt M, Pasco-Viel E, Arunachalam M, Li J, Wang X, Freyhof J, Saitoh K, Simons
 1612 AM, Miya M, He S, Mayden RL (2015) Phylogeny and polyploidy: resolving the classification of
 1613 cyprinine fishes (Teleostei: Cypriniformes). *Molecular Phylogenetics and Evolution* 85:97–116.
 1614 doi: 10.1016/j.ympev.2015.01.014
- 1615 Yavuz-Işık N (2008) Vegetational and climatic investigations in the Early Miocene lacustrine deposits
 1616 of the Güvem Basin (Galatean Volcanic Province), NW Central Anatolia, Turkey. *Review of*
 1617 *Palaeobotany and Palynology* 150:130–139. doi: 10.1016/j.revpalbo.2008.02.001
- 1618 Zachos J, Pagani M, Sloan L, Thomas E, Billups K (2001) Trends, rhythms, and aberrations in global
 1619 climate 65 Ma to present. *Science* 292:686–693. doi: 10.1126/science.1059412
- 1620 Zerova GA (1989) First find of the fossil erycin of the genus *Albaneryx* (Reptili, Boidae) in USSR.
 1621 *Vestnik Zoologii*:31–35
- 1622
- 1623
- 1624
- 1625
- 1626
- 1627
- 64

- 1628 **Figure captions**
- 1
2
3 1629 Figure 1. **a** an overview map of Turkey and **b** geographic locations of the studied localities on
4
5 1630 a topographic map. **c** stratigraphic chart with the studied fossil localities. The + and – in the
6
7 1631 brackets indicates correspondingly the normal or reverse polarity patterns of the fossiliferous
8
9 1632 layer according to Krijgsman et al. (1996) and Krijgsman (2003).
10
11
12
13 1633
14
15
16 1634 Figure 2. Images of the 3D models of the pharyngeal bones with teeth of the *Luciobarbus* and
17
18 1635 *Barbus* species. **a.** *Luciobarbus comizo* (MNCN 69304), **b.** *Luciobarbus longiceps* (MNCN E
19
20 1636 54), **c.** *Luciobarbus sclateri* (MNCN 69331), **d.** *Barbus barbuis* (SNSB SPAM-PI-00608), **e.**
21
22 1637 *Barbus sacratus* (MNCN GUI 17), **f.** *Barbus meridionalis* (MNCN 19933). The letters a, b, c
23
24 1638 correspond to the first (main), second and third row, the numbers (1-5) the tooth positions in
25
26 1639 those rows. The scale bars equal 1 mm.
27
28
29
30
31
32 1640
33
34
35 1641 Figure 3. Cyprinids from the studied localities. *Luciobarbus* sp., Morphotype d7 – from
36
37 1642 Hancılı, UU HAN 5315 (**a – b**); UU HAN 5316 (**c**); Morphotype d5 – UU HAN 5333 (**d**), UU
38
39 1643 HAR1 5300, loc. Hancılı (**e**); Morphotype d3 – UU HAN 5334, loc. Hancılı (**f**); UU HAN
40
41 1644 5305, loc. Hancılı (**g**). *Barbus* sp., Morphotype d6 from the loc. Harami 1, UU HAR1 5301
42
43 1645 (**h**), loc. Hancılı, UU HAN 5321 (**i**), UU HAN 5311 (**j – k**), UU HAN 5335 (**l**), Morphotype
44
45 1646 d4 - UU HAN 5308 (**m**), UU HAN 5309 (**n**). *Lucioarbus* vel *Barbus* sp., Morphotype d1 from
46
47 1647 loc. Hancılı, UU HAN 5300 (**o – p**), Morphotype d2, UU HAN 5303 (**q**), UU HAN 5306 (**r**);
48
49 1648 Morphotype s1, UU HAN 5324 (**s**); Morphotype s2, UU HAN 5325 (**t**), UU HAN 5326 (**u**);
50
51 1649 Morphotype s3, UU HAN 5329 (**v**). aff. *Capoeta* sp. from the loc. Hancılı, UU HAN 5317 (**w**,
52
53 1650 **x**). Barbini indet. (**z – dd**), UU KAR1 1304, loc. Kargı 1 (**y**), UU KAR1 1301, loc. Kargı 1
54
55 1651 (**z**), UU KAR2 1301, loc. Kargı 2 (**aa**), UU KAR2 1306, loc. Kargı 2 (**dd**), UU KAR2 1303,
56
57
58
59
60
61
62
63
64
65

- 1652 loc. Kargı 2 (**ee**), UU KE 5307, loc. Keseköy (**bb**), UU KE 5305, loc. Keseköy (**ce**).
 1
 21653 *Leuciscus* sp. from loc. Hancılı, UU HAN 5318 (**ff**).
 3
 4
 51654
 6
 7
 81655 Figure 4. Salamander and some frogs from Turkish localities. **a – l** *Salamandra* sp., **a – e**
 9
 10 trunk vertebra (UU BAG 1001) in anterior (**a**), posterior (**b**), right lateral (**c**), dorsal (**d**) and
 111656 ventral (**e**) views; **f – i** caudal vertebra (UU HAR1 5055) from loc. Harami 1 in anterior (**f**),
 12
 131657 left lateral (**g**), dorsal (**h**) and ventral (**i**) views; **j – l** humeri (UU BAG 1004 [**j**] and 1003 [**k** –
 14
 151658 **l**]) from loc. Bağıçi in ventral (**j, k**) and dorsal (**l**) views. **m – v** Pelobatidae indet. from **m – n**
 161659 loc. Harami 1, left maxilla (UU HAR1 5051) in outer (**m**) and inner (**n**) views; **o – p** loc.
 17
 181660 Bağıçi, right maxilla (UU BAG 1001) in outer (**o**) and inner (**p**) views; **q – r** loc. Keseköy,
 19
 201661 complete posterior half of right maxilla (UU KE 5006) in outer (**q**) and inner (**r**) views; **s – v**
 21
 221662 loc. Hancılı; right frontoparietal (UU HAN 5051) in ventral (**s**) and dorsal (**t**) views; left
 231663 frontoparietal (UU HAN 5052) in dorsal (**u**) and ventral (**v**) views. **w – y** Bufonidae indet.
 24
 251664 from loc. Keseköy, right ilium (UU KE 5001) in lateral (**w**), ventrolateral (**x**) and medial (**y**)
 26
 271665 views. **z – aa** Anura indet., fragment of left maxilla (UU KAR1 1051) in inner view (**z**), with
 28
 291666 magnified teeth of the same specimen in ventral view (**aa**); **bb** phalanx, morphotype A (UU
 30
 311667 HAR1 5056) in dorsal (**bb-1**) and ventral (**bb-2**) views; **cc** phalanx, morphotype B (UU
 32
 331668 HAR1 5057) in dorsal (**bb-1**) and ventral (**bb-2**) views.
 34
 351669
 36
 371670
 38
 391671 Figure 5. Remains of *Latonia* from the studied Turkish localities. **a – b** Left part of the
 40
 411672 frontoparietal (UU HAN 5055) in dorsal (**a**) and ventral (**b**) views. **c – d** Right scapula (UU
 42
 431673 HAR3 5051) in inner (**c**) and outer (**d**) views. **e – f** Atlas (UU CD 5002) in dorsal (**e**) and
 44
 451674 anterior (**f**) views. **g – h** Fragment of right maxilla (UU HAR1 5012-1) in lingual (**g**) and
 46
 471675 labial (**h**) views. The sulcus for the nasolacrimal duct, which runs posteroventrally on the
 48
 491676 inner surface of the bone, is marked by an arrow. **i – j** Left maxilla (UU HAR1 5012-2) in
 50
 51
 52
 53
 54
 55
 56
 57
 58
 59
 60
 61
 62
 63
 64
 65

- 1677 lingual (**i**) and labial (**j**) views. **k – e** Right maxilla (UU HAR1 5012-3) in labial (**k**) and
 1
 21678 lingual (**e**) views. **m – n** Right ilium (UU KAR3 1207) in lateral (**m**) and medial (**n**) aspects. **o**
 3
 4
 51679 urostyle (UU UU KE 5053) in dorsal view.
 6
 7
 81680
 9
 10
 111681 Figure 6. Cranial elements of Palaeobatrachidae. **a – c** Sphenethmoid UU HAR1 5005 from
 12
 131682 loc. Harami 1 in dorsal (**a**), ventral (**b**), and anterior (**c**) views. The arrow in (**a**) marks the
 14
 15
 161683 braincase cavity, the arrow in (**b**) marks the posterior orifice of the canal for the ramus
 17
 181684 medialis nervi ophthalmici. **d – f** Sphenethmoid UU HAR1 5006 from loc. Harami 1 in dorsal
 19
 20
 211685 (**d**), ventral (**e**), and anterior (**f**) views. **g** Left angular UU HAR1 5004 in dorsal view. Note a
 22
 231686 distinct ridge on the dorsal surface of the coronoid process, separating anterior and posterior
 24
 25
 261687 depression. The posterior margin of the coronoid process is nearly straight, reaching the
 27
 281688 medial margin of the bone at the level of the posterior end of the medial wall of the sulcus
 29
 30
 311689 Meckeli (marked by arrow). **h** Right angular UU HAR1 5002 in dorsal view. **i – j** Right
 32
 331690 angular UU HAR1 5001 in dorsolateral (**i**) and lateral (**j**) views; the arrows mark tubercle
 34
 351691 protruding from the medial wall of the Meckelian groove, and a distinct concavity on the
 36
 37
 381692 lateral surface. **k – l** Posterior part of right angular UU HAR1 5003 in dorsomedial (**k**) and
 39
 401693 medial (**l**) views; the longitudinal axis of the coronoid process is marked by a white broken
 41
 42
 431694 line, the arrow marks the medial wall of the Meckelian groove. Note absence of a tubercle or
 44
 451695 protuberance on dorsal margin of the wall. **m** Left angular UU HAR3 5001 from loc. Harami
 46
 47
 481696 3 in dorsomedial view; the arrow marks a tubercle protruding from the medial wall of the
 49
 501697 Meckelian groove, as in (**i**). **n** Left angular UU HAR3 5002 in dorsal view. **o – p** Right
 51
 521698 maxilla (UU HAR1 5059) in lingual (**o**) and labial (**p**) views. The white arrow in (**o**) points to
 53
 54
 551699 a contact ridge with the pterygoid, that in (**p**) marks a horizontal ledge that extends labially.
 56
 57
 581700
 59
 60
 61
 62
 63
 64
 65

- 1701 Figure 7. Postcranial elements of Palaeobatrachidae. **a – c** Left scapula (UU HAR1 5009)
 1
 21702 from loc. Harami 1 in lateral (**a**), medial (**b**) and posteromedial (**c**) views. The arrows in (**b**)
 3
 41703 mark the anterior and posterior margins of the bone, the arrows in (**c**) mark the external and
 5
 61704 internal surfaces of the bone. **d – e** Left ilium (UU HAR1 5008) in lateral (**d**) and medial (**e**)
 7
 81705 views. Note prominent spina iliaca (marked by an arrow in **e**). **f – g** Urostyle (UU KE 5011)
 9
 101706 from loc. Keseköy in dorsal (**f**) and anterior (**g**) views. **h** Right humerus (UU KAR2 5000)
 11
 121707 from loc. Kargı 2. **i – m** Variation of humeri from loc. Harami 3. **i** Right humerus (UU HAR3
 13
 141707 5006). **j** Left humerus (UU HAR3 5005). **k** Left humerus (UU HAR3 5007). **l** Left humerus
 15
 161708 (UU HAR3 5004). **m** Left humerus (UU HAR3 5008). **n – u** Variation of right humeri from
 17
 181709 loc. Harami 1. **n** UU HAR1 5022, **o** UU HAR1 5023 (mirrored for comparison), **p** UU HAR1
 19
 201710 5011, **q** UU HAR1 5026, **r** UU HAR1 5024, **s** UU HAR1 5021, **t** UU HAR1 5015, **u** UU
 21
 221711 HAR1-5031.
 23
 241712
 25
 261713
 27
 28
 29
 301714 Figure 8. Lizards remains from the studied Turkish localities. **a – b** *Pseudopus* sp. from loc.
 31
 321714 Kargı 1 (**a** – UU KAR1 1205) and loc. Kargı 2 (**b** – UU KAR2 1204), **c – e** Anguidae indet.
 33
 341715 from loc. Kargı 2 (UU KAR2 1203). **f-e** Lacertidae indet. 1 from Kargı 1 (UU KAR1 1206),
 35
 361716 in labial (**f**) and lingual (**g**), **e1** – magnified view on teeth. **i – o** Lacertiade indet. 2 from loc.
 37
 381717 Keseköy (**i** UU KE 5200, **j – k** UU KE 5206, **l – n** UU KE 5213, **o** UU KE 5219), magnified
 39
 401718 views on teeth of the specimens **k** UU KE 5206, and **n** UU KE 5213. **p – r, aa** Lacertidae
 41
 421719 indet. 3 from loc. Keseköy (**p – q** UU KE 5220) (**q** – magnified view on the teeth of the
 43
 441720 specimen UU KE 5220) (**aa** UU KE 5215), from loc. Çandır (**r** – UU CD 5210). **s – u**
 45
 461721 Lacertiade indet. 4 from loc. Çandır UU CD 5202, **u** magnified view on the teeth of the
 47
 481722 specimen UU CD 5202. **v – w** Lacertidae indet. from loc. Bağıcı (UU BAG 1201). **x – y**
 49
 501723 *Amphisbaena* indet. from loc. Çandır (UU CD 5204). All bones are figured from lingual view,
 51
 521724 except for **d, f, v, x** figured in labial view and **e** in ventral view.
 53
 54
 55
 56
 57
 58
 59
 601725
 61
 62
 63
 64
 65

- 1726
1
2
3 1727 Figure 9. Snake and crocodile remains from Turkish localities. **a – e** trunk vertebra of
4
5 1728 *Albaneryx* sp. from loc. Kargı 3 (UU KAR3 1204). **f – i** trunk vertebra of Erycinae indet. from
6
7
8 1729 loc. Harami 1 (UU HAR1 5200). **j – n** caudal vertebra of Erycinae indet. from the loc. Bağıçi
9
10 1730 (UU BAG 1202). **o – s** axis of Serpentes indet. from Bağıçi (UU BAG 1204), **t** – tooth of
11
12
13 1731 Serpentes indet. from loc. Kargı 1 (UU KAR1 1207). **u – w** Crocodylia indet. from loc. Kargı
14
15 1732 1, teeth **u** – UU KAR1 1202 and **v** – UU KAR1 1201, **w** – osteoderm UU KAR1 1204.
16
17
18 1733
19
20
21 1734 Figure 10. Paleogeographic relations of Anatolia (marked by red square) to Europe between
22
23
24 1735 late Oligocene and late Miocene. Noteworthy is permanent isolation of the area in northern
25
26 1736 Caucasus (marked by red arrow) where *Palaeobatrachus* was reported by Syromyatnikova
27
28
29 1737 (2018), which means that immigration from the main area of distribution had to occur
30
31 1738 relatively quick. Maps are from Rögl (1999).
32
33
34
35
36
37
38
39
40
41
42
43
44
45
46
47
48
49
50
51
52
53
54
55
56
57
58
59
60
61
62
63
64
65

Figure 1

[Click here to access/download;Figure;Fig_1.tif](#)

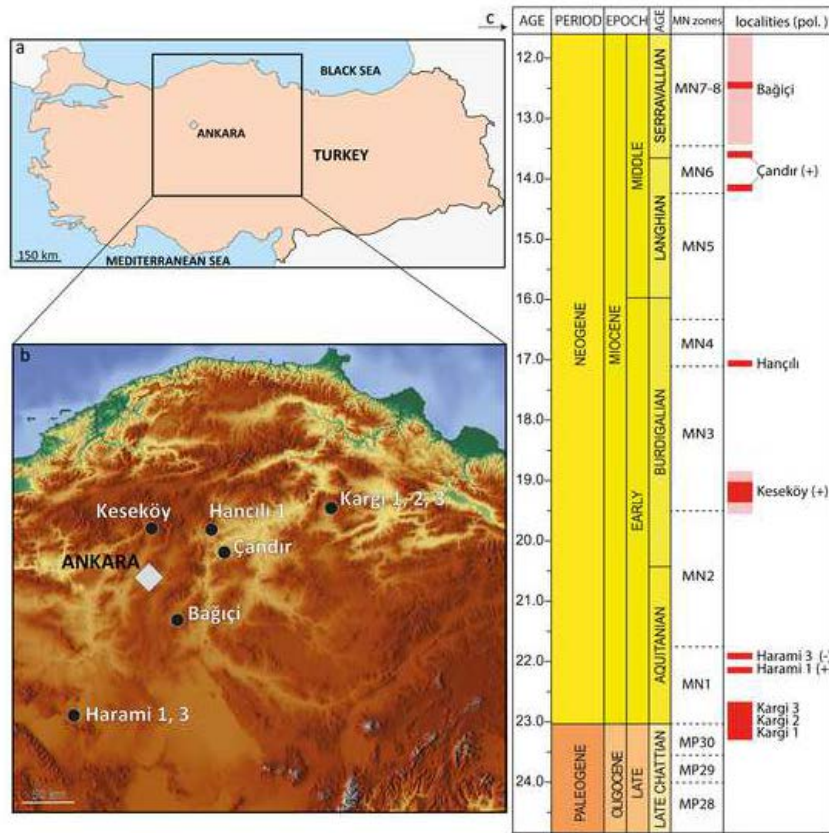


Figure 2

[Click here to access/download;Figure;Fig_2.tif](#)

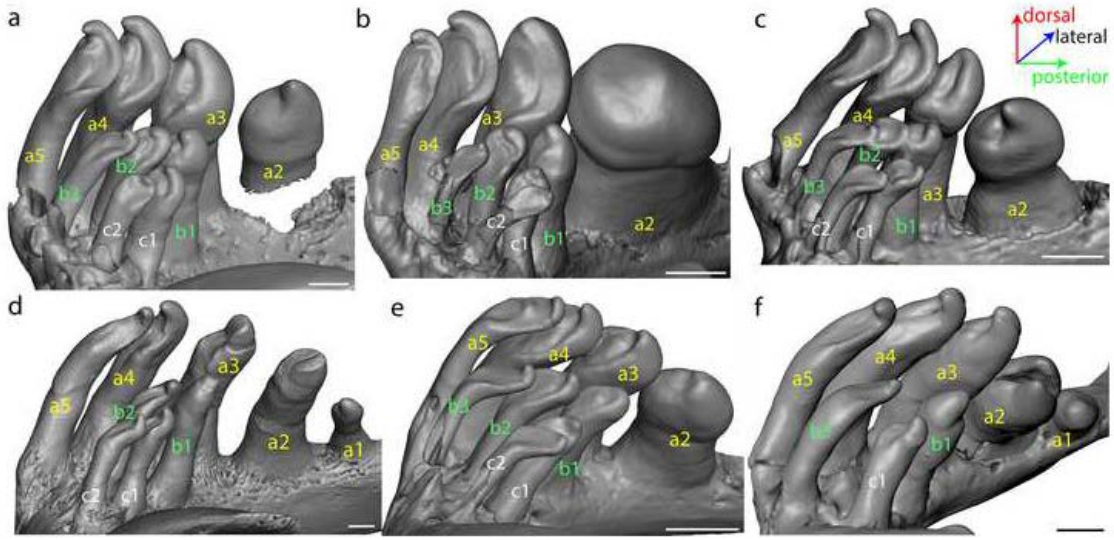


Figure 3

[Click here to access/download:Figure:Fig_3.tif](#)



Figure 5

[Click here to access/download;Figure;Fig_5.tif](#)

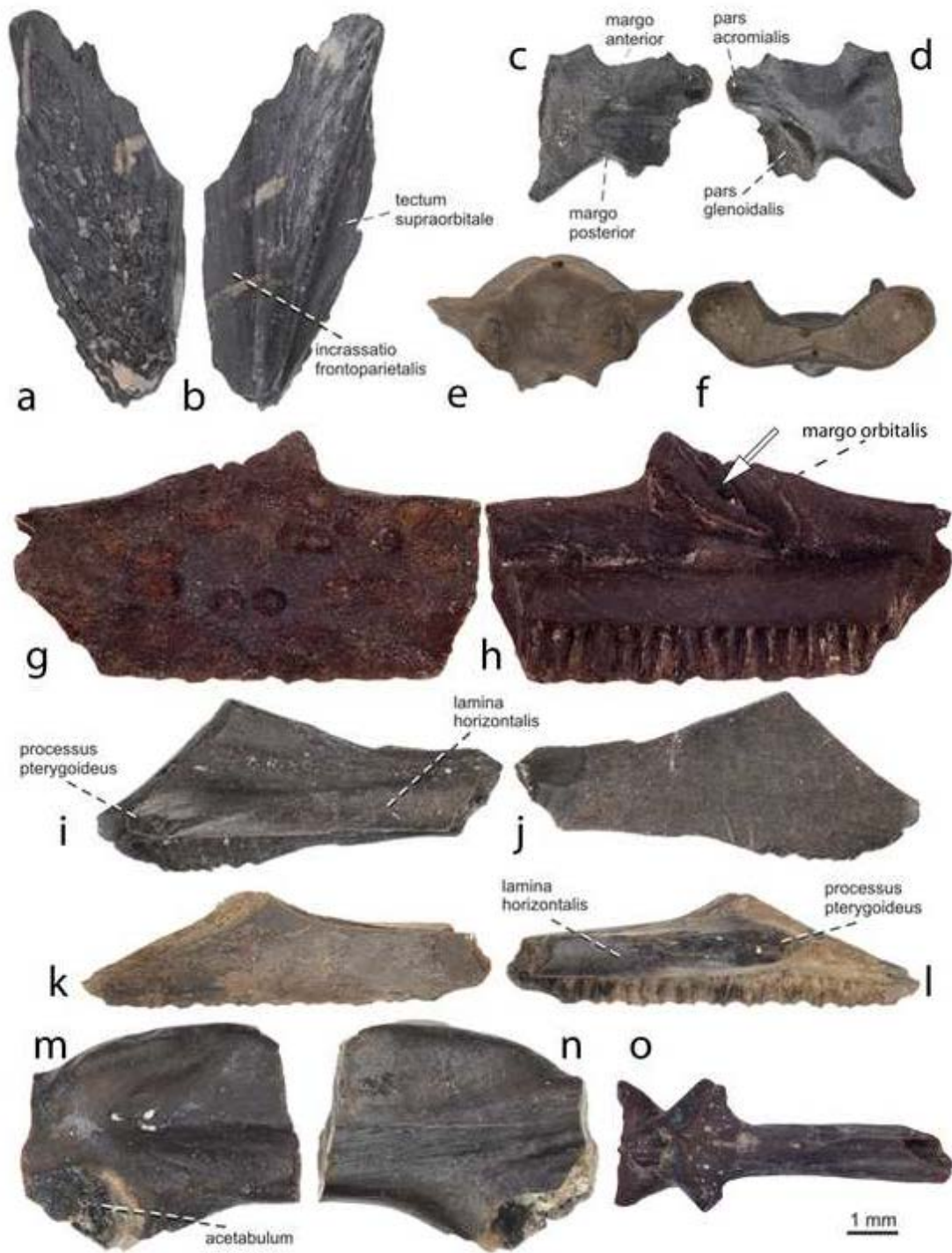


Figure 6

[Click here to access/download;Figure;Fig_6.tif](#)

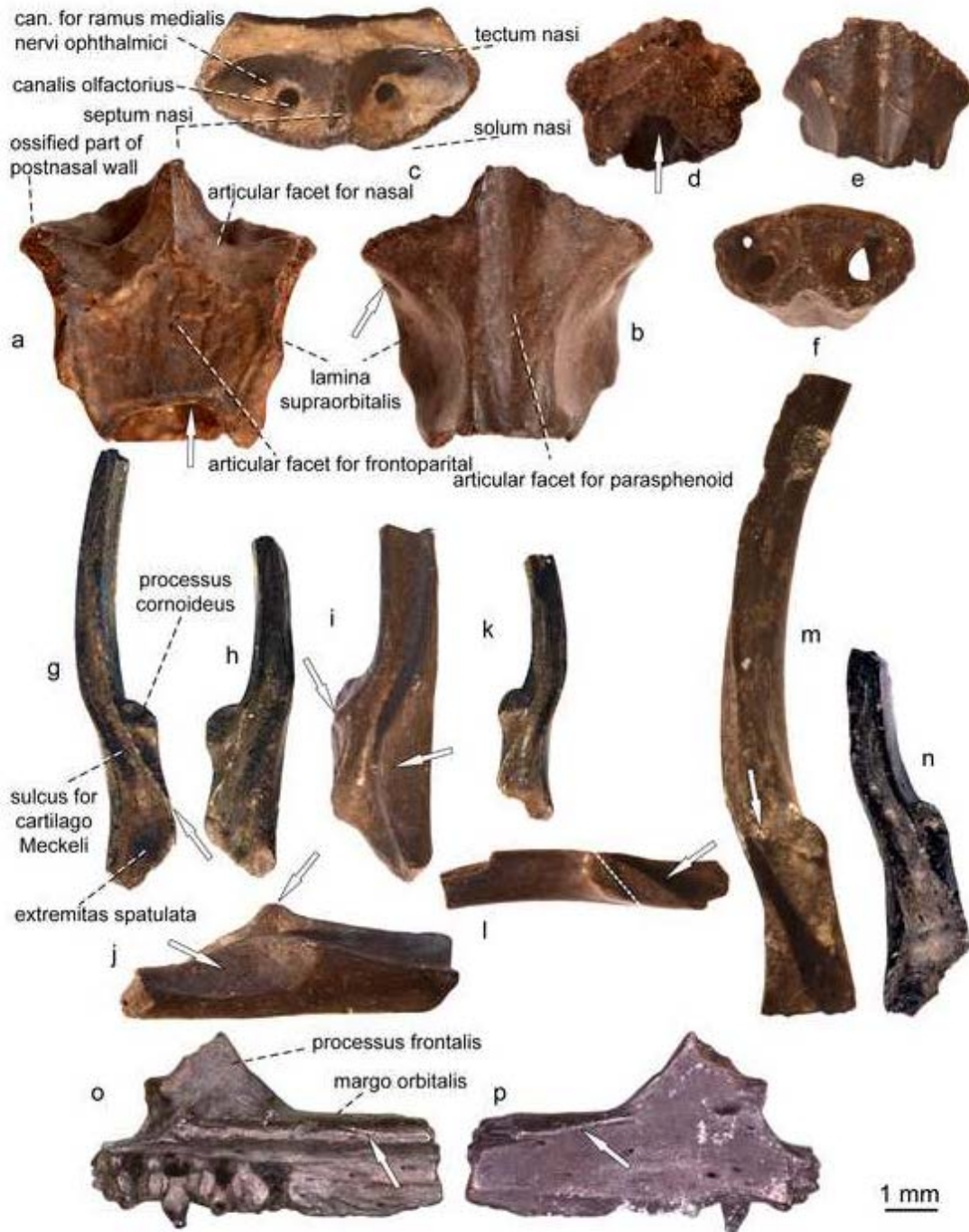


Figure 7

[Click here to access/download;Figure;Fig_7.tif](#)

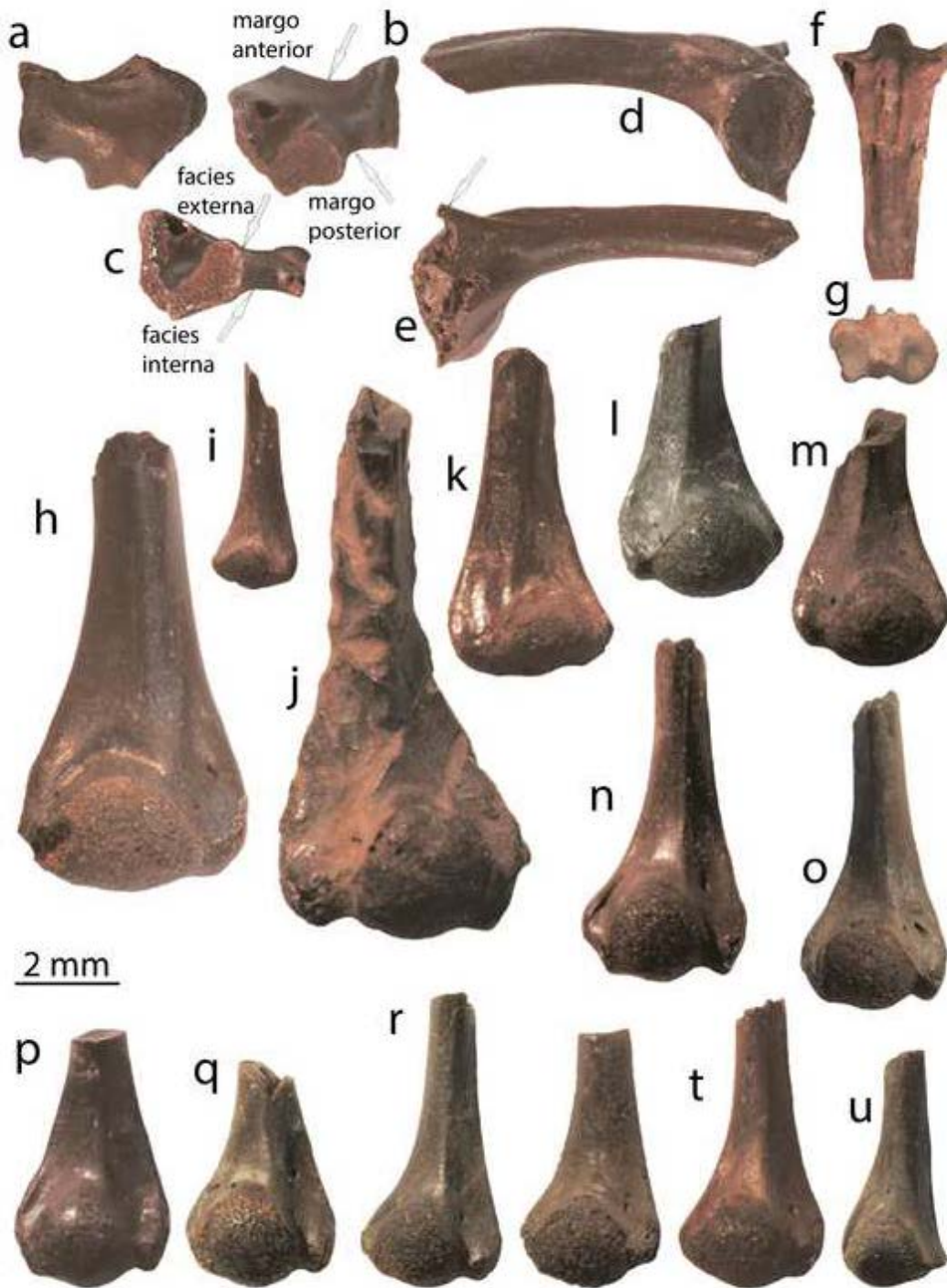


Figure 8

[Click here to access/download;Figure;Fig_8.tif](#)



Figure 9

[Click here to access/download;Figure;Fig_9.tif](#)

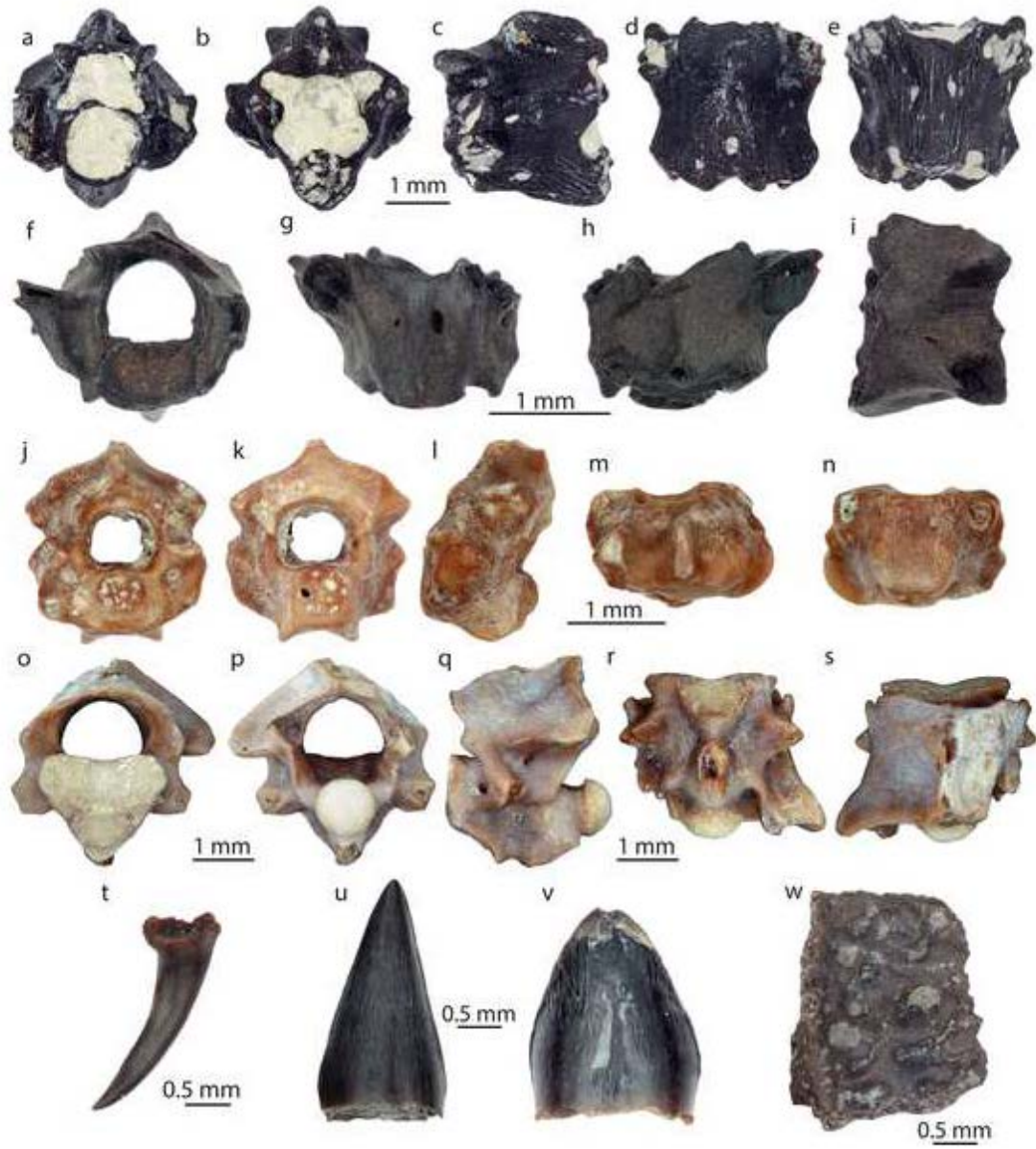


Figure 10

[Click here to access/download;Figure;Fig_10.tif](#)

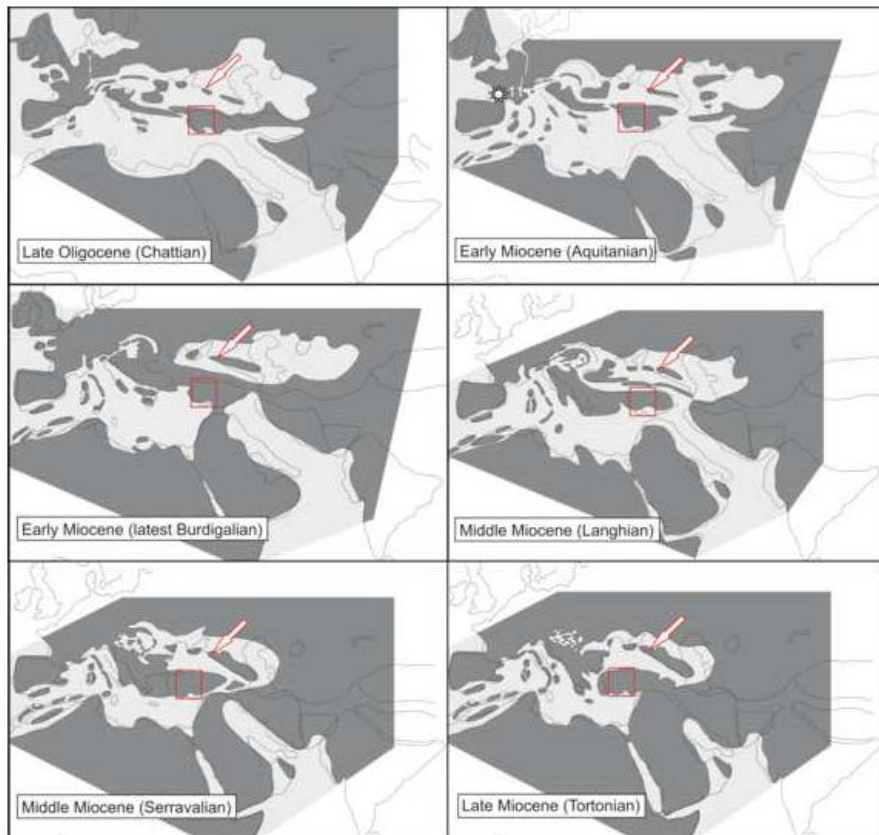


Table 1

Table 1. Review of literature data on the fossil record of ectothermic vertebrates from the O

		Locality	Kocayama & Kavakdare	Kargi 2
		Formation		
		Age	e. Oligocene	transition 1. Oligocene - e. Miocene
		Reference	Čerňanský et al. 2017	Čerňanský et al. 2017
Taxon	Teleostei	Cyprinidae		
	Urodela	Salamandridae		
	Anura	Ranidae		
		Pelobatidae		
	Lacertilia	Blanidae		
		Anguidae	Anguidae indet.	Anguidae indet. <i>Ophisaurus</i> sp.
	Crocodylia			
	Serpentes			
	Testudines	Boidae		
		Emydidae		
	Chelydridae			

ligocene to middle Miocene of Turkey.

	Kargi 1	Kurucan (54m-S10AT1) Medikdere	Kilçak 3b	Sabuncubeli
	e. Miocene	l. Oligocene - e. Miocene	e. Miocene	e. Miocene
	Čerňanský et al. 2017	Szyndlar and Hoşgör 2013	Čerňanský et al. 2017	Čerňanský et al. 2017
	Anguidae indet.		Anguidae indet.	Anguidae indet.
		<i>Bavarioboa</i> sp.		

Tuz-6 Turabi	Ağaöz (Aköz) Güvem Formation	Ahlath Dere Güvem Formation	Keseköy
e. Miocene	e. Miocene	e. Miocene	e. Miocene
Sen et al. 2011	Paicheler et al., 1978; Dubois et al., 2010	Dubois et al., 2010	Čerňanský et al. 2017
	<i>Leuciscus etilius</i> <i>Barbus bispinosus</i>		
	Salamandridae indet.		
	<i>Pelophylax</i> sp.		
	<i>Pelobates</i> sp.	<i>Pelobates</i> sp.	
			Anguidae indet. <i>Ophisaurus</i> sp.
	Crocodylia indet.		
	Colubroidea indet.		
	<i>Chelydropsis</i> sp.		
Çandır & Çandır HW	Bağıcı	Alpagut-Dodurga	
m. m. Miocene	l. m. Miocene	e. Miocene - m. Miocene	
Čerňanský et al. 2017	Čerňanský et al. 2017	Rückert-Ülkümen 1998, 2003	
		<i>Barbus guendogani</i> <i>Barbus schizakanthus</i> <i>Leuciscus dodurgaensis</i> <i>Leuciscus macrurus</i> <i>Tinca</i> cf. <i>furcatus</i>	
		<i>Rana</i> (? <i>Pelophylax</i>) sp.	
	Anguidae indet. <i>Ophisaurus</i> sp.	Anguidae indet. <i>Ophisaurus</i> sp. <i>Anguis</i> sp.	

Gebeceler	Küçükdoğanaca Kökü
Gebeceler	
(e.) m. Miocene	m. Oligocene - m. Miocene
Georgalis et al. 2018	Schleich 1994
<i>Blanus cf. strauschi</i>	
Crocodylia indet.	
Emydidae indet. "Palaeochelys" rueckerti "Palaeochelys" turcica Chelydropsis sp. Testudines indet.	

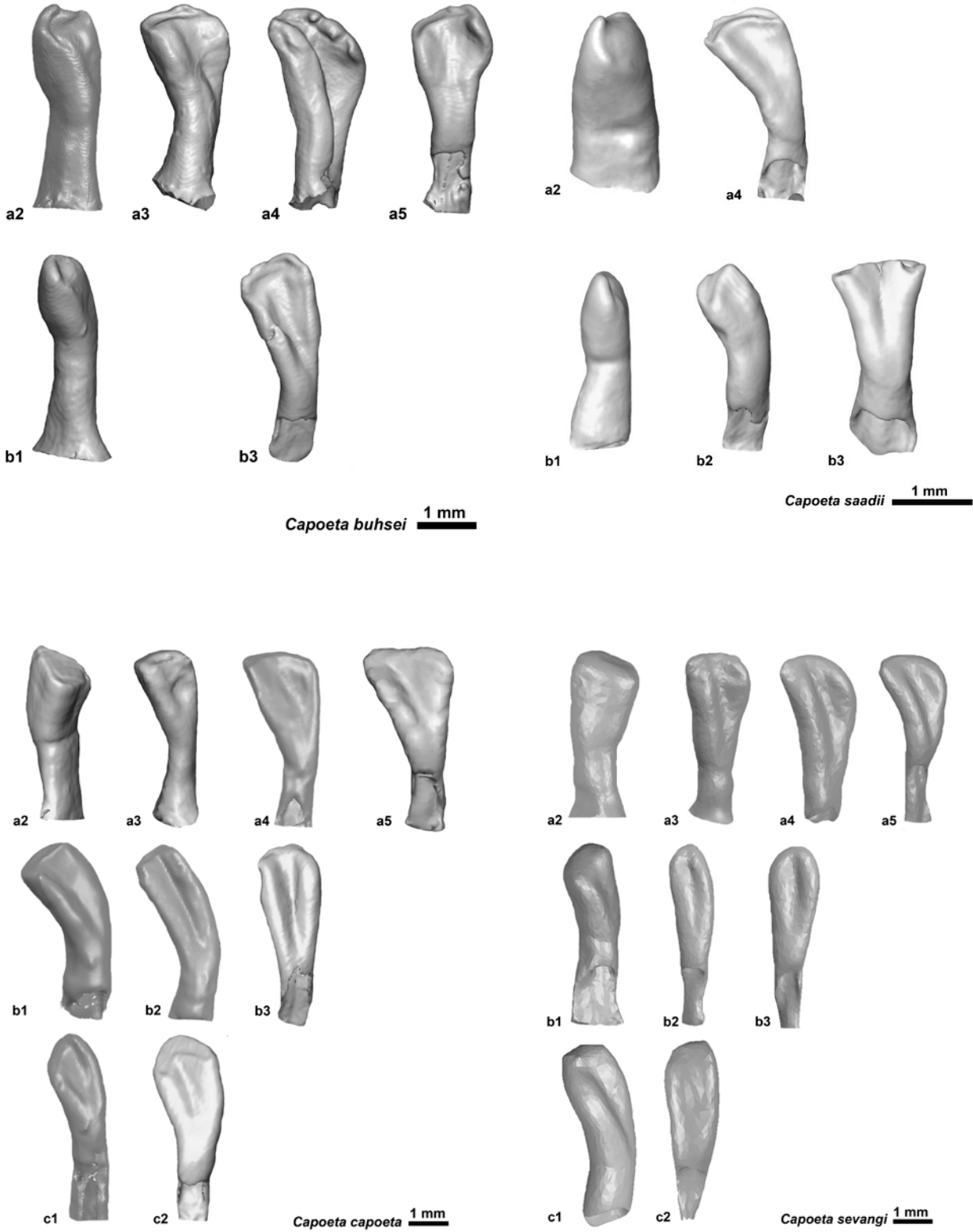
Table 2

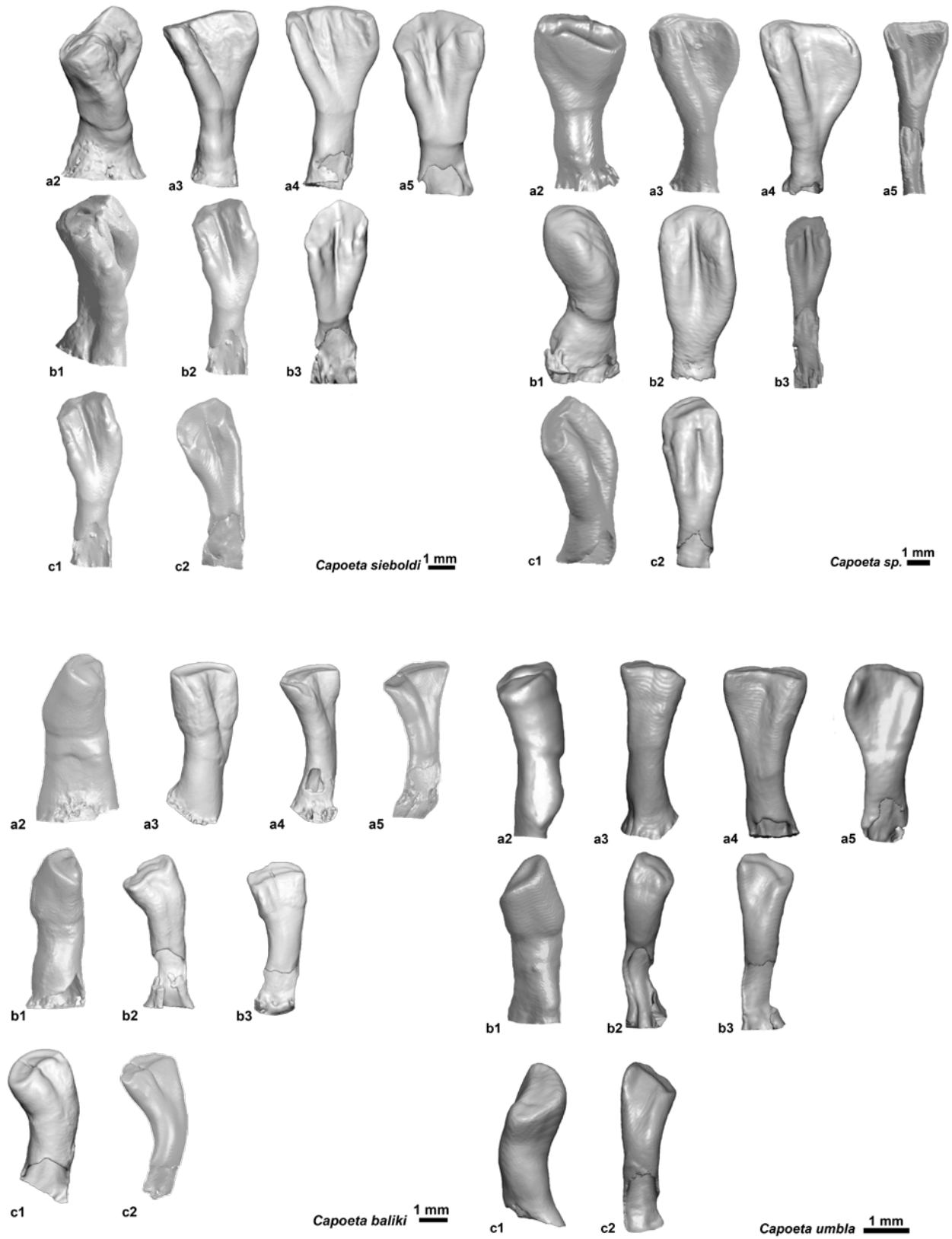
Table 2. Fauna of ectothermic vertebrates from the studied localities. Orange cells - results of the present study, green cells - Čerňanský et al. 2017

Taxa palaeoenvironment	locality									
	Kargı 1 swamp	Kargı 2 swamp	Kargı 3 lake	Harami 1 swamp	Harami 3 swamp	Keseköy lake	Hançılı swamp/lake	Çandır palaeosol	Bağcı lake ?	
Teleostei										
<i>Luciobarbus</i> sp.										
<i>Barbus</i> sp.										
<i>Luciobarbus</i> vel <i>Barbus</i> sp.										
aff. <i>Capoeta</i> sp.										
<i>Barbini</i> indet.										
<i>Leuciscus</i> sp.										
Cyprinidae indet.										
Teleostei indet.										
Lissamphibia										
<i>Salamandra</i> sp.										
Pelobatidae indet.										
Bufoindae indet.										
<i>Latonia</i> sp.										
Palaeobatrachidae indet.										
Anura indet.										
Reptilia										
<i>Pseudopus</i> sp.										
<i>Ophisaurus</i> sp.										
<i>Anguis</i> sp.										
Anguinae indet.										
Lacertidae indet. 1										
Lacertidae indet. 2										
Lacertidae indet. 3										
Lacertidae indet. 4										
Lacertidae indet.										
Lacertilia indet.										
Blaniidae indet. (? <i>Blanus</i> sp.)										
<i>Albanerx</i> sp.										
Erycinae indet.										
Serpentes indet.										
Crocodylia indet.										

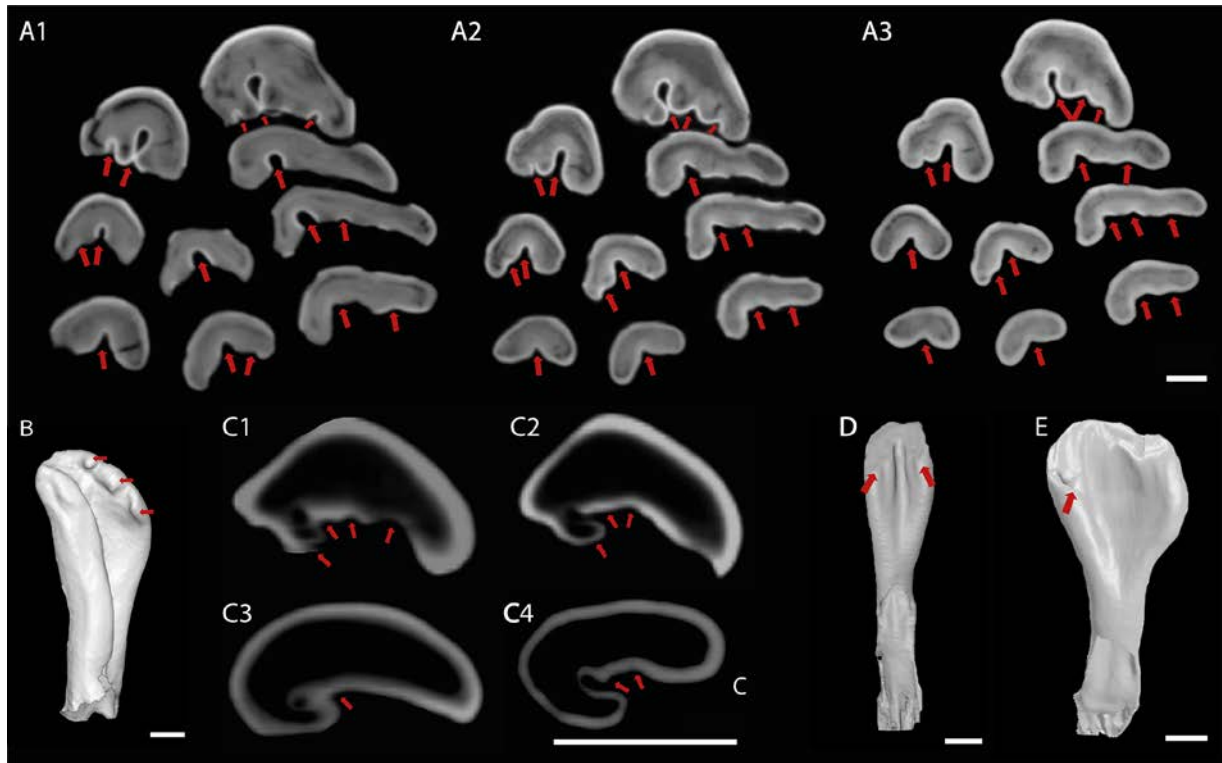
8. Appendix III: Supplementary material

This section includes supporting information in the cited order in the main text.





S1 Figure. Isolated pharyngeal teeth sets of the extant comparative material of *Capoeta*. Ayvazyan et al., 2018.



S2 Figure. Recorded variable morphologic characters of the grinding surface. (A) pharyngeal dentition of *C. sieboldi*, A1, A2, A3 correspond to the transverse cross-section of teeth at 0.57 mm, 0.87 mm and 1.42 mm below the top of the grinding surface. (B) *C. buhsei*, a4 tooth; C1, C2, C3, C4 correspond to 0,42 mm, 0,78 mm, 1,31 mm and 1,87 mm below the top of the grinding surface of the a4 tooth of *C. buhsei*; (D) *Capoeat sp.*, b3 tooth; (E) *C. trutta*, a5 tooth. The scale bars equal to 1mm. Ayvazyan et al., 2018.

Table S1 Description of the shape characters. * molariform tooth morphology indicates/includes well-distinguished foot-crown border; spatulate - not well distinguished foot-crown border, margins widen distally and bent ventrally/laterally; oblong-longer than broad and with nearly parallel sides; reniform-kidney shape, concave dorsally/posteriorly and deeply convex ventrally/anteriorly.

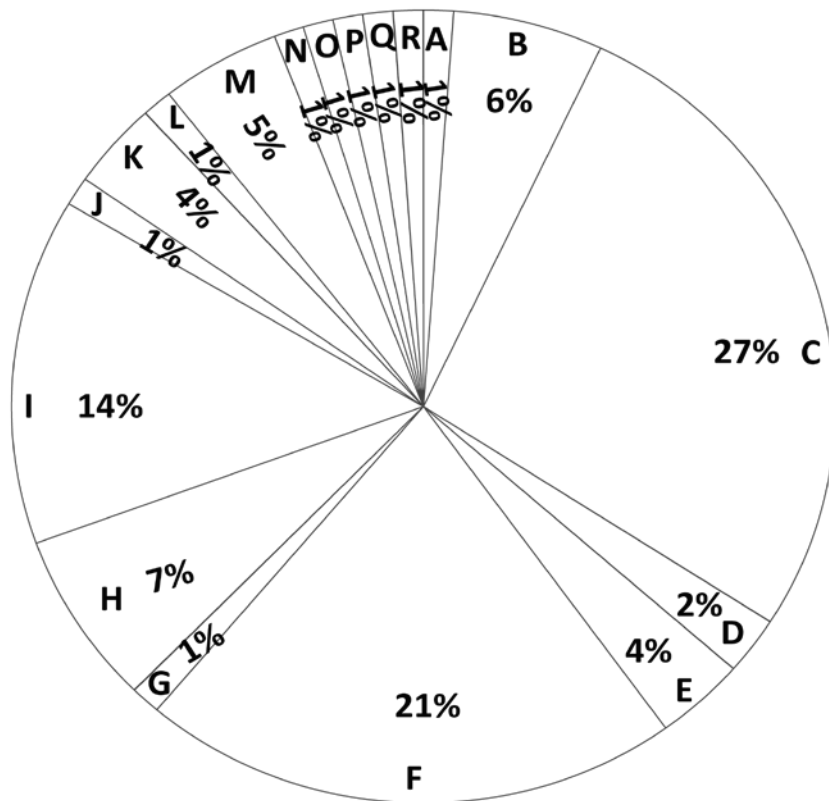
Shape characters	
Lateral outline (α)	
$\alpha 1$	is molariform*. Foot is longer than crown. The crown is convex ventrally. The width at foot and crown section is nearly the same.
$\alpha 2$	is spatulate* in shape.
$\alpha 3$	is similar to $\alpha 2$, but widen rapidly and the foot section is nearly two times narrower than the crown section.
$\alpha 4$	is molariform but flower bud in shape and compressed on foot-crown border.
$\alpha 5$	is linear. The foot-crown border is differentiated, where the crown bends laterally. The foot is shorter than the crown, but the width of tooth is equal/constant along the body.
$\alpha 6$	is ablong*.
$\alpha 7$	is molariform, but bends ventrally. The foot and crown section are nearly same in length and width.
$\alpha 8$	is ablong, but unlike to $\alpha 6$ it bends dorsally and slightly widen distally.
$\alpha 9$	is molariform, but the foot-crown border is not well differentiated and it bends slightly dorsally/anteriorly. The crown is wider than the foot.
$\alpha 10$	is similar to $\alpha 1$, but it widen distally and bends dorsally.
$\alpha 11$	is similar to $\alpha 1$, but bends dorsally and unlike to other molariforms slightly narrows distally.
$\alpha 12$	is molariform, but is widen rapidly, foot is shorter and narrower than the crown.
$\alpha 13$	is similar to $\alpha 11$, but foot is shorter than the crown.
$\alpha 14$	is narrow ablong but the foot-crown border is slightly differentiated.
Transverse cross-section (β)	
$\beta 1$	is more or less rounded in shape.
$\beta 2$	is slightly triangular in shape.
$\beta 3$	is bean-shaped (concave dorsally and convex ventrally).
$\beta 4$	is reniform.
$\beta 5$	is comma-shaped and narrows laterodistally.
$\beta 6$	is unciform (shaped like a hook).
$\beta 7$	is reniform but gibbous (extremely convex ventrally) with the irregular folds on the dorsal edge of the grinding surface.
$\beta 8$	is isosceles triangular, slightly convex ventrally with a cavity/fold on the dorsal edge of the grinding surface.
$\beta 9$	is similar to $\beta 3$ but gibbous and slightly convex dorsally.
$\beta 10$	is more or less ellipsoid and slightly narrows laterodistally.
$\beta 11$	is ovate, oblong but broader at one side (more or less oval in shape).

Table S2 Tooth shape classes in the studied recent *Capoeta* species.

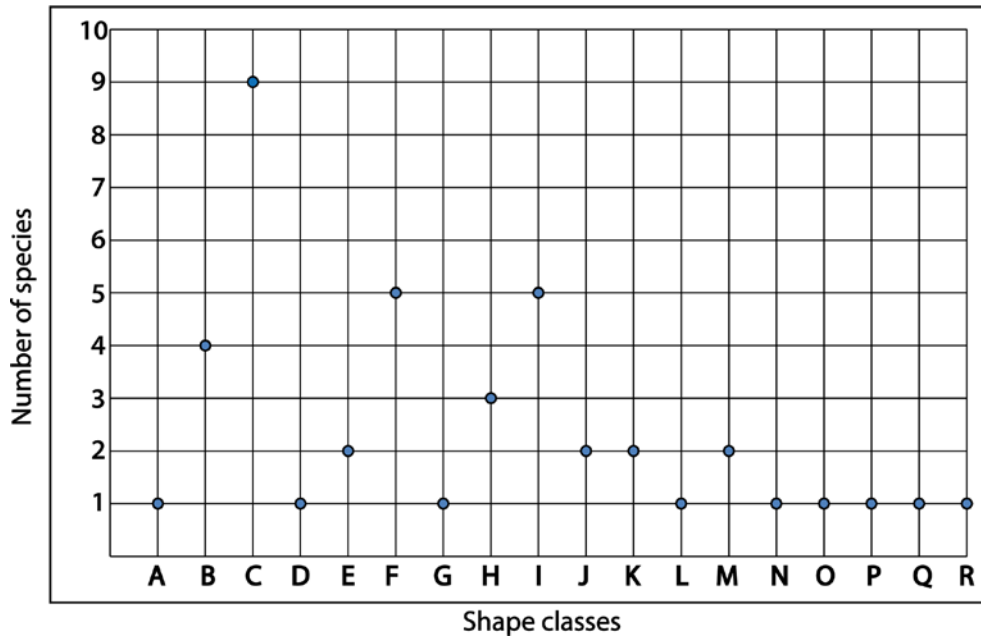
Teeth shape classes	Tooth position	Shape characters	Species
A	a2	$\alpha 8\beta 1$	<i>Capoeta umbla</i>
B	a3	$\alpha 2\beta 5$	<i>Capoeta umbla</i>
	a3, a4		<i>Capoeta baliki</i>
	a3		<i>Capoeta buhsei</i>
	a3		<i>Capoeta damascina</i>
C	a4, a5	$\alpha 3\beta 6$	<i>Capoeta umbla</i>
	a5		<i>Capoeta baliki</i>
	a3,a4,a5		<i>Capoeta sp.</i>
	a3,a4,a5		<i>Capoeta trutta</i>
	a3,a4,a5		<i>Capoeta sevangi</i>
	a3,a4,a5		<i>Capoeta capoeta</i>
	a3,a4,a5		<i>Capoeta sieboldii</i>
	a4, a5		<i>Capoeta buhsei</i>
	a4		<i>Capoeta saadii</i>
	a4, a5		<i>Capoeta damascina</i>
D	a2	$\alpha 4\beta 7$	<i>Capoeta sieboldii</i>
E	b1	$\alpha 7\beta 8$	<i>Capoeta sp.</i>
	a2,b1		<i>Capoeta trutta</i>
F	b2,b3,	$\alpha 2\beta 4$	<i>Capoeta sieboldii</i>
	c1,c2		
	b2,b3, c1,		<i>Capoeta trutta</i>
	c2		
	b2,b3, c1,		<i>Capoeta sp.</i>
	c2		
	b3, c1,c2		<i>Capoeta capoeta</i>
	b2,b3,c2		<i>Capoeta sevangi</i>
G	a2	$\alpha 12\beta 10$	<i>Capoeta sp.</i>
H	b1,c1	$\alpha 1\beta 2$	<i>Capoeta umbla</i>
	b1,c1		<i>Capoeta baliki</i>
	b1,c1		<i>Capoeta damascina</i>
I	b2, b3, c2	$\alpha 2\beta 3$	<i>Capoeta baliki</i>
	b2, b3		<i>Capoeta saadii</i>
	b2,b3,c2		<i>Capoeta damascina</i>
	b2, b3, c2		<i>Capoeta umbla</i>
	b3		<i>Capoeta buhsei</i>
J	a2	$\alpha 11\beta 9$	<i>Capoeta baliki</i>
K	b1	$\alpha 1\beta 11$	<i>Capoeta saadii</i>
	a2,b1		<i>Capoeta buhsei</i>
L	a2	$\alpha 6\beta 11$	<i>Capoeta saadii</i>
M	b1,b2	$\alpha 5\beta 4$	<i>Capoeta capoeta</i>
	b1,c1		<i>Capoeta sevangi</i>
N	a2	$\alpha 9\beta 10$	<i>Capoeta sevangi</i>
O	a2	$\alpha 10\beta 11$	<i>Capoeta capoeta</i>
P	a1	$\alpha 14\beta 1$	<i>Capoeta damascina</i>
Q	a2	$\alpha 13\beta 1$	<i>Capoeta damascina</i>
R	b1	$\alpha 7\beta 7$	<i>Capoeta sieboldii</i>

Table S3 The presence/absence of shape classes in the studied *Capoeta* species.

Shape classes	A	B	C	D	E	F	G	H	I	J	K	L	M	N	O	P	Q	R
<i>Capoeta umbla</i>	1	1	1	0	0	0	0	1	1	0	0	0	0	0	0	0	0	0
<i>Capoeta baliki</i>	0	1	1	0	0	0	0	1	1	1	0	0	0	0	0	0	0	0
<i>Capoeta trutta</i>	0	0	1	0	1	1	0	0	0	0	0	0	0	0	0	0	0	0
<i>Capoeta sp.</i>	0	0	1	0	1	1	1	0	0	0	0	0	0	0	0	0	0	0
<i>Capoeta capoeta</i>	0	0	1	0	0	1	0	0	0	0	0	0	1	0	1	0	0	0
<i>Capoeta sevangi</i>	0	0	1	0	0	1	0	0	0	0	0	0	1	1	0	0	0	0
<i>Capoeta sieboldii</i>	0	0	1	1	0	1	0	0	0	0	0	0	0	0	0	0	0	1
<i>Capoeta saadii</i>	0	0	1	0	0	0	0	0	1	0	1	1	0	0	0	0	0	0
<i>Capoeta buhsei</i>	0	1	1	0	0	0	0	0	1	0	1	0	0	0	0	0	0	0
<i>Capoeta damascina</i>	0	1	1	0	0	0	0	1	1	0	0	0	0	0	0	1	1	0



S3 Figure. The frequency (in % of all studied teeth, n=84) of the pharyngeal tooth shape classes in 10 studied species of the genus *Capoeta*. Ayvazyan et al., 2018.



S4 Figure. The commonness of occurrences (Y axis) of the shape classes (X axis) in the studied *Capoeta* species, shows that most shape classes occur in one or two species only, whereas certain shape classes appear commonly in several species (e.g. shape classes F and I), or characteristic to all species as shape class C (except *C.buhsei*, as the teeth are broken). Ayvazyan et al., 2018.

1 (8) Shape class F is present.....	2
2 (3) Shape classes D and R are present.....	<i>C. sieboldii</i>
3 (5) Shape class E is present.....	4
4 (4a) Shape class G is present.....	<i>C. sp.</i>
4a	<i>C. trutta</i>
5 Shape class M is present.....	6
6 (7) Shape class N is present	<i>C. sevangi</i>
7 Shape class O is present	<i>C. capoeta</i>
8 Shape classes B and I are present.....	9
9 (13) Shape class H is present.....	10
10 (11) Shape class J is present	<i>C. baliki</i>
11 (12) Shape Classes A is present.....	<i>C. umbla</i>
12 Shape classes P and Q are present	<i>C. damascina</i>
13 Shape class K is present	14
14 (15) Shape class L is present	<i>C. saadii</i>
15a.....	<i>C. buhsei</i>

S5 Figure. Identification key of the pharyngeal teeth for the genus *Capoeta*, according to the studied species, which all are provided by teeth of the shape class "C". *Capoeta*. Ayvazyan et al., 2018.

Shape classes	R					1				
	Q	1								
	P	1								
	O		1							
	N		1							
	M					2	1		2	
	L	1								
	K	1				2				
	J	1								
	I						4	4		3
	H					3			3	
	G	1								
	F						4	5	4	5
	E	1				2				
	D	1								
	C			5	9	9				
B			4	1						
A	1									
	a1	a2	a3	a4	a5	b1	b2	b3	c1	c2

Tooth positions

S6 Figure. Frequency of shape classes in relation to the tooth positions. Note that certain tooth positions can be characterized by few shape classes (e.g. at the tooth position a4 the shape class C occurs in nine species and the shape class B in one species), whereby other positions are quite heteromorphic among species (e.g. at the position a2, seven shape classes can occur). Similar to this, certain shape classes appear in only one species at one tooth position (e.g. shape classes G, J, and L), others appear in four or all species at many tooth positions (e.g. shape classes C and F). Ayvazyan et al., 2018.

Table S4 The scan settings of the scanned fossil material.

Speciemns	Fossil locality/horizon	Depository	Resolution mm*	Tube voltage kV**	Electrical current of tube mA***
<i>Capoeta sp.</i>	JZ-1	JRD-15/01	0.028	58	355
<i>Capoeta sp.</i>	JZ-1	JRD-17/07	0.001	180	150
<i>Capoeta sp.</i>	JZ-1	JRD-17/08	0.046	89	181
<i>Capoeta sp.</i>	JZ-1	JRD-17/09	0.046	89	181
<i>Capoeta nuntius</i>	Kisatibi	GNM 8-1	0.035	71	228
<i>Capoeta nuntius</i>	Kisatibi	GNM 10-1	0.037	94	162
<i>Capoeta nuntius</i>	Kisatibi	GNM 11-1	0.040	89	662
<i>Capoeta nuntius</i>	Kisatibi	GNM 13-4	0.035	67	288

*mm resolution

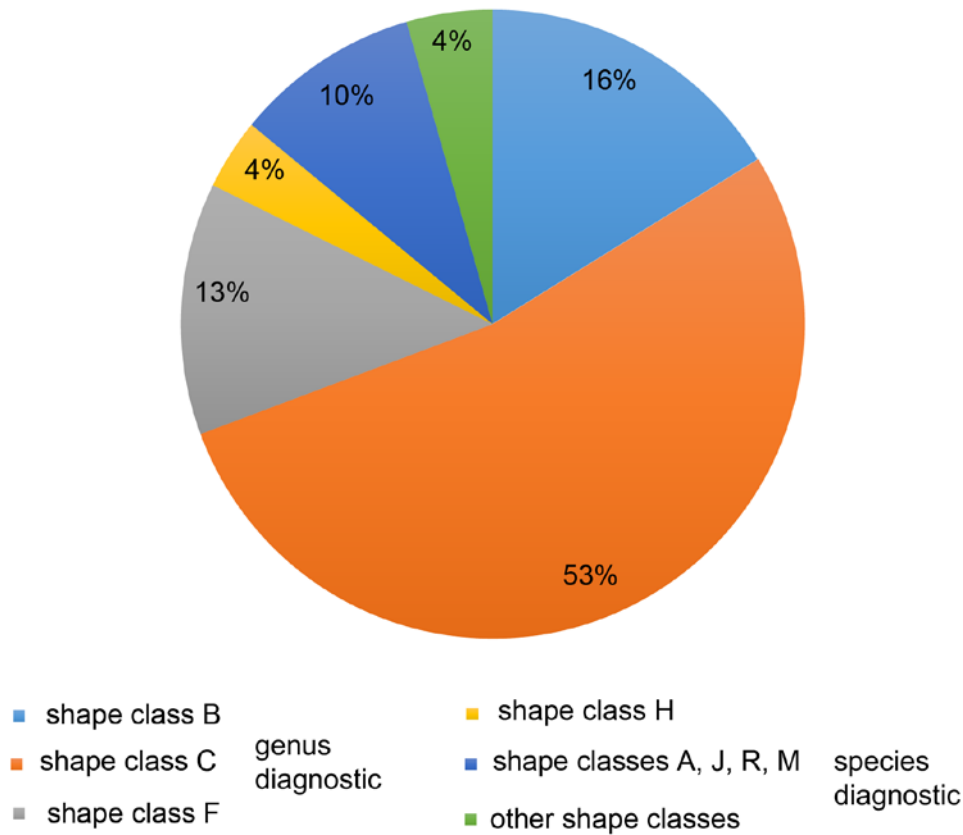
**kV (the voltage or electrical potential applied to the tube)

***mA (the electrical current that flows through the tube)

Table S6 Scan settings of the pharyngeal bones of barbins.

Species	Coll. Numbers	Resolution (mm)	Tube voltage (kV)	Electrical current of tube (mA)
<i>Luciobarbus comizo</i>	MNCN 69304	0.038	150	64
<i>Luciobarbus</i>	MNCN E 54	0.026	83	99

<i>longiceps</i>				
<i>Luciobarbus sclateri</i>	MNCN 69331	0.03	64	150
<i>Barbus barbatus</i>	SNSB SPAM- PI-00608	0.028	10	10
<i>Barbus meridionalis</i>	MNCN 19933	0.038	150	64
<i>Barbus sacratus</i>	MNCN GUI	0.026	83	99
	17			



S7 Figure. Frequency distribution of recorded shape classes in the Çevirme sample (n=247). Ayvazyan et al., 2019.

Table S7 Fossil material from latest Oligocene to middle Miocene localities Kargı 1, Kargı 2, Harami1, Hancılı and Keseköy (Turkey).

Specimens	Fossil locality	Number (n)	Morphotype	Depository
pharyngeal teeth				
<i>Luciobarbus</i> sp.	Hancılı	8	d3	UU HAN 5304, 5305, 5334
<i>Luciobarbus</i> sp.	Hancılı	4	d5	UU HAN 5332–5333
<i>Luciobarbus</i> sp.	Hancılı	1	d5	HAR1 5300

<i>Luciobarbus</i> sp.	Hancılı	21	d7	UU HAN 5313–5316
<i>Barbus</i> sp.	Hancılı	23	d4	UU HAN 5307, 5307-1, 5308, 5309
<i>Barbus</i> sp.	Hancılı	28	d6	UU HAN 5310-5312, 5321, 5335
<i>Barbus</i> sp.	Harami 1	1	d6	UU HAR1 5301
<i>Luciobarbus</i> vel <i>Barbus</i> sp	Hancılı	15	d1	UU HAN 5300, 5301, 5321
<i>Luciobarbus</i> vel <i>Barbus</i> sp	Hancılı	27	d2	UU HAN 5302, 5303, 5306
aff. <i>Capoeta</i> sp.	Hancılı	1	d8	UU HAN 5317
Barbini indet.	Kargı 1	15		UU KAR1 1300 – 1305
Barbini indet.	Kargı 2	19		UU KAR2 1301 – 1302, 1304-1306
Barbini indet.	Keseköy	116		UU KE 5305 – 5310
dorsal fin spine				
<i>Luciobarbus</i> vel <i>Barbus</i> sp	Hancılı		s1 (7 unbranched last spine of the dorsal fin)	UU HAN 5322 – 5324
<i>Luciobarbus</i> vel <i>Barbus</i> sp	Hancılı		s2 (5 unbranched last spine of the dorsal fin)	UU HAN 5325 – 5328
<i>Luciobarbus</i> vel <i>Barbus</i> sp	Hancılı		s3 (2 unbranched last spine of the dorsal fin)	UU HAN 5329 – 5330
Barbini indet.	Kargı 2		one unbranched dorsal fin ray	UU KAR2 1303